Miniaturisation of sensory systems in ants


Fiorella Carla Ramirez Esquivel

November 2017

A thesis submitted for the degree of Doctor of Philosophy of The Australian National University.

Declaration

This thesis contains original research carried out from March 2013 to November 2017 at the Australian National University, Canberra, Australia. I am the lead author, and principal contributor, of all publications contain within. Author contributions are outlined in detail at the start of each published chapter. The material presented here is, to the best of my knowledge, original research and has not been submitted in whole or in part for a degree at any other university.

I acknowledge the support of the Australian government in the form of an Australian Postgraduate Award (APA) scholarship and a Top-Up scholarship from the ARC Centre of Excellence in Vision Science.

Word count: 67,141

Fiorella Carla Ramirez Esquivel

Acknowledgements

First of all I would like to thank my supervisors Jochen and Ajay – thank you for your trust in affording me so much independence to pursue my own avenues of interest throughout my degree. Thank you for your kindness and support, and the extreme generosity with which you made so many resources and opportunities available to me. Your dedication and passion for science has been an inspiration right from those very first undergraduate lectures.

I'd like to thank my partner, Caleb. The last few years have been super packed with adventures and change and it has been really special to be able to go through it all with you. From all of the rock climbing to eating all the ramen in Japan to knee surgery and all the other crummy parts of life, I am so glad you were there for it all. I can't wait for our next adventure!

Thank you to all lab members and partners past and present from both ANU and Macquarie including Willi and Ladina Ribi, Zoltan and Kristina Kocsi, Trevor Murray and Camille Moray, Marcin Falkowski, Franne Kamhi and Yuri Ogawa. Particular thanks go to Trevor Murray for taking the time to give me very thoughtful comments on my unpublished chapters. Additionally, I'd like to thank the theoretical chemistry crew for including me in their social circle and just being super fun to be around. Thank you, in particular to Peter, Titou and Maude (and little Lucette and Celestine), Andrew, Simon, Giuseppe and Brigida, Marat, and Amanda.

I'd like to thank all the people who shared their expertise in microscopy at ANU Paul Cooper, Eldon Ball, Daryl Webb, Jo Lee, Hua Chen, Melanie Rug. I'd also like to thank Eric Warrant for organising the most amazing conference I've ever been to (ICIV 2013), for being my temporary office mate during his sabbatical in Canberra and for being always so kind.

I'd like to thank all the people I worked with during my time volunteering at the Australian National Insect Collection (CSIRO). I am super grateful I got to experience entomological research from a radically different perspective than the one I experience in my lab. Opening random drawers in the collection just to see what was inside was always my favourite thing to do and without this I doubt I'd have anywhere near as good a grasp of the sheer diversity of insect life. I'd like to thank my supervisors there over the years Nicole Fisher and John La Salle, as well as Debbie Jennings and Sara Pinzon Navarro whom I worked with during the start of my PhD.

I'd like to thank all the wonderful people I met at the HYM course of 2015. There is nothing quite like being in a room full of enthusiastic hymenopterists looking down microscopes, flipping through identification keys and completely taken with identifying specimens. The excitement was practically tangible and it was a wonderful experience. I really enjoy hearing about your ongoing adventures and I am glad I can count you among my circle of friends. I'd particularly like to thank my roommate Sara Fernandes and lab partner Dan Wiens for their friendship.

I'd like to thank Wolfgang Rössler for hosting me at his lab in Würzburg and his entire group for taking the time to teach me and make my stay fun. In particular I'd like to thank Jan Kropf, Frazi Schmitt, Anne Lindenberg, Agustina Falibene, and Vivien Landwirt. I'd also like to thank the two students from Arizona University I met while at Würzburg. Ted Smith for commiserating with me over Germans' apparently complete immunity to alcohol and for being a fun and understanding lab mate while I was making horrible high pitched sounds with a piezo element trying to vibrate sensilla off antennae. Although we only overlapped for a very brief and hectic time, I'm glad I ended up having wine at the bridge (practically an institution of Würzburg summertime) with Nicole Leitner. Not only was it awesome to find out someone had actually read my first publication but we also ended up working together on a new publication!

Work without friends and family is not very much fun. I'd like to thank my mum and step-dad for not minding too much when I was constantly stressed and grumpy. For cooking three different meals on Wednesday nights to accommodate all the different dietary requirements. For making more cheese than I could ever eat. For being the most indulgent doggy parents in the world. For being my safety net and for just being there always. I'd also like to thank my other parents, my "outlaws" Polly and Steve, for effectively adopting me into the Ball family and not even batting an eyelid when I turn up with live ducks for Christmas presents or spend entire afternoons digging up your yard.

Even though you are scattered far and wide I'd like to thank my extended family in Buenos Aires, Folkestone, Indianapolis, Canberra and Melbourne. I feel extremely fortunate to have grown up in a family with such diverse skills and interests from engineers, architects and health professionals to artists, dancers, musicians and journalists. Even though you might not really understand what exactly it is I do I know you'll be proud of me no matter what.

Thank you to the many friends who shared in the last four years and made them adventure-filled and awesome including Caleb Ball, Rob Janissen, Pete Appleby, Ben Noble, Jia Xie, Rachel Everett, Andrew May, Annette Zou, Snowy Haiblen, Andy Clark, Hannah Cliff, Sarah Buckerfield, Floyd Howard, Giuseppe Barca and Brigida Boticelli Barca, Theo Honing-Wassenburg, and Alec Coulson. Special thanks go to the climbing crew, my second family, without whom Friday night climbing would not have been the highlight of my weeks for such a long time! Special thanks to Ben for all that excellent Calvin Harris on Saturday mornings and for just being a generally awesome housemate. Thanks to my partner in crime, Sarah "Buckerchow!", for those two rad summers when we grew tomato jungles and so much food we didn't need to shop for veg for months and months. Thanks to Jia for being so considerate and fun and for making up the best Jia-isms ("fighting!" and "not moral" are forever part of our vocabulary now). Thanks to Smillin' Pete for just being the chillest dude ever. Thanks Rob for being the most bombastic and ridiculous human being alive.

Finally, I'd like to give a huge thanks to my brother and sister for being my favourite people. Over the last few years we've somehow managed to fit in a fair few things from building enormous veggie patches and exchanging plants, playing board games, going on coast trips with doggies, recovering from knee surgery and coming down from horrible painkillers while watching Looney Tunes, helping me to plant potatoes and do lab work when I was on crutches, sanding floors and painting houses, making wooden spoons and watching strange anime. These last years would have been much much duller without you guys around. "Los hermanos sean unidos, porque esa es la ley primera…"

To my dad, el abuelo Anibal and Betty.

Abstract

The main focus of this thesis is the study of sensory systems in the context of changing body-size. In particular the study of ant sensory systems and how these are shaped by miniaturisation. The study of insect visual ecology and physiology is used as a basis to develop a framework for the study of ant antennal sensilla and chemosensation, to interpret anatomical variation from a functional and organ design perspective. This thesis reviews the anatomy and nomenclature of antennal sensilla through two case studies on an extremely large species *Myrmecia pyriformis* and a small species *Temnothorax rugatulus*. These two studies additionally quantify intraspecific variation and discuss the potential functional consequences of this variation for self-organising insect societies and task allocation. A large scale comparative study takes the tools developed in previous chapters to focus in on how chemosensilla vary in their numbers, size and distribution through the Fomicid phylogeny. The gross anatomy of the antenna and changes in shape from club to filiform antennae are described in detail. Anatomical data are analysed to identify scaling trends and potential adaptations driven by miniaturisation. Ecological and phylogenetic considerations are discussed wherever relevant. The wide ranging impacts of body size changes are reviewed, incorporated into the interpretation of results and used to propose promising avenues for future research. Finally, ant body size and some of the different methods used in the literature to measure size and size variability are critically analysed. The functional implications of body size variability within species are discussed using *Iridomyrmex purpureus* as an example.

This thesis makes use of a variety of microscopy techniques. In addition to the methods sections of each chapter a dedicated methods chapter is included. This chapter reviews some of the techniques used in the main data chapters and in the additional publications produced over the course of this thesis.

Chapter outlines

Chapter 1: Introduction to miniaturisation – this chapter is intended as a standalone review on some of the important aspects of miniaturisation. It is currently in preparation for submission for publication under the following title:

> **Ramirez-Esquivel, F., in prep. Miniaturisation a complex trait: From genomics to sensory physiology.**

Chapter 2: Describing and identifying ant sensilla – this chapter represents an initial review of ant sensilla and a case study of the antennal array of a single polymorphic species. This chapter establishes the nomenclature and protocols used for the study of antennal arrays in this thesis. Its contents are based on the published work:

> **Ramirez-Esquivel, F., Zeil, J., Narendra, A., 2014. The antennal sensory array of the nocturnal bull ant *Myrmecia pyriformis*. Arthropod Structure & Development 43, 543-558.**

Chapter 3: Intraspecific variation in sensory systems – in this chapter both the visual and antennal arrays of a small monomorphic ant are described in detail. Sensory variability is identified among nest mates and the whole antenna is examined to reveal some previously undescribed features. This chapter is based on the following publication with the addition of some post-publication observations:

> **Ramirez-Esquivel, F., Leitner, N.E., Zeil, J., Narendra, A., 2017. The sensory arrays of the ant, *Temnothorax rugatulus*. Arthropod Structure & Development 46, 552-563.**

Chapter 4: A large-scale comparative study of ant sensilla – this chapter quantitatively documents, for the first time, the variation and scaling patterns of size, numbers and distribution of chemosensilla across Formicidae. The scaling of different antennal segments is also documented and miniaturisation specific adaptations are identified.

Chapter 5: Describing body size variation in ants – results from the previous chapters highlight the importance of within-species variability. This chapter attempts to address questions such as how much variability

do we expect to find in different species and what does this mean for sensory systems? The meaning of terms such as "monomorphic" and "polymorphic" are briefly reviewed and body size and visual system variability are examined in three populations of a monomorphic species.

Chapter 6 – Thesis Conclusions: Concluding remarks.

Chapter 7 – Methods Appendix: Techniques for the investigation of the ant visual system anatomy – this methods chapter outlines many of the techniques used in this thesis and in the publications produced during my PhD that are not included in this thesis. The contents of this chapter are based on the non-audio-visual component of the following published work:

> **Ramirez-Esquivel, F., Ribi, W., Narendra, A., in press. Techniques for Investigating the Anatomy of the Ant Visual System. JoVE.**

Additional publications not included in the thesis:

1. Narendra, A., **Ramirez-Esquivel, F.**, Ribi, W.A., 2016. Compound eye and ocellar structure for walking and flying modes of locomotion in the Australian ant, *Camponotus consobrinus*. Scientific Reports 6, 22331.
2. Narendra, A., **Ramirez-Esquivel, F.**, 2017. Subtle changes in the landmark panorama disrupt visual navigation in a nocturnal bull ant. Philosophical Transactions of the Royal Society B: Biological Sciences 372, 20160068.

A note on figures:

This thesis contains a large number of figures. With the exception of those contained in the introductory chapter the majority of the figures herein are composed of original images. Unless explicitly attributed to another author all images should be attributed to Fiorella Ramirez-Esquivel.

Table of contents

Chapter 1

Introduction to miniaturisation

Chapter contents

The study of miniaturisation in its modern formulation is a young field. Key works such as Hanken and Wake (1993) have gone a long way towards identifying key areas of interest but dedicated texts are only just starting to emerge (Polilov, 2016). Relevant literature is scattered far and wide and a holistic framework for the definition and study of miniaturisation has not been developed much further than Hanken and Wake's landmark publication. The first portion of this introduction is therefore dedicated to trying to address this problem by bringing together recent research on the subject, outlining areas of interest and important considerations for the study of miniaturisation.

The latter part of this introduction will outline the effects of miniaturisation on sensory systems, since they are the focus of this thesis. These effects include the physical constraints, the neural requirements, and how these may be shaped by body-size. I focus on vision and chemoreception, as model sensory systems, because these are the two primary senses that guide ant behaviour. Due to the complex differences between insect and vertebrate sensory systems, this section focuses generally on insects, but specifically hymenoptera and ants.

Miniaturisation is an intrinsically complex trait. There is no single "smallness" gene that natural selection can act on. As a result the effects of decreasing body size are diverse, affecting every aspect of an organism, including how it relates to the physical world, its development, physiology, genomics and behaviour. These diverse aspects of an organism often shape each other in very dramatic and complex ways. As a result a holistic approach must be taken, anything else is likely to result in a kind of tunnel vision that obfuscates the very adaptations we seek. Miniaturisation related adaptations may manifest differently in different lineages due to differences in evolutionary trajectories and may have even disparate effects among different structures or biological systems within a species.

In order to provide context, this introduction covers a wide range of topics since it is important to be aware of the diversity of competing factors that shape the biology of an organism. Otherwise, there is a danger of becoming

like the blind men of the parable[1], clutching different parts of the elephant unable to grasp the whole.

[1] *"A group of blind men heard that a strange animal, called an elephant, had been brought to the town, but none of them were aware of its shape and form. Out of curiosity, they said: "We must inspect and know it by touch, of which we are capable". So, they sought it out, and when they found it they groped about it. In the case of the first person, whose hand landed on the trunk, said "This being is like a thick snake". For another one whose hand reached its ear, it seemed like a kind of fan. As for another person, whose hand was upon its leg, said, the elephant is a pillar like a tree-trunk. The blind man who placed his hand upon its side said, "elephant is a wall". Another who felt its tail, described it as a rope. The last felt its tusk, stating the elephant is that which is hard, smooth and like a spear." – Goldstein, E.B., 2010. Encyclopedia of perception. Sage.*

1.1. Introduction to miniaturisation

1.1.1. Body-size

Animals vary in size; this is something we accept as an obvious observation and yet it is one of the most amazing feats of evolutionary engineering. Consider that all animals are composed of cells with the same basic components. Now let us consider the range of living things that are composed of these same basic building blocks (**Table 1.1**). From the smallest eukaryote to the largest there is a difference of 24 orders of magnitude.

Table 1.1. Modified after Schimdt-Nielsen (1977). Weights are meant to give an approximation of scale and are not precise population averages. Additional data from: (Caballero et al., 2004; Courties et al., 1994; Prescott, 1955).

Organism	Mass	
Ostreococcus tauri	1 fg	10^{-15} g
Amoeba proteus	10 ng	10^{-7} g
Springtail	10 µg	10^{-5} g
Bee	100 mg	10^{-1} g
Hamster	100 g	10^{2} g
Human	100 kg	10^{5} g
Blue whale	100 t	10^{8} g
Giant Sequoia	1000 t	10^{9} g

This is an unfathomably large figure. Let us instead consider an analogy. If cells are the building blocks of eukaryotic life then let us imagine Lego® blocks as an alternative building unit. If we were to build with standard Lego®, the smallest possible construction would consist of a single block of about 1g while the largest theoretically possible free standing Lego® structure would be about 400kg (Alexander, 2012). After this, additional modifications need to be made to the building units to overcome the weight bearing limits of the plastic and other problems that are likely to arise in terms of structural stability. This only spans five orders of magnitude compared to the 24 spanned by eukaryotes; increasing five orders of magnitude from the beginning of our eukaryote list does not even get us to multicellular organisms. Furthermore, consider that while our theoretical Lego® structure has only one function, structural integrity, a living cell must perform all the functions of autonomous life including metabolism of nutrients, respiration, reproduction, etc. Although this analogy is

extremely simplistic, it serves to illustrate the sheer complexity posed by the challenge of scaling living organisms over 24 orders of magnitude.

1.1.2. Miniaturisation

Body size is one of the most important characteristics of any living thing. The study of animal body size has existed for as long as the formal study of biology itself in the form of comparative biology and the study of allometry. The emergent field of miniaturisation can be thought of as a specialised branch of comparative biology, which focuses on any adaptations that accompany reductions in body size, relative to the ancestral state. While comparative anatomy is interested in the similarities and differences among species miniaturisation is specifically interested in the design limitation that prevent animals from becoming smaller and how those limits may be overcome through innovative design.

There has been a particular emphasis on studying taxa exhibiting extreme reductions in body size, since they test the lower limits of size attainable by living organisms. However, the study of miniaturisation need not limit itself to extremes, although these often provide useful insights, they are meaningless without an understanding of a particular taxon's larger relatives. Miniaturisation is a complex process which affects every aspect of an organism's biology. As a result comparative studies which include many related species, spanning a range of body sizes are often the most successful in contributing to our understanding of the design challenges faced by minute creatures (e.g. Eberhard, 2007; Fischer et al., 2013; Makarova et al., 2015; Quesada et al., 2011; Roth et al., 1988). However, in order to discuss the best way to study such scaling, we must first establish exactly what is meant by "miniaturisation". This introductory chapter attempts to review the state of knowledge of miniaturisation. To best illustrate the complexity of miniaturisation examples from throughout the Eukaryota are considered. However, the main focus will be on animals and in particular Hymenoptera, a group that has been at the forefront of miniaturisation research in the last decade.

Miniaturisation has been defined as a decrease in adult body size over an evolutionary timescale relative to the ancestral state (Hanken and Wake, 1993). Some extreme instances of miniaturisation in diverse taxa (**Figure 1.1**) include vertebrates (legless lizards: Bhullar and Bell, 2008; hummingbirds: Dial, 2003; chameleons: Glaw et al., 2012; salamanders: Hanken, 1983; bats: Pereira et al., 2006; frogs: Rittmeyer et al., 2012), arthropods (strepsiptera: Beutel et al., 2005; wasps, beetles, booklice:

Polilov, 2016; spiders: Quesada et al., 2011; ants: Seid et al., 2011), echinoderms (starfish: Byrne, 1996), other marine invertebrates (loriciferans: Kristensen, 1991; Minelli, 2003), and unicellular organisms (archaea: Comolli et al., 2009; picoeukaryote: Courties et al., 1994; ultramicrobacteria: Luef et al., 2015). Unfortunately, while numerous, small organisms can be difficult to find and difficult to study due to their size. The descriptions of most of the species listed above are limited to a few particular aspects of their biology and very few of these species have been comprehensively studied from the perspective of miniaturisation. This is understandable as it is difficult enough to amass a well-rounded body of knowledge (including, for example, energetics and metabolism, anatomy, behaviour and natural history) on a single animal at the best of times, let alone when that animal is a 7.7 mm frog in its natural habitat in remote tropical jungle. Consequently, it is challenging to find complete accounts of size related adaptations displayed by extremely small animals. In this respect, the study of small invertebrates has been unusually successful. While there is a multitude of reasons for this, perhaps the most important are the large range of body sizes exhibited by closely related insect taxa and their ubiquity. As such, suitable study systems are more plentiful and accessible than their vertebrate counterparts.

Invertebrates are evidently capable of attaining smaller minimum body-sizes, but why is this? What features of the invertebrate physiology make them more amenable to miniaturisation? Is there a limit to minimum size and what sets this? The answers to these questions are complex and so I will discuss many of the issues involved in answering them in the following sections. A good place to start is by discussing whether there is a point at which an organism qualifies as 'miniaturised'. At what point does a lineage go from being merely small to being miniature? Hanken and Wake (1993) identify such a 'critical size':

> *"…[the body size]… at which important physiological or ecological functions such as feeding, locomotion or reproductive biology are affected, necessitating a major change in the way an organism deals with its ancestral adaptive zone. Some instances of miniaturisation may represent a minimum body size below which further size decrease is not permitted because of the design limitations of a given bauplan…"*

However, developing criteria to define miniaturisation is difficult because different organs, sensory systems, ecological functions, etc. are differentially affected by a decreasing body size (Hanken and Wake, 1993). An organism may reach the limits of miniaturisation with respect to one

aspect of their biology, for example, egg size, while having, say, relatively large eyes. As such, there is no fixed criterion that defines whether or not an organism is miniaturised, since miniaturisation is a complex trait. It is perhaps then more pragmatic to speak of miniaturisation as it relates to specific aspects of an organism's biology and refer to taxa as having, for instance, a reproductive system that approaches the limits of miniaturisation in that lineage.

Phylogeny

As discussed above, there is no absolute criterion to define miniaturisation. Instead, we look at the relative size of a species compared to its ancestors. Miniaturisation is then a relative feature, as outlined in this example by Niven and Farris (2012):

> *"…although vertebrate nervous systems are large in comparison to those of many invertebrates, some vertebrate lineages may still be described as miniaturized in relation to an ancestor. Conversely, despite possessing small nervous systems in comparison to vertebrates, many insects possess much larger nervous systems than basal apterygotes (e.g. silverfish) and so, with reference to this node of their phylogeny, they are not miniaturized."*

Having a good understanding of the phylogenetic tree of a study species becomes extremely important for the interpretation of traits in the context of miniaturisation.

An interesting example to highlight the importance of phylogeny is the case of the kiwis (*Apteryx*). These peculiar birds from New Zealand were once thought to be the closest living relatives of the extinct giant moas (Dinornithiformes) and examples of miniaturised ratites, which is a group of flightless birds including emus and ostriches (Calder, 1984). This theory was encouraged by a peculiar feature of kiwi reproduction: the female kiwi produces a single, enormous egg per clutch, which is so large that in the days prior to laying it takes up the majority of the body cavity. In the past it was hypothesised that the kiwi had undergone miniaturisation but somehow retained its ancestral egg size from a moa-like ancestor (Calder, 1979, 1984). Modern phylogenetic analysis, however, contradicts this theory (Mitchell et al., 2014). Kiwis seem to be descended from a small-bodied, flying ancestor (Mitchell et al., 2014; Phillips et al., 2010). Their large eggs are probably not a product of miniaturisation but more likely evolved due to the unique ecology of New Zealand, which lacks mammalian

predators. The absence of terrestrial egg predators may have encouraged the production of precocious chicks that are less vulnerable to aerial predation, which is certainly present in the form of birds of prey (Worthy et al., 2013). Thus, careful examination of phylogenetic relationships reveals that the kiwi is not a miniaturised ratite but rather that most ratites are giantised birds.

Why become smaller?

Our first step in understanding miniaturisation is to understand what evolutionary advantages lead organisms to reduce their body size. Despite its prevalence the evolutionary advantages of miniaturisation are not obvious. In fact it is unlikely that there are many intrinsic benefits to miniaturisation itself, the advantages of miniaturisation are indirect and come from accessing new niches. The opposite scenario, evolutionary gigantism, provides an illustrative example of how shifts in body size give access to new niches. Specifically, let us consider the evolutionary radiation of mammals which gave rise to mammalian mega fauna, after the extinction of dinosaurs (Smith et al., 2010). In this scenario a dramatic shift in body-size enabled mammals to colonise new ecological niches, exploiting new resources, and escaping competition and predation. By increasing body-size mammals effectively colonised a niche space that they found suddenly vacated by dinosaurs, allowing their inter-specific relationships to be redefined. Miniaturisation allows for similar redefinitions: resources unusable for larger animals become accessible, for example the hyperparasitoid *Lysibia nana* is able to use the pupae of other minute *Cotesia* parasitoid wasps to provide nourishment for their offspring (Poelman et al., 2012); escape from saturated ecosystems provides the opportunity for evolutionary radiation into new ecological niches; and inter-species relationships (competition, predation and parasitism) can be redefined in the new context. An example of this is found in the evolutionary radiation of the diverse and minutely sized parasitic wasp lineages such as Figitidae, Mymarommatidae, and Chalcidoidea that make use of extremely small but abundant resources such as other insect's eggs. Accessing a new niche, such as this, propels the organism as a whole towards miniaturisation (Mckinney, 2013). "There's plenty of room at the bottom" (Feynman, 1960).

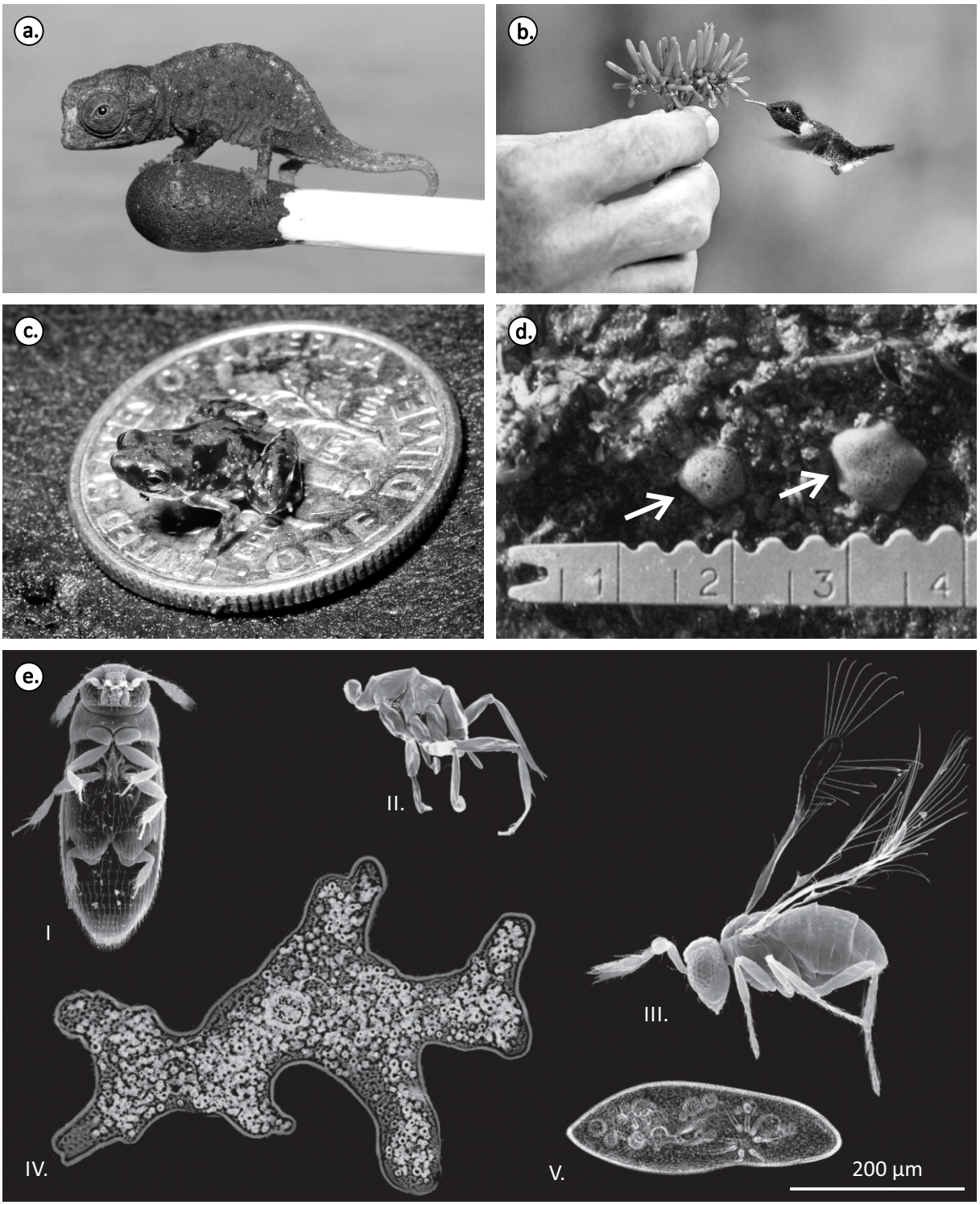

Figure 1.1. Examples of miniaturised animals: (a) chameleon *Brookesia micra*, modified from Glaw et al. (2012); (b) hummingbird *Mellisuga helenae*, modified from image by Rita Ivanauskas; (c) frog *Paedophyne amanuensis*, modified from Rittmeyer et al. (2012); (d) Two specimens of *Patiriella parvivipara* starfish, modified from Byrne (1996), ruler units = cm; (e) Microscopic invertebrates: (I) *Nanosella* sp., (II) *Dicopomorpha echmepterygis*, (III) *Megaphragma myrmaripenne*, (IV) *Amoeba proteus*, and (V) *Paramecium caudatum*, modified from Polilov (2015).

1.1.3. Costs and limits involved in miniaturisation

While the evolutionary advantages of miniaturisation are potentially great, there are many costs that need to be overcome to access those advantages. A drastic change in body size from the ancestral state implies much more than a simple up- or downscaling of existing structures and processes. The body size of an organism is not just pivotal in determining what ecological niches it can access, but also in shaping how its physiology functions and what physical forces predominate as it carries out basic functions such as locomotion and gas exchange (Calder, 1984; Pedley, 1977; Peters, 1983; Schmidt-Nielsen, 1984).

> *"Comparative anatomy is largely the story of the struggle to increase surface area in proportion to volume"*
>
> (Haldane, 1926)

One of the most important principles in illustrating the difficulty of changing body size is the square-cube law. This describes the relationship between the volume and the surface area of an object as its size changes (Haldane, 1926; Rensch, 1948; Schmidt-Nielsen, 1984). As an object of constant shape grows, its volume grows at a faster rate than its surface area (see **Figure 1.2**). The simplest example of this geometric relationship is that of the cube. If we take a cube of side length L, we know that the area of this cube will be proportional to L^2 and its volume will be proportional to L^3 (see **Figure 1.2**). This principle applies to bodies of any shape. As a result, if an animal were to decrease in size, without altering its shape, its volume would decrease more rapidly than its surface area.

This shifting ratio has a host of implications for many biological processes and can either facilitate or hamper them. For instance, while an increased surface area to volume ratio leads to a greater susceptibility to desiccation (e.g. Dromgoole, 1980; Pellegrino, 1984) it also facilitates gas exchange and the diffusion of substances across the body (e.g. nutrients, hormones, etc.) (Harrison et al., 2010). The differences in the respiratory systems of animals of different sizes are an interesting example of how shifts in the volume to surface area ratios can result in significant differences in the design of body systems of animals.

Large animals require elaborate respiratory systems with large surface areas to maintain adequate rates of gas exchange. They also use active respiration to speed up the rate of gas flow over their respiratory

membranes and have respiratory pigments (such as haemoglobin and haemocyanin) that increase the oxygen carrying capacity of blood. By comparison small animals, such as small insects, can attain sufficient rates of gas exchange by passive diffusion through a decentralised network of increasingly finer trachea throughout the body. These tracheae diffuse oxygen directly into the haemolymph and into tissues throughout the body cavity. Finally, some of the smallest arthropods such as some Collembolans respire directly through their porous cuticle (Calder, 1984; Davies, 1927; Schmidt-Nielsen, 1984).

In this particular example larger animals must invest in increasingly more elaborate respiratory systems because the rate of oxygen consumption is tied to the volume of tissue, while the rate of oxygen diffusion is tied to the area of the respiratory surface. As the surface area to volume ratio decreases with increasing body size, increases in the elaboration and modifications of the ancestral respiratory system become necessary to maintain adequate respiration.

The functioning of many biological processes is tightly bound to accessing adequate surface area. For example, nutrient absorption and gas exchange depend on convoluted epithelia with large surface areas (Rensch, 1948). As discussed, efficiency of nutrient absorption and gas exchange are dependent upon the relative area per volume. In contrast, other physiological processes such as vision (Land, 1997), are dependent on the absolute surface area available. Since miniaturisation impacts different physiological processes in different ways, we expect scaling to differ between organs and different anatomical structures. In insects, these differences include a decrease in relative spatial investment in respiration, waste filtration, and circulation of haemolymph, but an increase in spatial investment in sensory structures, brain, and the reproductive system (in females) (Polilov, 2016).

The non-linear scaling of surface area to volume in geometrically similar bodies is possibly the single most important geometric relationship to consider when studying miniaturisation. This is not to say that there are no other factors that shape physical, chemical and biological interactions as the limits of miniaturisation are approached. The following sections give an outline of some of the known constraints involved in miniaturisation.

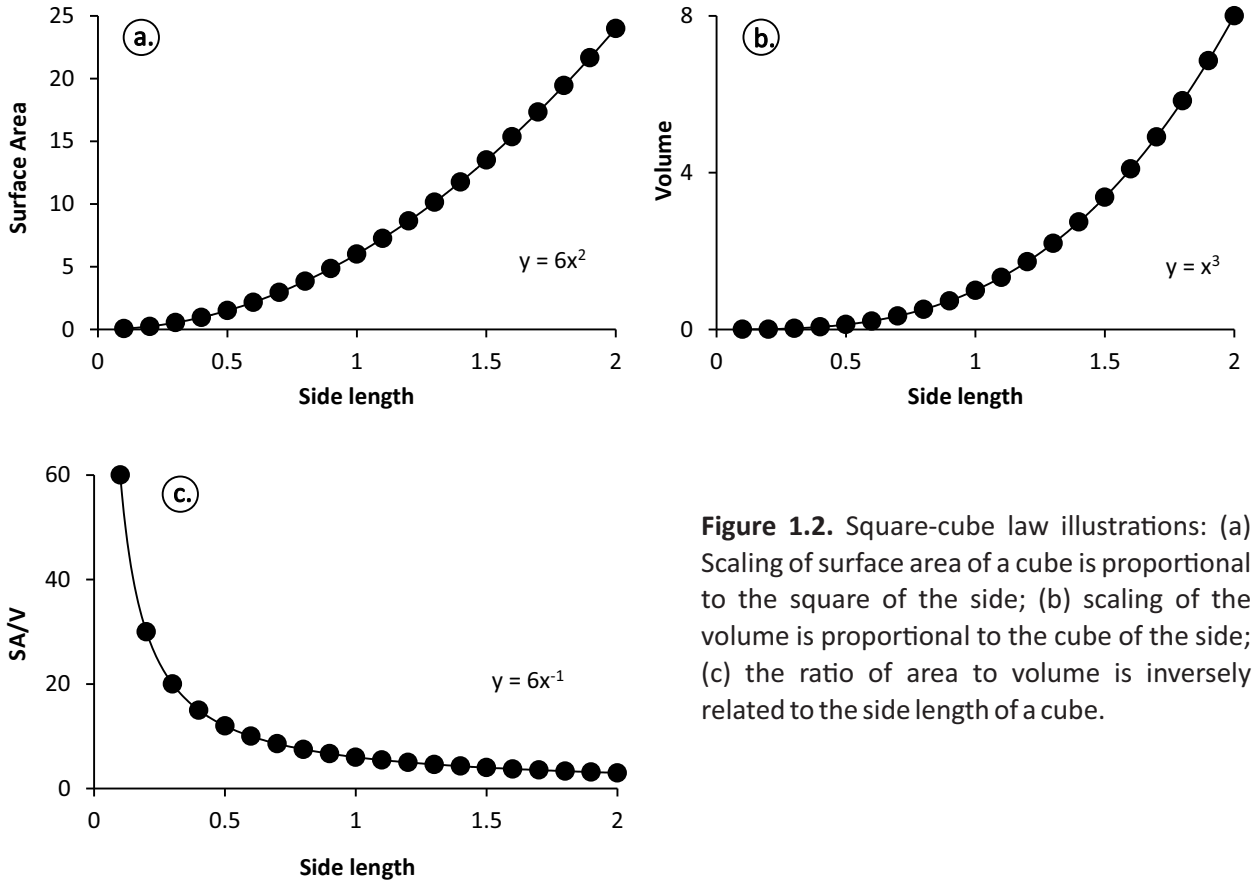

Figure 1.2. Square-cube law illustrations: (a) Scaling of surface area of a cube is proportional to the square of the side; (b) scaling of the volume is proportional to the cube of the side; (c) the ratio of area to volume is inversely related to the side length of a cube.

Physical properties of the environment

> *"The world we live in is governed by the laws of chemistry and physics, and animals must live within the bounds set by those laws."*
>
> (Schmidt-Nielsen, 1977)

The same laws of physics and chemistry apply regardless of an animal's body-size. However, interactions between bodies at micro-scales can appear fundamentally different from those we ourselves may experience as macro-animals. This is because the relative importance or predominance of different forces can shift with changes to the mass and surface area to volume ratio of bodies. At micro-scales the effects of forces such as surface tension, Brownian motion and Reynolds numbers become extremely important not just for physiological processes but also in defining how the whole organism interacts with the environment and the medium, be it air or water (Beebe et al., 2002). Meanwhile the effect of forces predominant at the macroscale such as inertial forces and the effects of gravity are greatly reduced and can have interesting effects on locomotion (e.g. Sane, 2016). These kinds of shifts in the physical laws and their consequences for interactions at the micro-scale are often surprising and difficult to intuitively understand. For example, no human being can directly perceive the effect of van der Waals forces and very few of us are aware of the ways in which surface tension and laminar flow shape our surroundings.

Let us consider some examples of locomotion, perhaps the most ubiquitous interaction between an animal and the physical world. The forces governing locomotion at a macro-scale are very different than those at a micro-scale (for an interesting review of scale effects in locomotion across taxa see: Pedley, 1977). While gravity and inertia define locomotion at a macro scale, Reynolds numbers, surface tension and van der Waals forces play a large role in defining the mechanics of movement at smaller scales. Consider, for instance, water striders; these small insects are able to literally walk on water as the surface tension of the water is too strong (see **Figure 1.3b**) to be overcome by the small downward pressure being exerted by their diminutive mass which is additionally spread out over the relatively large area provided by their six, setae covered, tarsi (Gao and Jiang, 2004). For a human to accomplish such a feat their weight would have to be spread out over such a large area that each foot would need to be about 1.6km long and 0.5km wide (Beebe et al., 2002).

A gecko's vertical running is another interesting mode of locomotion that capitalises on a large surface area to mass ratio and makes use of an

unusual physical interaction. Gecko feet have elaborate microstructures (see **Figure 1.3c**) that allow geckos to harness van der Waal's forces. The intimate contact and exact distance between the substrate and the precisely oriented, micro-setae on the feet of the gecko generate dipole interactions between the feet and the substrate, a unique and extremely unusual mode of adhesion that is only possible because of micro-scale interactions (Autumn et al., 2000).

Finally, let us consider the transition of flight modality from normal flapping flight in macro-animals (such as birds and most insects) to clap and fling in micro-animals (such as very small flies, beetles and wasps) (reviewed in Sane, 2016). This transition is necessary as the lack of inertia and the low Reynolds numbers in which they operate require an increase in stroke amplitude to minimise the loss of energy to viscous dissipation. The stroke amplitude is such that the wings 'clap' together at the end of the upstroke and must be peeled apart for the downstroke 'fling'. In order to mitigate the costs associated with peeling the wings apart in low Reynolds numbers various lineages of micro-insects have independently evolved hair-fringed wings (see **Figure 1.3a**), which increase the porosity of the wing.

Another aspect of locomotion that has been proposed to change with changing body size pertains to the structure of the environment, in particular the texture of the substrate, and is termed the size-grain hypothesis. This theory proposes that the way in which a walking animal interacts with a given terrain is size dependent and as size decreases the rugosity of the terrain will increase potentially leading to disproportionately long legs in smaller animals (Kaspari and Weiser, 1999).

There are many biologically relevant processes beyond locomotion that are governed by different scale-dependent physical principles. Many insects in the order Hemiptera feed on xylem sap using sucking mouthparts. However, as the diameter of the feeding tube becomes smaller, the force required to draw up xylem (which is under negative tension) increases. This may, in fact, place a hard limit to the miniaturisation of the Hemipteran bauplan (Novotny and Wilson, 1997). Other examples include the diffraction limits of light and its impact on eye design (Land, 1981), the diameter-dependent conduction velocity of neurons (e.g. Waxman, 1980), and the different modes of diffusion and dispersal of particles in a medium and their impact on chemosensory systems (e.g. Koehl, 2001). Some of these shall be discussed in detail later on in this chapter.

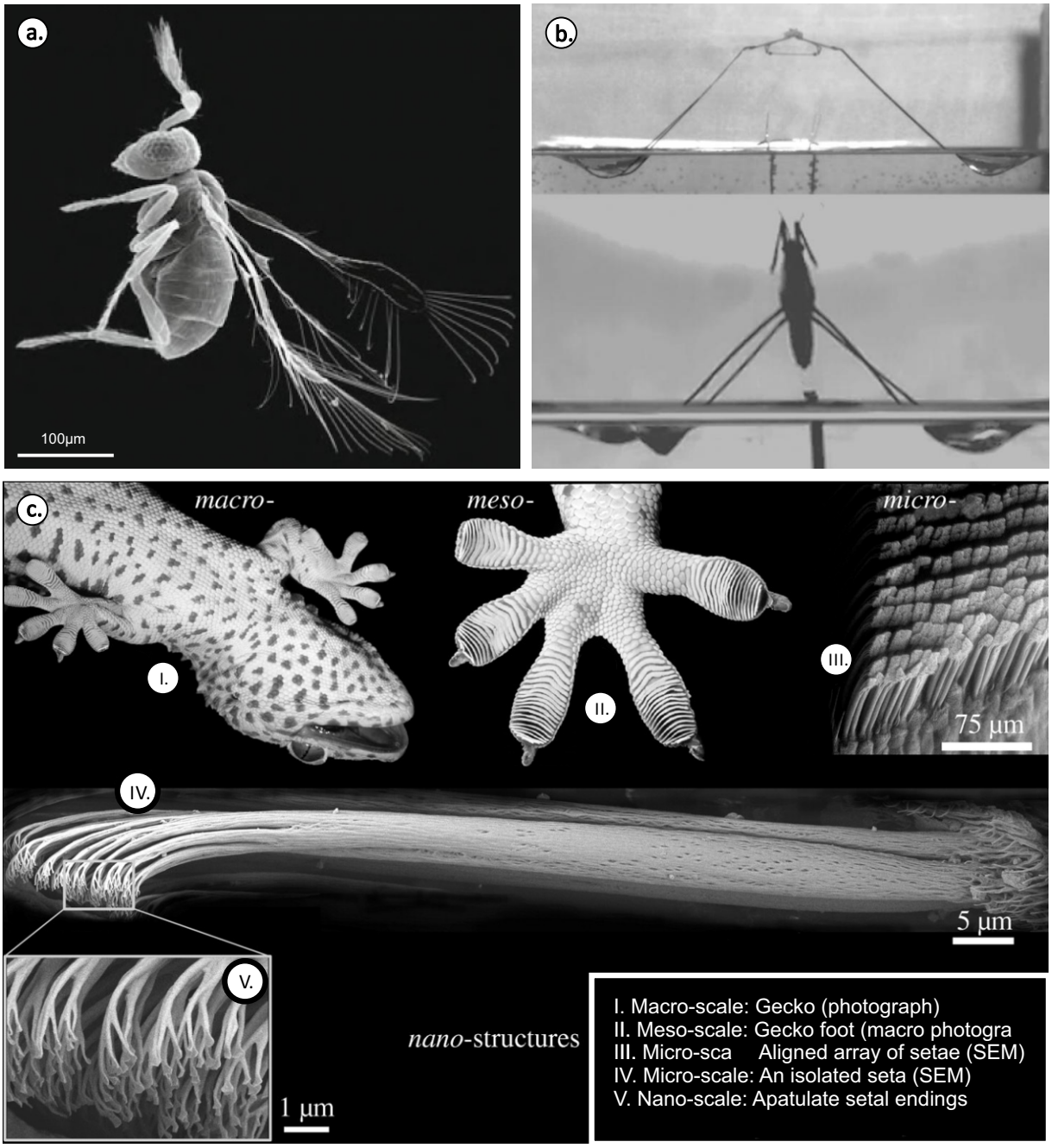

Figure 1.3. Physical interactions with the environment. (a) Fairy wasps with hair-fringed wings (modified from: Polilov, 2016). (b) A water strider (Gerroidea) exerting downward pressure on the water meniscus but failing to overcome surface tension even when jumping (bottom image), (modified from: Koh et al., 2015). (c) Structural organisation of Gecko feet at varying scales, note the microscopic setae responsible for the van der Waal's interactions with the substrate (modified from: Autumn and Gravish, 2008).

Biological constraints: Evolutionary history, development, life history and anatomy

> *"The consequences of miniaturization for organismal biology are ubiquitous and profound; virtually every attribute, from physiology, to behaviour, to ecology, may be affected."*
>
> (Hanken and Wake, 1993)

Although, in all the examples discussed in this section, the laws of physics impose limits on biological designs, the evolutionary history, ancestral bauplan and even the basic mechanisms of development and evolution can also constrain miniaturisation. In this section some of these considerations are explored. Throughout this discussion, a somewhat artificial divide has been drawn between the physical and biological constraints for ease of discussion. However, in reality, these two factors interact with one another and in complex systems it can be difficult to separate the two.

Genome and cell size

We began this chapter by describing cells as the basic building block of eukaryotes, but although the basic components of a cell are the same across eukaryotes, there are some important differences. Critically, the amount of DNA in eukaryote cells can vary dramatically from one species to the next (reviewed in: Gregory, 2005b). This is of interest to the study of body size because genome size is correlated with cell size in a variety of animals (e.g. eukaryotes: Cavalier-Smith, 1978; birds: Gregory, 2002; frogs: Olmo and Morescalchi, 1978; salamanders: Olmo and Morescalchi, 1975; fish: Pedersen, 1971; vertebrates: Szarski, 1976; rodents: Walker et al., 1991). As discussed, changing the size of the building blocks can affect the structure as a whole.

Cell size is almost always positively correlated with genome size (Gregory et al., 2000) (**Figure 1.4a** and **b**). The quantity of non-coding DNA appears to be the main factor driving variations in genome size among taxa. Extensive comparative studies support this theory; unfortunately, the underlying mechanisms that drive this relationship are beyond the scope of this chapter (reviewed in: Gregory, 2005a). Changes in genome size also affect rates of cell division, and depending on the biology of the organism, these two traits together with cell size can have a number of interesting

consequences on the organism. These include, changes to the metabolic rate, overall body size, organ complexity and developmental rate (Gregory, 2005b). Whether these effects manifest themselves, and to what extent, is highly dependent on the particular biology of the organism and a host of complex interactions.

A negative correlation between DNA content and cell size, and metabolism, was identified early on in vertebrate red blood cells. Vertebrates rely on erythrocytes for oxygen transport, and the greater the surface area to volume ratio of the cell, the greater the efficiency of the gas exchange and as a result animals with smaller genomes can maintain faster metabolisms (Szarski, 1983). This trend holds true across all vertebrate clades (reviewed in: Gregory, 2005a). Birds are renowned for their fast metabolism (a consequence of the high energetic costs of active flight) and do indeed have small genomes with little non-coding DNA (Kozłowski et al., 2003). Many mammals, especially rodents, match the metabolic rates observed in birds whilst having larger genomes (see **Figure 1.4c**). However, mammals are unusual in having enucleated erythrocytes (Cavalier-Smith, 1978; Gregory, 2000). This allows for a greater miniaturisation of the red blood cells relative to the size of the animal, which improves gas exchange, irrespective of whether that animal is small or large.

Examples of cell enucleation as a space saving adaptation have been recorded in miniaturising lineages. One example of this is another, independent, occurrence of enucleated erythrocytes in some salamanders with small body-size and large genomes (Mueller, 2000). In this case the decrease in erythrocyte size is thought to aid in the circulation of ancestrally inherited large cells in small blood vessels produced by an evolutionarily recent decrease in size, rather than aiding in the increase of metabolism. Cell enucleation has also been observed in one of the smallest recorded insects, the minute fairy wasp *Megaphragma mymaripenne*. Here, the size of the nervous system is reduced in the adult by the enucleation of a large proportion of the neurons in the last stages of pupation (Polilov, 2012).

Miniaturisation can take place at different levels of complexity within an organism, within a single animal some structures may be more miniaturised than others. This can lead to interesting examples such as the one above, of a small circulatory system with large blood cells. The above examples help to illustrate how important the size of the basic building blocks (cells) can be to the overall function of the organism. An even clearer illustration of this concept can be found in the work

undertaken by Roth et al. on the amphibian genome, cell size and its impact on organ complexity (Roth et al., 1994; Roth et al., 1990; Roth et al., 1988). Amphibians are somewhat peculiar compared to other vertebrates in that metabolism does not constrain genome size and, perhaps as a consequence of this, a remarkable variability in genome size can be observed within low-level phylogenetic groupings. As a result, the authors were able to measure brain structure complexity in a number of species with varying genome, cell and body size. Like in all vertebrate clades genome and cell size were positively correlated so that large genomes led to large cells. However, the body size of different species was not correlated to the size of the cells. As a result species of similar body size may have drastically different cell sizes. Because brain size is constrained by the size of the skull this resulted in a remarkable variation in brain structure complexity. Species with large cells could not physically accommodate as many cells within the skull resulting in a simplification of brain structure. Interestingly, this leads to a peculiar situation in which body size is not necessarily predictive of organ complexity, large species with large cells may have greater size constraints than smaller bodied species with small cells. This effectively results in a sort of cryptic miniaturisation.

The rate of cell division is constrained by genome size, because the time it takes to copy DNA scales with the number of base pairs (Gregory, 2005b). This is important for development generally, but it is especially crucial for holometabolous insects, which undergo complete metamorphosis such as ants and wasps. This is because metamorphosis, the transformation from the larval to the adult form, requires rapid cell division and differentiation. Although the exact mechanistic reasons are not well understood, Gregory (2005b) suggests that this fast development imposes a limit of about 2pg in genome size for holometabolous insects, since the vast majority of species fall below this threshold (see **Figure** 1.**4d**). This seemingly obligate reduction in genome size will, of course, have knock on effects. A reduced genome size may, for example, facilitate a high level of organ complexity in adult holometabolous insects compared to their hemimetabolous counterparts. Cells with smaller genomes tend to be smaller in size and permit a higher number of cells (higher complexity) in a given organ.

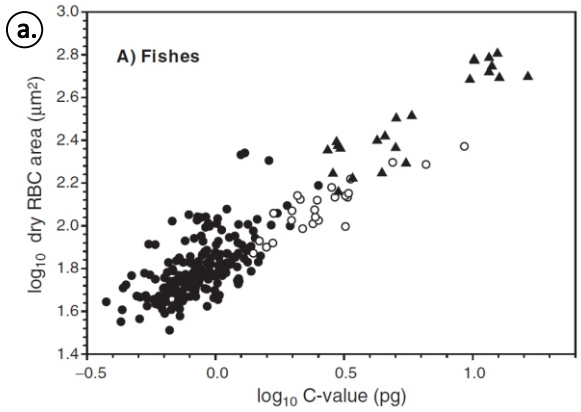
a.
A) Fishes
log10 dry RBC area (µm²)
log10 C-value (pg)

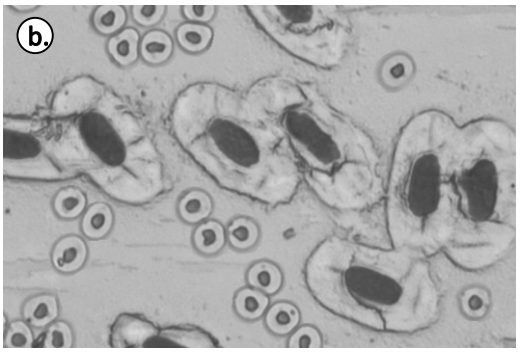
b.

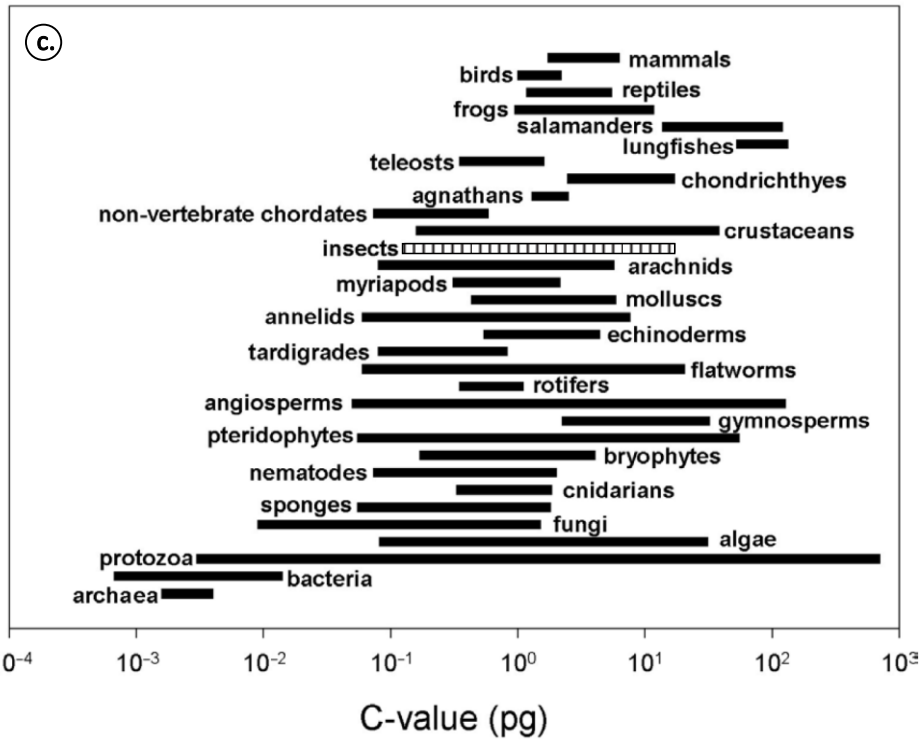
c.
mammals
birds
reptiles
frogs
salamanders
lungfishes
teleosts
chondrichthyes
agnathans
non-vertebrate chordates
crustaceans
insects
arachnids
myriapods
molluscs
annelids
echinoderms
tardigrades
flatworms
rotifers
angiosperms
gymnosperms
pteridophytes
bryophytes
nematodes
cnidarians
sponges
fungi
algae
protozoa
bacteria
archaea
C-value (pg)

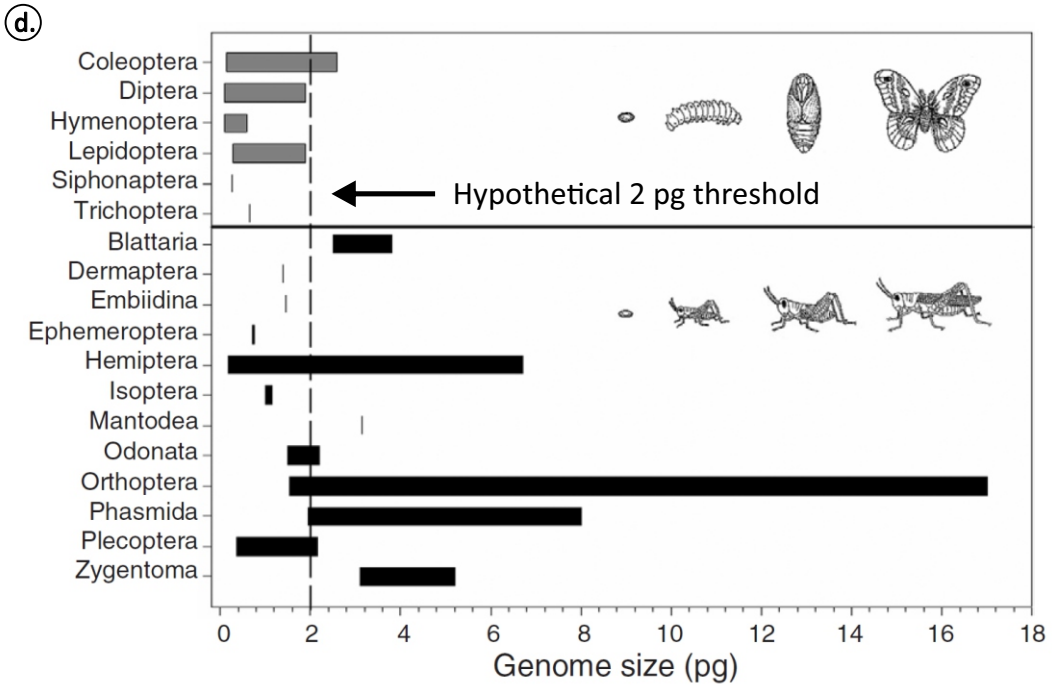
d.
Coleoptera
Diptera
Hymenoptera
Lepidoptera
Siphonaptera
Trichoptera
Hypothetical 2 pg threshold
Blattaria
Dermaptera
Embiidina
Ephemeroptera
Hemiptera
Isoptera
Mantodea
Odonata
Orthoptera
Phasmida
Plecoptera
Zygentoma
Genome size (pg)

Figure 1.4. Genome size examples, panels a-d modified from: Gregory (2005b). (a) Positive correlation between genome size (measured as DNA mass in haploid genome i.e. C-value pg) and red blood cell (RBC) area. (b) Light micrograph comparing erythrocyte size in two species of fish with differing genome size; small cells correspond to the Siamese fighting fish (*Betta splendens*) with a genome size 2C = 1.3pg, while the large cells correspond to the Australian lungfish (*Neoceratodus forsteri*) with a genome size 2C ≈ 105 pg. Note that the nucleus of the lungfish could not physically fit inside the cells of the fighting fish. (c) Genome size (C-value) of eukaryote clades (insects highlighted in black and white stripes). (d) Genome size across insect orders, the hypothesised genome size threshold of 2pg for holometabolous insects holds well across clades, with the exception of two beetle species.

The characteristic life history of holometabolous insects appears to make them especially well suited to miniaturisation. Indeed the smallest insects are holometabolous (Polilov, 2016). Besides a reduction in genome size, holometabolism may facilitate the evolution of small body size by de-coupling the adult and juvenile life-histories. Holometabolous larvae are greatly simplified, in terms of behaviour, ecology and physiological needs, relative to their adult forms. Larvae lack reproductive organs and a flight apparatus as reproduction and dispersal is often restricted to the adult phase. They often have simplified sensory organs and simplified walking limbs. Eggs are usually laid directly on the larval food source so that the newly hatched larvae need not search for suitable resources. These kinds of organismal simplifications should lead to a decrease in the number of tissues required in the larvae. As a consequence holometabous insects may require a more modest allocation of cellular starting material to develop into a larva compared to hemimetabolous larvae, which are not as simplified relative to the adult form (see **Development** section below). This, in turn, may mean that the holometabolous egg can be smaller, an important consideration which will be discussed in detail in the next section. Interestingly, the de-coupling of adult and juvenile life histories has additionally been identified as one of the key innovations leading to the radiation of insects (Rainford et al., 2014).

While I have, so far, omitted discussion of plant miniaturisation for simplicity's sake, it is worth pointing out that many (but not all) of the issues facing animals affect plants as well. Indeed, what we learn from plants can be applied to animals. For example, genome and cell size have been linked to growth patterns in plants. Where conditions are only sporadically favourable for growth plants may delay cell proliferation by

attaining a minimum size using fewer larger cells (with large genomes). This is thought to be metabolically more economical, as more cells require a greater quantity of lipids for cell membranes (Grime and Mowforth, 1982). For a comprehensive review on cell and genome size in plants refer to (Gregory, 2005a).

The effect of genome size on whole organism biology is a developing field, and so while I've outlined some general trends above, there is much left to learn. It is important to remember that these effects will be complex since many different aspects of an organism's biology will interact with genome size in different ways. For instance, while miniaturising lineages might benefit from small genomes and cells, ancestral genome size may lead to unusual combinations of large cells and small structures as discussed in the amphibian examples above. Ongoing advances in genomics and technology will, hopefully, make progress in the area progressively cheaper and more accessible.

Development

An interesting challenge faced by very small animals is that of reproduction since offspring must be, at least initially, smaller than their parents. Even in animals that produce large and well developed offspring such as mammals, offspring are always significantly smaller than the parent. When the adult form of an animal is already "toeing the line" of minimum body-size, what does this mean for the even smaller offspring?

Immature forms of most animals have the advantage of not needing to perform the full gamut of functions of their adult counterparts, and so can be simpler than their adult counterparts. Immature forms generally do not need to accommodate a fully developed reproductive system, they often do not have to search for food (due to parental provisioning) and generally are behaviourally limited relative to adults. This implies spatial and energy savings in reproductive organs, sensory systems, neural processing centres, and locomotory aparatus.

However, offspring (we shall restrict ourselves to discussing multicellular animals) need to be large enough to be able to develop all the basic tissues that make up the body. For this to occur, there needs to be enough cellular material since tissue differentiation requires a minimum anlage size (the primordium from which embryo tissues develop). In some animals a reduction in anlage size has been shown to lead to a reduction in the number of body parts that develop (Minelli, 2003). A substantial reduction in embryo body size can also disrupt the signalling systems that mediate

development. For instance, the arrangement of setae on the dorsal surface of beetle larvae is highly regular but in the minute scydmaenid beetle larvae (*Cephennium* and relatives) this arrangement is disrupted and setae are present in a seemingly random arrangement and in great numbers across the body surface. This is thought to be the result of a breakdown in the patterns of hormonal diffusion and signalling gradients that generate structure in an embryo during development (Minelli, 2003). This disruption is thought to be caused by the beetle's minute size relative to other species in its clade and the constrained volumes in which signalling gradients are forced to operate in.

Egg size hypothesis

The ability to reproduce is an intrinsic characteristic of all living things. However, for some organisms reproduction represents a larger relative investment than for others. For very small organisms the production of viable offspring seems to be one of the main factors limiting miniaturisation (Grebennikov, 2008; Polilov, 2016; Rensch, 1948).

The reason that offspring size is limiting is that, as discussed, tissues require a minimum size to develop correctly. This places a lower a limit on the size of the embryo, which, in an organism that is already approaching that limit, will lead to disproportionately large offspring. Such a pattern is evident in a number of lineages (see **Figure 1.5**), where only one or two offspring may be produced at a time and the embryo or egg takes up a large proportion of the body-cavity in the adult (for a more thorough discussion of the egg-size hypothesis in invertebrates see: Grebennikov, 2008; Polilov, 2016). The energetic investment required to produce such large offspring must also be huge, particularly in the face of a limited ability to store energy (normally in the form of fat bodies) in a body of extremely small volume.

The costs associated with disproportionately large offspring seem to have led miniaturising lineages to adopt alternative strategies to either: minimise the cost of reproduction or ensure maximum returns on investment. For instance, egg-size is not only dictated by the required embryo size but also by the provisions that the embryo relies on for development. Laying eggs directly into a food source can reduce the metabolic cost of producing eggs and minimise egg size. This is exactly what the smallest known insects, the minute parasitic wasps in Myrmaridae and Trichogrammatidae, do. In fact many hymenoptera either lay their eggs into other insects or provision brood chambers with insect

prey. These examples represent simple ways of reducing the cost of offspring production. Maximising returns on investment on the other hand is a more complex consideration which includes the number of offspring produced and their survival.

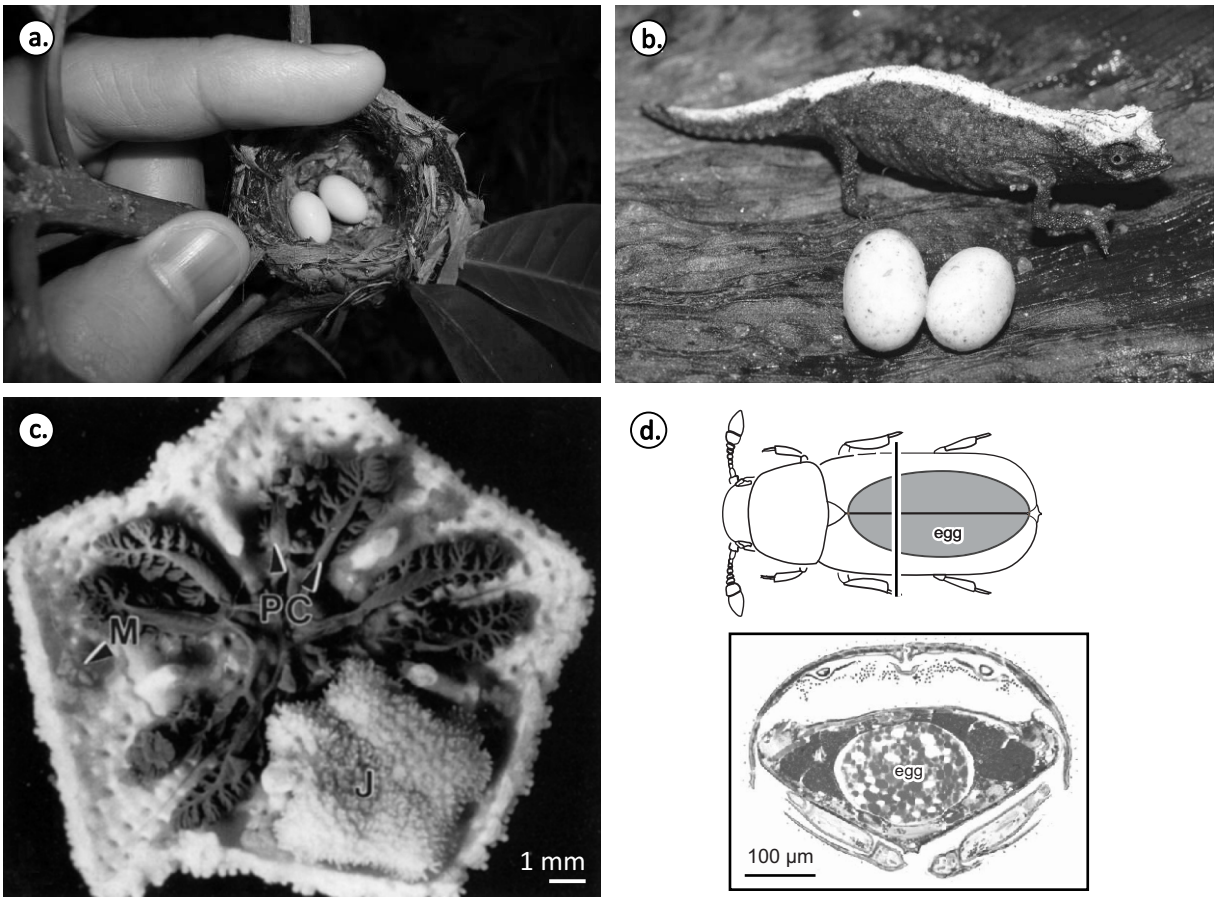

Figure 1.5. Examples of species with proportionally large offspring. (a) *Mellisuga helenae* nest displaying a small clutch of two eggs (source: Wikimedia Commons); (b) *Brookesia desperata* with clutch of two eggs next to the adult female, modified from Glaw et al. (2012); (c) *Patiriella vivipara* starfish adult dissected to show internal development of juvenile (30% of adult diameter), modified from Byrne (1996)(J=juvenile, M=male gonad, PC=pyloric caeca); (d) *Porophilla mystacea* beetle cartoon illustrating the relative size of the egg (Coleoptera: Ptiliidae), modified from Polilov(2015).

Despite the disproportionately large size of miniature offspring, their absolute size is still extremely small, as such they are likely to have a decreased chance of survival (e.g. Karban, 1986). This coupled with the decrease in adult fertility (i.e. only a limited number of offspring can be produced per reproductive cycle) may drive some miniaturising lineages to adopt extreme reproductive strategies and behavioural adaptations to ensure offspring survival. The reproductive strategies of the sea star *Patiriella* (Byrne, 1996; Roediger, 2011) and the frog *Paedophyne amanuensis* (Rittmeyer et al., 2012) are two excellent examples of this.

In the sea star *Patiriella,* the adult foregoes broadcast spawning (as is most common in Echinoderms) to instead, develop multiple offspring internally in a staggered manner. Once the more mature offspring develop mouthparts they undergo a period of secondary growth by feeding on their younger siblings. Finally, the adult gives birth to a live young through an unusual modified pore on the dorsum. Presumably this extremely unusual strategy permits this species to switch from the r strategy (broadcast spawning) predominant in echinoderms to a K strategy (large investment into few offspring). The energetically limited, minute adult seems to maximise fitness by producing very few fairly mature offspring rather than producing enormous numbers of vulnerable gametes.

Similarly, the frog *Paedophyne amanuensis* provides unusual levels of parental care to improve offspring survival. In this case a single egg is laid at a time in a froth nest, instead of under water, which protects the offspring from predation. The parent guards the nest and the embryo develops into a small, but fully formed adult within the egg without going through a tadpole stage (Rittmeyer et al., 2012). Direct development allows offspring to skip the highly competitive aquatic life stage where mortality is greatest. Differing levels of parental investment can be observed in many amphibians, in fact all three of these reproductive features are seen in other relatives of this species but the presence of all three strategies in a single species is somewhat unique. There are many other examples of K strategists in the amphibians. This type of strategy is not restricted to species with unusually small body size (e.g. Wake, 1978). However, this rich ancestral adaptive zone may be a contributing factor towards the apparent success of frogs at miniaturising by permitting a large range of behaviours (Almeida-Santos et al., 2011; Estrada and Hedges, 1996; Rittmeyer et al., 2012).

A compelling piece of evidence to support the theory that offspring size can strongly constrain adult body size comes from fact that in miniaturised species males tend to be smaller than females. Grebennikov (2008) makes

the argument that this disparity is due to the differences in space and energy allocations associated with the female reproductive system. He cites the many fairy wasp species, which have evolved to have smaller males than females.

Anatomical simplification/oligomerisation/condensation

A feature thought to be associated with miniaturisation is the simplification of anatomical structures. This has been a popular area of study as it is relatively simple to quantify. Simplification may take the form of a reduction or absence of certain structures. There are multiple evolutionary and developmental avenues that may lead to these kinds of phenotypes. However, the mechanisms mediating these simplifications are not always well understood. Anatomical simplifications may be the result of truncated development (e.g. heterogeneously truncated phases of development) or may arise due to a disruption of signalling systems during development (e.g. Hanken and Wake, 1993; Minelli, 2003).

Unfortunately, examples of these kinds of traits can sometimes be difficult to locate in the literature and interpret. For example, the term "oligomerisation" is used in the miniaturisation literature (e.g. Minelli, 2003; Polilov, 2016) to refer to a reduction in the number of true body segments (the developmental units in arthropods, chordates and annelids). It is also used, by extension, to refer to other forms of anatomical simplifications that lead to a reduction in the number of distinguishable anatomical units. The use of this term may be somewhat problematic for two reasons. Firstly, it is not clear whether it should refer strictly to a reduction of true body segments or if it can refer to any reduction in anatomical units. Secondly, it seems to be a loanword from chemistry where its meaning is at odds with its use in miniaturisation. An oligomer is a molecule composed of very few repeating units (a monomer, or in a biological analogy body segments) whereas a polymer is made up of very many repeating units, so far so good. However, the word "oligomerisation" refers to the process of monomers coming together into a short chain, an oligomer, and not to the reduction of a polymer into an oligomer. Semantics aside, there is something to be said for having a specific term for this kind of structural simplification. The multidisciplinary nature of the study of miniaturisation poses a problem for collecting all the puzzle pieces; appropriate terminology can help or hamper the articulation between different fields.

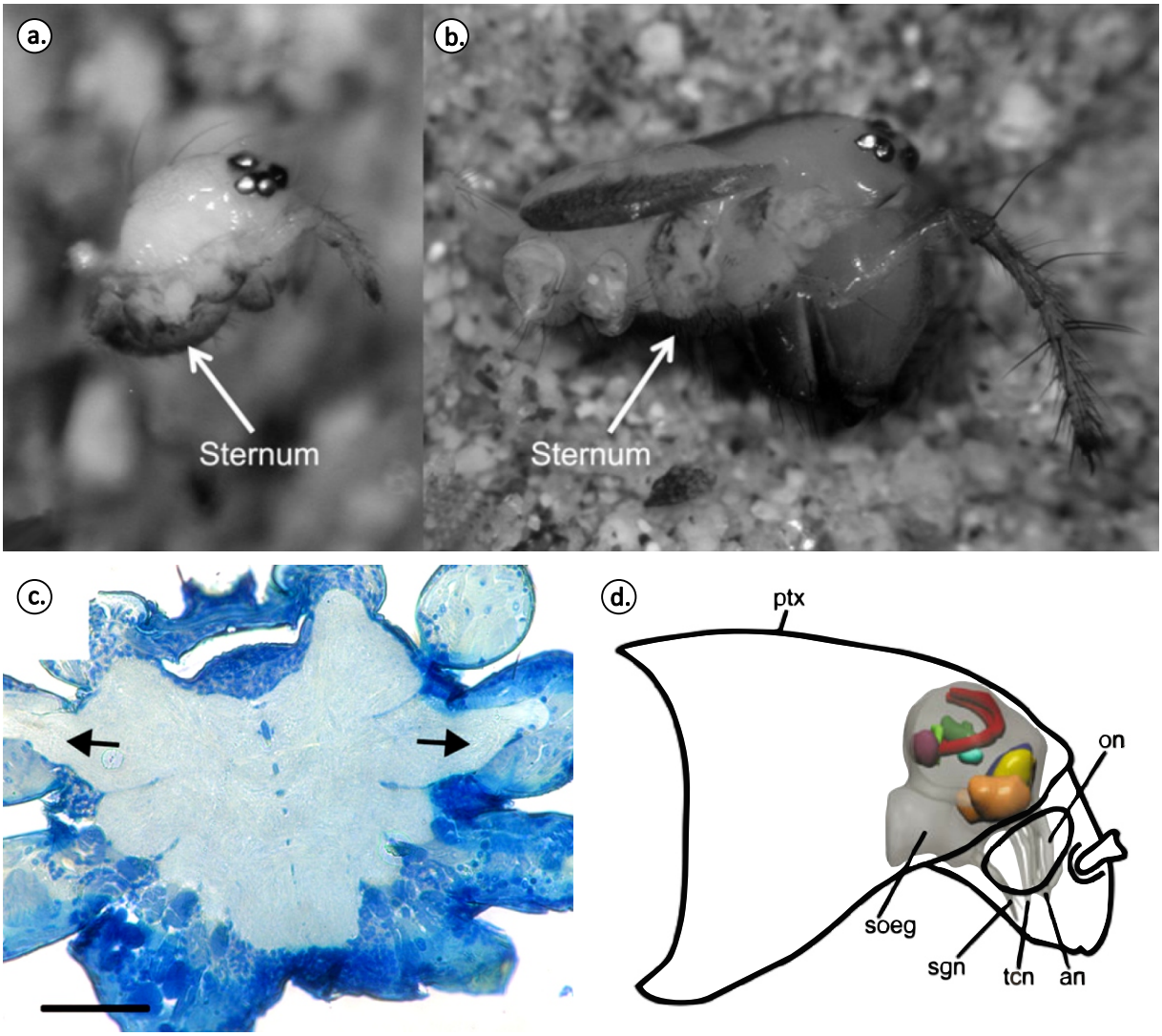

Figure 1.6. Brain and nervous tissue expanding beyond normal limits in very small invertebrates. (a,b) spider nymphs have a distended sternum (a) compared to the adult (b) to accommodate the relatively large brain (Eberhard and Wcislo, 2011). (c) in some spiders the brain extends beyond the cephalothorax and into the coxae (leg segments) (Quesada et al., 2011). (d) The brain of the beetle Corylophidae is shifted into the prothorax (ptx), other labelled features include the optic nerves (on), antennal nerve (an), paired nerves of the tritocerebrum (tcn), nerves of the suboesophageal ganglion (sgn), suboesophageal ganglion (soeg) (p.150 Polilov, 2016). (e) The brain of Strepsiptera extends past the head (red line) and into thoracic segments 1 and 2 (Beutel et al., 2005). Labelled structures: medulla (me), lamina (lg), lobula (lo), oesophagus (oes), circumoesophageal connective (coec), suboesophageal complex (soes), prothoracic ganglion (g1), base of the hind wing (wb).

Common examples of miniaturisation related structural simplifications are reductions of skeletal elements, asymmetry in paired organs and a reduction in the number of cell nuclei in particular tissues. Reduced skeletal structures have been recorded in some miniaturised frogs, such as reduced skull elements, fewer digits and reduction of vomerine teeth (Almeida-Santos et al., 2011; Estrada and Hedges, 1996). While some arthropods show cuticular skeletal simplification in the form of a reduction in the number of segments, or in some examples, segmentation may become indistinct and articulations incomplete (e.g. Minelli, 2003; Polilov, 2017; Polilov and Beutel, 2009, 2010; Polilov and Shmakov, 2016). The very smallest invertebrates can display various reductions of the reproductive system, from asymmetric or unpaired gonads, to extremely low numbers of ovarioles (Polilov, 2016). There are also reports of "oligomerisation and condensation" of nervous ganglia (Heath and Evans, 1990). In the wasp genus *Megaphragma,* the number of cell bodies in the central nervous system of the adult is greatly reduced (Polilov, 2012) while some salamanders have evolved enucleated erythrocytes (see "Genome and cell size"). Although these examples may seem roughly equivalent, all of these reductions involve complex traits with likely disparate underlying causes, developmental and evolutionary mechanisms.

The loss of regularity, for example in the distribution of repeating structures, is associated with simplification as a characteristic of miniaturisation. As discussed above, loss of regularity is thought to reflect a disruption of the embryological signalling systems that regulate development (Minelli, 2003). However, many extremely small organisms retain exquisitely complex structures (fairy wasps: Fischer et al., 2011; beetles: Grebennikov and Beutel, 2002; loriciferans: Kristensen, 1991; mites, p. 99: Minelli, 2003). For example, mites and spiders of similar size, have differing regularity in their pit sensors. Small spiders show a disrupted distribution of pit sensors, while those of mites are perfectly regular (Minelli, 2003). Given that mites are often much smaller than the smallest spiders this seems to suggest that maybe loss of regularity is not a necessary feature of miniaturisation. Furthermore, thorough studies on the smallest insects have found it difficult to make a clear case for overall simplification of structures (Beutel and Haas, 1998; Polilov, 2016). Simplifications and loss of regularity are not always present and even when present seem to affect select anatomical features.

Given these contradictory examples, it seems reasonable to conclude that these kinds of features (simplification and loss of regularity) may not be an intrinsic feature of miniaturisation. Minelli (2003) suggests that these features may instead be diagnostic of the recent miniaturisation of a

lineage and a consequence of a lack of an accompanying reduction in cell size. This may, in turn, be the result of a large genome that has not undergone a reduction in non-coding DNA relative to the ancestral state (see **Genome and cell size** section above). As such, we may expect species that have recently undergone a rapid and significant reduction in body size to exhibit some loss of regularity and simplification of structures, whereas species with a long evolutionary history of miniaturisation would not be expected to show these features.

Central and peripheral nervous systems

Throughout this introductory chapter the complex and diverse effects of miniaturisation have been highlighted. It should be clear now that certain biological systems are more dramatically affected by miniaturisation than others. Second only to the reproductive system, the effects of miniaturisation are probably most wide-ranging and dramatic in the nervous system. The central and peripheral nervous systems are responsible for transducing relevant sensory cues that inform an animal on the external and internal environments, processing inputs, and generating behaviours. As a consequence of this the study of nervous systems is of interest to a wide variety of audiences from anatomists, physiologists and ecologists to roboticists and systems engineers.

A particularly interesting aspect of miniaturisation is balancing the costs of sensory structures against the benefits that they provide. The neural tissues that make up both the peripheral sensory structures and the peripheral and central processing units are known to be metabolically costly tissues (Attwell and Laughlin, 2001; Niven et al., 2007; Niven and Laughlin, 2008; Safi et al., 2005). Niven and Laughlin (2008) present two stunning examples from the vertebrate and invertebrate world to illustrate this point. In humans the brain represents 2% of the body mass but utilises about 20% of the basal metabolic rate. Similarly, in the blowfly *Calliphora vicina* the retina alone consumes approximately 8% of the resting metabolic rate (Niven and Laughlin, 2008). The argument is then made that this huge energy investment places strong evolutionary pressure to optimise the trade-off between the level of investment and the fitness returns obtained from sensory systems (Niven, 2005; Niven and Laughlin, 2008; Safi et al., 2005). Energy that is allocated to sensory systems cannot be invested into other aspects of an animal's biology that may be more directly linked with fitness such as reproduction. Therefore, the returns from investment in neural tissue must contribute significantly to fitness in order for the investment to be adaptive.

Small animals are under additional pressure to optimise their returns on neural tissues and sensory structures because these metabolically expensive structures typically increase in relative size with decreasing body size (e.g. Beutel and Haas, 1998; Eberhard and Wcislo, 2011; Grebennikov and Beutel, 2002; Quesada et al., 2011; Rensch, 1959, pp. 142-143; Seid et al., 2011). This is known as Haller's rule and has been recorded across vertebrates and invertebrates alike (reviewed in: Eberhard and Wcislo, 2011) although the underlying causes are debated. Eberhard and Wcislo (2011) discuss three factors of interest in the modern literature: the size of the neuron nucleus, the axon thickness, and the number of neurons. The size of the neuron cell body is primarily limited by the size of the nucleus, which is in turn tied to the genome size (reviewed in: Gregory, 2005a). Axon diameter is closely tied to conductance speeds with diminishing diameters leading to slower conductance (e.g. Waxman, 1980). An absolute lower limit to axon diameter is additionally imposed by noise generated by the stochastic opening of sodium channels on the axon membrane (Faisal et al., 2005; but see: Hustert, 2012; Perge et al. 2012). Lastly, although there is little information on how the number of neurons in the central nervous system changes in miniaturising lineages, in the periphery, sensory systems have fewer sensory units. There is evidence that smaller insects have fewer sensory units in their eyes and antennae (Chapman, 1982; Jander and Jander, 2002; Kelber, 2009; Ramirez-Esquivel, 2012; Rutowski, 2000; Spaethe et al., 2007; Spaethe and Chittka, 2003; Streinzer et al., 2013; Wcislo, 1995). However, the number of cells per sensory unit may have a lower limit. Studies on the sensory systems of extremely small insects indicate that major design modifications are not common (Fischer et al., 2012; Makarova et al., 2015; van der Woude and Smid, 2015). Instead small species retain all the cell types found in larger species arranged in a more compact fashion and reduce the number of sensory units. Miniaturisation seems to be limited by the minimum cell size that permits adequate function of the sensory unit. Whether an analogous principle is true of brain organisation is not clear.

Whatever the underlying causes may be, small animals have proportionally large brains that they need to accommodate in their small bodies. To handle this problem extremely small insects often undergo a change in body proportions, or an extension of their central nervous system into adjacent body segments (see **Figure 1.6**). For instance Beutel and Haas (1998) note a disproportionally large head and brain on the miniature larvae of the beetle *Hydroscapha natans*. To accommodate the disproportionately large nervous system, the packing or organisation of organs may differ between the miniaturised and the ancestral states. Some

studies have observed organs that are more densely packed (Beutel and Haas, 1998); brain tissues that take up a much larger proportion of the head capsule (Grebennikov and Beutel, 2002); or even brain tissues that extend past the head capsule into later thoracic segments in insects, or into the coxae in spiders (Beutel and Haas, 1998; Beutel and Hörnschemeyer, 2002; Grebennikov and Beutel, 2002; Quesada et al., 2011). The fact that the body cavity can be so dramatically rearranged to accommodate the expanding nervous system tells us that there are strict limits to the miniaturisation of neural structures.

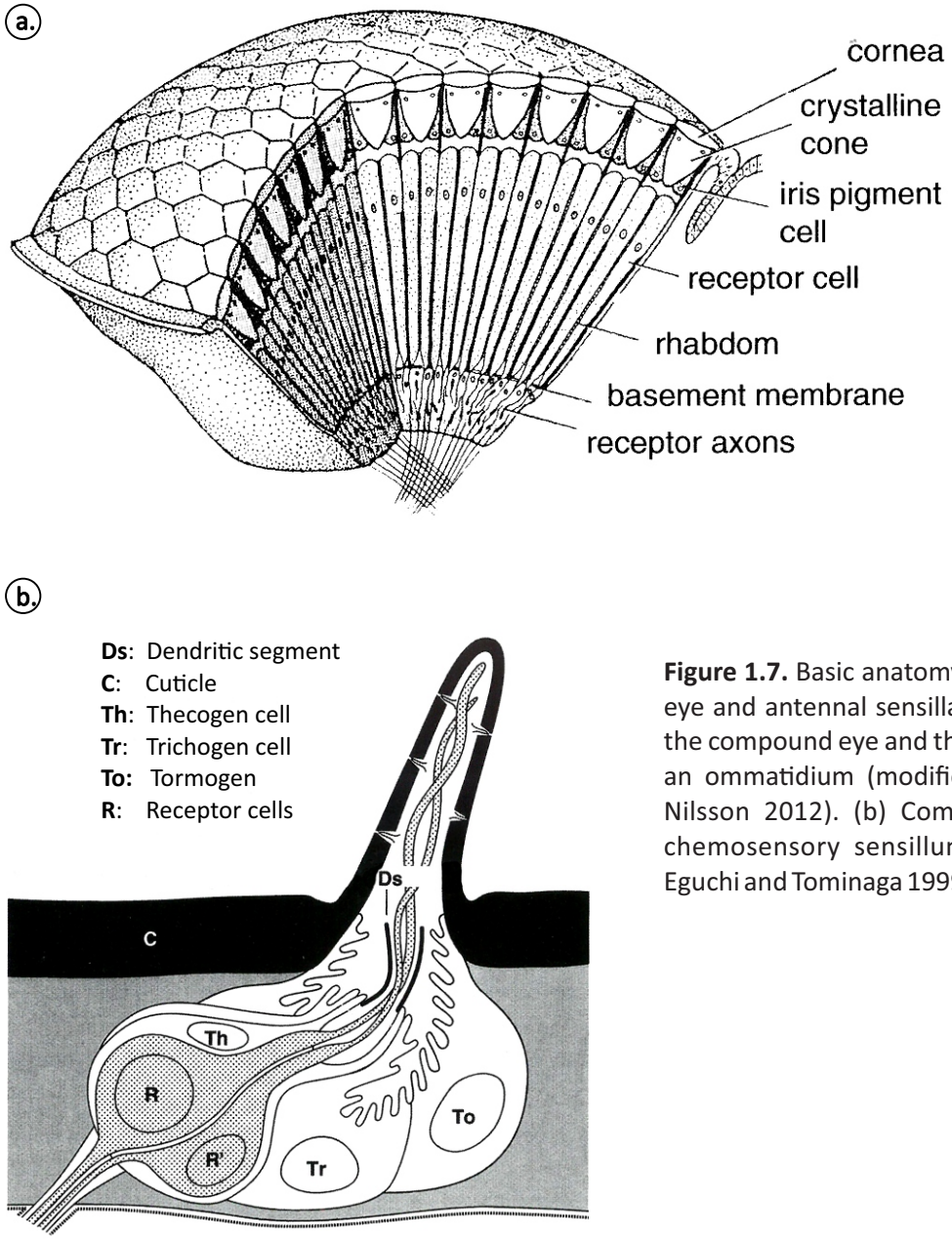

Figure 1.7. Basic anatomy of the compound eye and antennal sensilla. (a) Illustration of the compound eye and the basic anatomy of an ommatidium (modified from Land and Nilsson 2012). (b) Component cells of a chemosensory sensillum (modified from Eguchi and Tominaga 1999).

1.1.4. Focus of the Thesis: Miniaturisation of sensory systems

Sensory systems, although part of the nervous system, are shaped not only by biological constraints but also by the physical characteristics of their target signals. Because our understanding of the way light travels through space or the way chemicals diffuse through a medium are rather better than our understanding of nervous systems, it is easier to intuit design limitations in sensory systems than in brains. After all an eye that can't see or an antenna that can't smell is of no use.

Sensory systems are concerned with the transduction of physical signals such as light and odour molecules into neural signals, but can a sensor be too small to process these signals? Insect sensors such as compound eyes and sensilla occur in arrays made up of repeating units. Our current knowledge of sensory arrays indicates that individual sensory units have lower size limits. Beyond these limits, decreases in body size lead to a decrease in the number (rather than the size) of the units.

This is particularly well studied in the vision literature. In the Hymenoptera, as in other insects, the compound eye consists of repeating units called ommatidia each with their own lens and photoreceptor (see **Figure 1.7a**). Here we know that sensitivity (the eye's ability to capture light) imposes a hard lower limit to the size of ommatidia in compound eyes. An eye that cannot capture light cannot see. How large an eye needs to be can be determined by using the sensitivity equation (Warrant and Nilsson, 1998):

$$S = \left(\frac{\pi}{4}\right)^2 A^2 \left(\frac{d}{f}\right)^2 \left(\frac{kl}{2.3 + kl}\right)$$

Where A is the aperture diameter (in this case the lens diameter), d is the receptor diameter, f is the focal length, k is the photoreceptor absorption coefficient, and l is the receptor length. From this equation we can see that sensitivity is predominantly determined by the size of the lens and the rhabdom. Lenses must allow enough light into the eye and rhabdoms must be large enough to house sufficient photopigment to signal reliably (otherwise receptor noise will interfere). In addition we know that the minimum size of a lens is limited by diffraction (Land, 1981). These factors place quantitative limits on the minimum size of an eye which have been studied in apposition and superposition eyes (e.g. Meyer-Rochow and Gál, 2004; Warrant and McIntyre, 1993). The smallest recorded lens diameter in Hymenoptera is 5.90μm in the male of the minute fairy wasp

Trichogramma evanescens, which does not disperse, has limited visual requirements and is restricted to operate in bright conditions (Fischer et al., 2011).

Apart from size, the ecological niche of an animal determines its sensory requirements and therefore shapes its sensors; insect sensory systems are perhaps most often studied in this context. In vision there is an important trade-off between sensitivity and resolution (how coarse or fine grained visual information is), for a given eye size in order to increase one the other must decrease. Ecological adaptations mediate the balance between these two factors by determining what information is most important to an animal. For example, in night active species, attaining adequate sensitivity in the dim environment will be the priority, whereas fast moving species that inhabit brightly lit conditions may prioritise resolution. These trade-offs have been well documented in insects and in particular hymenoptera (e.g. Greiner et al., 2007; Greiner et al., 2004; Kirschfeld and Wenk, 1976; Narendra et al., 2016; Narendra et al., 2011; Streinzer et al., 2013; Streinzer et al., 2016; Yilmaz et al., 2014). The interaction between these opposing parameters can even be observed in comparative studies of related species with different activity schedules (Greiner et al., 2007; Narendra et al., 2011), in comparisons between flying and walking forms within a single species (Narendra et al., 2016), and even within a single eye with specialised ventral and dorsal visual fields (e.g. Zeil, 1983) (see **Figure 1.8**). Animals that require high resolution vision are often restricted to high light intensities while night active animals often have relatively poor resolution.

In the case of miniature species sensitivity is expected to be prioritised over resolution leading to a decrease in the number of ommatidia in small species (Fischer et al., 2011). A resolution limited eye can still effectively be used for certain purposes such as phototaxis and orientation but lenses below 10μm incur huge losses in sensitivity which eventually lead to a loss of eye function (Fischer et al., 2011; Land and Nilsson, 2012). In other words, the number of units in a compound eye can be reduced down to 1 and still there will be some visual function, while reducing ommatidium size past a certain threshold (dependent on the wavelength of light and the brightness of the environment) will lead to a total loss of visual function regardless of how many ommatidia are retained.

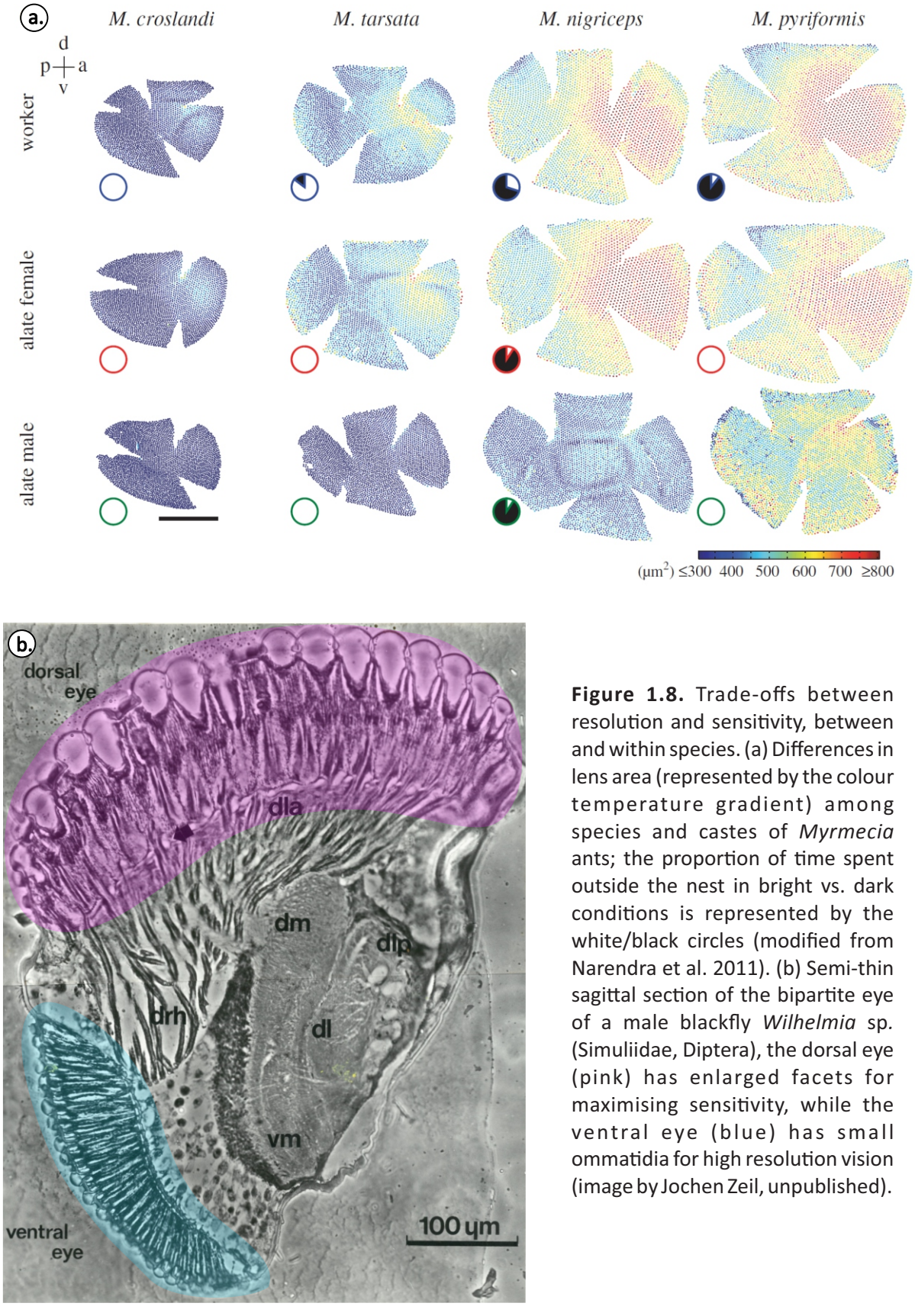

Figure 1.8. Trade-offs between resolution and sensitivity, between and within species. (a) Differences in lens area (represented by the colour temperature gradient) among species and castes of *Myrmecia* ants; the proportion of time spent outside the nest in bright vs. dark conditions is represented by the white/black circles (modified from Narendra et al. 2011). (b) Semi-thin sagittal section of the bipartite eye of a male blackfly *Wilhelmia* sp. (Simuliidae, Diptera), the dorsal eye (pink) has enlarged facets for maximising sensitivity, while the ventral eye (blue) has small ommatidia for high resolution vision (image by Jochen Zeil, unpublished).

Although chemosensilla are not as well understood, it might be reasonable to expect some similar trends. While there are no established theoretical limits to the size of a chemosensillum, it is logical to suggest that there must be a lower physical limit to these sensory units as well. At the very least, the number and size of the cells that make up a sensillum should limit miniaturisation in a similar way to what is observed in the central nervous system (see discussion above). Metabolic costs will also apply and the physical properties of odour cues will shape the limits of sensor design.

Chemosensilla are composed of a number of cells including the sensory neurons and accessory cells (see **Figure 1.7b**). The sensory neuron projects dendritic endings into the lumen of the sensillum peg (the external cuticular component) where it detects odour molecules that enter through perforations in the cuticle surface (Ryan, 2002). The accessory cells perform important functions such as secreting the sensillum lymph that surrounds the dendritic endings in the sensillum lumen, which prevents desiccation and removes old odorant molecules. The number of cells underlying a sensillum varies among species (e.g. Esslen and Kaissling, 1976; Kelber et al., 2006; Lee and Strausfeld, 1990; Ruschioni et al., 2012; Venkatesh and Singh, 1984).

Although in chemosensilla there is not an exact analogue of the resolution vs. sensitivity trade-off of compound eyes, there are some similarly competing parameters. Sensitivity, as a measure of sensory competence, may be somewhat comparable in vision and in chemosensation. In both cases it refers to the probability that a particle will be detected (either photons or odorant molecules). A handful of studies have associated an increase in sensilla numbers with increased sensitivity (Chapman, 1982; Gill et al., 2013; Jayaweera and Barry, 2017; Spaethe et al., 2007). This implies that an increase in sensory area leads to an increase in sensitivity.

In simple systems it can be shown that sensitivity (the probability of detection) is dependent on the size of the receptor. The processes involved in bacterial chemotaxis are similar to the very fine scale interactions that take place in sensilla. At this scale odours disperse through diffusion and Brownian motion (Beebe et al., 2002) and the probability of capture can be modelled using the following equation (Berg and Purcell, 1977):

$$\frac{\delta c}{c} = \frac{1}{\sqrt{Drc_m t}}$$

Where D is the diffusion coefficient of a stimulus molecule, r is the receptor radius, c_m is the concentration of the stimulus molecule and t is the detection time. From this equation we can see that the size of the receptor is important. For a given odour concentration, diffusion medium and integration time the only way to improve sensitivity is to enlarge the receptor. This is similar to increasing receptor size in vision to improve photon capture. We might then expect that sensitivity to a given odour is tied to the area allocated to its reception.

Unfortunately, determining sensory competence is not a simple task in chemosensory arrays. One of the reasons for this is that while in vision there are a limited number of photopigments which absorb light across the spectrum in chemosensory systems there are scores or hundreds of molecular receptors that bind to different odour molecules (Vosshall et al., 1999). These receptors may have a very specific sensitivity to a particular molecule or may be more broadly tuned to respond to a class of compounds (Hallem and Carlson, 2006). Broadly tuned receptors may change the number of odorants that they are receptive to depending on the stimulus concentration (Hallem and Carlson, 2006). Additionally, a single sensory neuron may express more than one kind of chemoreceptor (Goldman et al., 2005). So while an increased sensory area achieved, for example through an increase in the number of sensilla, may lead to increased sensitivity to some odour cues it is unlikely that this increase will apply homogeneously throughout an animal's odour space (i.e. all the odour chemicals an animal is receptive to). However, it is likely that there is a trade-off in chemosensory arrays between increasing sensitivity to a target odour and the size of the odour space. Increasing the number of receptors allocated to detecting a given odour to increase sensitivity will preclude those receptors from being allocated to the detection of other odours.

What does this mean for miniaturising arrays of sensilla? Like in compound eyes we might expect there to be some variation in the size of sensilla with a lower limit past which sensor function is impaired. At this lower limit we might expect that there is not sufficient dendritic membrane interacting with the environment to signal reliably (like in any other neuron stochastic opening of sodium channels will create noise). In miniature ants we would expect that once this limit is reached the number of sensilla will diminish. However, in order to preserve sensitivity and/or odour space miniature ants may develop adaptations to maximise the number of sensilla. In compound eyes the cells of the ommatidium are very tightly packed in special arrangements not seen in larger species. Although this may not be visible in the external anatomy of the antenna the sensilla themselves may become denser on the antennal surface.

Ants, and arthropods in general, have been particularly successful at taking miniaturisation to extremes. The insect bauplan may provide a flexible starting point for the reduction of body size. The lack of a closed circulatory system and the passive (diffusion dependent) respiratory system are just two examples of functional aspects of insect biology which minimise structural clutter and may facilitate the reduction of body size. Conversely there is some evidence that these same factors may be at least partly responsible for limiting the maximum body size attainable by insects (see Harrison et al., 2010).

Ants present a number of useful traits for the study of miniaturisation. As a group the Formicidae cover a large range of body sizes (approximately 0.8mm to 30mm) and yet the vast majority of species in this family share a number of important characteristics. Ants are eusocial, this means that despite the diversity of habitats and ecological niches occupied by different species there are some important common needs such as the necessity of communication among nest mates and the ability to navigate to and from a central place (the nest). These commonalities impose certain minimum requirements on the sensory systems and the information that they should provide. This facilitates, to some extent, the comparison of sensory organs across species within Formicidae. In contrast, a higher taxonomic grouping such as Hymenoptera includes species with such divergent biologies (e.g. eusocial, solitary and parasitic species) that differentiating between life history and size effects on the sensory structures of these insects becomes much more difficult. Additionally, some species of ant exhibit marked polymorphism within a single colony (e.g. Myrmecia pyriformis), which permits us to examine size effects on the sensory systems of a single species.

This thesis will address the issue of miniaturisation of sensory systems in ants with a particular emphasis on antennal sensilla. The first two chapters set the scene by identifying the different types of antennal sensilla, developing methods, and quantifying variation within species. This is done through two case studies one in a large species, *Myrmecia pyriformis* and a small species *Temnothorax rugatulus*:

Chapter 2: Describing and identifying ant sensilla: "The antennal sensory array of the nocturnal bull ant *Myrmecia pyriformis*"

Chapter 3: Intraspecific variation in sensory systems: "The sensory arrays of the ant, *Temnothorax rugatulus*"

A large scale comparative chapter then explores the scaling of antennae and antennal sensilla across the Formicidae:

Chapter 4: Miniaturisation of the antennal array

Chapter 5: Describing body size variation in ants

Chapter 6: Thesis Conclusions: Concluding remarks on miniaturisation

An additional chapter present descriptions of methods used:

Chapter 7: Methods Appendix: Techniques for investigating the ant visual system anatomy

1.2. References

Alexander, R., 2012. How tall can a Lego tower get?, BBC News. BBC.

Almeida-Santos, M., Siqueira, C.C., Van Sluys, M., Rocha, C.F.D., 2011. Ecology of the Brazilian flea frog *Brachycephalus didactylus* (Terrarana: Brachycephalidae). Journal of Herpetology 45, 251-255.

Attwell, D., Laughlin, S.B., 2001. An energy budget for signaling in the grey matter of the brain. Journal of Cerebral Blood Flow & Metabolism 21, 1133-1145.

Autumn, K., Liang, Y.A., Hsieh, S.T., Zesch, W., Chan, W.P., Kenny, T.W., Fearing, R., Full, R.J., 2000. Adhesive force of a single gecko foot-hair. Nature 405, 681-685.

Beebe, D.J., Mensing, G.A., Walker, G.M., 2002. Physics and applications of microfluidics in biology. Annual review of biomedical engineering 4, 261-286.

Berg, H.C., Purcell, E.M., 1977. Physics of chemoreception. Biophysical Journal 20, 193-219.

Beutel, R., Haas, A., 1998. Larval head morphology of *Hydroscapha natans* (Coleoptera, Myxophaga) with reference to miniaturization and the systematic position of Hydroscaphidae. Zoomorphology 118, 103-116.

Beutel, R., Hörnschemeyer, T., 2002. Larval morphology and phylogenetic position of *Micromalthus debilis* LeConte (Coleoptera: Micromalthidae). Systematic Entomology 27, 169-190.

Beutel, R.G., Pohl, H., Hünefeld, F., 2005. Strepsipteran brains and effects of miniaturization (Insecta). Arthropod Structure & Development 34, 301-313.

Bhullar, B.-A.S., Bell, C.J., 2008. Osteoderms of the California legless lizard *Anniella* (Squamata: Anguidae) and their relevance for considerations of miniaturization. Copeia 2008, 785-793.

Byrne, M., 1996. Viviparity and intragonadal cannibalism in the diminutive sea stars *Patiriella vivipara* and *P. parvivipara* (family Asterinidae). Marine Biology 125, 551-567.

Caballero, M., Baquero, E., Ariño, A.H., Jordana, R., 2004. Indirect biomass estimations in Collembola. Pedobiologia 48, 551-557.

Calder, W.A., 1979. The kiwi and egg design: evolution as a package deal. Bioscience 29, 461-467.

Calder, W.A., 1984. Size, function, and life history. Courier Corporation, Cambridge.

Cavalier-Smith, T., 1978. Nuclear volume control by nucleoskeletal DNA, selection for cell volume and cell growth rate, and the solution of the DNA C-value paradox. Journal of Cell Science 34, 247-278.

Chapman, R., 1982. Chemoreception: the significance of receptor numbers. Advances in Insect Physiology 16.

Comolli, L.R., Baker, B.J., Downing, K.H., Siegerist, C.E., Banfield, J.F., 2009. Three-dimensional analysis of the structure and ecology of a novel, ultra-small archaeon. The ISME journal 3, 159-167.

Courties, C., Vaquer, A., Troussellier, M., Lautier, J., Chrétiennot-Dinet, M.J., Neveux, J., Machado, C., Claustre, H., 1994. Smallest eukaryotic organism. Nature 370, 255-255.

Davies, W.M., 1927. Memoirs: on the tracheal system of Collembola, with special reference to that of *Sminthurus viridis*, Lubb. Journal of Cell Science 2, 15-30.

Dial, K.P., 2003. Evolution of avian locomotion: correlates of flight style, locomotor modules, nesting biology, body size, development, and the origin of flapping flight. The Auk 120, 941-952.

Dromgoole, F., 1980. Desiccation resistance of intertidal and subtidal algae. Botanica Marina 23, 149-160.

Eberhard, W.G., 2007. Miniaturized orb-weaving spiders: behavioural precision is not limited by small size. Proceedings of the Royal Society B: Biological Sciences 274, 2203-2209.

Eberhard, W.G., Wcislo, W.T., 2011. Grade changes in brain-body allometry: morphological and behavioural correlates of brain size in miniature spiders, insects and other invertebrates. Advances in Insect Physiology 40, 155.

Esslen, J., Kaissling, K.-E., 1976. Zahl und Verteilung antennaler Sensillen bei der Honigbiene (*Apis mellifera* L.). Zoomorphologie 83, 227-251.

Estrada, A.R., Hedges, S.B., 1996. At the lower size limit in tetrapods: a new diminutive frog from Cuba (Leptodactylidae: *Eleutherodactylus*). Copeia, 852-859.

Faisal, A.A., White, J.A., Laughlin, S.B., 2005. Ion-channel noise places limits on the miniaturization of the brain's wiring. Current Biology 15, 1143-1149.

Feynman, R.P., 1960. There's plenty of room at the bottom. Engineering and science 23, 22-36.

Fischer, S., Meyer‐Rochow, V.B., Müller, C.H., 2012. Challenging limits: ultrastructure and size-related functional constraints of the compound eye of *Stigmella microtheriella* (Lepidoptera: Nepticulidae). Journal of Morphology 273, 1064-1078.

Fischer, S., Meyer‐Rochow, V.B., Müller, C.H., 2013. Compound eye miniaturization in lepidoptera: a comparative morphological analysis. Acta Zoologica.

Fischer, S., Müller, C.H., Meyer-Rochow, V.B., 2011. How small can small be: the compound eye of the parasitoid wasp *Trichogramma*

evanescens (Westwood, 1833)(Hymenoptera, Hexapoda), an insect of 0.3 to 0.4 mm total body size. Vis Neurosci 28, 295-308.

Gao, X., Jiang, L., 2004. Biophysics: water-repellent legs of water striders. Nature 432, 36-36.

Gill, K.P., van Wilgenburg, E., Macmillan, D.L., Elgar, M.A., 2013. Density of antennal sensilla influences efficacy of communication in a social insect. The American naturalist 182, 834-840.

Glaw, F., Köhler, J., Townsend, T.M., Vences, M., 2012. Rivaling the world's smallest reptiles: discovery of miniaturized and microendemic new species of leaf chameleons (*Brookesia*) from northern Madagascar. PloS one 7, e31314.

Goldman, A.L., van Naters, W.V.d.G., Lessing, D., Warr, C.G., Carlson, J.R., 2005. Coexpression of two functional odor receptors in one neuron. Neuron 45, 661-666.

Goldstein, E.B., 2010. Encyclopedia of perception. Sage.

Grebennikov, V.V., 2008. How small you can go: factors limiting body miniaturization in winged insects with a review of the pantropical genus *Discheramocephalus* and description of six new species of the smallest beetles (Pterygota: Coleoptera: Ptiliidae). European Journal of Entomology 105.

Grebennikov, V.V., Beutel, R.G., 2002. Morphology of the minute larva of *Ptinella tenella*, with special reference to effects of miniaturisation and the systematic position of Ptiliidae (Coleoptera: Staphylinoidea). Arthropod Structure & Development 31, 157-172.

Gregory, T.R., 2000. Nucleotypic effects without nuclei: genome size and erythrocyte size in mammals. Genome 43, 895-901.

Gregory, T.R., 2002. A bird's-eye view of the C-value enigma: genome size, cell size, and metabolic rate in the class Aves. Evolution 56, 121-130.

Gregory, T.R., 2005a. The evolution of the genome. Academic Press.

Gregory, T.R., 2005b. Genome size evolution in animals, In: Gregory, T.R. (Ed.), The evolution of the genome. Academic Press, San Diego.

Gregory, T.R., Hebert, P.D., Kolasa, J., 2000. Evolutionary implications of the relationship between genome size and body size in flatworms and copepods. Heredity 84, 201-208.

Greiner, B., Narendra, A., Reid, S.F., Dacke, M., Ribi, W.A., Zeil, J., 2007. Eye structure correlates with distinct foraging-bout timing in primitive ants. Current Biology 17, R879-R880.

Greiner, B., Ribi, W.A., Warrant, E.J., 2004. Retinal and optical adaptations for nocturnal vision in the halictid bee *Megalopta genalis*. Cell and Tissue Research 316, 377-390.

Grime, J., Mowforth, M., 1982. Variation in genome size—an ecological interpretation. Nature 299, 151-153.

Haldane, J.B.S., 1926. On being the right size. Harper's Monthly Magazine 152, 424-427.

Hallem, E.A., Carlson, J.R., 2006. Coding of Odors by a Receptor Repertoire. Cell 125, 143-160.

Hanken, J., 1983. Miniaturization and its effects on cranial morphology in plethodontid salamanders, genus *Thorius* (Amphibia, Plethodontidae): II. The fate of the brain and sense organs and their role in skull morphogenesis and evolution. Journal of Morphology 177, 255-268.

Hanken, J., Wake, D.B., 1993. Miniaturization of body size: organismal consequences and evolutionary significance. Annual Review of Ecology and Systematics 24, 501-519.

Harrison, J.F., Kaiser, A., VandenBrooks, J.M., 2010. Atmospheric oxygen level and the evolution of insect body size. Proceedings of the Royal Society B: Biological Sciences 277, 1937-1946.

Heath, R., Evans, M., 1990. The relationship between the ventral nerve cord, body size and phylogeny in ground beetles (Coleoptera: Carabidae). Zoological Journal of the Linnean Society 98, 259-293.

Hustert, R., 2012. Giant and dwarf axons in a miniature insect, Encarsia formosa, (Hymenoptera, Calcididae). Arthropod Structure & Development 41, 535-543.

Jander, U., Jander, R., 2002. Allometry and resolution of bee eyes (Apoidea). Arthropod Structure & Development 30, 179-193.

Jayaweera, A., Barry, K.L., 2017. Male antenna morphology and its effect on scramble competition in false garden mantids. The Science of Nature 104, 75.

Karban, R., 1986. Prolonged development in cicadas, In: Taylor, F., Karban, R. (Eds.), The Evolution of Insect Life Cycles. Springer, New York, pp. 222-235.

Kaspari, M., Weiser, M., 1999. The size–grain hypothesis and interspecific scaling in ants. Functional Ecology 13, 530-538.

Kelber, C., 2009. The olfactory system of leaf-cutting ants: neuroanatomy and the correlation to social organization. Julius-Maximilians-Universität, Würzburg, p. 87.

Kelber, C., Rössler, W., Kleineidam, C.J., 2006. Multiple olfactory receptor neurons and their axonal projections in the antennal lobe of the honeybee *Apis mellifera*. Journal of Comparative Neurology 496, 395-405.

Kirschfeld, K., Wenk, P., 1976. The dorsal compound eye of simuliid flies. Zeitschrift für Naturforschung C 31, 764-765.

Koehl, M.A.R., 2001. Fluid dynamics of animal appendages that capture molecules: arthropod olfactory antennae, In: Fauci, L.J., Gueron, S. (Eds.), Computational Modeling in Biological Fluid Dynamics. Springer Verlag, New York.

Kozłowski, J., Konarzewski, M., Gawelczyk, A., 2003. Cell size as a link between noncoding DNA and metabolic rate scaling. Proceedings of the National Academy of Sciences 100, 14080-14085.

Kristensen, R.M., 1991. Loricifera, In: Harrison, F.W., Ruppert, E.E. (Eds.), Microscopic Anatomy of Invertebrates Wiley-Liss, New York.

Land, M.F., 1981. Optics and vision in invertebrates, In: Autrum, H. (Ed.), Handbook of Sensory Physiology. Springer, Berlin Heidleberg New York, pp. pp. 471-592.

Land, M.F., 1997. Visual acuity in insects. Annual Review of Entomology 42, 147-177.

Land, M.F., Nilsson, D.-E., 2012. Animal Eyes, Second ed. Oxford University Press, Oxford.

Lee, J., Strausfeld, N., 1990. Structure, distribution and number of surface sensilla and their receptor cells on the olfactory appendage of the male moth *Manduca sexta*. Journal of neurocytology 19, 519-538.

Luef, B., Frischkorn, K.R., Wrighton, K.C., Holman, H.-Y.N., Birarda, G., Thomas, B.C., Singh, A., Williams, K.H., Siegerist, C.E., Tringe, S.G., 2015. Diverse uncultivated ultra-small bacterial cells in groundwater. Nature communications 6.

Makarova, A., Polilov, A., Fischer, S., 2015. Comparative morphological analysis of compound eye miniaturization in minute hymenoptera. Arthropod Structure & Development 44, 21-32.

Mckinney, M., 2013. Heterochrony in evolution: a multidisciplinary approach. Springer Science & Business Media.

Meyer-Rochow, V.B., Gál, J., 2004. Dimensional limits for arthropod eyes with superposition optics. Vision research 44, 2213-2223.

Minelli, A., 2003. The Development of Animal Form: Ontogeny, Morphology, and Evolution. Cambridge University Press.

Mitchell, K.J., Llamas, B., Soubrier, J., Rawlence, N.J., Worthy, T.H., Wood, J., Lee, M.S.Y., Cooper, A., 2014. Ancient DNA reveals elephant birds and kiwi are sister taxa and clarifies ratite bird evolution. Science 344, 898-900.

Mueller, R., 2000. Who needs a nucleus? Red blood cells in the genus *Batrachoseps*, American Zoologist. American Zoologist 1041 New Hampshire St, Lawrence, KS 66044 USA, pp. 1142-1142.

Narendra, A., Ramirez-Esquivel, F., Ribi, W.A., 2016. Compound eye and ocellar structure for walking and flying modes of locomotion in the Australian ant, *Camponotus consobrinus*. Scientific Reports 6, 22331.

Narendra, A., Reid, S.F., Greiner, B., Peters, R.A., Hemmi, J.M., Ribi, W.A., Zeil, J., 2011. Caste-specific visual adaptations to distinct daily activity schedules in Australian *Myrmecia* ants. Proceedings of the Royal Society B: Biological Sciences 278, 1141-1149.

Niven, J.E., 2005. Brain evolution: Getting better all the time? Current Biology 15, R624-R626.

Niven, J.E., Anderson, J.C., Laughlin, S.B., 2007. Fly photoreceptors demonstrate energy-information trade-offs in neural coding. PLoS Biol 5, e116.

Niven, J.E., Farris, S.M., 2012. Miniaturization of nervous systems and neurons. Current Biology 22, R323-R329.

Niven, J.E., Laughlin, S.B., 2008. Energy limitation as a selective pressure on the evolution of sensory systems. Journal of Experimental Biology 211, 1792-1804.

Novotny, V., Wilson, M.R., 1997. Why are there no small species among xylem-sucking insects? Evolutionary Ecology 11, 419.

Olmo, E., Morescalchi, A., 1978. Genome and cell sizes in frogs: a comparison with salamanders. Cellular and Molecular Life Sciences 34, 44-46.

Olmo, O., Morescalchi, A., 1975. Evolution of the genome and cell sizes in salamanders. Cellular and Molecular Life Sciences 31, 804-806.

Pedersen, R.A., 1971. DNA content, ribosomal gene multiplicity, and cell size in fish. Journal of Experimental Zoology 177, 65-78.

Pedley, T., 1977. Scale Effects in Animal Locomotion, International Symposium on Scale Effects in Animal Locomotion (1975: Cambridge University). Academic Press.

Pellegrino, C.R., 1984. The role of desiccation pressures and surface area/volume relationships on seasonal zonation and size distribution of four intertidal decapod Crustacea from New Zealand: implications for adaptation to land. Crustaceana, 251-268.

Pereira, M.J.R., Rebelo, H., Teeling, E.C., O'Brien, S.J., Mackie, I., Bu, S.S.H., Swe, K.M., Khin, M.M., Bates, P.J., 2006. Status of the world's smallest mammal, the bumble-bee bat *Craseonycteris thonglongyai*, in Myanmar. Oryx 40, 456-463.

Perge, J.A., Niven, J.E., Mugnaini, E., Balasubramanian, V., Sterling, P., 2012. Why do axons differ in caliber? Journal of Neuroscience 32, 626-638.

Peters, R.H., 1983. The ecological implications of body size, Cambridge.

Phillips, M.J., Gibb, G.C., Crimp, E.A., Penny, D., 2010. Tinamous and moa flock together: mitochondrial genome sequence analysis reveals independent losses of flight among ratites. Systematic Biology 59, 90-107.

Poelman, E.H., Bruinsma, M., Zhu, F., Weldegergis, B.T., Boursault, A.E., Jongema, Y., van Loon, J.J., Vet, L.E., Harvey, J.A., Dicke, M., 2012. Hyperparasitoids use herbivore-induced plant volatiles to locate their parasitoid host. PLoS biology 10, e1001435.

Polilov, A.A., 2012. The smallest insects evolve anucleate neurons. Arthropod Structure & Development 41, 29-34.

Polilov, A.A., 2016. At the Size Limit: Effects of Miniaturization in Insects. Springer.

Polilov, A.A., 2017. Anatomy of adult *Megaphragma* (Hymenoptera: Trichogrammatidae), one of the smallest insects, and new insight into insect miniaturization. PloS one 12, e0175566.

Polilov, A.A., Beutel, R.G., 2009. Miniaturisation effects in larvae and adults of *Mikado* sp.(Coleoptera: Ptiliidae), one of the smallest free-living insects. Arthropod Structure & Development 38, 247-270.

Polilov, A.A., Beutel, R.G., 2010. Developmental stages of the hooded beetle *Sericoderus lateralis* (Coleoptera: Corylophidae) with comments on the phylogenetic position and effects of miniaturization. Arthropod Structure & Development 39, 52-69.

Polilov, A.A., Shmakov, A.S., 2016. The anatomy of the thrips *Heliothrips haemorrhoidalis* (Thysanoptera, Thripidae) and its specific features caused by miniaturization. Arthropod Structure & Development 45, 496-507.

Prescott, D., 1955. Relations between cell growth and cell division: I. Reduced weight, cell volume, protein content, and nuclear volume of *Amoeba proteus* from division to division. Experimental cell research 9, 328-337.

Quesada, R., Triana, E., Vargas, G., Douglass, J.K., Seid, M.A., Niven, J.E., Eberhard, W.G., Wcislo, W.T., 2011. The allometry of CNS size and consequences of miniaturization in orb-weaving and cleptoparasitic spiders. Arthropod Structure & Development 40, 521-529.

Rainford, J.L., Hofreiter, M., Nicholson, D.B., Mayhew, P.J., 2014. Phylogenetic distribution of extant richness suggests metamorphosis is a key innovation driving diversification in insects. PloS one 9, e109085.

Ramirez-Esquivel, F., 2012. From large to small, from day to night: The sensory costs of miniaturisation in ants, Evolution, Ecology and Genetics. The Australian National University, Canberra p. 46.

Rensch, B., 1948. Histological changes correlated with evolutionary changes of body size. Evolution 2, 218-230.

Rensch, B., 1959. Evolution Above the Species Level. Methuen, London.

Rittmeyer, E.N., Allison, A., Gründler, M.C., Thompson, D.K., Austin, C.C., 2012. Ecological guild evolution and the discovery of the world's smallest vertebrate. PloS one 7, e29797.

Roediger, L.M., 2011. Population and reproductive ecology of the direct-developing sea stars *Parvulastra parvivipara* and *Cryptasterina hystera*, School of Biological Sciences. Flinders University, Adelaide, p. 172.

Roth, G., Blanke, J., Wake, D.B., 1994. Cell size predicts morphological complexity in the brains of frogs and salamanders. Proceedings of the National Academy of Sciences 91, 4796-4800.

Roth, G., Rottluff, B., Grunwald, W., Hanken, J., Linke, R., 1990. Miniaturization in plethodontid salamanders (Caudata: Plethodontidae) and its consequences for the brain and visual system. Biological Journal of the Linnean Society 40, 165-190.

Roth, G., Rottluff, B., Linke, R., 1988. Miniaturization, genome size and the origin of functional constraints in the visual system of salamanders. Naturwissenschaften 75, 297-304.

Ruschioni, S., Romani, R., Riolo, P., Isidoro, N., 2012. Morphology and distribution of antennal multiporous gustatory sensilla related to host recognition in some *Trichogramma* spp. Bull. Insectol. 65, 171-176.

Rutowski, R.L., 2000. Variation of eye size in butterflies: inter - and intraspecific patterns. Journal of Zoology 252, 187-195.

Ryan, M.F., 2002. Insect Chemoreception. Kluwer Academic Publishers, Dordrecht.

Safi, K., Seid, M.A., Dechmann, D.K., 2005. Bigger is not always better: when brains get smaller. Biology Letters 1, 283-286.

Sane, S.P., 2016. Neurobiology and biomechanics of flight in miniature insects. Current Opinion in Neurobiology 41, 158-166.

Schmidt-Nielsen, K., 1977. Problems of Scaling: Locomotion and Physiological Correlates, In: Pedley, T. (Ed.), Scale Effects in Animal Locomotion. Academic Press, London.

Schmidt-Nielsen, K., 1984. Scaling: Why is animal size so important? Cambridge Unversity Press, Cambridge.

Seid, M.A., Castillo, A., Wcislo, W.T., 2011. The allometry of brain miniaturization in ants Brain, Behavior and Evolution 77, 5-13.

Smith, F.A., Boyer, A.G., Brown, J.H., Costa, D.P., Dayan, T., Ernest, S.M., Evans, A.R., Fortelius, M., Gittleman, J.L., Hamilton, M.J., 2010. The evolution of maximum body size of terrestrial mammals. Science 330, 1216-1219.

Spaethe, J., Brockmann, A., Halbig, C., Tautz, J., 2007. Size determines antennal sensitivity and behavioral threshold to odors in bumblebee workers. Naturwissenschaften 94, 733-739.

Spaethe, J., Chittka, L., 2003. Interindividual variation of eye optics and single object resolution in bumblebees. Journal of Experimental Biology 206, 3447-3453.

Streinzer, M., Brockmann, A., Nagaraja, N., Spaethe, J., 2013. Sex and caste-specific variation in compound eye morphology of five honeybee species. PloS one 8, e57702.

Streinzer, M., Huber, W., Spaethe, J., 2016. Body size limits dim-light foraging activity in stingless bees (Apidae: Meliponini). Journal of Comparative Physiology A 202, 643-655.

Szarski, H., 1976. Cell size and nuclear DNA content in vertebrates. International Review of Cytology 44, 93-111.

Szarski, H., 1983. Cell size and the concept of wasteful and frugal evolutionary strategies. Journal of Theoretical Biology 105, 201-209.

van der Woude, E., Smid, H.M., 2015. How to escape from Haller's rule: olfactory system complexity in small and large *Trichogramma evanescens* parasitic wasps. Journal of Comparative Neurology 524, 1876-1891.

Venkatesh, S., Singh, R.N., 1984. Sensilla on the third antennal segment of *Drosophila melanogaster* Meigen (Diptera: Drosophilidae). International Journal of Insect Morphology and Embryology 13, 51-63.

Vosshall, L.B., Amrein, H., Morozov, P.S., Rzhetsky, A., Axel, R., 1999. A spatial map of olfactory receptor expression in the *Drosophila antenna*. Cell 96, 725-736.

Wake, M.H., 1978. The reproductive biology of *Eleutherodactylus jasperi* (Amphibia, Anura, Leptodactylidae), with comments on the evolution of live-bearing systems. Journal of Herpetology, 121-133.

Walker, L., Spotorno, A., Sans, J., 1991. Genome size variation and its phenotypic consequences in *Phyllotis* rodents. Hereditas 115, 99-107.

Warrant, E.J., McIntyre, P.D., 1993. Arthropod eye design and the physical limits to spatial resolving power. Progress in neurobiology 40, 413-461.

Warrant, E.J., Nilsson, D.-E., 1998. Absorption of white light in photoreceptors. Vision research 38, 195-207.

Waxman, S.G., 1980. Determinants of conduction velocity in myelinated nerve fibers. Muscle & nerve 3, 141-150.

Wcislo, W.T., 1995. Sensilla numbers and antennal morphology of parasitic and non-parasitic bees (Hymenoptera: Apoidea). International Journal of Insect Morphology and Embryology 24, 63-81.

Worthy, T.H., Worthy, J.P., Tennyson, A.J., Salisbury, S.W., Hand, S.J., Scofield, R.P., 2013. Miocene fossils show that kiwi (*Apteryx*, Apterygidae) are probably not phyletic dwarves, Paleornithological Research 2013—Proceedings of the 8th International Meeting of the Society of Avian Paleontology and Evolution. Vienna: Natural History Museum Vienna, pp. 63-80.

Yilmaz, A., Aksoy, V., Camlitepe, Y., Giurfa, M., 2014. Eye structure, activity rhythms, and visually-driven behavior are tuned to visual niche in ants. Frontiers in behavioral neuroscience 8.

Zeil, J., 1983. Sexual dimorphism in the visual system of flies: The compound eyes and neural superposition in Bibionidae (Diptera). Journal of comparative physiology 150, 379-393.

Chapter 2

Describing and identifying ant sensilla:
"The antennal sensory array of the nocturnal bull ant Myrmecia pyriformis"

Chapter contents

The first step towards studying antennal arrays was to review what was already known about the different types of sensilla and to establish a methodology. This chapter represents an attempt to review the conflicting nomenclature in the literature, identify all the different types of sensilla present in ants, and establish a methodology to identify, map, count and measure sensilla in ants. The ant *Myrmecia pyriformis* was chosen for a number of reasons, its large size means it is easier to handle and mount as well as providing an example of a large ant for the comparative study that was to follow. This species was also widely used in behavioural and anatomical studies in the lab, this meant that it was possible to interpret results in the context of natural history, anatomy and behaviour as information on these aspects of *Myrmecia pyriformis* biology was available.

The contents of this chapter are based on the following publication:

> **Ramirez-Esquivel, F., Zeil, J., Narendra, A., 2014. The antennal sensory array of the nocturnal bull ant *Myrmecia pyriformis*. Arthropod Structure & Development 43, 543-558.**

It differs from the original only in minor editorial details and some expansion of the discussion section.

Author contributions:
Data collection and analysis: FRE; first draft of the manuscript and figure design: FRE; critical revision of the manuscript: FRE, JZ, AN.

2.1. Introduction

The antennae and the compound eyes represent the main sensory organs which provide information about an ant's surroundings. Although compound eyes are theoretically well understood, this is not the case for many aspects of insect antennae. This is hardly surprising as antennae are complex sensory arrays studded with different types of sensilla which process a range of inputs in different modalities. They also vary markedly in appearance, despite a common underlying architecture.

The gross external morphology of sensory sensilla is given by the outer cuticular element and generally follows the same basic structure (Frazier, 1985). An outer hair, peg or other stimulus conducting structure is attached to a socket or protrudes through an opening (or more correctly an invagination) in the cuticular surface (Altner and Prillinger, 1980). Some sensilla are found sunken within the antennal lumen but these still follow a similar general structure. The morphology of the external cuticular elements is, at least in part, dictated by the function of the particular sensillum. For instance, chemoreceptors must have pores, slits or other inlets to allow molecules to penetrate into the lumen of the sensillum. This permits different types of sensilla to be identified, to a certain degree, based on external morphology alone (Nakanishi et al., 2009).

Apart from chemoreception, ant sensilla provide information about mechanical cues, humidity, temperature and CO_2 levels in the surrounding area (Fresneau, 1979; Ozaki et al., 2005; Roces and Kleineidam, 2000; Soroker et al., 1995; Wilson, 1972). Sensing these environmental conditions is important for most insects but it takes on additional importance in social insects where coordinating activities among individuals, living in an enclosed space and caring for young adds an extra layer of complexity to sensory requirements. Despite the heavy reliance of ants on their antennae, we know relatively little about sensilla, especially regarding their distribution and abundance. Some studies have addressed this in trail-following species such as *Solenopsis invicta* (Renthal et al., 2003) and *Lasius fuliginosus* (Dumpert, 1972b) and also in tandem running and individually foraging ants such as *Camponotus compressus* (Barsagade et al., 2013; Mysore et al., 2010) and *Dinoponera lucida* (Marques-Silva et al., 2006) respectively. Furthermore, an initial attempt towards comparing the morphology of sensilla across the ant phylogeny was made (Hashimoto, 1990a, b). However, the qualitative comparisons carried out in this case were made with different purposes in mind and therefore are of limited value without access to all of the raw data.

Unfortunately, what is largely missing are comprehensive datasets containing basic information on the numbers, size and distribution of different sensilla types. These are necessary for thorough comparisons of the antennal arrays of different species.

Here, we studied the ant *Myrmecia pyriformis,* which belongs to the Australian ant genus *Myrmecia* (Hymenoptera: Formicidae: Myrmeciinae). This genus is unusual among ants in having large eyes, a potent sting and workers that forage solitarily (Narendra et al., 2013; Reid et al., 2013). In addition, their morphology and behaviour are relatively unspecialised in comparison to other ants, which perhaps hints at the conditions under which eusociality in ants arose (Ward and Brady, 2003). This genus is speciose and ecologically diverse with different species being diurnal, crepuscular, or nocturnal (Greiner et al., 2007; Narendra et al., 2011). Our particular study species *M. pyriformis* emerges from the nest during the evening twilight, spends the night foraging on a single food tree, and returns to the nest in the morning twilight (Narendra et al., 2010). Workers of this species are polymorphic with a continuous gradient of body sizes and ants of all sizes appear to engage in foraging activities. Given their large size (12-26mm (Narendra et al., 2011)), solitary foraging habits, and visually driven navigation this species has been the subject of a number of studies on night vision and navigation (Jayatilaka et al., 2011; Narendra et al., 2011; Narendra et al., 2010; Narendra et al., 2013; Reid et al., 2011; Reid et al., 2013). The present study is part of a larger comparative project investigating the sensory costs of miniaturisation. We are particularly interested in the types of sensilla, their size, their shape variation and their distribution in the polymorphic nocturnal ant *M. pyriformis* and how these features compare across different species. Such comparisons are, however, difficult to make given the inconsistent use of sensillum nomenclature and the difficulties associated with reliably identifying different sensillum types. Hence, here we attempt to consolidate the known ant sensilla literature to make possible interspecific comparisons.

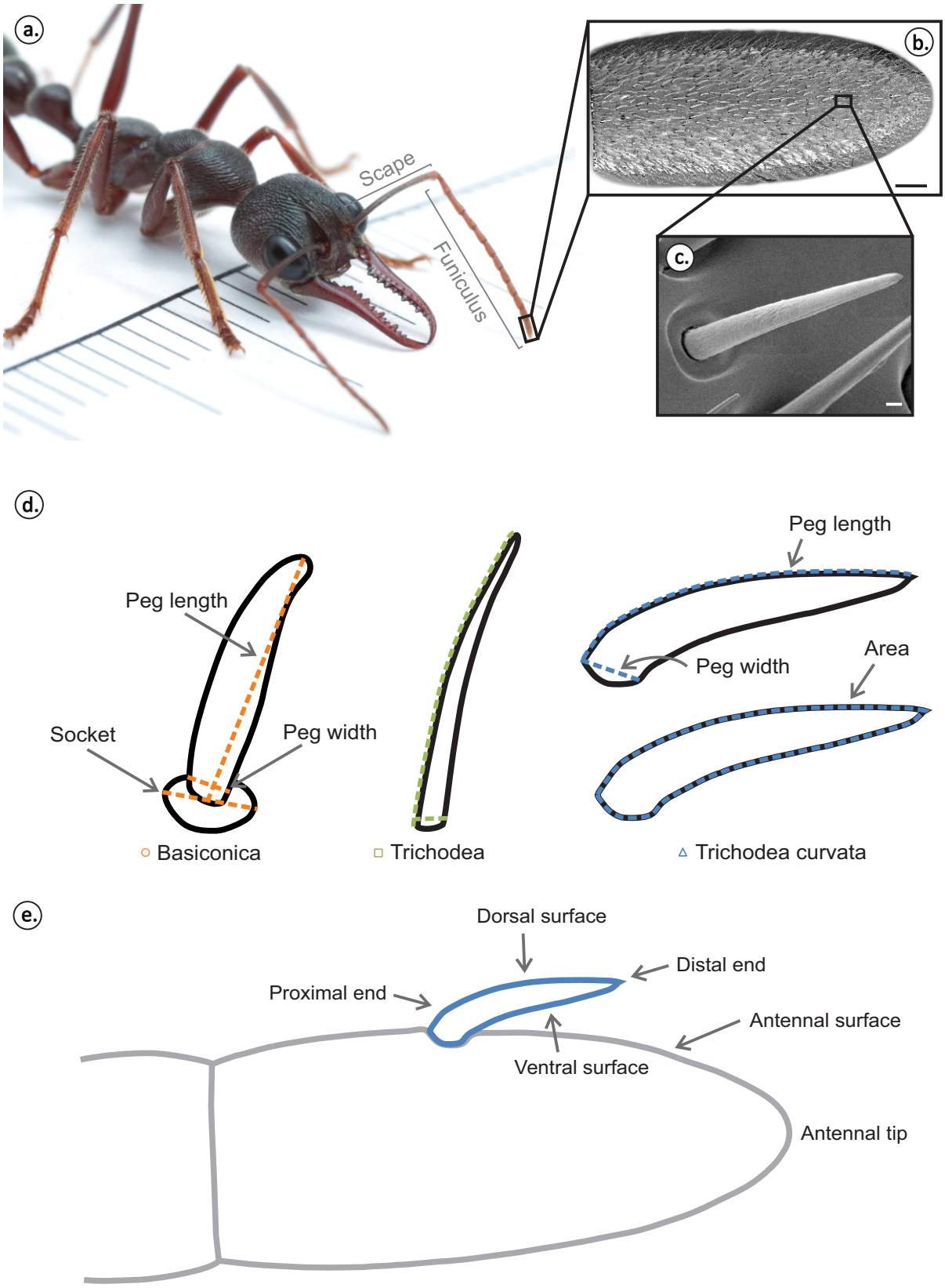

Figure 2.1. The study species, *Myrmecia pyriformis*. (a) Profile view of the worker ant indicating the scape, funiculus (composed of the flagellum and pedicel) and apical segment, the region of the antenna studied. Photo credit: Ajay Narendra. Scanning electron micrographs of the (b) apical segment of the flagellum and (c) a single sensillum. Scale bar = (a) 1mm; (b) 50µm; (c) 1µm. (d) Schematics of sensilla basiconica, trichodea and trichodea curvata showing how different measurements were taken. (e) Schematic of sensilla trichodea curvata explaining dorsal and ventral surface of a sensillum as well as proximal and distal ends in relation with the rest of the antenna (drawing is not to scale).

2.2. Methods

2.2.1. Study species

Worker ants were collected from a single colony located at the Campus Field Station at The Australian National University, Canberra (35°16'50.14"S, 149°6'42.13"E). Individuals used for scanning electron microscopy (SEM) analysis were killed by immersion in 50% ethanol and stored in vials until further processing. We studied the dorsal side of the apical antennomere in nine workers of varying size (1-9 in **Table 2.1**) and in addition compared the dorsal and ventral surfaces of the apical segment in a very small and a fairly large worker (1 and 7 in **Table 2.1**). A total of 78 workers were additionally photographed to determine the relation between body length and head width (**Figure 2.2**).

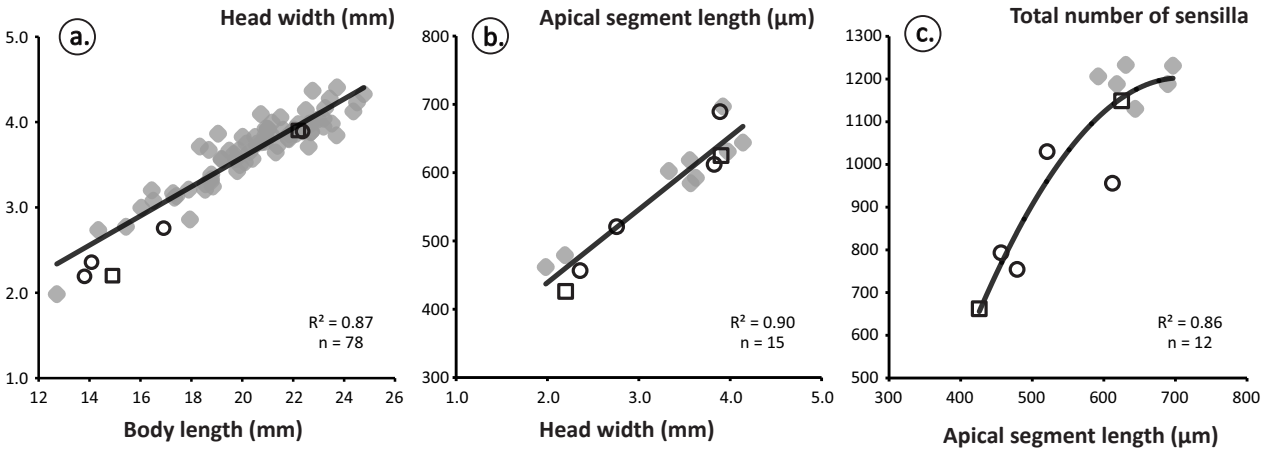

Figure 2.2. Morphometric measurements in *Myrmecia pyriformis*. Relationship between (a) head width and body length, (b) apical segment length and head width and (c) total number of sensilla and apical segment length. Black open circles: represent the four individuals in Figure 10; black open squares: represent the two individuals in Figure 11; grey markers: represent other sampled individuals. A line of best fit is shown in black.

2.2.2. SEM specimen preparation

Ants were photographed, and body length and head width were measured. Antennae were separated from the head capsule and mounted on aluminium stubs with adhesive, conductive carbon tape. The antennae were positioned with either the ventral or the dorsal side facing upwards and allowed to air dry. Samples were then coated with Au/Pd (60:40) for 2 – 4 minutes at 20 mA and observed using one of two instruments, either a Hitachi S-4300 SE/N scanning electron microscope or a Zeiss UltraPlus FESEM, under an accelerating voltage of 3kV. To obtain images of the internal aspect of the apical segment, it was split with a scalpel blade. Soft tissue was removed by placing the resulting halves in 10% KOH solution for 12 hours. The cleaned cuticle was then prepared for SEM observation as described above.

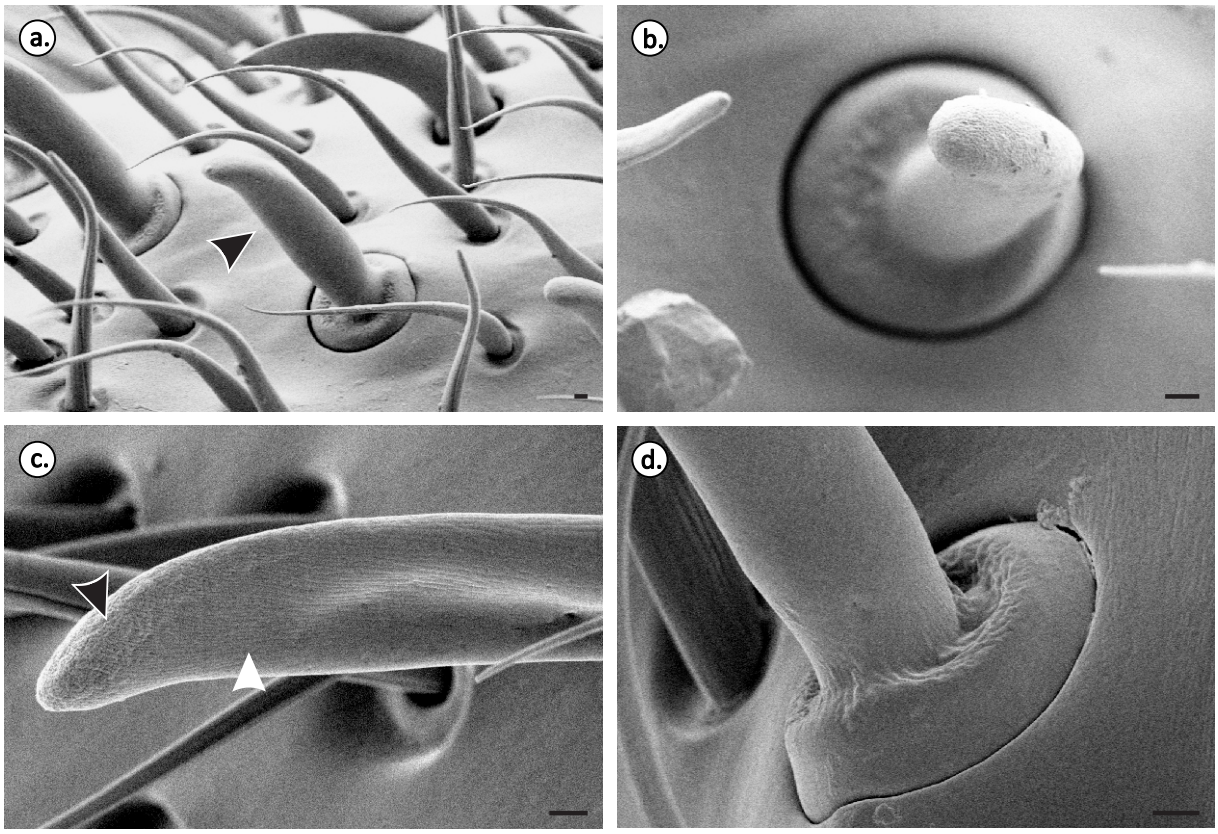

Figure 2.3. Scanning electron micrographs of sensilla basiconica. (a) Overview of a sensillum basiconicum (black arrow) amongst other sensilla. (b) Top view of the sensillum shows a circular socket surrounding the base of the peg. (c) Pores cover the dorsal, distal surface of the peg (black arrow) and striations cover the proximal ventral surface (white arrow). (d) Structure of the socket and the base of the peg. All scale bars = 1µm.

2.2.3. Analysis

We focussed mainly on the dorsal surface of the apical antennomere as this segment bears the largest number of chemo-, hygro- and CO_2- receptors in ants (Dumpert, 1972b; Jaisson, 1969; Mysore et al., 2010; Nakanishi et al., 2009; Renthal et al., 2003). Studying the dorsal region provided us the best opportunity to study all sensillum types in detail. Images were stitched, cropped and adjusted for contrast using CorelDRAW® Graphics Suite X5 (2010 Corel). No other modifications were made. The abundance of each type of sensillum was determined from the stitched images of the apical segment, with each image taken at x1.5k magnification. Maps of the antennal tip showing the location of each individual sensillum were created using a Matlab (2007a Matworks Natick, Massachusetts) based custom-written program Digilite (Jan Hemmi and Robert Parker, The Australian National University). In most analyses we have used the apical segment length rather than area to represent size of antennomere We provide information on both the apical segment length (ASL) and apical segment area (ASA), which in *M. pyriformis* are highly correlated (R^2=0.986). ASA has inherent errors acquired from measuring a curved surface, but is a good measure for representing sensilla density. In contrast, ASL is a more reliable measurement as it is does not take curvature into account. However, ASA may be more appropriate for inter-species comparison as it provides an accurate representation of apical segment shape. Hence, for most analyses we have used ASL to represent size of antennomere and used ASA only to represent sensilla density.

Eight distinct sensillum types were identified using previous descriptions of the external morphology in other ant species (Dumpert, 1972a, b; Hashimoto, 1990b; Kleineidam et al., 2000; Kleineidam and Tautz, 1996; Marques-Silva et al., 2006; Nakanishi et al., 2009; Ozaki et al., 2005; Renthal et al., 2003; Rutchy et al., 2009). In the past, different studies have used different nomenclatures to name sensillum types hampering comparisons. Here we follow the nomenclature of Dumpert (1972b) as this has been most widely used and provides names for most of the sensilla we identified. For the only two sensilla not covered by Dumpert's nomenclature (1972b) we have used "trichoid-II sensillum" and "coelocapitular sensillum" as per Nakanishi et al. (2009; 1982). Additionally, for ease of comparison between studies the homologies in terminology have been listed in Appendix 1.

Measurements of individual sensilla were carried out using ImageJ 1.45s (Rusband, National Institutes of Health, USA). For each sensillum type the length, diameter, and 2D area (see **Figure 2.1d** for examples) were

measured from at least five sensilla for each specimen. In the case of sensilla trichodea, trichodea curvata and trichoid-II sensilla a curved line was traced on the outer edge of the sensillum to measure the length (see **Figure 2.1d**). In the case of other sensilla the longest straight line between the tip and the base was measured. Only 'above ground' structures were measured to determine the length of sensilla. For the width of sensilla and the diameter of sockets or openings we always measured the widest possible diameter. Measurements were only carried out on sensilla that were clearly imaged in full profile (**Figure 2.1e**). Sensilla that were at an angle, pointing away or towards the observer, were ignored. This ensured that the measurements taken were representative of the true dimensions of sensilla but limited the sample size. When describing the anatomy of sensilla we use the terms ventral, dorsal, proximal and distal as indicated in **Figure 2.1e**.

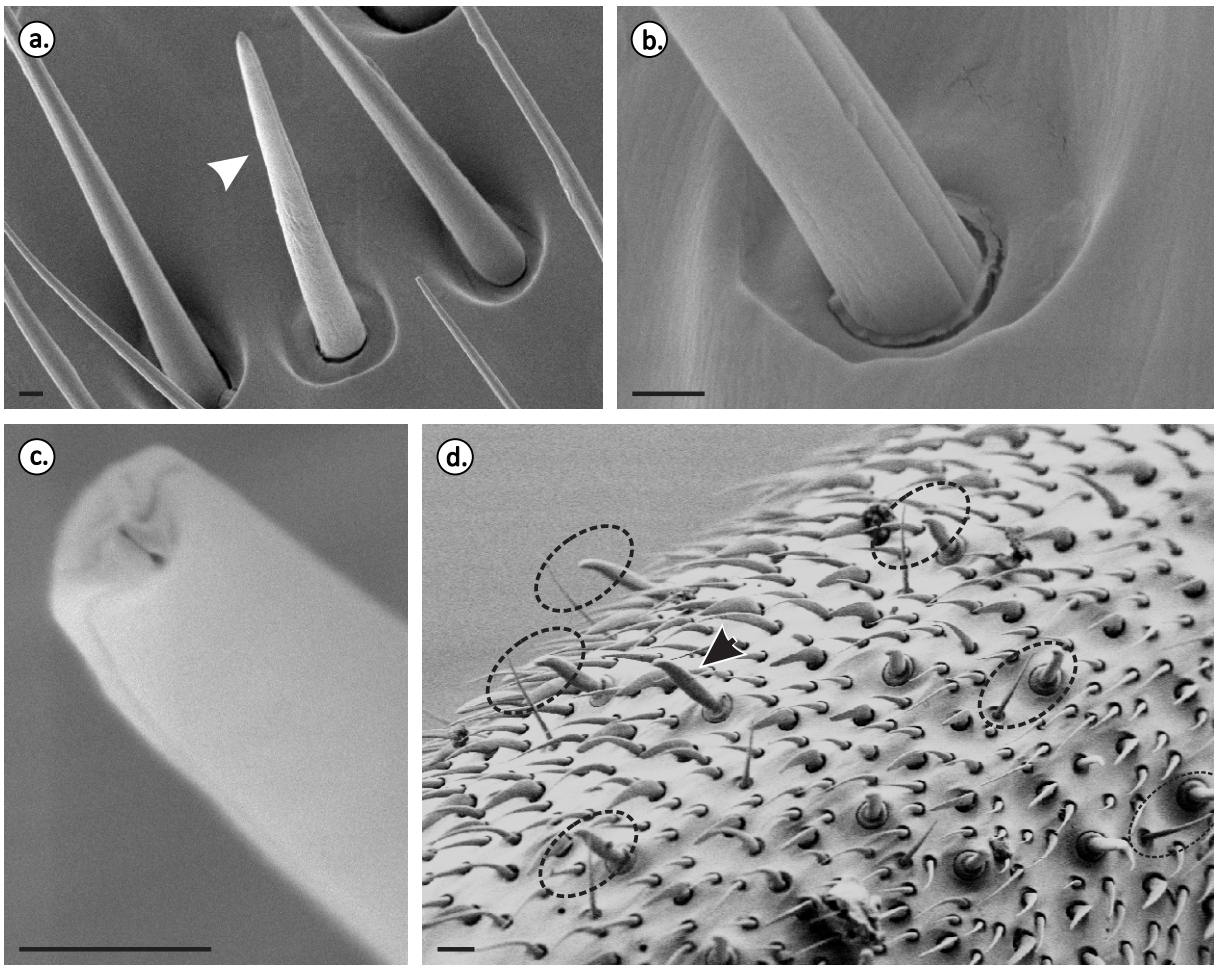

Figure 2.4. Scanning electron micrographs of sensilla trichodea. (a) Overview of sensilla trichodea (white arrow) amongst other sensilla. (b) Base of the peg. (c) Peg tip shows a closed terminal pore and lateral grooves. (d) Paired basiconica and sensilla trichodea (dashed ovals) and unpaired sensilla basiconica (black arrow). Scale bars for (a), (b), (c) = 1µm, (d) = 10µm.

2.3. Results and Discussion

2.3.1. Overview

Sensory hairs in *M. pyriformis* are located throughout most of the body but are most abundant and diverse on the antennae, particularly in the apical antennomere (**Figure 2.1a** and **b**). Despite the minute size of the sensilla (**Figure 2.1c**), their sheer density (**Figure 2.1b**) sometimes makes them visible to the naked eye as fine pilosity. The body length of the workers studied ranged from 12.7 -24.8 mm (**Figure 2.2a**) with larger animals generally having larger heads (**Figure 2a**) and larger apical antennomeres (**Figure 2.2b**). The number of sensilla also increased with the size of apical segment (**Figure 2.2c**, **Table 2.1**). We identified eight different types of sensilla on the apical segment of *M. pyriformis* with one, the coelocapitular sensillum, found mostly on the ventral region.

2.3.2. Morphology and function

This section outlines the external morphology of each type of sensillum and gives some indication of its function based on its anatomy and on evidence from previous studies. Some of the terminology used here, such as the 'dorsal' and 'ventral' sides of sensilla, and length of each sensillum are explained in the methods section above and in **Figure 2.1**. We refer to the external apertures of pit sensilla as 'openings' as that is how they appear externally. However, they are not true openings into the underlying haemolymph, but depressions or invaginations of the cuticle.

Sensilla basiconica

These sensilla are one of the shortest (25.2µm±2.1; n=65) and have thickened pegs (3.9µm±0.4; n=65) with a rounded tip (**Figure 2.3a** and **b**, **Table 2.2**). Pores are visible along the dorsal surface, particularly around the tip, (**Figure 2.3c**, black arrow) while striations cover the distal, ventral portion (**Figure 2.3c**, white arrow). A thick, circular socket surrounds the base of the sensilla (**Figure 2.3b** and **d**). This socket is elevated above the level of the antennal surface, similar to that of *Myrmecia gulosa* (Hashimoto, 1990b). These sensilla have not been observed in male ants (e.g., *Camponotus compressus*, Mysore et al., 2010). Anatomical, electrophysiological and behavioural evidence indicates that

sensilla basiconica function as contact chemoreceptors (*Camponotus vagus*: Masson, 1974; *Camponotus japonicus*: Ozaki et al., 2005).

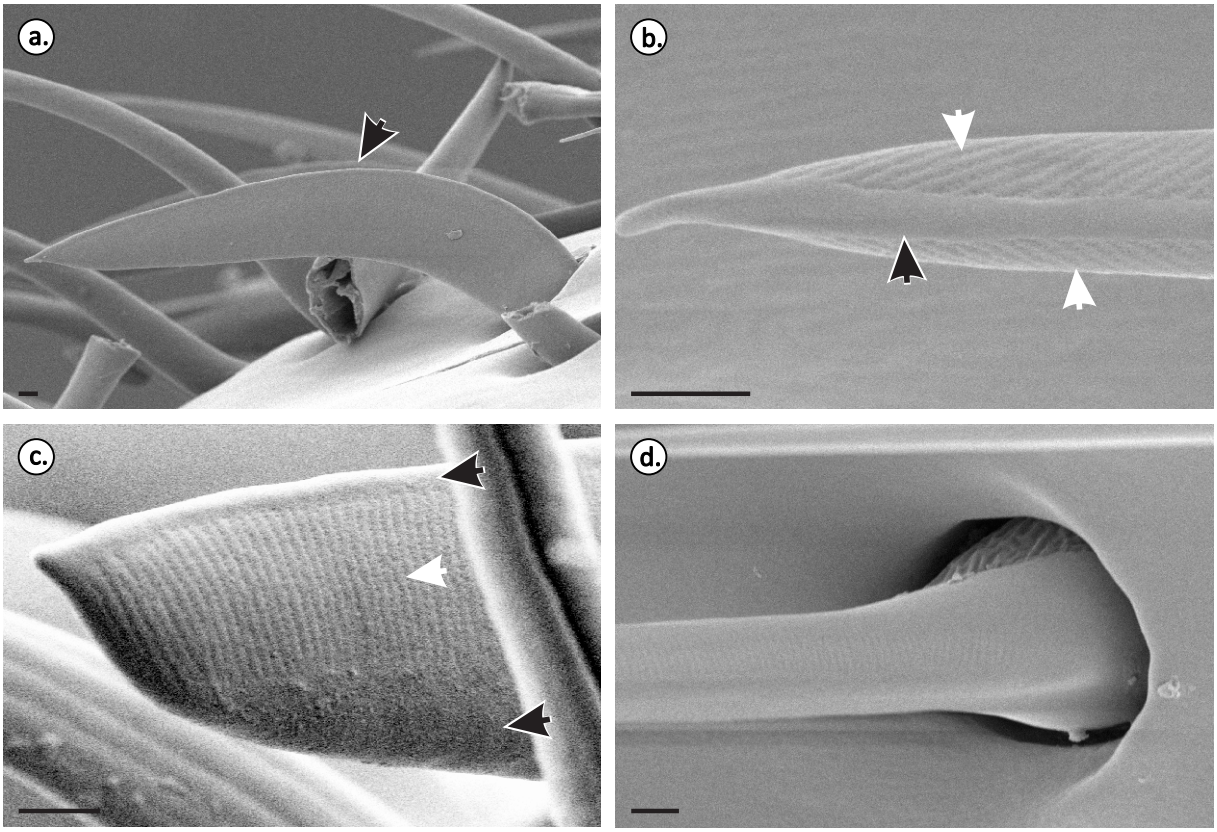

Figure 2.5. Scanning electron micrographs of sensilla trichodea curvata. (a) Overview of a sensillum trichodeum curvatum (black arrow) amongst other sensilla. (b) Sensillum tip shows bands of pores on either side of the peg (white arrows) with an unperforated band at the top (black arrow). (c) Lateral aspect of the peg tip shows rows of pores (white arrow) and unperforated regions (black arrows). (d) Base of the peg and insertion. All scale bars = 1µm.

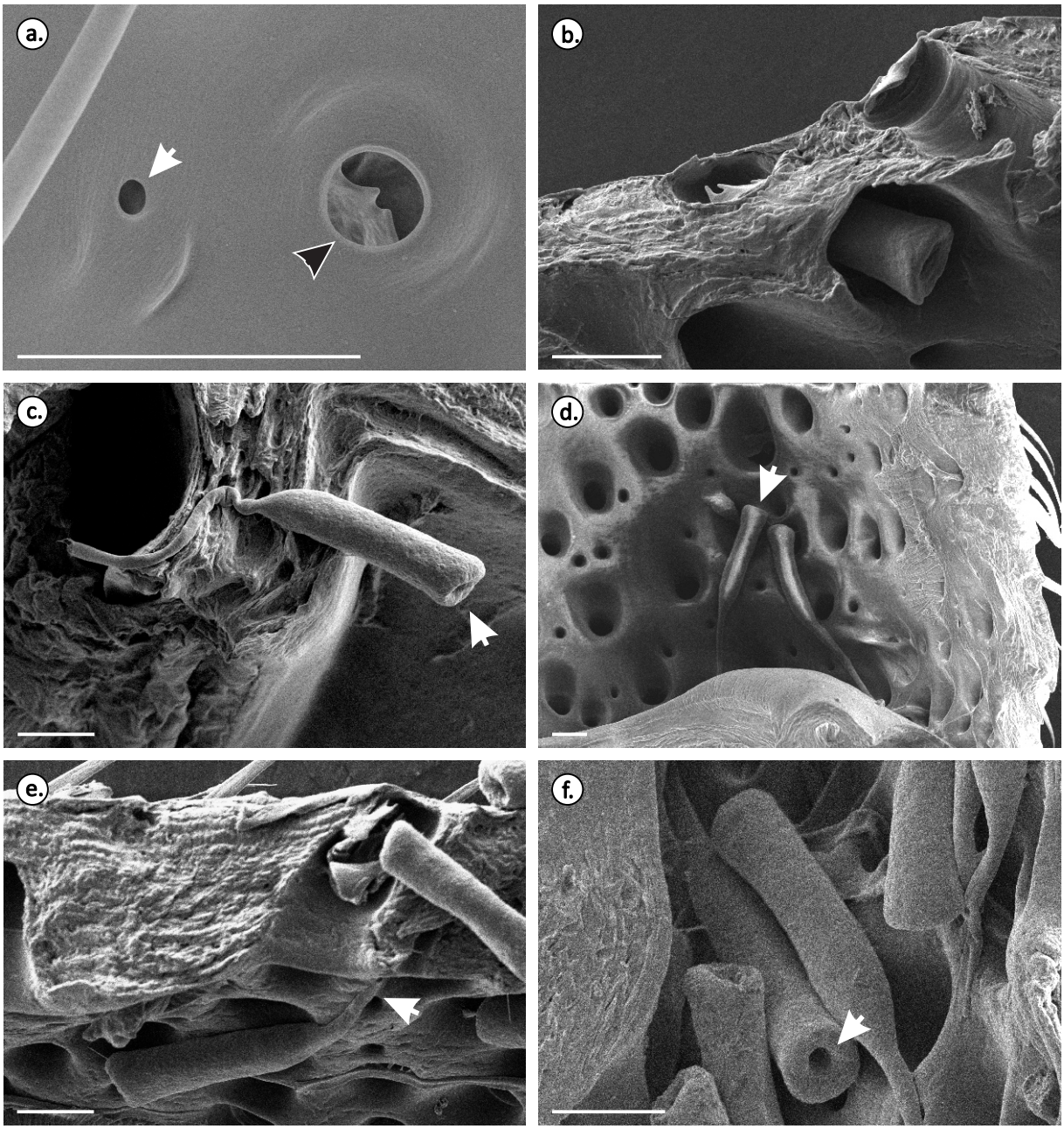

Figure 2.6. Scanning electron micrographs of the internal and external structure of the apical segment of the antenna show sensilla ampullacea and coeloconica. (a) External structure of sensilla ampullacea (white arrows) and coeloconica (black arrow). (b) Cross-section through the antennal cuticle shows the peg of a sensillum coeloconicum within the chamber. (c) Detached ampoule of the sensillum ampullaceum reveals no porosity, but a single large opening (white arrow). (d) Micrograph of an uncoated specimen reveals the sensory peg within the enclosing ampoule of sensilla ampullacea (white arrow). (e) Cross-section through the cuticle shows a sensillum ampullaceum hanging within the antennal lumen by a slender tube (white arrow) connecting to the external opening. (f) Detached sensilla ampullacea showing opening for neural innervation (white arrow). All scale bars = 1µm.

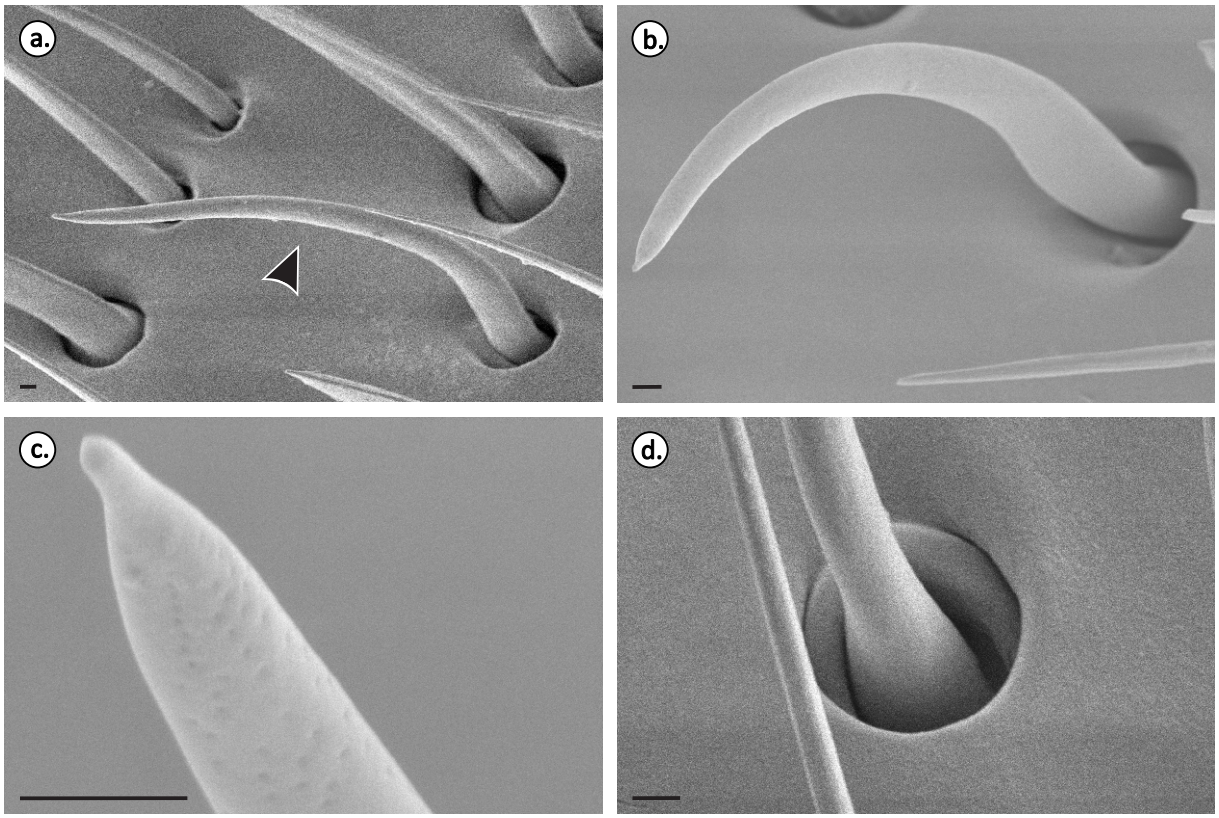

Figure 2.7. Scanning electron micrographs of trichoid-II sensilla. (a) Overview of the trichoid-II sensillum (black arrow) amongst other sensilla. (b) Top view of the sensillum. (c) Tip of the sensillum and the sparse pores that cover the majority of the peg. (d) Socket and base of the peg. All scale bars = 1µm.

Sensilla trichodea

These sensilla have slender pegs (width=2.0µm±0.2; n=53), which are comparable in length to sensilla basiconica (25.8µm±3.0; n=53). They have deep longitudinal grooves (**Figure 2.4a** to **c**) and an apical pore which was always observed in an either closed or collapsed state as seen in **Figure 2.4c** (this may be due to desiccation or to the high vacuum in the SEM column). The peg inserts into an opening surrounded by a region of smooth slightly depressed cuticle of oval shape (**Figure 2.4b**). In contrast to other sensilla that are angled towards the tip of the antenna, these sensilla project almost perpendicularly from the antennal surface, which makes them quite conspicuous. We are unaware of any studies that have identified the function of sensilla trichodea, but their close association with sensilla basiconica (a known contact chemoreceptor) and the presence of a large terminal pore in many ant species suggest that they may function as contact chemoreceptors (see Hashimoto, 1990b).

Sensilla trichodea curvata

Unlike most other sensilla, the peg is not comprised of a tapering cylinder but is instead bilaterally flattened and strongly bent towards the antennal tip (**Figure 2.5a**). As a result they are quite wide (5.1µm±0.5; n=77) for their length (25.7µm±3.1; n=77). These sensilla have pores arranged in a band of transverse rows that narrows proximally. The pores are extremely small (approximately 0.04 µm) and collectively appear as grooves at low magnification. Pores are absent from the base of the sensillum, from the dorsal ridge and also from the ventral surface (**Figure 2.5b** and **c**). The peg inserts into an opening in the cuticular surface without a socket. Intricate corrugations were observed at the ventral base of the sensillum (**Figure 2.5d**). The slender forms of this sensillum tapered to a sharp point, while the thicker forms had a bevelled tip (**Figure 2.5a** and **c**). Electrophysiological evidence indicates that sensilla trichodea curvata are sensitive to various volatile compounds, including alarm pheromones (e.g., *Lasius fuliginosus* Dumpert, 1972a).

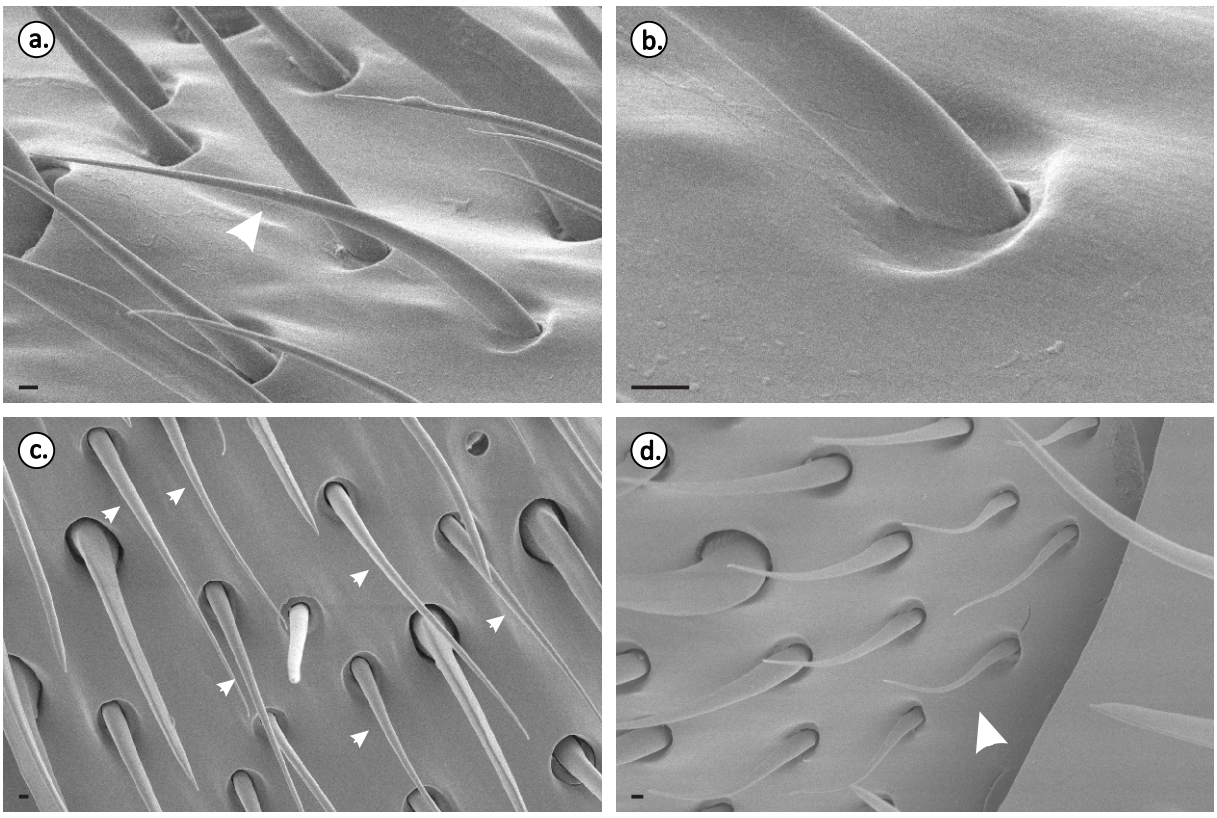

Figure 2.8. Scanning electron micrographs of sensilla chaetica. (a) Overview of a sensillum chaeticum (white arrow) amongst other sensilla. (b) Base of the peg and insertion into the cuticular surface. (c) Top view of several sensilla chaetica (white arrows) amongst other sensilla. (d) Small sensilla chaetica (white arrow) near the articulation between the apical and the preceding segment. All scale bars = 1µm.

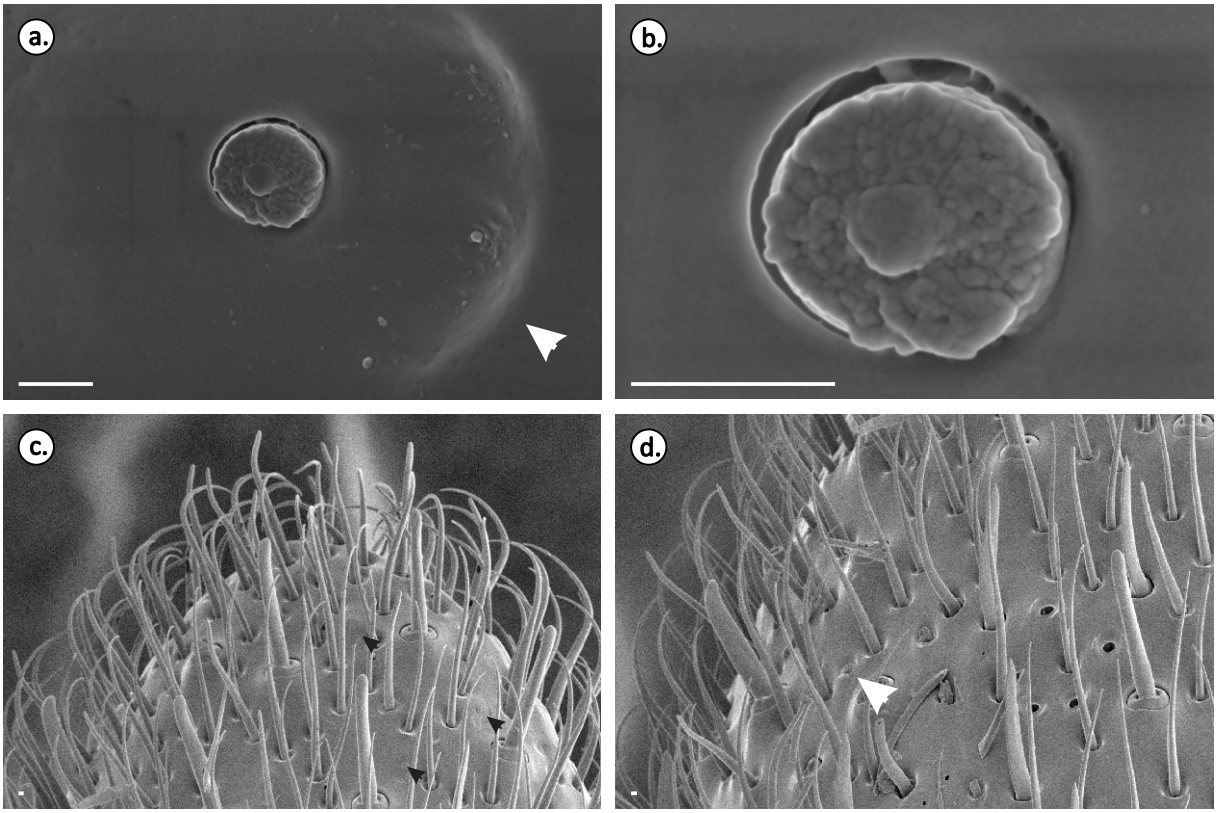

Figure 2.9. Scanning electron micrographs of coelocapitular sensilla. (a) Overview of a coelocapitular sensillum with surrounding depression of the cuticle (white arrow). (b) High magnification image of the peg with surface sculpturing. (c) Overview image of the tip of the apical segment of the antenna (ventral surface) showing inconspicuous coelocapitular sensilla (black arrows). (d) Overview image of a section of the apical segment of the antenna (ventral surface) showing broken sensillum (white arrow) resembling a coelocapitular sensillum. All scale bars = 1µm.

Sensilla ampullacea

Externally, sensilla ampullacea appear as small, round openings on the cuticular surface (diameter =0.8µm±0.1; n=63) (**Table 2.1**, **Figure 2.6a**, white arrow). Examination of the internal structure of the cuticle reveals a long, thin tube leading into a larger chamber or ampoule containing the sensory peg (**Figure 2.6c**). In uncoated samples the peg seems to collect electrical charge making it visible through the wall of the ampoule (**Figure 2.6d**, white arrow). The tube which connects the external opening to the ampoule traverses the entire thickness of the cuticle and allows the ampoule to hang inside the antennal lumen (**Figure 2.6e**). A round opening at the base of the chamber allows innervation of the sensillum (**Figure 2.6f**). Electrophysiological evidence from the leaf-cutter ants, *Atta cephalotes* and *Atta sexdens* indicates that sensilla ampullacea have a warm and a CO_2 receptor neuron (Kleineidam et al., 2000; Kleineidam and Tautz, 1996).

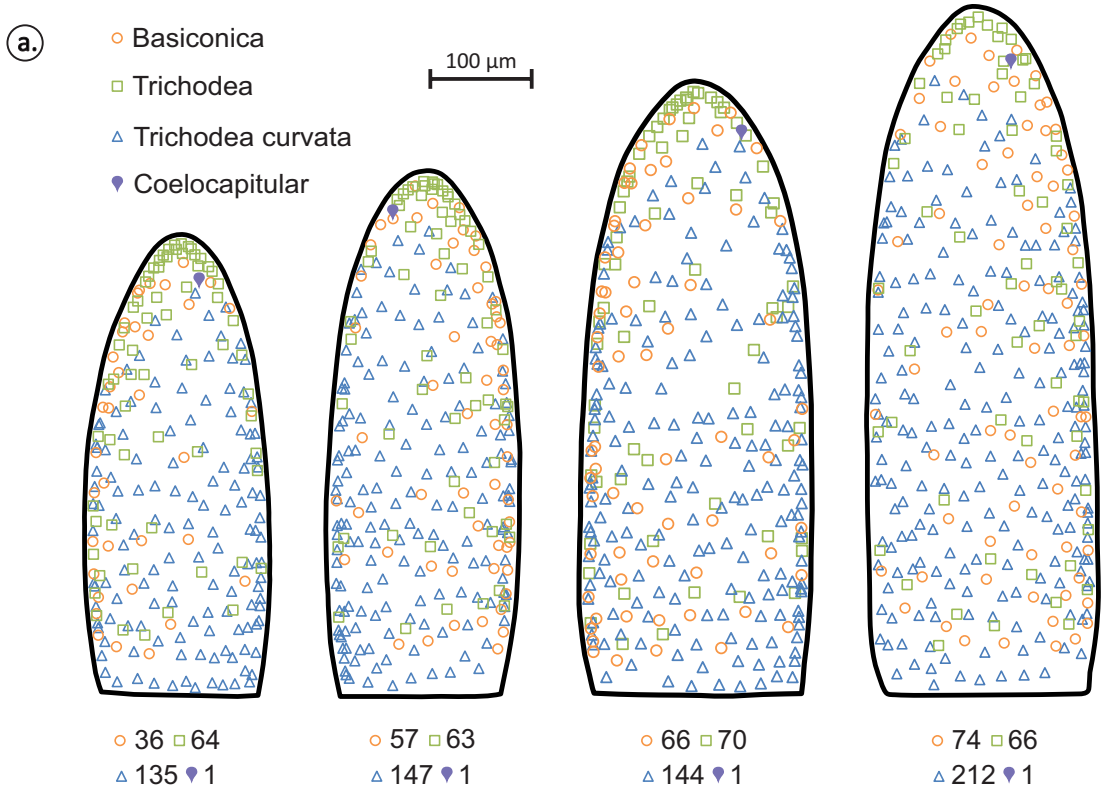

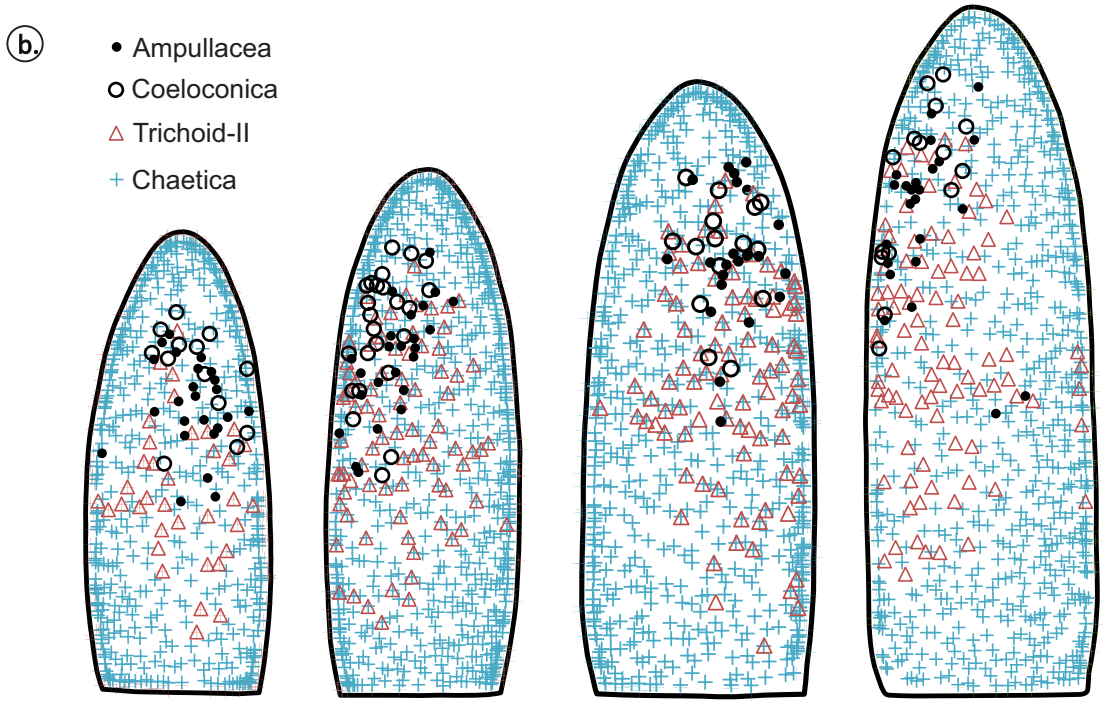

Specimen 2 (L)
Dorsal Surface
ASL=456µm
HW=2.4mm
BL=14.1mm

Specimen 4 (L)
Dorsal Surface
ASL=521µm
HW=2.8mm
BL=16.9mm

Specimen 5 (R)
Dorsal Surface
ASL=612µm
HW=3.8mm
BL=20.5mm

Specimen 7 (R)
Dorsal Surface
ASL=689µm
HW=3.9mm
BL=22.4mm

Figure 2.10. Distribution maps of different sensilla on the dorsal surface of the apical antennal segment in Myrmecia pyriformis workers. (a) Distribution of sensilla basiconica, sensilla trichodea, sensilla trichodea curvata, and coelocapitular sensilla. (b) Distribution of sensilla ampullacea, coeloconica, trichoid-II and chaetica. Numbers of each type of sensillum are shown together with the corresponding symbol. Each column corresponds to a single individual, various measures of size are given as apical segment length (ASL), head width (HW) and body length (BL). Data from right (R) and left (L) antennae (all right antennae have been mirror-imaged for ease of comparison with left antennae). It must be noted that although the density of sensilla appears to increase towards the margins of the segment this is due to the curvature of the antenna.

Sensilla coeloconica

In these sensilla the external opening is substantially larger than in sensilla ampullacea (diameter=2.5µm±0.3; n=56) making the tip of the sensory peg occasionally visible just below the surface (**Figure 2.6a**, black arrow). The peg of sensilla coeloconica is contained within a chamber embedded within the antennal cuticle and it possesses a bilaterally flattened end with a number of points (**Figure 2.6a** and **b**). Rutchy et al. (2009) measured sensory neuron activity and established that sensilla coeloconica responds to changes in atmospheric temperature.

Trichoid-II sensilla

The peg is long and tapering (length=32.8µm±3.5; width=2.6µm±0.3; n=60), it can be either straight or curved (**Figure 2.7a** and **b**) ending in a 'pinched' tip (**Figure 2.7c**). Pores are present along the length of the sensillum, but they are much sparser than in sensilla basiconica and sensilla trichodea curvata, there is also no visible apical pore. The peg inserts into an opening in the antennal surface where a cuticular half ring appears to surround the base of the peg where it inserts into the opening (**Figure 2.7d**). To our knowledge the only other ant, in which this sensillum has been documented is *Camponotus japonicus* and it is not clear what its function may be (Nakanishi et al., 2009). It has also been observed in other Hymenoptera including parasitoid wasps (Bethylidae) and in honeybees (Apidae) where it has been referred to as sensilla trichodea II and sensilla trichodea B respectively (Li et al., 2011; Suwannapong et al., 2012). We believe that in the past this sensillum has been grouped with sensilla trichodea curvata as they can look very similar

at low magnification or in information-poor images (e.g. low resolution, low contrast, blurry, etc.).

Sensilla chaetica

These are slender hair-like sensilla (width=2.0µm±0.4; n=97) (**Figure. 2.8a-c** white arrows) which vary in length (34.9µm±7.1; n=97), with the shortest found in the area just ahead of the joint with the next segment (**Figure 2.8d**, white arrows) and the longest found just below, projecting over the joint. They have smooth surfaces, appear not to have any pores and lack a socket (**Figure 2.8b**). Such filliform sensilla that have no pores, striations or openings are usually considered to be mechanoreceptors (Dumpert, 1972b; Marques-Silva et al., 2006; McIver, 1975).

Coelocapitular sensilla

These sensilla are quite small and inconspicuous. They appear as small, nub-like projections (diameter=1.4µm±0.1; n=5) around which there is a circular depression of the surrounding cuticle (**Figure 2.9a** and **b**). At higher magnification the external surface of the 'nub' or peg appears highly convoluted with spongy looking, globular irregularities with no visible pores (see **Figure 2.9b**). At low magnification this inconspicuous sensillum (**Figure 2.9c**, black arrows) resembles the stumps left behind by broken sensilla (**Figure 2.9d**, white arrow). It is also present in *C. japonicus* (Nakanishi et al., 2009), in honeybees (Yokohari et al., 1982), and in other insect orders such as Coleoptera and Mantophasmatodea (Drilling and Klass, 2010; Giglio et al., 2008). This type of sensillum has been thoroughly studied in the honeybee where its anatomy has been described, its function tested electrophysiologically and its neural connections to the glomeruli mapped (Nishino et al., 2009; Yokohari, 1983; Yokohari et al., 1982). This sensillum acts as both a hygro- and a thermoreceptor.

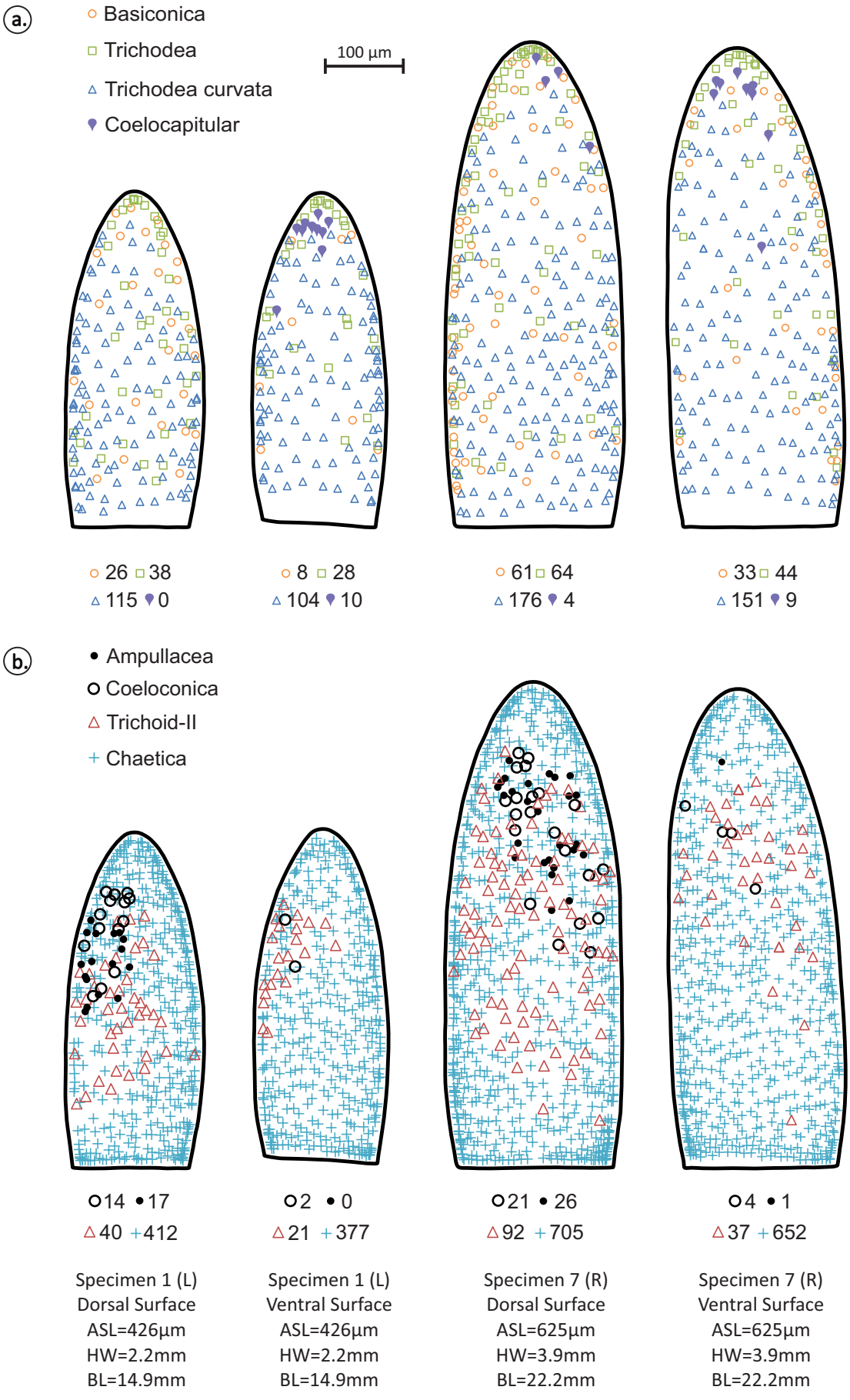
a.
Basiconica
Trichodea
Trichodea curvata
Coelocapitular
100 µm
26 38
115 0
8 28
104 10
61 64
176 4
33 44
151 9
b.
Ampullacea
Coeloconica
Trichoid-II
Chaetica
14 17
40 412
2 0
21 377
21 26
92 705
4 1
37 652
Specimen 1 (L)
Dorsal Surface
ASL=426µm
HW=2.2mm
BL=14.9mm
Specimen 1 (L)
Ventral Surface
ASL=426µm
HW=2.2mm
BL=14.9mm
Specimen 7 (R)
Dorsal Surface
ASL=625µm
HW=3.9mm
BL=22.2mm
Specimen 7 (R)
Ventral Surface
ASL=625µm
HW=3.9mm
BL=22.2mm

Figure 2.11. Distribution maps of different sensilla on the dorsal and ventral surface of the apical antennal segment in *Myrmecia pyriformis* workers. (a) Distribution of sensilla basiconica, sensilla trichodea, sensilla trichodea curvata, and coelocapitular sensilla. (b) Distribution of sensilla ampullacea, coeloconica, trichoid-II and chaetica. Numbers of each type of sensillum are shown together with the corresponding symbol. The first two columns correspond to a small individual (column 1 = dorsal, column 2 = ventral, as indicated) and the last two columns to a large individual. Various measures of size are given as apical segment length (ASL), head width (HW) and body length (BL). Data from right (R) and left (L) antennae (all right antennae have been mirror-imaged for ease of comparison with left antennae). It must be noted that although the density of sensilla appears to increase towards the margins of the segment this is due to the curvature of the antenna.

2.3.3. Distribution of sensilla in the apical segment

Dorsal surface

Each of the eight types of sensillum identified in *M. pyriformis* has a specific distribution and occupies distinct regions of the dorsal side of the apical segment. Among the chemoreceptors, sensilla trichodea curvata (**Figure 2.5**) were the most abundant sensilla present throughout the dorsal surface of the apical segment, except at the extreme tip (**Figure 2.10a**, blue triangles). Sensilla basiconica (**Figure 2.3**) were the least common chemoreceptors but were fairly evenly distributed along the surface of the apical segment (**Figure 2.10a**, orange circles). However, they were missing from a small area around the tip and were sometimes more prominent towards one of the sides. Sensilla basiconica were often found paired with sensilla trichodea (**Figure 2.4**) with the latter always being the more distal of the two. This is similar to what has been observed in *Solenopsis invicta* (Renthal et al., 2003) and various other ant species (Hashimoto, 1990b). Sensilla trichodea also occur unpaired and this is particularly evident at the tip of the apical segment where they are present in unusually high numbers (**Figure 2.10a**, green squares). Apart from this area of high density, sensilla trichodea occur evenly throughout the apical segment but are absent at its base. The rarest sensillum overall was the coelocapitular sensillum (**Figure 2.9**) which only occurred between one to four times per dorsal apical segment and was altogether missing in some individuals; when present this sensillum was found close to the tip (**Figure 2.10a**, **2.11a**, purple pointers). Conversely, the most common and abundant sensilla are sensilla chaetica (**Figure 2.8**), which are found throughout the apical segment (**Figure 2.10b**, blue crosses).

Trichoid II sensilla (**Figure 2.7**) are present in numbers similar to sensilla trichodea and basiconica, and are found in the middle portion of the apical antennomere (**Figure 2.10b**, red triangles). Both sensilla ampullacea and coeloconica (**Figure 2.6**) are typically found together and exhibit a clumped distribution in the sub-apical region of the segment (**Figure 2.3b**, black closed and open circles).

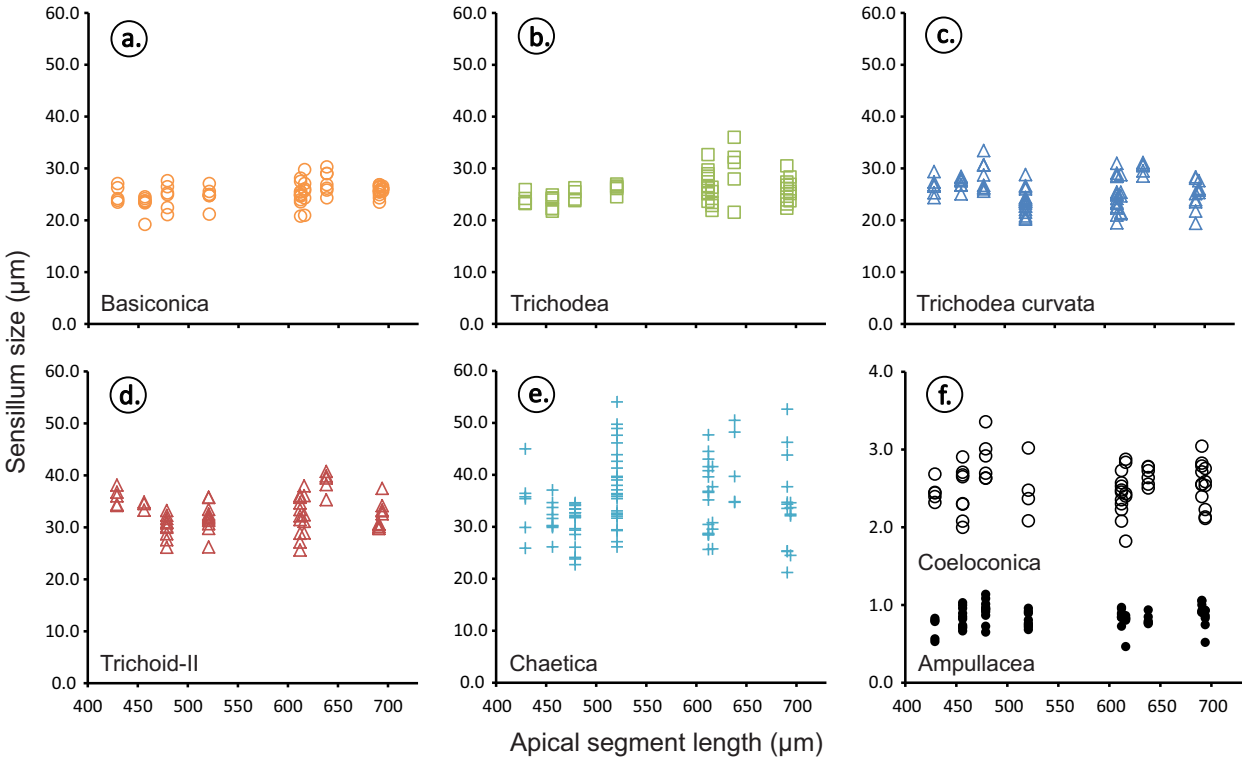

Figure 2.12. Size variation of sensilla in nine differently sized *Myrmecia pyriformis* workers. Sensillum size is shown for (a) sensilla basiconica, (b) trichodea, (c) trichodea curvata, (d) trichoid-II, (e) chaetica and (f) sensilla coeloconica (open circles) and ampullacea (closed circles). Sensillum size refers to sensillum length in panels a-e (extracuticular sensilla) and diameter of the opening for panel f (intracuticular sensilla). The data of individual scatterplots are arranged in columns, which represent individuals of different sizes corresponding to specimens 1 to 9 from left to right.

Ventral Surface

While the distribution of sensilla is very similar in the dorsal and ventral surfaces, the abundance of certain types of sensillum drops very noticeably on the ventral surface. The main differences are that there are far fewer sensilla basiconica, trichodea and trichoid-II sensilla on the ventral surface (**Figure 2.11**). Sensilla ampullacea and coeloconica are extremely rare and sometimes absent from the ventral surface but the abundance of sensilla

trichodea curvata and chaetica does not change much (**Figure 2.11**). Lastly, and in contrast to all other sensillum types, coelocapitular sensilla are most abundant on the ventral surface (**Figure 2.11**). Interestingly, there are ten coelocapitular sensilla in the small worker (D1) and nine in the large worker (D2) which suggests that individuals, regardless of size, may have a very similar total number of coelocapitular sensilla on the ventral surface of the apical segment. Similarly, in *C. japonicus* six coelocapitular sensilla are present on the ventro-lateral side of the apical segment of the workers of *C. japonicus* (Nakanishi et al., 2009).

Sensilla campaniformia

We did not observe these sensilla on the ventral or dorsal surfaces of the apical segment of *M. pyriformis*. However, sensilla campaniformia have been described in a number of ants including *Lasius fuliginosus*, *Dinoponera lucida* and *Solenopsis invicta* (Dumpert, 1972b; Marques-Silva et al., 2006; Renthal et al., 2003). These sensilla are rare and their location on the antennae seems to vary between species. About 3-4 of these sensilla occur on the apical segment in *L. fuliginosus* (Dumpert, 1972b), about 3-4 on the most proximal funicular segment (see **Figure 2.1a**) but not elsewhere on the funiculus in *S. invicta* (Renthal et al., 2003) and about 2-3 on the apical segment of *D. lucida* (Marques-Silva et al., 2006). It is worth noting that there have been instances of sensilla coelocapitular being mistakenly named sensilla campaniformia (see Yokohari, 1983).

Table 2.1. Numbers of each type of sensillum on the dorsal surface of the apical segment of *Myrmecia pyriformis*. The split-level rows show the absolute number of sensilla (unshaded rows) and the number of sensilla relative to the apical segment area (shaded rows). Each row represents a different worker ant labelled from 1 to 9. BL=Body Length (mm), HW=Head Width (mm), ASL=Apical Segment Length (µm), ASA=Apical Segment Area (µm^2).

	BL	HW	ASL	ASA	Basiconica	Trichodea	Trichodea curvata	Coelocapitular	Ampullacea	Coeloconica	Trichoid-II	Chaetica	Σ
1	14.9	2.2	426	630	26	38	115	0	17	14	40	412	662
					0.04	0.06	0.18	0.00	0.03	0.02	0.06	0.65	1.05
2	14.1	2.4	456	670	36	64	135	1	24	13	36	484	792
					0.05	0.10	0.20	0.00	0.04	0.02	0.05	0.72	1.18
3	13.8	2.2	479	710	34	49	143	2	21	12	51	443	753
					0.05	0.07	0.20	0.00	0.03	0.02	0.07	0.62	1.06
4	16.9	2.8	521	890	57	63	147	1	24	24	81	633	1029
					0.06	0.07	0.17	0.00	0.03	0.03	0.09	0.71	1.16
5	20.5	3.8	612	1150	66	70	144	1	22	15	90	547	954
					0.06	0.06	0.13	0.00	0.02	0.01	0.08	0.48	0.83
6	19.2	3.6	618	1290	60	69	202	0	24	17	107	690	1169
					0.05	0.05	0.16	0.00	0.02	0.01	0.08	0.53	0.91
7	22.2	3.9	625	1090	61	64	176	4	26	21	92	705	1149
					0.06	0.06	0.16	0.00	0.02	0.02	0.08	0.65	1.05
8	22.4	3.9	689	1090	74	66	212	1	24	15	91	706	1188
					0.07	0.06	0.19	0.00	0.02	0.01	0.08	0.65	1.09
9	21	3.9	697	1290	85	81	216	0	21	26	105	697	1231
					0.07	0.06	0.17	0.00	0.02	0.02	0.08	0.54	0.95

2.3.4. Number and size of sensilla

Numbers

Among *M. pyriformis* individuals, the number of sensilla on the apical antennomere tends to increase with the size of the antennomere (**Table 2.1**). This is true across all types of sensilla except in the case of the three types of intracuticular sensilla (sensilla ampullacea, coeloconica and coelocapitular) which all seem to have relatively stable numbers across different sized workers. This is particularly evident in the case of sensilla ampullacea where, irrespective of size, there are 21-24 sensilla present on the dorsal surface. In other species, however, this number is not conserved. There are about half as many sensilla ampullacea in the extremely large *Atta sexdens*, and all other species, regardless of size, have similar numbers as *A. sexdens* (see **Table 2.3**). A similar trend is also observed in sensilla coeloconica but there is not much information on sensilla coelocapitular. Meanwhile, the extracuticular sensilla (all other types studied here) seem to increase proportionally with increasing apical segment area (see **Table 2.1**, shaded rows). In sensilla basiconica the number of sensilla per unit area seems to consistently increase with increasing apical segment size but the increase is very small and similar consistent changes are not observed in the other sensillum types. Therefore, based on this small sample, it seems most likely that the numbers of extracuticular sensilla in *M. pyriformis* scale proportionally. This increase in sensillum numbers with size, however, does not hold true in other studied species. For instance, in the polymorphic ant *C compressus*, minor workers have the highest numbers of sensilla basiconica, trichodea and trichodea curvata despite having shorter apical segments (345μm) relative to the majors (407μm) (Mysore et al., 2010).

Unfortunately direct comparisons of the absolute numbers of sensilla between species are difficult to make because either different areas of the antenna were studied or abundance was estimated in different ways (see **Table 2.3**). However, we can still make some rough comparisons. For instance, **Table 2.3** shows that minor workers of *M. pyriformis* and *Camponotus japonicus* have similar head widths and similar numbers of sensilla basiconica, trichodea, and trichodea curvata. But, because the numbers available for *M. pyriformis* represent the abundance of sensilla on the dorsal surface alone while in *C. japonicus* the whole apical segment is represented we can conclude that *M. pyriformis* must have nearly twice as many sensilla. This may be because the apical segment of *M. pyriformis* is

longer (456µm) than in major workers of *C. japonicus* (290µm). However, the similarly sized minor workers of *C. compressus* also have shorter apical segments (354µm) than *M. pyriformis* but seem to have many more sensilla. It is interesting to note that even within the *Camponotus* genus, ants of comparable sizes (minor worker of *C. compressus* and worker of *C. japonicus*) exhibit large variation in the number of sensilla basiconica (204 and 54), but very little variation in sensilla trichodea (61 and 60) and trichodea curvata (181 and 168). These differences point to the fact that size alone does not dictate the number of sensilla that are present across different species.

Table 2.2. Dimensions of each type of sensillum on the dorsal surface of the apical segment of *Myrmecia pyriformis* (mean ± standard deviation). Peg l.: Peg length; Peg w.: Peg width. Measurements taken from all 9 individuals from Table 2.1. In the case of sensilla basiconica 'opening' refers to the maximum width of the socket, in sensilla ampullacea and coeloconica to the maximal width of the external opening of the sensilla and in trichoid-II sensilla to the maximum width of the opening in the cuticular surface around the base of the peg.

	Basiconica	Trichodea	Trichodea curvata	Coelocapitular	Ampullacea	Coeloconica	Trichoid-II	Chaetica
Peg l. (µm)	25.2 ± 2.1	25.8 ± 3.0	25.7 ± 3.1	N/A	N/A	N/A	32.8 ± 3.5	34.9 ± 7.1
Peg w. (µm)	3.9 ± 0.4	2.0 ± 0.2	5.1 ± 0.5	N/A	N/A	N/A	2.6 ± 0.3	2.0 ± 0.4
'Opening' (µm)	7.9 ± 0.7	N/A	N/A	1.4 ± 0.1	0.8 ± 0.1	2.5 ± 0.3	4.7 ± 0.4	N/A
Area (µm²)	97.5 ± 15.2	35.5 ± 6.5	83.5 ± 12.2	1.4 ± 0.1	0.5 ± 0.1	4.1 ± 1.0	49.6 ± 7.7	38.0 ± 15.6
n (sensilla)	65	53	77	5	63	56	60	97

It is likely that the lifestyle of a species plays a significant role in the ratios of sensilla found on the antennae. For instance, workers of *M. pyriformis* are nocturnal (Narendra et al., 2010) and are exclusively solitary foraging animals, whereas workers of *C. compressus* are strictly diurnal, forage individually, but also engage in tandem running (Narendra and Kumar, 2006). Another example may be the similarly sized *C. compressus* and *M. pyriformis* minors. The lower numbers of sensilla basiconica in *M. pyriformis* (**Table 2.3**) may reflect the simple social

structure of their colonies. Behavioural and immunohistochemical assays have shown that this sensillum is involved in the recognition of nest-mates' cuticular hydrocarbons (Ozaki et al., 2005). When foraging, *M. pyriformis* workers of the same colony do not seem to interact or recognise each other (AN, personal observation), it seems likely that the relatively small number of sensilla basiconica may be correlated with this lack of recognition. From this perspective it would be interesting to know more about the function of sensilla, particularly which olfactory sensilla respond to what olfactory cues, and to see if it is possible to map differences in lifestyle onto changes in the antennal topography.

Finally, while it can be difficult to draw comparisons between different ant species due to differences in methodology, it seems that in general, in the apical antennomere, sensilla chaetica are the most abundant, while sensilla coelocapitular, coeloconica and ampullacea are the least abundant sensilla (**Table 2.3**).

Table 2.3. Abundances of each type of sensillum in different species of ants as reported in available publications. The body size of each species is given as head width (HW) based on information from the relevant publication (labelled by number) or, when size is not reported, from measurements taken from photographed collection specimens found at www.antweb.org (largest size always reported unless data are given for multiple castes; labelled *). Area of the antenna studied and source publication as follows: [1]Dorsal surface of apical segment (present publication); [2]Not specified (Jaisson, 1969); [3]Entire surface of apical segment (Kleineidam et al., 2000); [4]Entire surface of apical segment (Mysore et al., 2010); [5]Entire surface of apical segment (Nakanishi et al., 2009); [6]Not specified (Marques-Silva et al., 2006); [7]Estimates of the entire surface of the apical segment reported here (Fresneau, 1979); [8]Entire surface of apical segment, examined by splitting the antennomere in two halves (Dumpert, 1972b); [9]Mysore et al. (2009).

	HW (mm)	Basiconica	Trichodea	Trichodea curvata	Coelocapitular	Ampullacea	Coeloconica	Trichoid-II	Chaetica
Myrmecia pyriformis (minor)[1]	2.4[1]	36	64	135	1	24	13	36	484
Myrmecia pyriformis (major)[1]	3.9[1]	85	81	216	0	21	26	105	697
Aphaenogaster gibbosa[2]	0.9*					8	4		
Atta sexdens[3]	4.9*					10			
Camponotus compressus (minor)[4]	2.3[9]	204	61	181					
Camponotus compressus (medium)[4]	4.0[9]	188	57	167					
Camponotus compressus (major)[4]	5.6[9]	157	43	139					
Camponotus japonicus[5]	2.5*	54	60	168	6	10	10	60	823
Dinoponera lucida[6]	5.1*						8		
Formica polyctena[7]	2.4*	43		62		9	6		
Lasius fuliginosus[8]	1.6*	36	69	152		9	8		440
Myrmica laevinodis[2]	1.0*					9	8		

Size

The size of some sensilla varies not only between species, but also within a single species and surprisingly even within individuals (see **Figure 2.12**, **Table 2.2** and **2.4**). In *M. pyriformis*, the peg length was most variable, particularly in sensilla chaetica and trichodea, while the peg diameter in each sensillum type did not vary much. Some individuals displayed a larger range of sensillum size than others (**Figure 2.12**). However, this is probably due to the small number of sensilla that were sampled. For each individual we measured a minimum of 5 sensilla of each type. This is a substantial proportion of the total sensillum population for certain types such as sensilla coeloconica and ampullacea but a tiny fraction for others. Therefore, at the individual level, this may not capture a complete picture of the size variation. Despite this, the overlapping ranges of small and large individuals indicate that there is no clear trend of increase in the size of sensilla with increase in the size of the apical segment. It is possible that individuals with larger apical segments may have a sensillum population that is biased towards larger sensilla but, if present, this bias must be relatively subtle as it is not apparent in our data. A comparison across different species indicates that the dimensions of sensilla trichodea,

trichodea curvata, ampullacea and coeloconica observed in *M. pyriformis* were consistent with those found in other species while other sensilla varied in size across species. This indicates that the large apical segment of *M. pyriformis* does not lead to a consistent increase in the size of sensilla.

The variability in sensillum length and other parameters, which was observed in individuals of *M. pyriformis* may be related to the local architecture of the apical segment. The array of sensilla on this antennomere is the most complex in the antenna and because of the limited amount of space there must be trade-offs at play. In the case of chemoreceptors, at least, it is beneficial to increase the surface area of the sensillum (Wicher, 2012), but in order to maximise the total receptivity of the apical antennomere to different types of information it may be worthwhile to sacrifice the size of some sensilla in order to be able to fit larger numbers of them. Thus it may be that any given sensillum may vary in size depending on what other sensilla are around it and how much space they take up, both above and below 'ground'. If this is the case it would be expected that on more proximal antennomers where space is not at such a prime, and sensilla are not so closely packed, the size of sensilla of a particular type would be much less variable.

Table 2.4. Size of sensilla across different species. Peg l.: Peg length; Peg w.: Peg width. Source publications: for [1-9] see Table 2.3; [10](Barsagade et al., 2013); [11](Renthal et al., 2003). All measurements are given in µm.

	Basiconica	Trichodea	Trichodea curvata	Ampullacea	Coeloconica	Trichoid-II	Chaetica
Myrmecia pyriformis[1]	Peg l. 24.4 Peg w. 3.8	Peg l. 24.9 Peg w. 2.8	Peg l. 25.5 Peg w. 5.1	Opening 0.9	Opening 2.5	Peg l. 31.1 Peg w. 2.7	Peg l. 34.3 Peg w. 1.9
Atta sexdens[3]				Opening 1 to 2			
Camponotus compressus[10]	Peg l. 5.7 Peg w. 1.2						
Camponotus japonicus[5]	Peg l. 20.0 Peg w. 6.0	Peg l. 20.0 Peg w. 2.0	Peg l. 30.0 Peg w. 6.0	Opening <1	Opening 1.2	Peg l. 70.0 Peg w. 3.0	
Dinoponera lucida[6]							Peg l. 20-30; 140-160
Solenopsis invicta[11]	Peg l. 13.0 Peg w. 3.0		Peg l. 15-25 Peg w. 1.0-2.5				

2.4. Conclusions

As discussed in the introduction, workers of *M. pyriformis* have highly developed vision and forage solitarily (do not follow foraging trails), spending large portions of their foraging bouts in an arboreal environment. Such marked visual specialisation can lead to a decrease in investment in other senses. This kind of trade-off has been previously observed in other taxa, for example a review of mammalian sensory interactions revealed that arboreal species (although *M. pyriformis* is not strictly arboreal) tended to exhibit a greater investment in visual structures and a lesser investment in olfactory ones (Nummela et al., 2013). This makes sense as sensory systems are metabolically expensive to maintain (Niven and Laughlin, 2008). If greater elaboration in one sensory system can reduce reliance on another, evolutionarily there is strong pressure to reduce investment on the latter. The catch here is that one sensory system may furnish an animal with a particular type of information that another sensory system, no matter how elaborate, may not be able to provide. Whether trade-offs between sensory systems can take place or not is up for debate and the answer is likely to be highly dependent on the specific sensory requirements of a given animal.

This study found that workers of *M. pyriformis* have an antennal array comparable to that of other species in terms of the sensilla type, size and numbers. This indicates that the heavy reliance on vision of *M. pyriformis* does not have detrimental effects on their level of investment on antennal sensilla. Whether this holds true in terms of the underlying neural circuitry associated with the antennae is not known at this point. However, the apparent absence of a trade-off between senses perhaps should not come as a surprise. Although *M. pyriformis* does not follow pheromone trails it must still respond to chemical social cues within the colony, a function that cannot be replaced by vision. Furthermore, within the dark environment of the nest tactile and chemosensory cues must supersede vision. In this case, both visual and antennal arrays provide very different types of information that guide animals through different facets of their lives.

Of the eight sensilla we identified in *M. pyriformis* six have been concurrently described in a variety of other ants (Dumpert, 1972b; Hashimoto, 1990b; Renthal et al., 2003), other studies have identified subsets of these six sensilla (Marques-Silva et al., 2006; Mysore et al., 2010; Ozaki et al., 2005), while Nakanishi et al. (2009) found all eight types. While we observed coelocapitular sensilla on the antennae of *M.*

pyriformis many studies on other ant species do not report their presence. Conversely, we did not observe sensilla campaniformia while studies on other species have. However, it is not entirely clear whether both of these are present in ants or if both names have been used to refer to the same type of sensillum (see Yokohari, 1983). Furthermore, these sensilla tend to occur in very low numbers and are very small and inconspicuous, often resembling the stumps of broken sensilla (see **Figure 2.9c** and **d**). This would make them easy to miss and hard to identify, particularly when high quality, high magnification images are not available. Similarly the trichoid-II sensillum has only been described in *M. pyriformis* and *C. japonicus*. However, this receptor can be extraordinarily hard to distinguish from sensilla trichodea curvata or sensilla chaetica at low magnifications and has most likely been identified as one of these two types in the past; it is not until the eye has been trained to identify specific diagnostic features that it becomes apparent at all. Therefore, it is probable that most differences in the types of sensilla described for different species are not due to actual differences in the array but due to differences in classification, the difficulty in distinguishing between similar sensilla and, on occasion misidentification of sensilla.

With respect to the size and numbers of sensilla it is hard to draw firm conclusions about differences across different species from the information that is currently available (see **Table 2.4**). The main change observed was a reduction in the number of sensilla basiconica in *M. pyriformis* relative to other species; as discussed above, this may tie in with the simple social structure of *M. pyriformis* colonies. This observation along with other factors, such as the variability among species in the ratios at which different types of sensilla are found, lead us to speculate that, while certain aspects of the antennal array, such as the total number of sensilla, may be explained to some degree by the size of the animal and the size of the apical segment, it appears that lifestyle may play an important role in shaping the antennal array. However, three types of sensilla seem to be less prone to variability. Numbers of sensilla ampullacea, coeloconica and coelocapitular across species seem to be very similar indicating that these sensilla have very little to do with lifestyle specialisations and that they must provide essential information for life in an ant colony. This is consistent with their function as monitors of ambient temperature and CO_2 levels, factors that would appear to be important environmental conditions in ant colonies with limited ventilation.

Within *M. pyriformis* it seems that the size of sensilla does not increase with the size of the worker while the numbers do (see **Figure 2.12** and **Table 2.1** respectively). Furthermore, the number of sensilla seemed to

increase proportionally with worker size. While this seems intuitive, the scenario is exactly the opposite in *C. compressus* (Mysore et al., 2010) where the number of sensilla decreased with increasing worker size (see **Table 2.3**). It remains to be tested whether: (a) large workers of *M. pyriformis* need better chemoreceptive abilities or (b) the major workers of *C. compressus* have fewer sensilla since they typically do not engage in foraging, unlike in *M. pyriformis* where animals of all sizes engage in foraging. We suspect the latter to be the most likely scenario.

2.5. References

Altner, H., Prillinger, L., 1980. Ultrastructure of invertebrate chemo-, thermo-, and hygroreceptors and its functional significance. International Review of Cytology 67, 69-139.

Barsagade, D.D., Tembhare, D.B., Kadu, S.G., 2013. Microscopic structure of antennal sensilla in the carpenter ant *Camponotus compressus* (Fabricius)(Formicidae: Hymenoptera). Asian Myrmecology 5, 113-120.

Drilling, K., Klass, K.-D., 2010. Surface structures of the antenna of Mantophasmatodea (Insecta). Zoologischer Anzeiger-A Journal of Comparative Zoology 249, 121-137.

Dumpert, K., 1972a. Alarmstoffrezeptoren auf der Antenne von *Lasius fuliginosus* (Latr.)(Hymenoptera, Formicidae). Journal of Comparative Physiology A 76, 403-425.

Dumpert, K., 1972b. Bau und Verteilung der Sensillen auf der Antennengeißel von *Lasius fuliginosus* (Latr.)(Hymenoptera, Formicidae). Zoomorphology 73, 95-116.

Frazier, J.L., 1985. Nervous System: Sensory System, In: Blum, M.S. (Ed.), Fundamentals of Insect Physiology. Wiley-Interscience, New York, pp. 287-356.

Fresneau, D., 1979. Étude du role sensoriel de l'antenne dans l'ethogenese des soins aux cocons chez *Formica polyctena* Forst (Hymenoptera: Formicidae). Insectes Sociaux 26, 170-195.

Giglio, A., Brandmayr, P., Ferrero, E.A., Perrota, E., Romeo, M., Zetto, T., Talarico, F., 2008. Comparative antennal morphometry and sensilla distribution pattern of three species of Siagoninae (Coleoptera, Carabidae), In: Penev, L., Erwin, T., Assmann, T. (Eds.), Back to the Roots and Back to the Future: Towards a New Synthesis Amongst Taxonomic, Ecological and Biogeographical Approaches in Carabidology. Pensoft, Sofia-Moscow, pp. 143-158.

Greiner, B., Narendra, A., Reid, S.F., Dacke, M., Ribi, W.A., Zeil, J., 2007. Eye structure correlates with distinct foraging-bout timing in primitive ants. Current Biology 17, R879-R880.

Hashimoto, Y., 1990a. Phylogenetic study of Formicidae based on the sensillum structures of the antenna and mouthparts, Graduate School of Science and Technology. Kobe University, Kobe, p. 95.

Hashimoto, Y., 1990b. Unique features of sensilla on the antennae of Formicidae (Hymenoptera). Applied Entomology and Zoology 25, 491-501.

Jaisson, P., 1969. Étude de la distribution des organes sensoriels de l'antenne et de leurs relations possibles avec le comportement chez deux fourmis myrmicines: *Myrmica laevinodis* Nyl. et

Aphaenogaster gibbosa Latr. récoltées dans la région des Eyzies. Insectes Sociaux 16, 279-312.

Jayatilaka, P., Narendra, A., Reid, S.F., Cooper, P., Zeil, J., 2011. Different effects of temperature on foraging activity schedules in sympatric *Myrmecia* ants. The Journal of Experimental Biology 214, 2730-2738.

Kleineidam, C., Romani, R., Tautz, J., Isidoro, N., 2000. Ultrastructure and physiology of the CO_2 sensitive sensillum ampullaceum in the leaf-cutting ant *Atta sexdens*. Arthropod Structure and Development 29, 43-55.

Kleineidam, C., Tautz, J., 1996. Perception of carbon dioxide and other "air-condition" parameters in the leaf cutting ant *Atta cephalotes*. Naturwissenschaften 83, 566-568.

Li, X., Lu, D., Liu, X., Zhang, Q., Zhou, X., 2011. Ultrastructural characterization of olfactory sensilla and immunolocalization of odorant binding and chemosensory proteins from an ectoparasitoid *Scleroderma guani* (Hymenoptera: Bethylidae). International journal of biological sciences 7, 848.

Marques-Silva, S., Matiello-Guss, C.P., Delabie, J.H.C., Mariano, C.S.F., Zanuncio, J.C., Serrão, J.E., 2006. Sensilla and secretory glands in the antennae of a primitive ant: *Dinoponera lucida* (Formicidae: Ponerinae). Microscopy Research and Technique 69, 885-890.

Masson, C., 1974. Quelques données sur l'ultrastructure de récepteurs gustatifs de l'antenne de la fourmi *Camponotus vagus* Scop. (Hymenoptera, Formicinae). Zeitschrift für Morphologie der Tiere 77, 235-243.

McIver, S.B., 1975. Structure of cuticular mechanoreceptors of arthropods. Annual Review of Entomology 20, 381-397.

Mysore, K., Shyamala, B.V., Rodrigues, V., 2010. Morphological and developmental analysis of peripheral antennal chemosensory sensilla and central olfactory glomeruli in worker castes of *Camponotus compressus* (Fabricius, 1787). Arthropod Structure & Development 39, 310-321.

Mysore, K., Subramanian, K.A., Sarasij, R.C., Suresh, A., Shyamala, B.V., VijayRaghavan, K., Rodrigues, V., 2009. Caste and sex specific olfactory glomerular organization and brain architecture in two sympatric ant species *Camponotus sericeus* and *Camponotus compressus* (Fabricius, 1798). Arthropod Structure & Development 38, 485-497.

Nakanishi, A., Nishino, H., Watanabe, H., Yokohari, F., Nishikawa, M., 2009. Sex-specific antennal sensory system in the ant *Camponotus japonicus*: structure and distribution of sensilla on the flagellum. Cell and Tissue Research 338, 79-97.

Narendra, A., Kumar, S.M., 2006. On A Trail With Ants: A Handbook of the Ants of Peninsular India. Tholasi Prints, Bangalore.

Narendra, A., Reid, S.F., Greiner, B., Peters, R.A., Hemmi, J.M., Ribi, W.A., Zeil, J., 2011. Caste-specific visual adaptations to distinct daily activity schedules in Australian *Myrmecia* ants. Proceedings of the Royal Society B: Biological Sciences 278, 1141-1149.

Narendra, A., Reid, S.F., Hemmi, J.M., 2010. The twilight zone: ambient light levels trigger activity in primitive ants. Proceedings of the Royal Society B: Biological Sciences 277, 1531-1538.

Narendra, A., Reid, S.F., Raderschall, C.A., 2013. Navigational efficiency of nocturnal *Myrmecia* ants suffers at low light levels. PloS one 8, e58801.

Nishino, H., Nishikawa, M., Mizunami, M., Yokohari, F., 2009. Functional and topographic segregation of glomeruli revealed by local staining of antennal sensory neurons in the honeybee *Apis mellifera*. The Journal of Comparative Neurology 515, 161-180.

Niven, J.E., Laughlin, S.B., 2008. Energy limitation as a selective pressure on the evolution of sensory systems. Journal of Experimental Biology 211, 1792-1804.

Nummela, S., Pihlström, H., Puolamäki, K., Fortelius, M., Hemilä, S., Reuter, T., 2013. Exploring the mammalian sensory space: co-operations and trade-offs among senses. Journal of Comparative Physiology A 199, 1077-1092.

Ozaki, M., Wada-Katsumata, A., Fujikawa, K., Iwasaki, M., Yokohari, F., Satoji, Y., Nisimura, T., Yamaoka, R., 2005. Ant nestmate and non-nestmate discrimination by a chemosensory sensillum. Science's STKE 309, 311.

Reid, S.F., Narendra, A., Hemmi, J.M., Zeil, J., 2011. Polarised skylight and the landmark panorama provide night-active bull ants with compass information during route following. Journal of Experimental Biology 214, 363-370.

Reid, S.F., Narendra, A., Taylor, R.W., Zeil, J., 2013. Foraging ecology of the night-active bull ant *Myrmecia pyriformis*. Australian Journal of Zoology 61, 170-177.

Renthal, R., Velasquez, D., Olmos, D., Hampton, J., Wergin, W.P., 2003. Structure and distribution of antennal sensilla of the red imported fire ant. Micron 34, 405-413.

Roces, F., Kleineidam, C., 2000. Humidity preferences for fungus culturing by workers of the leaf-cutting ant *Atta sexdens rubropilosa*. Insectes Sociaux 47, 348-350.

Rutchy, M., Romani, R., Kuebler, L.S., Ruschioni, S., Roces, F., Isidoro, N., Kleineidam, C.J., 2009. The thermo-sensitive sensilla coeloconica of leaf-cutting ants (*Atta vollenwenderi*). Arthropod Structure and Development 38, 195-205.

Soroker, V., Vienne, C., Hefetz, A., 1995. Hydrocarbon dynamics within and between nestmates in *Cataglyphis niger* (Hymenoptera: Formicidae). Journal of Chemical Ecology 21, 365-378.

Suwannapong, G., Noiphrom, J., Benbow, M.E., 2012. Ultramorphology of antennal sensilla in Thai single open nest honeybees (Hymenoptera: Apidae). LEPCEY: The Journal of Tropical Asian Entomology 1, 1-12.

Ward, P.S., Brady, S.G., 2003. Phylogeny and biogeography of the ant subfamily Myrmeciinae (Hymenoptera: Formicidae). Invertebrate Systematics 17, 605-605.

Wicher, D., 2012. Functional and evolutionary aspects of chemoreceptors. Frontiers in Cellular Neuroscience 6:48.

Wilson, E.O., 1972. The Insect Societies. The Belknap Press of Harvard University Press, Cambridge, Massachusetts

Yokohari, F., 1983. The coelocapitular sensillum, an antennal hygro- and thermoreceptive sensillum of the honey bee, *Apis mellifera* L. Cell and Tissue Research 233, 355-365.

Yokohari, F., Tominaga, Y., Tateda, H., 1982. Antennal hygroreceptors of the honey bee, *Apis mellifera* L. Cell and Tissue Research 226, 63-73.

2.6. Appendices

Appendix 2.1. Nomenclatures used by referenced studies in chronological order. When denominations are used that do not seem to correlate to an established type of sensillum these data are ignored. Highlighted are the terms which compose the nomenclature used herein.

Jaisson (1969)	Basiconica				Organes en forme de bouteille	Organes en "bouchon de champagne"		
Dumpert (1972)	Basiconica	Trichodea	Trichodea curvata		Ampullacea	Coeloconica		Chaetica
Fresneau (1979)	Basiconica		Trichodea curvata					
Hashimoto (1990)	Basiconica	Chaetica	Trichodea curvata		Ampullacea	Coeloconica		Bristle
Renthal et al. (2003)	Basiconica	Trichodea	Trichodea curvata		Ampullacea	Coeloconica		Trichodea
Marques-Silva et al. (2006)	Basiconica					Coeloconica		Trichodea
Nakanishi et al. (2009)	Basiconic	Chaetic-A	Trichoid-I	Coelocapitular	Ampullaceal	Coeloconic	Trichoid-II	Chaetic
Mysore et al. (2010)	Basiconica	Trichodea	Trichodea curvata					
Barsagade (2013)	Basiconica							Trichodea/ trichodea curvata?

Chapter 3

Intraspecific variation in sensory systems:
"The sensory arrays of the ant, Temnothorax rugatulus"

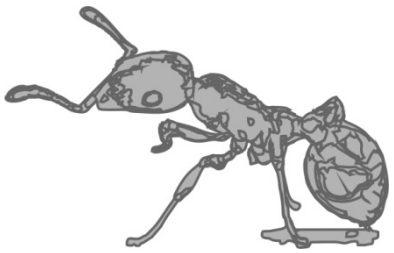

Chapter contents

The idea for this work arose out of conversations with a fellow PhD candidate, Nicole E. Leitner, who was studying the sensory systems of the ant *Temnothorax rugatulus* in Arizona University. We met while we were both training at the Wolfgang Rössler lab in Würzburg, Germany, learning techniques to study ant neuroanatomy. Previous studies had shown significant differences in the level of activity of seemingly uniform worker ants. Studying differences in the sensory arrays was a logical next step in this avenue of research. Nicole had trialled a number of light microscopy techniques trying to investigate the antennal array and had been unable to find differences in the total number of sensilla. Results from my work on *M. pyriformis* had made it apparent to me that the vast majority of sensilla on the antennae would be mechanoreceptors and that scanning electron microscopy would be better suited to detecting differences in olfactory sensilla. It was decided that I would attempt to re-examine the external antennal and visual arrays using SEM while Nicole attempted to identify differences in the anatomy of the antennal lobe in the brain and behavioural differences in olfactory discrimination. As a result of the mode of its conception this chapter represents a slight diversion from the main direction of this thesis. However, the opportunity to collaborate and cross-pollinate was too great to pass up. Furthermore, studying *T. rugatulus* provided me with a number of opportunities that fit well with the research interests addressed in this thesis.

T. rugatulus seemed like a good fit for my thesis for three main reasons. Its small size provided a first point of contrast with *M. pyriformis* and secondly permitted me to examine the whole antenna in detail for the first time. Lastly, having examined a polymorphic species I felt quantifying variation in a non-polymorphic species was important to defining an adequate sample size per species for the comparative dataset.

T. rugatulus worked well as a comparison species on the other size end of the spectrum to *M. pyriformis*. The two species have comparable ecologies despite their size differences and occurring in different continents. *M. pyriformis* workers generally travel 20m or less from the nest and forage individually, they don't follow pheromone trails; they either hunt insects in surrounding grass (e.g. small moths, spiders or earwigs) or climb a nearby eucalyptus tree in search of honeydew produced by sap sucking insects, (Narendra et al., 2013; Reid et al., 2013, personal observation FRE). *T. rugatulus* travel individually between 2 to 16 meters (Bengston and Dornhaus, 2013) foraging for small arthropods (Bengston and Dornhaus,

2013; Fisher and Cover, 2007). Their source of carbohydrates though unknown, is most likely honeydew from hemipterans or exudates from trees. They typically nest in preformed rock cavities, with colony size ranging between 50 to 400 individuals (Bengston and Dornhaus, 2013; Cao and Dornhaus, 2012). *M. pyriformis* nests vary from 50 to over 2200 workers (Reid et al., 2013) but nests at our study site for **Chapter 2** most likely contained only a few hundred workers[2]. Although, *M. pyriformis* nests were also terrestrial, unlike *T. rugatulus*, bull ant nests are multi-chambered and dug into the soil (Gray, 1974).

Both species inhabit cold semi-arid climates, they are terrestrial but may climb trees while foraging and inhabit visually comparable environments at our two study sites. Although the focal species of this chapter, *T. rugatulus* is distributed widely across the western forests of North America (see www.antwiki.org) at our study site in the Santa Catalina Mountains (Arizona, USA) the ants inhabit pine and juniper forests. These pine forests are somewhat sparsely wooded with an even sparser understory (Niering and Lowe, 1984). Their habitat substrate is often dry, rocky soil that may be blanketed by dense layers of fallen pine needles, likely offering very few proximate navigational cues (Bengston and Dornhaus, 2014; Creighton, 1950; Rüppell and Kirkman, 2005). Similarly, *M. pyriformis* in our study site inhabited temperate grassy woodlands characterised by native grasses and sparsely wooded with eucalyptus trees. During the warmer months when ants are active the heavy clay soils are quite hard and dry. *M. pyriformis* and *T. rugatulus* are not particularly closely related and belong to different subfamilies (*T. rugatulus*: Myrmicinae; *M. pyriformis*: Myrmeciinae).

Unfortunately, many of the precise details on the foraging ecology of *T. rugatulus* under natural conditions are unknown at present (e.g. mode of prey capture). However, it is evident that there are similarities between these two species. One prominent difference between these two species lies in the visual system. While *M. pyriformis* has extremely large, well-developed eyes with thousands of facets (see **Figure 2.1.**) *T. rugatulus* has much smaller eyes with under a hundred facets (see **Figure 3.6.**). This difference is likely to be reflected in their approach to tasks such as prey capture. *M. pyriformis* is a known active predator that can visually track its prey and chase after and jump after other insects (personal observation, FRE). In contrast, the prey capture strategies of *T. rugatulus* are not known. However, antennae are likely to play a more prominent role other

[2] These nests depend on eucalyptus trees and the population size of individual nests may be limited by resources in smaller remnant woodlands such as our study site (Gray, 1974).

tasks such as the location of honeydew and social communication among nest-mates; tasks that both of these species have in common.

Additionally, neither species exhibits highly specialised behaviours such as plant mutualisms that are likely to lead to important differences in the sensory pressures placed on the antennae. Mutualistic relationships with specific plant species may lead to a strong pressure to identify certain plant odours or lead to nesting in particular conditions (e.g. leaf nests) that may differ in their thermal and ventilation properties to terrestrial nests (conditions that are monitored by specialised sensilla on the antennae). As a result comparisons between these two species were an adequate foundation to start with in my examination of body size differences.

This second antennal "case study" was extremely useful in expanding my understanding of ant antennae. Focusing in on a small area such as the apical flagellomere for my first case study was important to make the workload manageable. However, there were questions about the rest of the antenna that needed to be addressed. The small size of *Temnothorax* ants allowed me to image the whole antenna in high resolution, something that is not easily accomplished in larger ants because of the much greater number of images that must be collected for a high-resolution montage (*M. pyriformis* apical flagellomere montage at x1000 magnification: 25 images, *T. rugatulus* whole flagellum montage at x1000 magnification: 14 images). Examining the whole antenna allowed me to identify the location of what appear to be true sensilla campaniformia on the pedicel, a described sensillum type that had gone unaccounted for in my previous studies. I was also able to record the presence of unusual branched sensilla or hairs on the scape. It also sparked questions about the different shapes of antennae in large vs. small species, why did *M. pyriformis* have a fairly straight filliform antenna while *T. rugatulus* had these strange club shaped antennae? This second case study was vital in formulating questions for the comparison of large and small species and to further develop workflows for specimen preparation, imaging and analysis.

Examination of worker size and sensillum numbers in this chapter unfortunately revealed that worker size in *T. rugatulus* was not as uniform as initially expected. The variability found in this study made it obvious that sampling sizes that adequately captured the range of variability in each species could not realistically be achieved for the comparative dataset given the time consuming nature of this type of study. However, some interesting questions about monomorphism and intraspecific variability were sparked by this project which resulted in what is now **Chapter 5** of this thesis.

Although studying *T. rugatulus* initially seemed like a bit of diversion from the main direction of this thesis it has resulted in many insights that helped to develop the direction of **Chapter 4 – Miniaturisation of the antennal array** and instigated the research for **Chapter 5 – Describing body size variation in ants**. The contents of this chapter are based on the published work:

> **Ramirez-Esquivel, F., Leitner, N.E., Zeil, J., Narendra, A., 2017. The sensory arrays of the ant, *Temnothorax rugatulus*. Arthropod Structure & Development 46, 552-563.**

It differs from the original publication in some minor editorial points but also includes additional content. This consists of a short discussion on sensilla campaniformia ("A special note on sensilla campaniformia") and a special appendix on palmate sensilla outlining post-publication observations of branched sensilla in various ant species and additional SEM records of branched sensilla morphology.

Author contributions:

All of the data for the publication was gathered by me with the exception of some of the body size measurements, which were done by me and NEL. Ants were collected and kept by NEL. The manuscript planning and first draft of the introduction were carried out by NEL and me. The data analysis was carried out by me with the exception of optical calculations, which were carried out by Jochen Zeil (JZ). The remainder of the manuscript and the figure design was carried out by myself with help from NEL, JZ, and AN. All additional materials presented in this chapter were collected by me.

3.1. Introduction

Ants are social insects and as such their societies are characterised by the division of labour among individuals, in the case of ants this includes the distribution of different tasks among workers ants. Task allocation among workers is based on genetic and epigenetic variation, differences in developmental conditions and trajectories, and experience-dependent processes, including learning and memory (e.g. Charbonneau and Dornhaus, 2015a; Maleszka, 2016). One potential mechanism involved in task allocation lies in the variable thresholds with which individuals respond to task-related cues, whether they be sensory or cognitive (e.g. Charbonneau and Dornhaus, 2015a). This may apply even in cases where there is limited variability among individuals such as in monomorphic species. Variations in response thresholds can be due to any number of reasons, amongst them genetic and epigenetic variation, developmental conditions, differences in body size or age (reviewed in Charbonneau and Dornhaus, 2015a). Independent of underlying causes, one relatively easily quantifiable trait that must affect response thresholds is the number and type of sensors available to an ant. Investigating the variation in this trait with the aim of correlating it with variations in task allocation for any given species of ant may establish an important link between genetic, epigenetic and developmental processes and the behavioural plasticity underlying task allocation in social insects.

Body size variation is associated with differences in the compound eyes and the antennal array of sensilla, which can lead to functional differences among workers. The eyes and antennae are the two most important sensory organs for providing ants with information about the external environment. Combined, these sensory organs detect visual, chemical and mechanical cues as well as information about temperature, humidity and CO_2 levels. In bumblebees, differences in the number of antennal sensilla and ommatidia have been shown to respectively affect a worker's odour sensitivity and visual resolution (e.g. Spaethe et al., 2007; Spaethe and Chittka, 2003). At the behavioural level, larger bumblebee workers are more likely to engage in foraging behaviours than their smaller counterparts (Spaethe et al., 2007; Spaethe and Chittka, 2003). Although having a larger body-size may be advantageous for a number of reasons it is likely that increased sensory capabilities contribute towards larger workers being more efficient foragers.

Here, we examine both the compound eyes and the antennae of *Temnothorax rugatulus* ants, the behaviour of which has been well

documented, to identify morphological variations potentially affecting individual behaviour. We investigate whether there are body-size dependent differences in the sensory arrays of workers.

3.2. Methods

3.2.1. Study site and study species

Worker ants for this study were opportunistically sampled from a single experimental colony, all ants were collected indiscriminately and preserved in ethanol. The colony was collected from the Santa Catalina mountain range, Tucson, Arizona, USA ($32^0$23'43.00"N, $110^0$41'27.69"W) in May 2015. In the laboratory, the colony was housed in an artificial nest and periodically fed with sugar solution and dead fruit flies (for full methods see: Charbonneau and Dornhaus, 2015b). All imaging of the eyes and antennae was done using this single colony.

Body size and head width variation among workers was recorded by photographing dead specimens under dissecting microscopes (Olympus SZX9, Nikon DS-Fi1). Measurements of the head width (measured in dorsal view just behind the compound eyes) were taken in a total of 100 workers; the sample was made up of 46 workers from the colony mentioned above plus 54 workers from another laboratory colony collected at the same location to boost sample size (the mean and standard deviation were identical for both colonies). Additionally, body length (clypeus to the end of the gaster) and head length (clypeus to apex) measurements were taken for comparison. Measurements were taken from digital images using ImageJ 1.45s (Rusband, National Institutes of Health, USA).

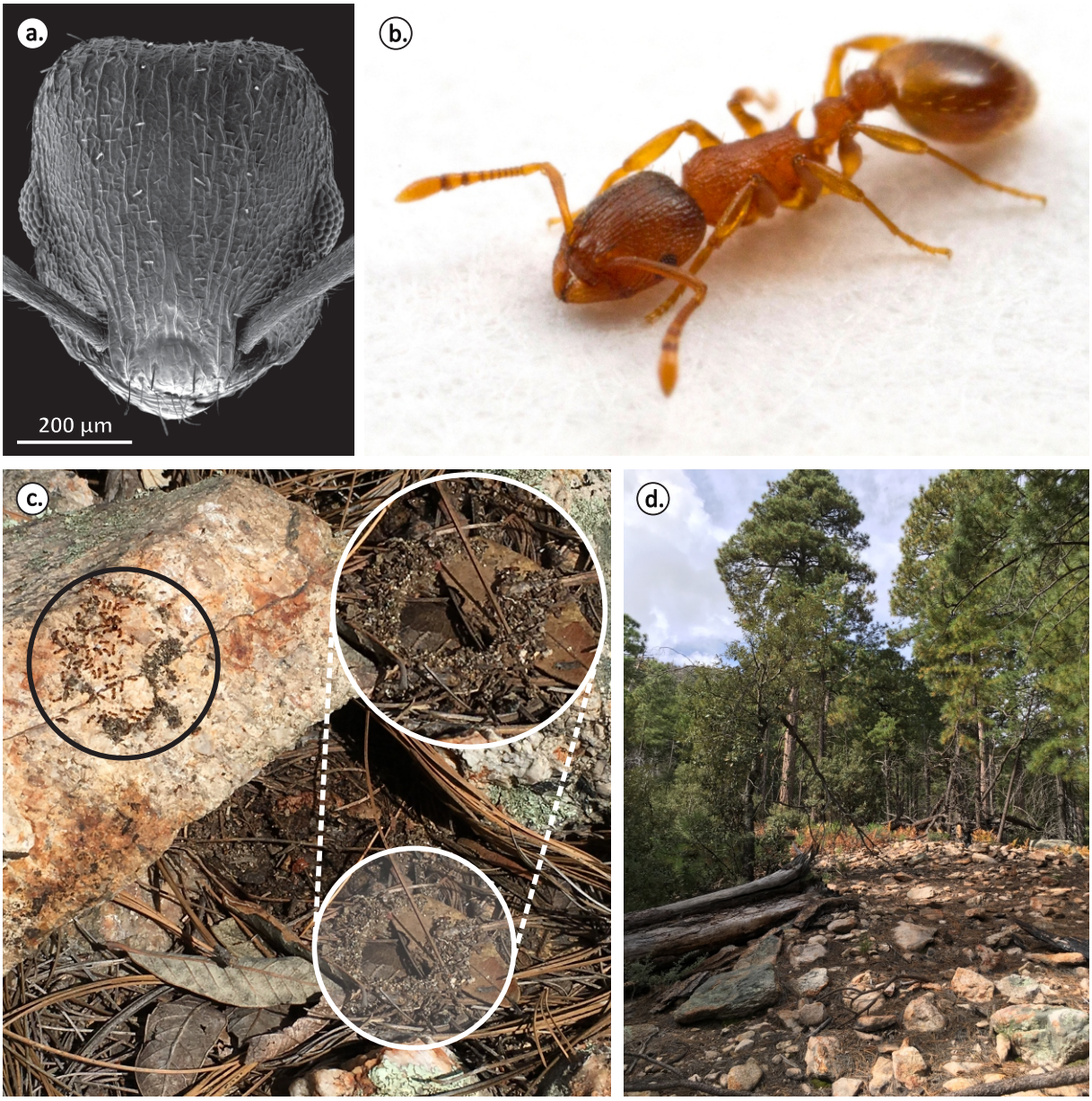

Figure 3.1. Overview of the study species *Temnothorax rugatulus*. (a) Scanning electron micrograph of the worker head showing laterally placed compound eyes and characteristic rugosities of the cuticle on the head. (b) Overview photograph of worker: note yellow-brown colouration and club antennae. Photo credit: Michele Lanan (c) Nesting site under an upturned rock: the white circle indicates the nest location on the substrate denoted by a semicircle made of plant detritus; the black circle indicates the corresponding surface on the upturned rock with workers and queen clinging on. (d) Overview of the environment surrounding the nest site, the rocky landscape is dominated by pine trees with patchy understorey.

3.2.2. SEM specimen preparation

Whole specimens were stored in 70% ethanol. The amputated antennae or whole heads were then mounted on aluminium stubs using conductive carbon tape. Specimens were coated with Au/Pd (60:40) for 2 minutes at 20 mA and imaged on a Hitachi S-4300 SE/N scanning electron microscope. For detailed methods see Ramirez-Esquivel et al. (2014).

3.2.3. Compound eye histology

For the study of the internal anatomy of the eyes live specimens were immobilised using wax under a dissection microscope, the mandibles were removed and the back of the head capsule was quickly opened up. The remainder of the head capsule, bearing the two compound eyes, was immediately placed in ice-cold aldehyde fixative (50:50 mixture of 4% formaldehyde and 4% glutaraldehyde, pH 7.2) and left for 5 hours while the remainder of the body was immersed in 100% ethanol to kill the ant. The samples were then rinsed in PBS (5x3 minutes) and post-fixed in 2% OsO_4 solution for 90-120 minutes. The samples were once again rinsed in PBS (5x3 minutes) and stained with 2% uranyl acetate overnight. After rinsing, as above, the samples were dehydrated in an ethanol series (50-100%) and transferred into propylene oxide for resin infiltration. The Epoxy (Epon) infiltrated tissues were polymerised in an oven at 60° for 12 hours. For detailed methods see Greiner et al. (2007) and Narendra et al. (2013) .

Samples were sectioned with a HistoJumbo diamond knife (Diatome, Biel/Bienne, Switzerland) to 2 μm thickness on a Leica EM UC7 ultramicrotome , mounted on glass slides, heat fixed and stained for contrast with toluidine blue. They were later imaged on a Zeiss Axioskop compound microscope equipped with a SPOT Flex 16MP colour camera.

3.2.4. Image processing and measurements

All image processing, including SEM colourisation, was carried out with CorelDraw® Graphics Suite X6 (2012 Corel). Measurements were made directly from digital images with ImageJ 1.45s (Rusband, National Institutes of Health, USA).

To estimate the variability of the antennal sensillum array between different individuals we quantified the abundance of the different types of

sensilla and measured the length of sensilla basiconica, trichodea and trichodea curvata in six worker ants of different sizes (head width varied from 0.46 to 0.63 mm). We focused on the dorsal surface of the antenna but also examined the ventral surface in three individuals for comparison. Antenna area estimations are based on measurements of the visible area from SEM images, not taking into account the effects of curvature. Sensillum length was measured on sensilla which were clearly visible in profile (for full details see Ramirez-Esquivel et al., 2014). We concentrated on the filiform chemoreceptors as these were relatively plentiful (unlike peg-in-pit sensilla, i.e. sensilla coeloconica, ampullacea, coelocapitular and campaniformia).

Compound eye facets were counted in SEM images. Internal eye structures were measured in semi-thin sections from three individuals. These measurements were used to calculate resolution (inter-ommatidial and acceptance angles) and optical sensitivity (the eye's ability to capture photons when viewing a scene of broad spectral content) (Land and Nilsson, 2012). Optical sensitivity, S, is given in $\mu m^2 \cdot sr$ (Land, 1981; Warrant and Nilsson, 1998) as:

$$S = \left(\frac{\pi}{4}\right)^2 A^2 \left(\frac{d}{f}\right)^2 \left(\frac{kl}{2.3+kl}\right),$$

where, A = facet diameter (μm); d = diameter of the rhabdom (μm); f = focal length, determined by the distance from the nodal point of the lens to the tip of the rhabdom (μm); l = the rhabdom length (μm); k = absorption coefficient, assumed to be 0.0067 μm^{-1} (see Warrant and Nilsson, 1998) . We used the thick lens equation (see Schwarz et al., 2011; Stavenga, 2003) to determine the position of the nodal point, the focal length and the location of the focal plane, assuming a homogeneous refractive index of the lens and the crystalline cone.

3.3. Results

3.3.1. Gross morphology and body size

T. rugatulus are yellowish brown ants, with rugose sculpturing on the cuticle of the head, thorax and petiole (**Figure 3.1a, b**). Workers were small with a body length of 2.6 to 3.8 mm (n=46). Throughout this study we have chosen to omit body length from the analyses and use head width as a proxy for body size, since body length, which includes the gaster, can

vary greatly according to nutritional state and satiety. Head width is a commonly used proxy in the ant literature (e.g. Hölldobler and Wilson, 1990; Kaspari and Weiser, 1999; Tschinkel et al., 2003), it has been previously used to describe size variation in *T. rugatulus* (Westling et al., 2014), and in this species it scales linearly with both body length (R^2=0.67, n=46) and head length (R^2=0.93, n=54). We found head width varied from 0.45 to 0.66 mm (n=100), representing a variation of approximately ±20% around the mean (**Figure 3.2**). The size distribution was similar to a previously described distribution (Westling et al., 2014) but with a relatively limited range of head widths (**Figure 3.2**). It did not significantly deviate from a normal distribution (D'Agostino and Pearson test, P=0.7127).

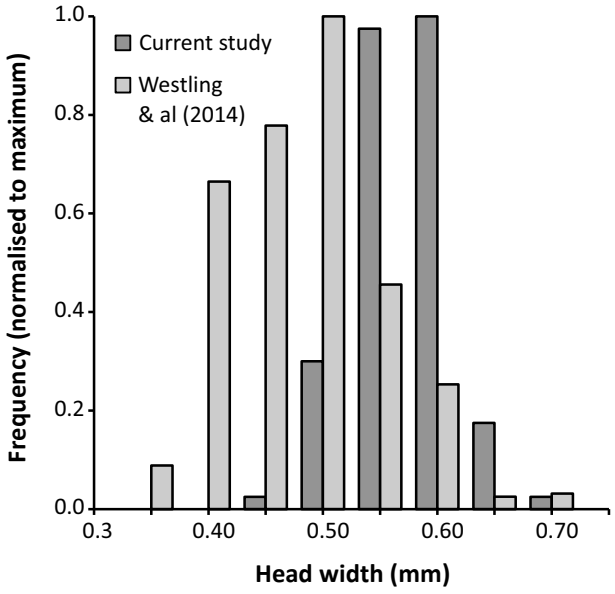

Figure 3.2. Frequency histogram of worker size variation in *Temnothorax rugatulus*. Head width acts as a proxy for body size. Data from the current study overlayed with previous data from Westling & al (2014) for comparison (n=100 and 522 respectively). See Discussion for details.

3.3.2. Antennal array

General anatomy and characteristics of the antenna

The antennae consisted of a scape, a pedicel and nine flagellar segments. The pedicel and the flagellum are jointly referred to as the funiculus (**Figure 3.3a**). Of the funicular segments, F1-3 were the largest and formed a club while F4-9 were greatly reduced and formed a thin straight shaft (**Figure 3.3a**). The dorsal surface area of the club was in fact over three times larger than that of the shaft (**Figure 3.3b**), despite being comprised of fewer segments. Smaller funicular segments bore fewer sensilla, and chemosensitive sensilla in particular dropped in abundance as segments became smaller and were altogether missing from the small shaft segments (**Figure 3.3c**). Larger workers tended to have a larger total antennal area (R^2=0.70, n=6 workers), where an increase of 0.01mm in head width was accompanied by an increase of approximately 900μm^2 of antennal area.

Sensillum types and their distributions

We surveyed the dorsal surface of the entire antenna and found ten different types of sensilla, each with their own particular distributions, which were consistent across individuals (**Figure 3.4a**). Seven of the ten types of sensilla were confined to the club: sensilla basiconica, trichodea, trichodea curvata, trichoid-II, coeloconica, ampullacea and coelocapitular (**Figure 3.4 a-c**). The filiform mechanoreceptors, sensilla chaetica, were present throughout the antenna (**Figure 3.4a, b**) while sensillum campaniformium (**Figure 3.4d**) was restricted to the distal border of the pedicel (**Figure 3.4a**).

We discovered a pair of peculiar branched sensilla on the scape, which to the best of our knowledge have not been previously described in hymenoptera. This sensillum has a hand-like appearance with variable numbers (3-10) of digitate or finger-like projections (**Figure 3.5a, c**). These sensilla project over the scape-pedicel joint and generally occurred as a single pair on the dorsal surface (**Figure 3.5a, c**), although there can occasionally be 1 or 3 sensilla instead of 2. The peg length was longer than in most other sensilla (see "Size of sensilla" section below), at 39.0±5.5 μm (mean±s.d., n=11). Similarly branched sensilla are present on the dorsal surface of the head, mesosoma and gaster (**Figure 3.5b, e, f**) where they are longer (head: 53.0±8.1 μm, n=11; mesosoma: 62.8±10.2 μm, n=15;

gaster: 68.5±8.6 µm, n=16) and have their projections arranged in different configurations (**Figure 3.5c, c, g, h**). It is possible that not all of these sensilla are homologous.

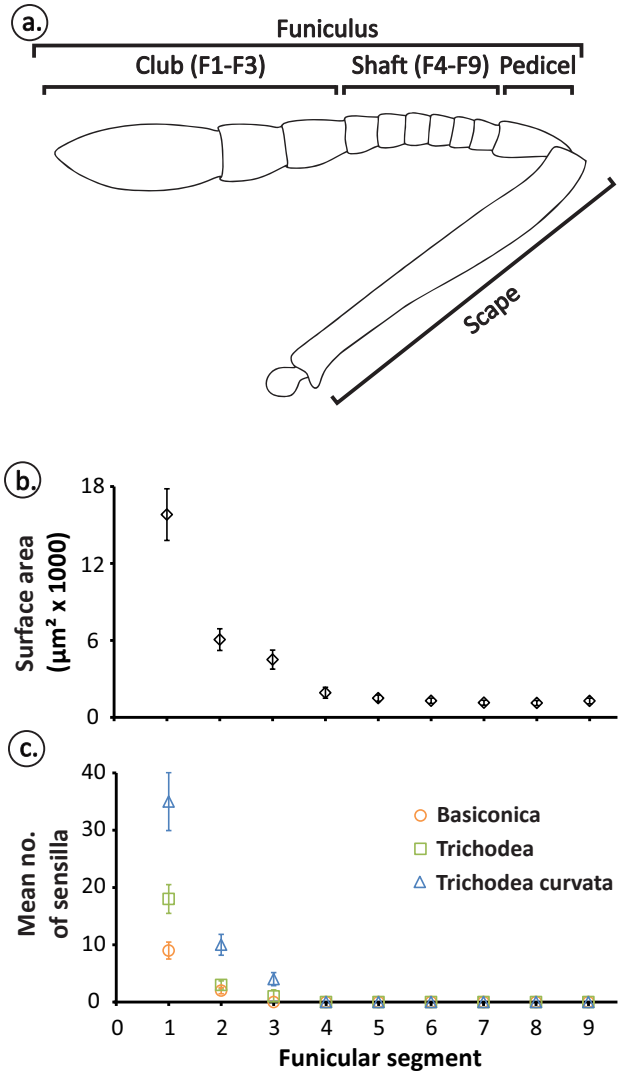

Figure 3.3. Overview of the antennal anatomy of *Temnothorax rugatulus*. (a) Parts of the antenna including the club (segments F1 to F3), shaft (F4 to F9), pedicel and scape. (b) Size variation across flagellar segments. (c) Average number of filiform chemosensitive sensilla across flagellar segments. Error bars represent standard deviations, n=5.

Sensillum variation among individuals: Size and numbers of sensilla

In order to gather sufficient, reliable data to investigate the effects of worker size variation on the sensillar array we concentrated on the filiform sensilla (sensilla basiconica, trichodea, trichodea curvata, chaetica and TII) on the dorsal surface of the club (**Figure 3.4b**), as these were most abundant.

Numbers of sensilla

The number of sensilla varied with worker size but the manner in which they varied was dependent on the sensillum type. The relative numbers of sensilla basiconica and Trichoid II (TII) increased considerably and consistently with head width (from 8 to 13 and from 20 to 36 respectively), and in both of these cases there was a strong, positive, linear relationship between the number of sensilla and worker head width normalized to maximum (R^2=0.98 and 0.81 respectively, F<0.05, orange and red dashed lines, **Figure 3.6a**). The head width of workers examined varied from 0.46 to 0.63 mm which equates to a 36% increase in head width (relative to the minimum), compared to a 63% increase in sensilla basiconica and an 80% increase in TII sensilla. In contrast, there was no strong correlation (R^2<0.30, F>0.05) between numbers of sensilla and worker size in the case of sensilla trichodea, trichodea curvata and chaetica (green and dark purple dashed lines, **Figure 3.6a**).

The average absolute abundance of different sensillum types differed greatly and as a consequence so did their relative contributions to the total sensillum array (**Figure 3.6b**). The vast majority (72%) of the sensilla found on the club were mechanoreceptive sensilla chaetica while the remaining 28% of filiform sensilla were comprised of four different types of chemoreceptors and a putative chemoreceptor. Among the chemoreceptors the smallest contribution (3%) was made by sensilla basiconica and the largest by sensilla trichodea curvata (12%) (**Figure 3.6b**).

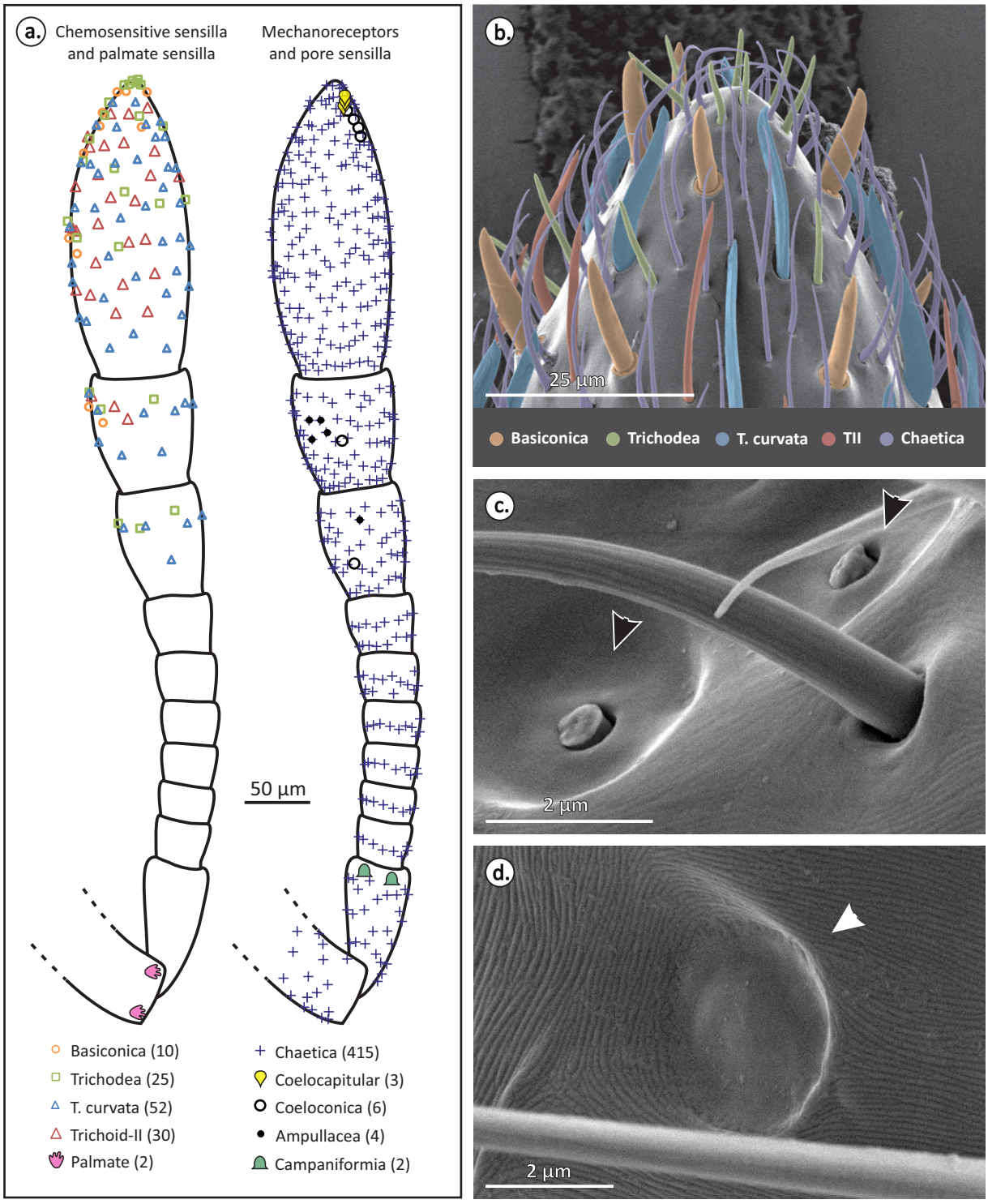

Figure 3.4. Types of sensilla and their distributions on the *Temnothorax rugatulus* antenna. (a) Example map of locations of filiform chemosensilla and palmate sensilla (left), and sensilla chaetica and peg-in-pit sensilla (right) on the dorsal surface of the antenna of *Temnothorax rugatulus*. Data are from the right antenna of a single worker (head width=0.58) but mapped separately for clarity. Legend lists sensillum types and abundances. (b) Colourised SEM of the antennal tip; colour-coded are the various types of filiform sensilla. Two examples of peg-in-pit sensilla: (c) a pair of coelocapitular sensilla (black arrows) and (d) sensilla campaniformia (white arrow).

The relative increase from the minimum to the maximum observed abundance of a sensillum type across different individuals was unrelated to the absolute abundance of that sensillum (**Figure 3.6c**). That is to say, the relative variability of a sensillum type was unrelated to its absolute abundance. The most variable sensilla were sensilla basiconica (63% increase relative to the minimum) and TII (80%) while the least variable were sensilla chaetica (38%) and trichodea (19%).

Comparing the dorsal (n=5 workers) and ventral (n=3 workers) surfaces of the club, we found that the ventral surface has, overall, fewer sensilla. As compared to the dorsal surface, there were approximately 20% fewer sensilla trichodea and trichodea curvata and approximately 70% fewer TII sensilla on the ventral surface. Sensilla chaetica did not vary dramatically between the two surfaces while sensilla basiconica were similar in abundance both dorsally and ventrally or, in the case of one worker, they were more abundant ventrally.

Size of sensilla

Here we restricted our analysis to the three filiform chemosensilla: sensilla basiconica, trichodea and trichodea curvata (see methods). Sensilla basiconica and trichodea were of similar length while sensilla trichodea curvata were much longer (**Figure 3.7a**). We found that sensillum size could not be predicted by worker head width. Sensilla basiconica ranged continuously from 10 to 20 µm (n=38 sensilla, 6 workers) with approximately the whole range of variation being displayed in every individual examined independently of head width (data not shown). Similarly sensilla trichodea ranged from 8 to 18 µm (n=38 sensilla, 6 workers) and trichodea curvata from 20 to 34 µm (n=69 sensilla, 6 workers). Within individuals, sensilla are roughly organised from smallest to largest on the apical segment. Peg length varied with proximity to the apex of the antenna following a power relationship where the closer a sensillum was to the tip the shorter its peg (**Figure 3.7b**).

3.3.3. Optical system

T. rugatulus workers possess a pair of apposition compound eyes and no ocelli. The compound eyes were laterally placed (e.g. **Figure 3.1a**) and measured 107.0±10.2 µm (mean±s.d.) along the dorso-ventral axis (n=17) and 141.0±15.8 µm along the anterior-posterior axis (n=17). Eye size was not correlated with head width (R^2<0.05). Each eye was made up of 55.2±6.5 ommatidia (mean±s.d., n=39, Figure 8 A); however, the number of ommatidia varied considerably with worker size, ranging from 45 to 76 (**Figure 3.8b**). This represents, relative to the mean, a 19% decrease in the ants with the fewest facets and a 37% increase in the ants with the most. Within individuals, the number of facets between the left eye (55.25±1.94; mean±s.d.) and the right eye (55.94±2.01) did not differ significantly (paired t-test, n=16, p=0.102, t=1.741, df=15). The facets were not arrayed to form a regular hexagonal pattern as in larger ants but were irregularly arranged (**Figure 3.8a**) (see also Pix et al., 2000).

Across the horizontal plane the visual field spanned approximately 120°, and the maximum number of facets in a horizontal row ranged between individuals from 8 to 11 facets, as judged from horizontal sections (**Figure 3.8c**). This translates into horizontal inter-ommatidial angles ($\Delta\phi$) of between 11° and 15°. In the vertical plane the field of view spans about 130° with a maximum of 7 to 9 facets ($\Delta\phi$ = 14°-19°). The full extent of the visual field of one eye is thus approximately 15600 deg² (120°x130°) with each ommatidium covering 15600/55=284 deg², which equates to an average inter-ommatidial angle of 16.8°. The average facet diameter is 16.5±1.1 µm (range: 14.7 to 19.0 µm; n=41), which produces a blur circle half-width of $\Delta\rho_{lens}$ = 1.5-1.9 µm ($\Delta\rho_{lens} = \lambda/A$ [rad], with wavelength of light λ = 0.5µm; facet diameter A = 16.5µm). Measuring the facet diameters of the whole central horizontal row in 22 workers revealed that facet diameter was not correlated with head width (R^2<0.13). The photosensitive structures (the rhabdoms) are 5.7±0.0 µm wide (n=3; **Figure 3.8e**) and approximately 27.4±1.9 µm long (n=6; **Figure 3.8c**).

Figure 3.5. Previously undescribed, branched 'palmate' sensilla as seen in various body parts of Temnothorax rugatulus. 'Palmate' sensilla at the (a, c) scape-pedicel joint, (b, d) dorsal surface of the head, (e, g) dorsal surface of the mesosoma and (f, h) dorsal surface of the gaster. The 'palmate' sensilla are artificially colourised in pink in panels a, b, e, and f.

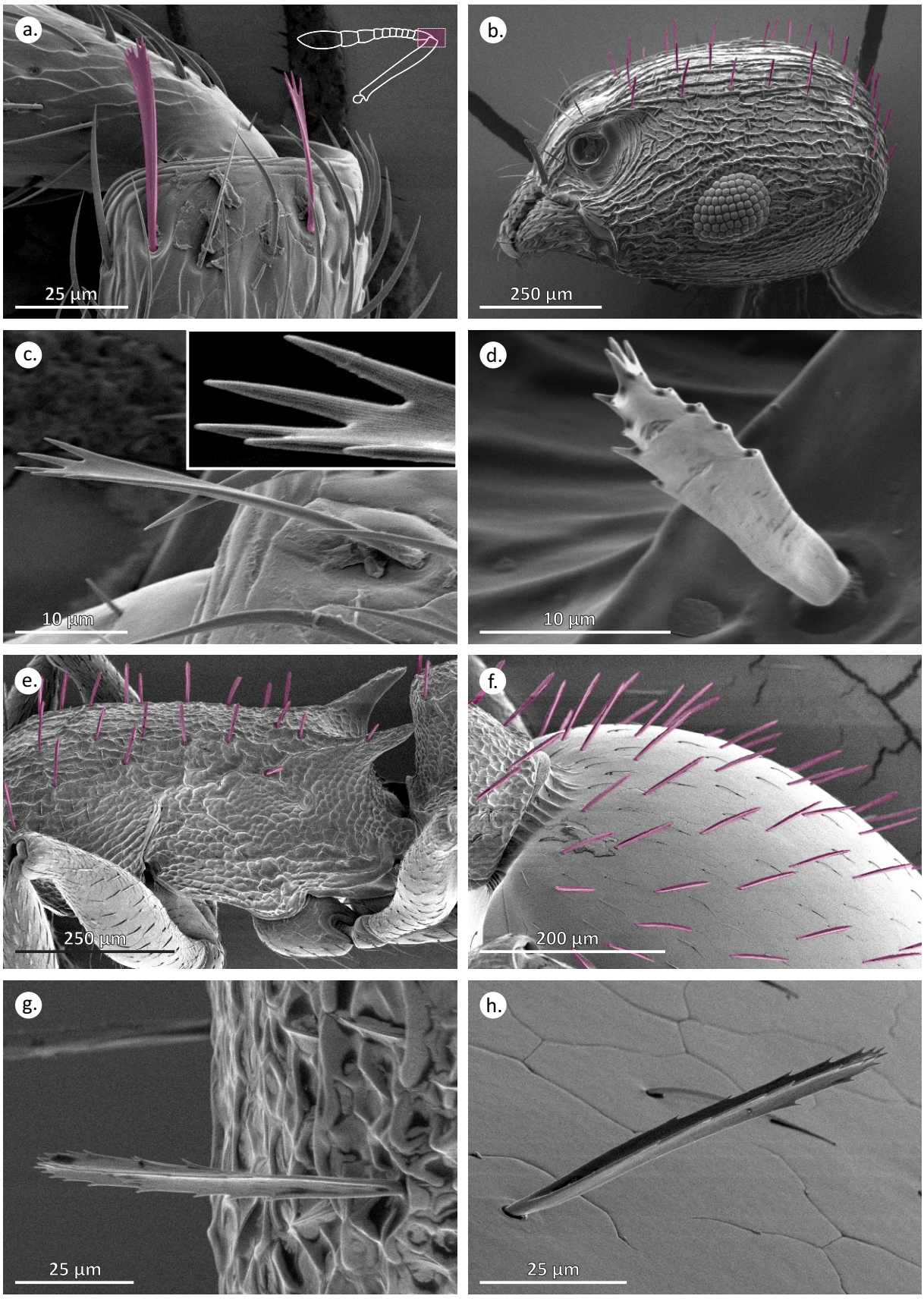
a.
25 µm
b.
250 µm
c.
10 µm
d.
10 µm
e.
250 µm
f.
200 µm
g.
25 µm
h.
25 µm

Given they had unusually large rhadboms for a day-active species, we aimed to determine their optical sensitivity. For this, we first determined the distance between the nodal point of the lens and the focal plane by applying the thick lens equation with the outer lens surface radius of r1=11.2 µm (n=3), the inner lens radius r2=-6.1 µm (n=3), the distance between vertices 11.1 µm (n=3) and refractive indices of 1.43 for the lens and 1.34 for the crystalline cone, assuming a uniform distribution of refractive indices in both compartments. Interestingly, these parameters place the plane of best focus more than 10 µm proximal of the distal tip of the rhabdom (**Figure 3.8d**, red cross). Taking the distance between the distal tip of the rhabdom and the nodal point (9.0 µm, see **Figure 3.8d**) as the effective focal distance for the acceptance angle of the rhabdom, we arrive at an acceptance angle $\Delta\rho_{rhabdom} = 36^{o}$ ($\Delta\rho_{rhabdom}$ = d/f [rad], with rhabdom diameter d and focal length f), which is only slightly larger than the optimal value of twice the average inter-ommatidial angle of 16.8^{o}. It needs to be noted, however, that the light distribution at this point in the optical pathway is much more diffuse compared to the focal plane. With this value of the acceptance function ($\Delta\rho_{rhabdom}$) the optical sensitivity of the *T. rugatulus* eye would be comparatively high for a miniature compound eye at 4.1 $\mu m^2 sr^{-1}$ (c.f. Fischer et al., 2011; Makarova et al., 2015), even compared with large night-active bull dog ants (1-1.6 $\mu m^2 sr^{-1}$; (Greiner et al., 2007)) and night-active bees and wasps (2.7 $\mu m^2 sr^{-1}$, (Warrant and Dacke, 2011)).

Another feature of interest in the *T. rugatulus* eye was that while most rhabdoms have circular or almost square cross sections (**Figure 3.8e**), a few rhabdoms in the dorsal region of the eye are rectangular in shape, with the long axis measuring 4.4±0.4 µm (n=4), on average 1.44 times wider than the short axis (**Figure 3.8f**). Such modified rhabdoms are typical for the dorsal rim area (DRA) of insect compound eyes, which is involved in the detection of polarized sky light.

Figure 3.6. Abundance of filiform sensilla on the club of *Temnothorax rugatulus*. (a) Variation in sensillum abundance on the club among workers of different size (n=5 workers). Sensillum types colour-coded as per panel B. Note that head width normalized to maximum is plotted on the x-axis. (b) Average contributions of different filiform sensillum types towards total average filiform sensilla on the club. (c) Comparison of maximum and minimum observed abundances for each sensillum type, the percentage increase from minimum to maximum (relative to the minimum value) is stated for each sensillum type.

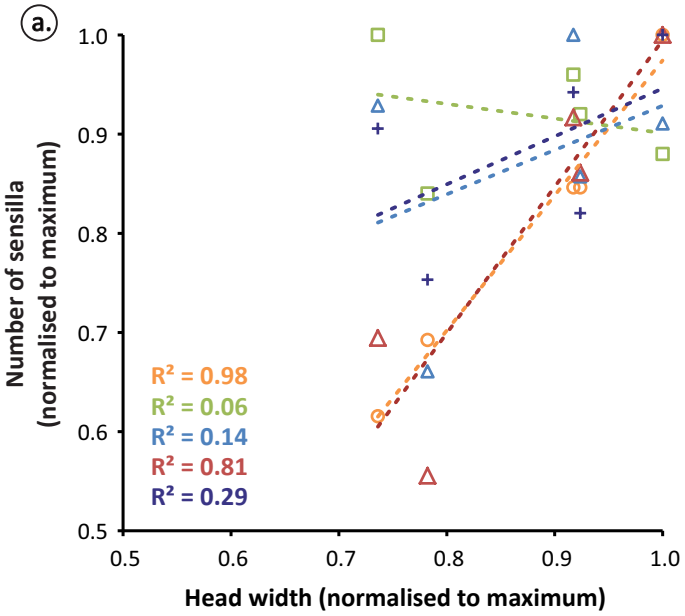
a.
Number of sensilla (normalised to maximum)
1.0
0.9
0.8
0.7
0.6
0.5
0.5
0.6
0.7
0.8
0.9
1.0
Head width (normalised to maximum)
R² = 0.98
R² = 0.06
R² = 0.14
R² = 0.81
R² = 0.29

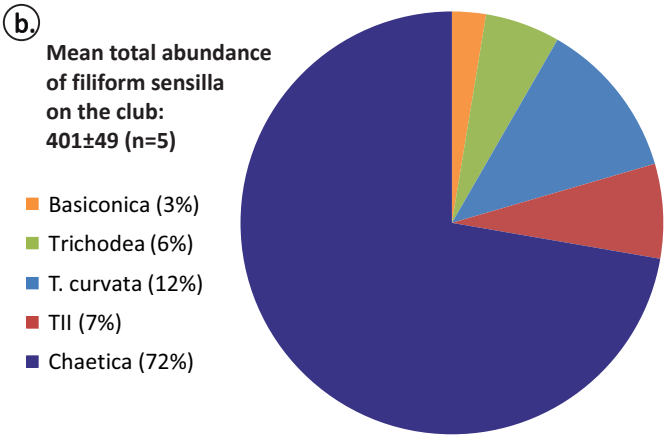
b.
Mean total abundance of filiform sensilla on the club: 401±49 (n=5)
Basiconica (3%)
Trichodea (6%)
T. curvata (12%)
TII (7%)
Chaetica (72%)

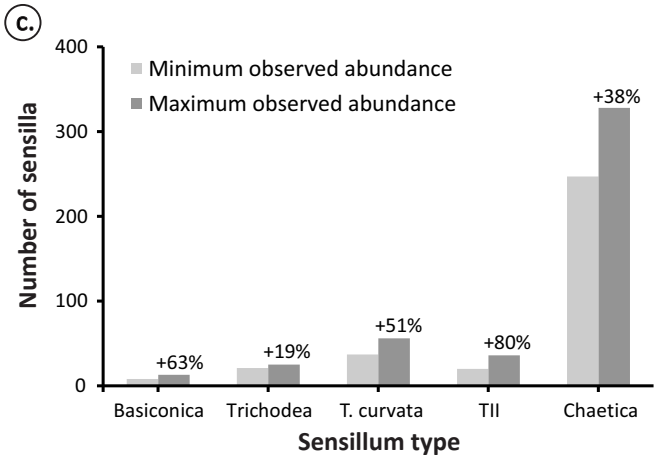
c.
Number of sensilla
400
300
200
100
0
Minimum observed abundance
Maximum observed abundance
+63%
+19%
+51%
+80%
+38%
Basiconica
Trichodea
T. curvata
TII
Chaetica
Sensillum type

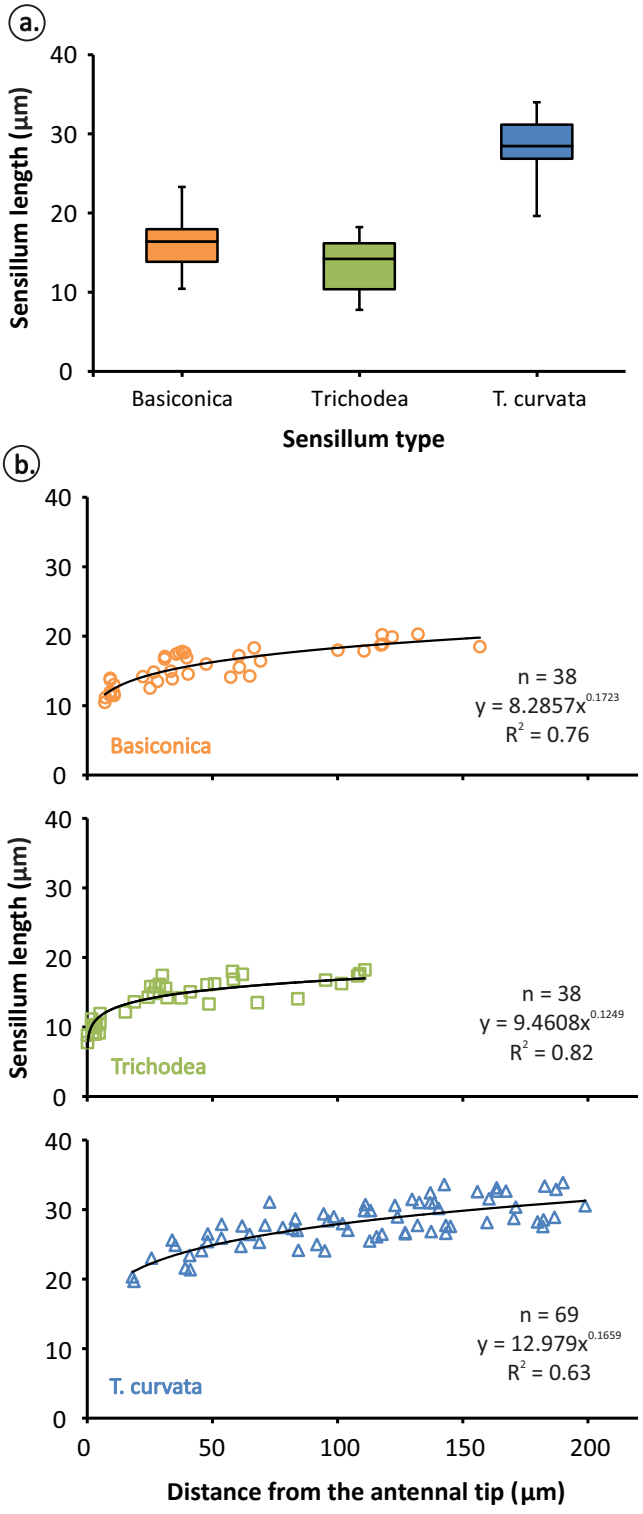

Figure 3.7. Variability in peg length of filiform chemoreceptors in *Temnothorax rugatulus*. (a) Comparison of the distribution of peg lengths in sensilla basiconica, trichodea and trichodea curvata. Boxplot represent median, 1st and 3rd quartile, and minimum and maximum peg length. (b) Peg lengths relative to distance from the tip of the antenna for three sensilla. Sensilla closer to the tip tend to be shorter.

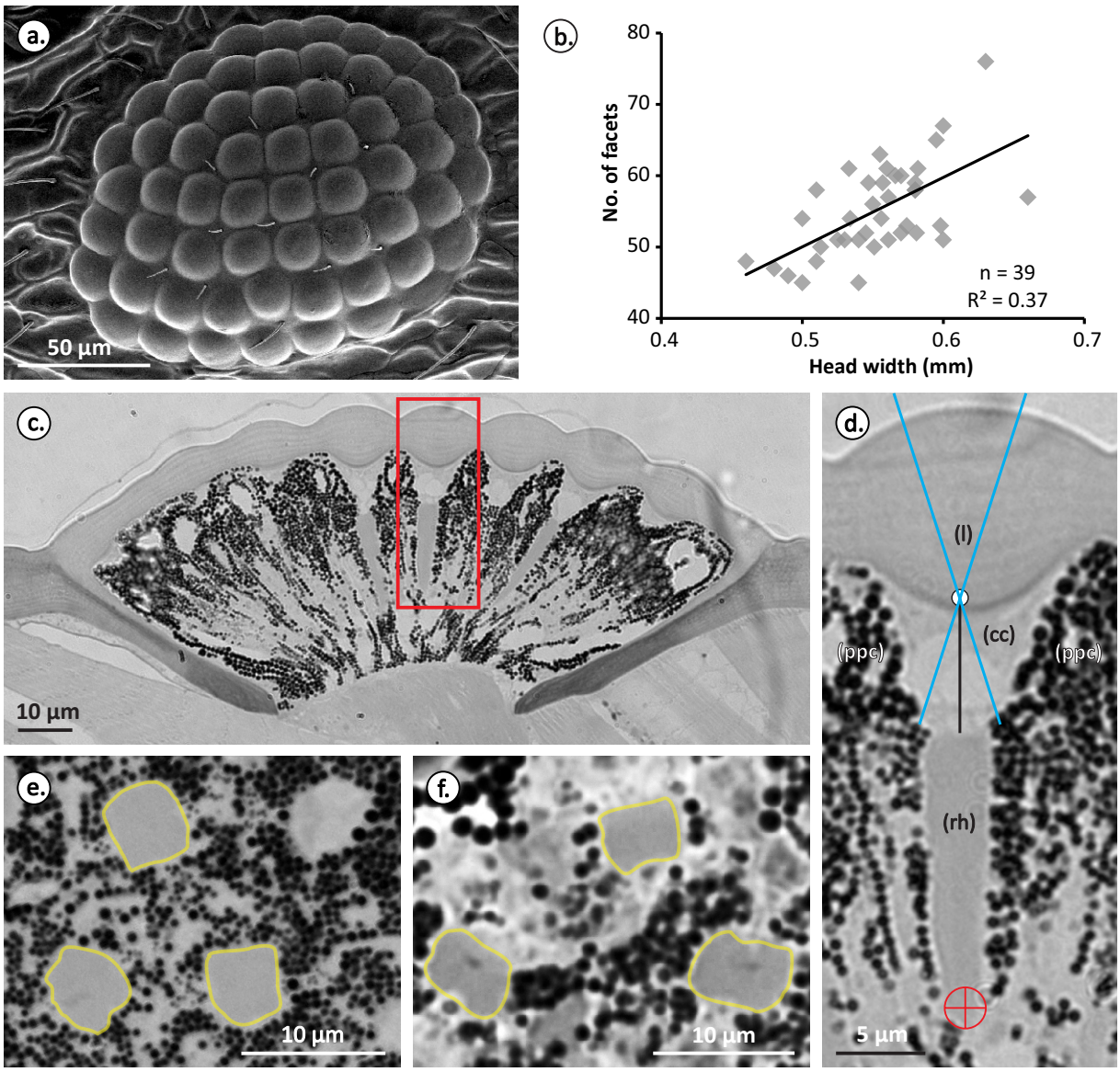

Figure 3.8. Eye anatomy of *Temnothorax rugatulus* worker. (a) Overview Scanning Electron Micrograph of the compound eye. (b) Relation between the number of facets and head width. (c) Horizontal section through the compound eye showing longitudinal sections of the ommatidia at the equator of the eye. (d) A single ommatidium with its lens (l), crystalline cone (cc), rhabdom (rh) and primary pigment cells (ppc). (e) Cross-section at the level of distal rhabdoms in the frontal region of the eye. (f) Cross-section of the distal rhabdoms of the dorsal rim area of the eye. Outline of the rhabdoms is shown in yellow.

3.4. Discussion

Despite being a popular study system for behavioural studies there have been no descriptions of the sensory systems of *Temnothorax* ants. We present detailed descriptions of the compound eyes and the antennal sensilla array uncovering some unexpected features. We compare variability between workers and speculate on the possible functional implications of such variation.

The workers of *T. rugatulus* we examine vary in body-size by ±20% around the mean. Accompanying this variation there are quantifiable differences in the elaboration of the sensory arrays. Larger workers tend to have larger antennae with more sensilla basiconica and TII sensilla as well as eyes with more ommatidia. However, body-size alone does not explain all of the variation observed. Most sensillum types did not scale with size and body-size only explained about half of the variation seen in facet numbers (R^2=0.47, Fig. 9). These trends should result in a certain degree of variation in the sensory information gathering capabilities of individuals in a manner that is linked to, but not exclusively dependent on, body-size. Unfortunately, the opportunistic nature of our sample prevented us from behaviourally identifying intranidal and extranidal workers and the limited sample size meant we did not capture the full range of body-size variation previously described (Westling et al., 2014). Notwithstanding these limitations, we believe that the degree of variability we observed warrants further studies incorporating behavioural observations.

3.4.1. The antennal array

Temnothorax ants rely on pheromones to orchestrate complex behaviours such as colony emigrations and communication among nest-mates. During recruitment to new nest sites, for example, workers leading tandem runs discharge a recruitment pheromone from the poison gland (Möglich et al., 1974). Nest scouts use pheromone markings to select favourable nests during colony emigrations (Cao and Dornhaus, 2012) and secrete negative signals to prevent fellow scouts from selecting unsuitable nest sites (Franks et al., 2007; Sasaki et al., 2014; Stroeymeyt et al., 2011; Stroeymeyt et al., 2014). Finally and perhaps most remarkable of all, some *Temnothorax* species lay not only colony-specific but also individually distinct trails. Experiments have shown that individuals are able to identify and preferentially follow their own trails (Maschwitz et al., 1986). It is clear then that *Temnothorax* ants are capable of behaviours which

rely on sophisticated chemosensory abilities. Perhaps then it comes as no surprise that despite their small size *T. rugatulus* display the full complement of sensillum types observed in larger ant species although at much lower numbers (see Table 3 in: Ramirez-Esquivel et al., 2014). The low numbers of sensilla may mean that small variations in the sensillum array may have a significant impact on the sensory capabilities of individuals which may result in behavioural differences. To study the variability of the antennal array we compared sensillum sizes and numbers across individuals of different sizes.

It is hard to assess the functional significance of variations in sensillum size. Steinbrecht (1973) found in *Bombyx mori* that long sensilla trichodea almost always were innervated by two receptor cells, while a shorter type of sensilla trichodea contained one to three receptor cells. The situation was different for sensilla basiconica, with large sensilla containing three and a smaller form of the sensillum containing only one receptor cell. In addition, at least in flies, dendritic branching patterns can be quite complicated independently of sensillum size (Lewis, 1971). So all we can say at the moment is that larger sensilla may contain more wall pores and longer dendrites and thus could express more receptor proteins, which would make them more sensitive. However, sensillum length measurements from three filiform sensilla showed quite considerable variability within individuals and no clear differences in sensillum size between different individuals. There was no relationship between sensillum length and head width. This result is consistent with previous observations (Ramirez-Esquivel et al., 2014; van der Woude and Smid, 2015). At this point it is not clear why there is such dramatic intra-individual size variation in sensilla but one possibility is that packing of both external structures such as the cuticular elements of the sensilla and internal structures such as the underlying neurons may constrain the size of sensilla in certain locations of the antenna (Schneider, 1964).

In contrast, the number of sensilla of a given type varied from one individual to another but not all sensilla are affected by changes in head width in the same way. While sensilla chaetica and trichodea curvata were present in variable numbers without a clear dependence on worker head width, sensilla trichodea seemed to remain relatively constant across different head widths. This could point to a very specific and narrow function unrelated to size or task allocation or to a density dependent function. In contrast, sensilla basiconica and TII consistently increased with head width, suggesting that perhaps extranidal workers benefit from enhancing these sensory channels to perform more informationally demanding behaviours such as foraging.

The functional significance of relative increases in sensillum abundance with increasing head width is not immediately obvious and cannot be ascertained with certainty based on external anatomy alone. However, the variability we observe is an encouraging sign that differences in the peripheral component of ant chemosensation may produce individual differences in how chemical cues are perceived and therefore drive task specialisation.

There are many aspects of the chemosensory array that may affect how an ant perceives an odour cue including the specificity and sensitivity of the chemoreceptors present in the olfactory receptor neurons (ORNs) (e.g. Duchamp-Viret et al., 1999; Sachse et al., 1999), the number of ORNs, the combinations of olfactory receptors present in a single sensillum (e.g. Getz and Akers, 1995), and how olfactory information is organised in the antennal lobe and how it outputs into higher order processing centres of the brain (e.g. Faber et al., 1999; Galizia and Menzel, 2000; Sachse et al., 1999). Of all these variables we can only speculate on the number of ORNs based on our data. Although, sensillum numbers do not directly measure ORN numbers it is likely that the two are at least loosely associated (Kleineidam et al., 2007).

If an increase in the number of sensilla is indeed accompanied by an increase in ORNs this could have a number of consequences including greater sensitivity, an improved ability to discriminate between compounds or sensitivity to a greater number of compounds (Kelber et al., 2006). Previous studies have linked increased sensillum numbers in larger workers within single species to increased olfactory sensitivity leading to differences in foraging and trail following efficiencies (leaf-cutting ants: Kleineidam et al., 2007; bumblebees: Spaethe et al., 2007). Studying the underlying neuroanatomy and differences in behavioural responses to odour cues may reveal further differences in *T. rugatulus* workers which may help explain differences in task allocation.

A special note on sensilla campaniformia

Due to their similarity, sensilla coelocapitular were sometimes miss-identified as sensilla campaniformia (see **Figure 3.4c, d**) (see Yokohari, 1983). We believe that studies that report sensilla campaniformia in the distal segments of the flagellum may have fallen into this trap as this sensillum monitors distortions of the cuticle that are unlikely to occur at the tip. While the scape-pedicel joint contains intrinsic musculature that permits active movement, the flagellum does not, it is moved passively

along with the rest of the antenna. If the flagellum collides with an object while the pedicel's position remains constant this would create mechanical stress at the flagellum-pedicel joint. The sensilla campaniformia at the base of the pedicel probably monitor these stresses.

A similar arrangement of sensilla campaniformia occurs in locusts and is named Hick's organ. Heinzel and Gewecke (1979) showed that individual sensilla campaniformia have directional sensitivity, this is thought to be achieved by "fan-shaped" structures on the terminal ends of the dendrites innervating the sensilla. While Hick's organ is comprised of an estimated 70 sensilla in *Locusta migratoria*, we estimate that there are only 4 to 8 sensilla campaniformia in the pedicel of *T. rugatulus* (this is similar to what Renthal et al. (2003) observed in *Solenopsis invicta*). This diversity in sensillum numbers is probably driven by the large difference in body size but also by the likely function of the organ in either organism. In locusts it is thought to help in flight control (Heinzel and Gewecke, 1979) while in ants it probably acts as a safeguard to prevent the overextension of the flagellum. Given these different tasks, the resolution in proprioception required is likely to be very different.

Johnston's organ

Contained within the pedicel is also the Johnston's organ. This organ is composed of a group of scolopidia or mechanosensors. This organ is known to be present in most insects, it can act as a proprioceptor but it is also capable of detecting external input. In some species it can help to coordinate flight (Sane et al., 2007) or it can detect external vibrations (Yack, 2004). In the case of ants these are vibrations of the substrate such as those created by ant species with stridulatory organs (Roces and Tautz, 2001). In other families Johnston's organ is known to be sensitive to airborne vibrations (e.g. mosquitoes; Yack, 2004). Unfortunately, given its location on the internal aspect of the pedicel this study was unable to collect any data on the Johnston's organ.

An undescribed type of sensillum in ants: Palmate sensilla

We observed the scape of *T. rugatulus* has a branched type of sensillum that has not been found in other ants (Barsagade et al., 2013; Dumpert, 1972; Hashimoto, 1990; Jaisson, 1969; Kleineidam et al., 2000; Marques-Silva et al., 2006; Mysore et al., 2010; Nakanishi et al., 2009; Ramirez-Esquivel et al., 2014; Renthal et al., 2003). This sensillum closely resembles the palmate sensilla seen in the weevil *Pissodes nitidus*

(Coleoptera) (Yan et al., 2011). Yan et al. (2011) suggest that these may be olfactory sensilla as there are grooves on the surface of the sensillum and ultrathin sections indicate the presence of openings connecting the exterior to the lumen typical of olfactory sensilla. Consistent with this, the palmate sensilla of *T. rugatulus* have longitudinal grooves covering the surface (**Figure 3.5c**, inset) but analysis of the internal anatomy will be necessary to determine if these grooves do contain openings into the lumen.

Upon further examination we observed other branched sensilla on the head, mesosoma, petiole and gaster. However, these were quite different in form to those on the scape, suggesting that they may not be homologous. While the palmate sensilla found on the scape are shaped like a scoop (**Figure 3.5a**, **c**), the branched sensilla found elsewhere roughly resemble a pyramidal prism where the three sides are strongly concave (**Figure 3.5d, g, h**). Furthermore, while the palmate sensilla on the weevil *P. nitidus* numbered in the hundreds and covered the apical segment of the antenna, the palmate sensilla we observed on the scape were very rare (maximum of 3). Yan et al. (2011) also classified their palmate sensilla according to the number of finger-like protrusions. They describe sensilla with 1, 2, 3, and 4 digits and about 200 sensilla in each category, while the sensilla in *T. rugatulus* varied seemingly randomly in the number of digits from 3 to 10. It is not clear then whether the *P. nitidus* and *T. rugatulus* palmate sensilla are homologous but their resemblance is such that we feel it is appropriate for them to share a name. Although the branched sensilla found on the head, mesosoma, petiole and gaster look somewhat different, until further studies show whether they are functionally different or not it seems convenient to refer to them under the same name.

To the best of our knowledge this is the first time palmate sensilla have been described in Formicidae. It is possible that they have been overlooked in other ants due to their location outside of the flagellum. Preliminary observations showed that palmate sensilla are present on the head, mesosoma, petiole, and gaster in some small species of ant (*Pheidole sp.*, *Paraparatrechina minitula*, *Technomyrmex sp.*), but not in all (*Meranoplus ferrugineus*) (Ramirez-Esquivel, unpublished observation). However, in none of these species were palmate sensilla found on the scape, making T. *rugatulus* an exception.

3.4.2. The optical system

Vision is crucial for most ants to navigate between food resources and the nest, be it in exclusively solitary foraging species or for scouts in species

that recruit by laying pheromone trails. The majority of studies on visual navigation to date have focussed on ants with large eyes (e.g. *Cataglyphis bicolor*: 1300 facets (Menzi, 1987), *Camponotus consobrinus:* 798 facets (Narendra et al., 2016), *Formica integroides*: 700 facets (Bernstein and Finn, 1971), *Gigantiops destructor*: 4100 facets (Gronenberg and Hölldobler, 1999), *Melophorus bagoti*: 590 facets (Schwarz et al., 2011), *Myrmecia croslandi*: 2363 facets, *Myrmecia pyriformis*: 3593 facets (Greiner et al., 2007; Narendra et al., 2011), *Polyrhachis sokolova*: 596 facets (Narendra et al., 2013). *Temnothorax* is one of the very few ants that we are aware of that have been shown to navigate visually with just over 50 ommatidia in each eye. *T. albipennis*, for instance, does indeed use visual landmarks for navigation (Pratt et al., 2001). *T. rugatulus* tends to forage individually in an environment where the undergrowth is relatively sparse, with few proximate landmarks. Foraging workers therefore most likely rely on distant cues that appear above the horizon such as tree trunks for navigation.

We observed considerable variation in the number of facets per eye in these ants (range=45-76), which raises the question of what impact such significant variations in the 'number of pixels' and the sensitivity between individuals within a single colony may have on task allocation (e.g. Perl and Niven, 2016). It is important to note in this context that visual navigation does not necessarily require high-resolution vision (e.g. Milford, 2013; Stürzl et al., 2015; Wystrach et al., 2016). However, differences in resolution do affect target detection (e.g. Spaethe and Chittka, 2003) which may impact worker foraging efficiency. This will be dependent on the foraging strategies employed by *Temnothorax* ants in natural conditions, which are unfortunately not well studied. Detection of small objects and detection distances will be improved in workers with greater visual resolution. Adding a word of caution in this context, we note that we had to estimate compound eye properties such as visual fields and inter-ommatidial angles from SEM preparations and light-microscopy sections, because *in-vivo* optical analysis is practically impossible in these small heavily pigmented eyes. It thus remains to be investigated how the number of ommatidia and eye curvature vary in these ants which will both determine the variations in resolution and visual fields. Studying foraging behaviours and visual tasks in a natural setting should tell us more about what is required from the compound eyes of *Temnothorax* ants.

The lens diameters of the ants do not vary with head width, but vary within each individual. Their lens diameters in the compound eyes of *T. rugatulus* (range: 14.7-19.0 μm) place them in the company of much larger day-active ants (e.g., *M. bagoti*: 19 μm (Schwarz et al., 2011); *M. croslandi*:

18 µm (Greiner et al., 2007)). However, their large rhabdom diameter and in particular the very short effective focal length in these eyes generate an optical sensitivity that is much higher (S=4.1 $\mu m^2 sr^{-1}$) than that found in large nocturnal ants (e.g. *M. pyriformis*: S=1-1.6 $\mu m^2 sr^{-1}$; (Greiner et al., 2007)) and nocturnal bees (e.g. *Megalopta genalis*, S=2.7 $\mu m^2 sr^{-1}$; (Greiner et al., 2004)). This unexpectedly high sensitivity in *T. rugatulus* may be an adaptation for the dim-lit leaf litter habitat in which these ants forage. In *T. rugatulus* facet diameters did not vary with head width, but if rhabdom diameters decreased in smaller individuals, this would reduce their optical sensitivity.

Our modelling of the optical properties of *T. rugatulus* ommatidia indicates that given the assumption of uniform refractive indices, the lens and crystalline cone do not focus light on the distal tip of the rhabdom, but at a point about 10µm down the length of the rhabdom. This severe under-focussing has not been found in other miniature compound eyes (e.g. Fischer et al. 2011; Makarova et al. 2015). However, a discussion of the functional significance of this arrangement would be premature, because we do not know whether there is a refractive index gradient in the facet lenses of *T. rugatulus* ommatidia that would increase the refractive power of the optical system, bringing the focal plane closer to the distal tip of the rhabdom.

We also found what seem to be specialised rhabdoms, which appear rectangular in cross-section (**Figure 3.8f**). These are similar to the specialised photoreceptors found in the dorsal rim area of several ants such as *Cataglyphis fortis*, *Camponotus consobrinus*, *M. pyriformis*, *Nothomyrmecia macrops*, and *P. sokolova* (Narendra et al., 2016; Zeil et al., 2014). In these specialised rhabdoms the microvilli of retinular cells are typically oriented at 90° relative to each other and do not twist along the length of the rhabdom, making them sensitive to the direction of polarised light. Although we were unable to confirm these properties in *T. rugatulus*, the rectangular cross sections of dorsal rhabdoms hint at the possibility that in addition to using landmark information for navigation, *Temnothorax* ants may also rely on the pattern of polarised skylight to derive compass information for path integration.

3.4.3. Worker size variation

Workers in our sample vary in head width from 0.45 to 0.66 mm (n=100) and had a normal frequency distribution. By comparison, Westling et al. (2014) examined worker size variation in great detail and found worker

head width ranged from 0.35 to 0.70 (n=522). Furthermore, Westling et al. (2014) also identified a small intranidal class of workers and a large extranidal class. These two sub-populations had overlapping distributions which when pooled give rise to a distribution similar to ours. However, the small intranidal workers described were much smaller than any workers we observe in our sample. The greater range in distribution and the bias towards larger workers we observe might be explained by differences in sample sizes in the two studies or it may be because the two colonies we sampled do not represent mature colonies. There may be costs associated with producing fully specialised workers before the colony has reached maturity and achieved a full complement of workers. Young and small colonies in other species have previously been shown to produce worker size distributions that differ from those of mature colonies (Tschinkel, 1998; Tschinkel, 1988; Wood and Tschinkel, 1981).

Although the range and frequency distribution of worker head widths shown here is not fully consistent with those previously reported this does not imply that workers in our sample were uniform. Even the limited range of body-sizes we observe seems considerable for a "monomorphic" species and is sufficient to produce variability in the sensory arrays.

3.5. Conclusions

We observe variability in the sensory systems of *T. rugatulus*, which is linked, to some extent, to worker head width. We suggest that these variations, both of the compound eyes and antennal sensor arrays, may have functional implications in terms of a worker's access to information about her social and physical environment. This may in turn play a role in worker specialisation and task allocation although this remains to be tested using behavioural experiments, which identify not just worker size but also intra- or extranidal behavioural castes.

3.6. References

Barsagade, D.D., Tembhare, D.B., Kadu, S.G., 2013. Microscopic structure of antennal sensilla in the carpenter ant *Camponotus compressus* (Fabricius)(Formicidae: Hymenoptera). Asian Myrmecology 5, 113-120.

Bengston, S., Dornhaus, A., 2013. Colony size does not predict foraging distance in the ant *Temnothorax rugatulus*: a puzzle for standard scaling models. Insectes Sociaux 60, 93-96.

Bengston, S., Dornhaus, A., 2014. Be meek or be bold? A colony-level behavioural syndrome in ants. Proceedings of the Royal Society of London B: Biological Sciences 281, 20140518.

Bernstein, S., Finn, C., 1971. Ant compound eye: size-related ommatidium differences within a single wood ant nest. Experientia 27, 708-710.

Cao, T., Dornhaus, A., 2012. Ants use pheromone markings in emigrations to move closer to food-rich areas. Insectes Sociaux 59, 87-92.

Charbonneau, D., Dornhaus, A., 2015a. When doing nothing is something. How task allocation strategies compromise between flexibility, efficiency, and inactive agents. Journal of Bioeconomics 17, 217-242.

Charbonneau, D., Dornhaus, A., 2015b. Workers 'specialized' on inactivity: Behavioral consistency of inactive workers and their role in task allocation. Behavioral Ecology and Sociobiology 69, 1459-1472.

Creighton, W.S., 1950. The Ants of North America. Bulletin of the Museum of Comparative Zoolology, Harvard College.

Duchamp-Viret, P., Chaput, M., Duchamp, A., 1999. Odor response properties of rat olfactory receptor neurons. Science 284, 2171-2174.

Dumpert, K., 1972. Bau und Verteilung der Sensillen auf der Antennengeißel von *Lasius fuliginosus* (Latr.)(Hymenoptera, Formicidae). Zoomorphology 73, 95-116.

Faber, T., Joerges, J., Menzel, R., 1999. Associative learning modifies neural representations of odors in the insect brain. Nat Neurosci 2, 74-78.

Fischer, S., Müller, C.H., Meyer-Rochow, V.B., 2011. How small can small be: the compound eye of the parasitoid wasp *Trichogramma evanescens* (Westwood, 1833)(Hymenoptera, Hexapoda), an insect of 0.3 to 0.4 mm total body size. Vis Neurosci 28, 295-308.

Fisher, B.L., Cover, S.P., 2007. Ants of North America: a guide to the genera. Univ of California Press.

Franks, N.R., Hooper, J.W., Dornhaus, A., Aukett, P.J., Hayward, A.L., Berghoff, S.M., 2007. Reconnaissance and latent learning in ants. Proceedings of the Royal Society of London B: Biological Sciences 274, 1505-1509.

Galizia, C.G., Menzel, R., 2000. Odour perception in honeybees: coding information in glomerular patterns. Current Opinion in Neurobiology 10, 504-510.

Getz, W.M., Akers, R.P., 1995. Partitioning non-linearities in the response of honey bee olfactory receptor neurons to binary odors. Biosystems 34, 27-40.

Gray, B., 1974. Nest structure and populations of *Myrmecia* (Hymenoptera: Formicidae), with observations on the capture of prey. Insectes Sociaux 21, 107-120.

Greiner, B., Narendra, A., Reid, S.F., Dacke, M., Ribi, W.A., Zeil, J., 2007. Eye structure correlates with distinct foraging-bout timing in primitive ants. Current Biology 17, R879-R880.

Greiner, B., Ribi, W.A., Warrant, E.J., 2004. Retinal and optical adaptations for nocturnal vision in the halictid bee *Megalopta genalis*. Cell and Tissue Research 316, 377-390.

Gronenberg, W., Hölldobler, B., 1999. Morphologic representation of visual and antennal information in the ant brain. Journal of Comparative Neurology 412, 229-240.

Hashimoto, Y., 1990. Unique features of sensilla on the antennae of Formicidae (Hymenoptera). Applied Entomology and Zoology 25, 491-501.

Heinzel, H.-G., Gewecke, M., 1979. Directional sensitivity of the antennal campaniform sensilla in locusts. Naturwissenschaften 66, 212-213.

Hölldobler, B., Wilson, E.O., 1990. The Ants. The Belknap Press of Harvard University Press, Cambridge, Massachusetts.

Jaisson, P., 1969. Étude de la distribution des organes sensoriels de l'antenne et de leurs relations possibles avec le comportement chez deux fourmis myrmicines: *Myrmica laevinodis* Nyl. et *Aphaenogaster gibbosa* Latr. récoltées dans la région des Eyzies. Insectes Sociaux 16, 279-312.

Kaspari, M., Weiser, M., 1999. The size–grain hypothesis and interspecific scaling in ants. Functional Ecology 13, 530-538.

Kelber, C., Rössler, W., Kleineidam, C.J., 2006. Multiple olfactory receptor neurons and their axonal projections in the antennal lobe of the honeybee *Apis mellifera*. Journal of Comparative Neurology 496, 395-405.

Kleineidam, C., Romani, R., Tautz, J., Isidoro, N., 2000. Ultrastructure and physiology of the CO_2 sensitive sensillum ampullaceum in the leaf-cutting ant *Atta sexdens*. Arthropod Structure and Development 29, 43-55.

Kleineidam, C., Rössler, W., Hölldobler, B., Roces, F., 2007. Perceptual differences in trail-following leaf-cutting ants relate to body size. Journal of insect physiology 53, 1233-1241.

Land, M.F., 1981. Optics and vision in invertebrates, In: Autrum, H. (Ed.), Handbook of Sensory Physiology. Springer, Berlin Heidleberg New York, pp. pp. 471-592.

Land, M.F., Nilsson, D.-E., 2012. Animal Eyes, Second ed. Oxford University Press, Oxford.

Leponce, M., Delsinne, T., Laurent, Y., Cillis, J., Bachy, I., Heughebaert, A., Desmet, P., Youdjou, N., 2008. RBINS Ant eMuseum: Paraguay Collection. Royal Belgian Institute of Natural Sciences.

Lewis, C., 1971. Superficial sense organs of the antennae of the fly, Stomoxys calcitrans. Journal of insect physiology 17, 449-461.

Makarova, A., Polilov, A., Fischer, S., 2015. Comparative morphological analysis of compound eye miniaturization in minute hymenoptera. Arthropod Structure & Development 44, 21-32.

Maleszka, R., 2016. Epigenetic code and insect behavioural plasticity. Current Opinion in Insect Science 15, 45-52.

Marques-Silva, S., Matiello-Guss, C.P., Delabie, J.H.C., Mariano, C.S.F., Zanuncio, J.C., Serrão, J.E., 2006. Sensilla and secretory glands in the antennae of a primitive ant: *Dinoponera lucida* (Formicidae: Ponerinae). Microscopy Research and Technique 69, 885-890.

Maschwitz, U., Lenz, S., Buschinger, A., 1986. Individual specific trails in the ant *Leptothorax affinis* (Formicidae: Myrmicinae). Experientia 42, 1173-1174.

Menzi, U., 1987. Visual adaptation in nocturnal and diurnal ants. Journal of Comparative Physiology A 160, 11-21.

Milford, M., 2013. Vision-based place recognition: how low can you go? The International Journal of Robotics Research 32, 766-789.

Möglich, M., Maschwitz, U., Hölldobler, B., 1974. Tandem calling: a new kind of signal in ant communication. Science 186, 1046-1047.

Mysore, K., Shyamala, B.V., Rodrigues, V., 2010. Morphological and developmental analysis of peripheral antennal chemosensory sensilla and central olfactory glomeruli in worker castes of *Camponotus compressus* (Fabricius, 1787). Arthropod Structure & Development 39, 310-321.

Nakanishi, A., Nishino, H., Watanabe, H., Yokohari, F., Nishikawa, M., 2009. Sex-specific antennal sensory system in the ant *Camponotus japonicus*: structure and distribution of sensilla on the flagellum. Cell and Tissue Research 338, 79-97.

Narendra, A., Alkaladi, A., Raderschall, C.A., Robson, S.K.A., Ribi, W.A., 2013. Compound eye adaptations for diurnal and nocturnal lifestyle in the intertidal ant, *Polyrhachis sokolova*. PloS one 8, e76015.

Narendra, A., Ramirez-Esquivel, F., Ribi, W.A., 2016. Compound eye and ocellar structure for walking and flying modes of locomotion in the Australian ant, *Camponotus consobrinus*. Scientific Reports 6, 22331.

Narendra, A., Reid, S.F., Greiner, B., Peters, R.A., Hemmi, J.M., Ribi, W.A., Zeil, J., 2011. Caste-specific visual adaptations to distinct daily activity schedules in Australian *Myrmecia* ants. Proceedings of the Royal Society B: Biological Sciences 278, 1141-1149.

Narendra, A., Reid, S.F., Raderschall, C.A., 2013. Navigational efficiency of nocturnal *Myrmecia* ants suffers at low light levels. PloS one 8, e58801.

Niering, W.A., Lowe, C.H., 1984. Vegetation of the Santa Catalina Mountains: community types and dynamics. Vegetatio 58, 3-28.

Perl, C.D., Niven, J.E., 2016. Differential scaling within an insect compound eye. Biology Letters 12, 20160042.

Pix, W., Zanker, J.M., Zeil, J., 2000. The optomotor response and spatial resolution of the visual system in male *Xenos vesparum* (Strepsiptera). Journal of Experimental Biology 203, 3397-3409.

Pratt, S.C., Brooks, S.E., Franks, N.R., 2001. The use of edges in visual navigation by the ant *Leptothorax albipennis*. Ethology 107, 1125-1136.

Ramirez-Esquivel, F., Zeil, J., Narendra, A., 2014. The antennal sensory array of the nocturnal bull ant *Myrmecia pyriformis*. Arthropod Structure & Development 43, 543-558.

Reid, S.F., Narendra, A., Taylor, R.W., Zeil, J., 2013. Foraging ecology of the night-active bull ant *Myrmecia pyriformis*. Australian Journal of Zoology 61, 170-177.

Renthal, R., Velasquez, D., Olmos, D., Hampton, J., Wergin, W.P., 2003. Structure and distribution of antennal sensilla of the red imported fire ant. Micron 34, 405-413.

Roces, F., Tautz, J., 2001. Ants are deaf. The Journal of the Acoustical Society of America 109, 3080-3082.

Rüppell, O., Kirkman, R., 2005. Extraordinary starvation resistance in *Temnothorax rugatulus* (Hymenoptera, Formicidae) colonies: Demography and adaptive behavior. Insectes Sociaux 52, 282-290.

Sachse, S., Rappert, A., Galizia, C.G., 1999. The spatial representation of chemical structures in the antennal lobe of honeybees: steps towards the olfactory code. European Journal of Neuroscience 11, 3970-3982.

Sasaki, T., Hölldobler, B., Millar, J.G., Pratt, S.C., 2014. A context-dependent alarm signal in the ant *Temnothorax rugatulus*. The Journal of Experimental Biology 217, 3229-3236.

Schneider, D., 1964. Insect antennae. Annual Review of Entomology 9, 103-122.

Schwarz, S., Narendra, A., Zeil, J., 2011. The properties of the visual system in the Australian desert ant *Melophorus bagoti*. Arthropod Structure & Development 40, 128-134.

Spaethe, J., Brockmann, A., Halbig, C., Tautz, J., 2007. Size determines antennal sensitivity and behavioral threshold to odors in bumblebee workers. Naturwissenschaften 94, 733-739.

Spaethe, J., Chittka, L., 2003. Interindividual variation of eye optics and single object resolution in bumblebees. Journal of Experimental Biology 206, 3447-3453.

Stavenga, D., 2003. Angular and spectral sensitivity of fly photoreceptors. II. Dependence on facet lens F-number and rhabdomere type in *Drosophila*. Journal of Comparative Physiology A 189, 189-202.

Steinbrecht, R.A., 1973. Der feinbau olfaktorischer sensillen des Seidenspinners (Insecta, Lepidoptera). Zeitschrift für Zellforschung und mikroskopische Anatomie 139, 533-565.

Stroeymeyt, N., Franks, N.R., Giurfa, M., 2011. Knowledgeable individuals lead collective decisions in ants. The Journal of Experimental Biology 214, 3046-3054.

Stroeymeyt, N., Jordan, C., Mayer, G., Hovsepian, S., Giurfa, M., Franks, N., 2014. Seasonality in communication and collective decision-making in ants. Proceedings of the Royal Society of London B: Biological Sciences 281, 20133108.

Stürzl, W., Grixa, I., Mair, E., Narendra, A., Zeil, J., 2015. Three-dimensional models of natural environments and the mapping of navigational information. Journal of Comparative Physiology A 201, 563-584.

Tschinkel, W., 1998. Sociometry and sociogenesis of colonies of the harvester ant, *Pogonomyrmex badius*: worker characteristics in relation to colony size and season. Insectes Sociaux 45, 385-410.

Tschinkel, W.R., 1988. Colony growth and the ontogeny of worker polymorphism in the fire ant, *Solenopsis invicta*. Behavioral Ecology and Sociobiology 22, 103-115.

Tschinkel, W.R., Mikheyev, A.S., Storz, S.R., 2003. Allometry of workers of the fire ant, *Solenopsis invicta*. Journal of Insect Science 3, 2.

van der Woude, E., Smid, H.M., 2015. How to escape from Haller's rule: olfactory system complexity in small and large *Trichogramma evanescens* parasitic wasps. Journal of Comparative Neurology 524, 1876-1891.

Warrant, E., Dacke, M., 2011. Vision and visual navigation in nocturnal insects. Annual Review of Entomology 56, 239-254.

Warrant, E.J., Nilsson, D.-E., 1998. Absorption of white light in photoreceptors. Vision research 38, 195-207.

Westling, J., Harrington, K., Bengston, S., Dornhaus, A., 2014. Morphological differences between extranidal and intranidal workers in the ant *Temnothorax rugatulus*, but no effect of body size on foraging distance. Insectes Sociaux 61, 367-369.

Wood, L.A., Tschinkel, W.R., 1981. Quantification and modification of worker size variation in the fire ant *Solenopsis invicta*. Insectes Sociaux 28, 117-128.

Wystrach, A., Dewar, A., Philippides, A., Graham, P., 2016. How do field of view and resolution affect the information content of panoramic scenes for visual navigation? A computational investigation. Journal of Comparative Physiology A 202, 87-95.

Yack, J.E., 2004. The structure and function of auditory chordotonal organs in insects. Microscopy Research and Technique 63, 315-337.

Yan, S.C., Meng, Z.J., Peng, L., Liu, D., 2011. Antennal sensilla of the pine weevil *Pissodes nitidus* Roel.(Coleoptera: Curculionidae). Microscopy Research and Technique 74, 389-396.

Yokohari, F., 1983. The coelocapitular sensillum, an antennal hygro- and thermoreceptive sensillum of the honey bee, *Apis mellifera* L. Cell and Tissue Research 233, 355-365.

Zeil, J., Ribi, W.A., Narendra, A., 2014. Polarisation Vision in Ants, Bees and Wasps, In: Horváth, G. (Ed.), Polarized Light and Polarization Vision in Animal Sciences. Springer, pp. 41-60.

3.7. Appendices

3.7.1. Additional notes on palmate sensilla

Branched sensilla on the additional species that I examined for this chapter varied in appearance. In *Paraparatrechina minitula* branched sensilla were present on the head, mesosoma (two longitudinal rows) and gaster (at the distal edge of each gastral segment) and resembled the branched sensilla found on the thorax and gaster of *T. rugatulus* (see **Figure 3.9**). In *Technomyrmex* sp. 1 branched sensilla were found in the same organisation as in *P. minitula* but the head and gaster sensilla differed in appearance to the mesosoma sensilla (see **Figure 3.10**). In *Pheidole* sp.2 the branched sensilla were found on the mesosoma, petiole and gaster and looked very different from those in other species. In *Pheidole* sp.1 branched sensilla were only branched distally and there were very many fewer branches (see **Figure 3.11**).

After the publication of this chapter I observed branched sensilla documented on SEMs of a variety of ant species in the RBINS Ant eMuseum (Leponce et al., 2008), an online resource hosted by the Royal Belgian Institute of Natural Sciences (http://projects.biodiversity.be/ants/). At this point it is difficult to say if all of these branched sensilla are analogous or even if they are all innervated or not. With that in mind I've recorded the species that have any kind of branched sensillum on any part of the body as they may be useful in further studies.

The following species from the RBINS database seem to have branched sensilla:

- *Brachymyrmex luederwalti*
- *Caponotus* sp. 07 (see **Figure 3.12a** and **b**)
- *Crematogaster quadriformis* (unclear from available images)
- *Crematogaster* sp. 08
- *Paratrechina* sp. 02
- *Pogonomyrmex cunicularius* (see **Figure 3.12c**)
- *Pogonomyrmex naegelli* (unclear from available images)
- *Strumigenys* sp. 04 (unclear from available images)
- *Thaumatomyrmex* sp. 01 (unclear from available images, see **Figure 3.12d**)

Note: Not all *Crematogaster* species have branched sensilla, and not all species with branched sensilla have them in the same body segments. Because of this presence/absence of branched sensilla within a single genus *Crematogaster* ants may be an interesting species to focus further studies on. Additionally, these ants are extremely widely distributed and generally common.

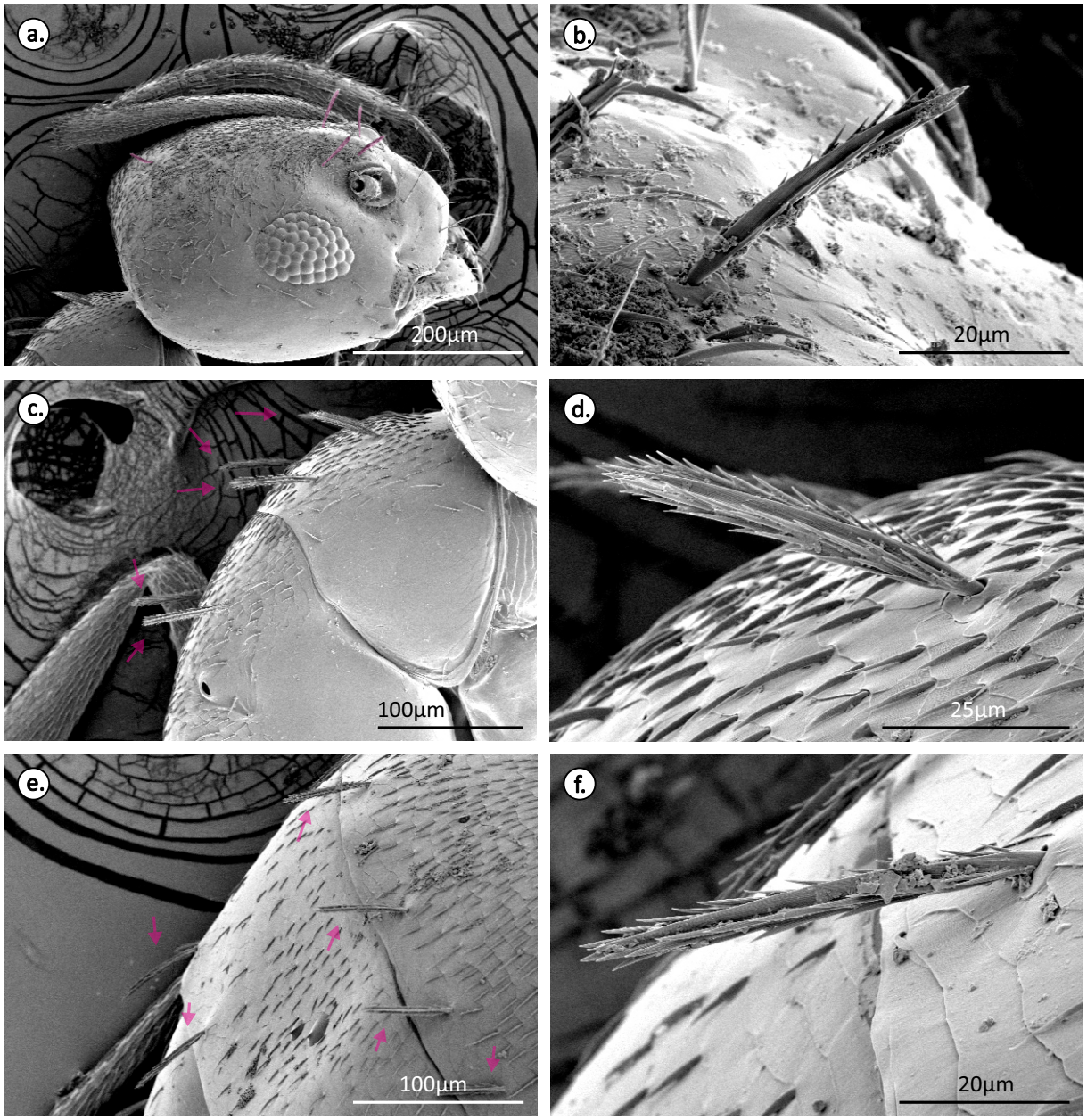

Figure 3.9. Branched sensilla in *Paraparatrechina minitula.* Branched or palmate sensilla are found on the head (a, b); mesosoma (c, d) and dorsal gaster (e, f).

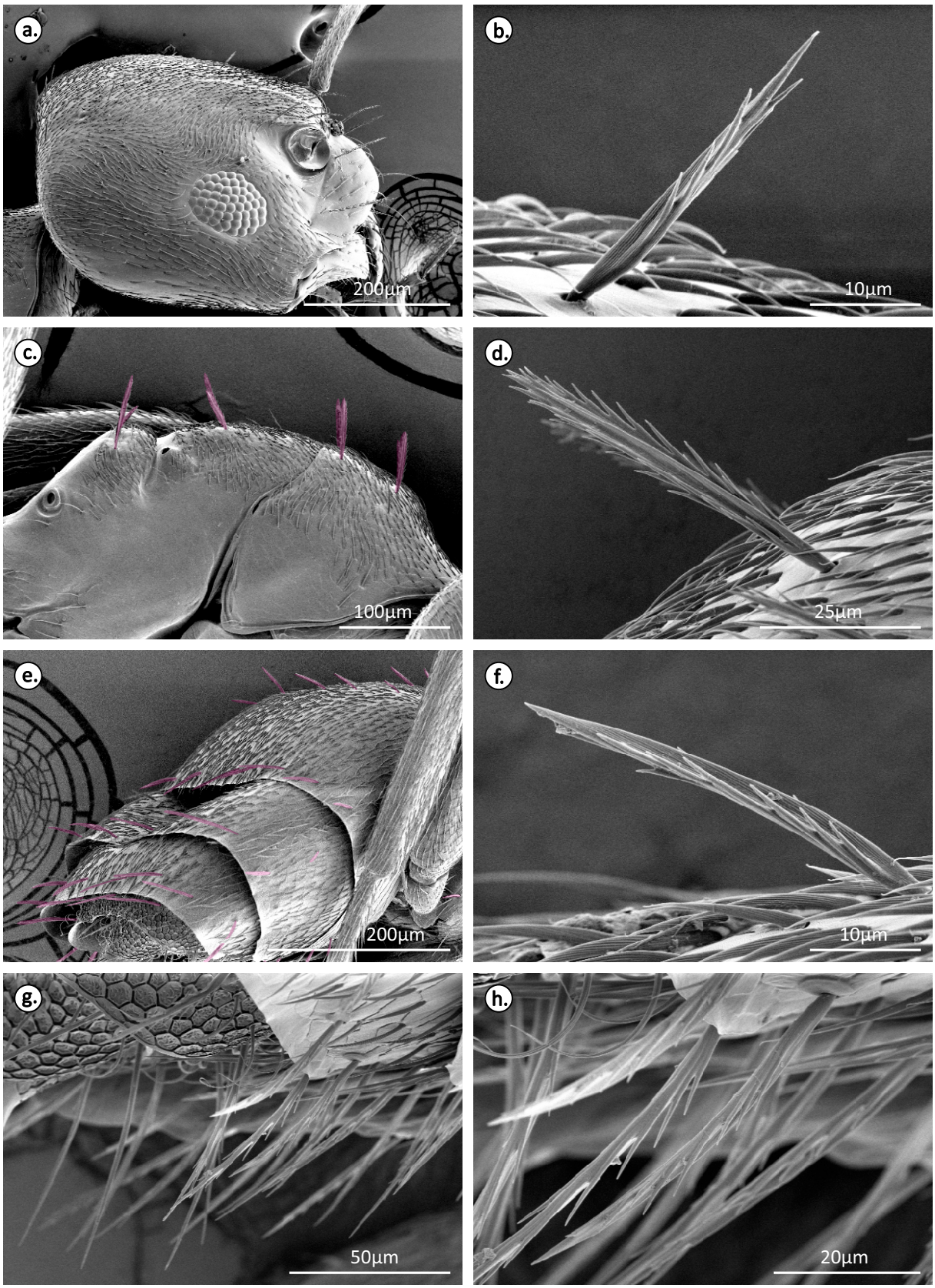

Figure 3.10. Branched sensilla in *Technomyrmex* sp. 1. Branched hairs or palmate sensilla are found on the head (a, b); mesosoma (c, d); dorsal gaster (e, f) and ventral gaster (g, h). Pink colouring is added during post-processing to highlight the location of the sensilla in low magnification images.

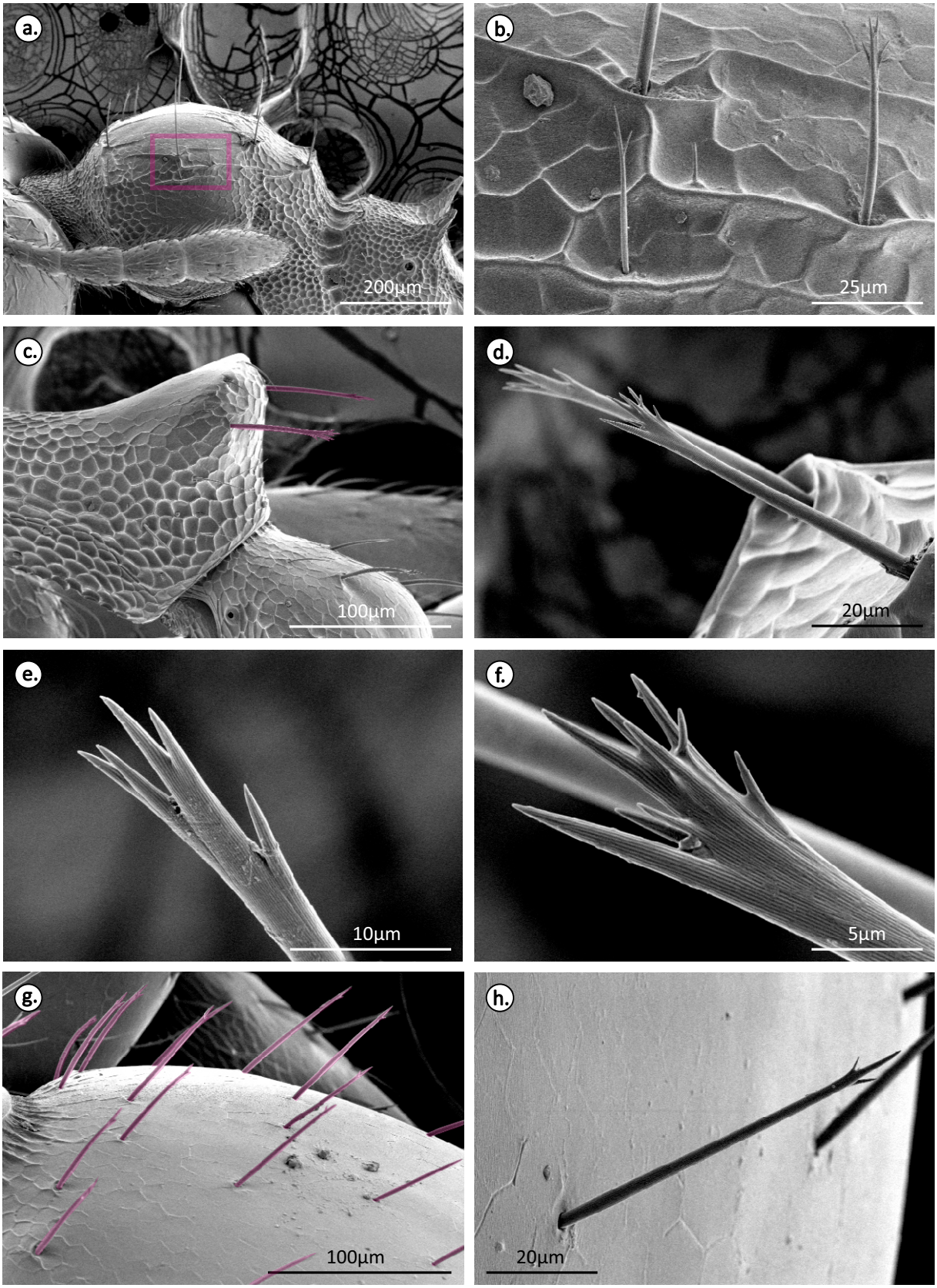

Figure 3.11. Branched sensilla in *Pheidole* sp.2. Long branched sensilla on the mesosoma (a), inset area shown in greater magnification in (b); two long branched sensilla on the petiole (highlighted in pink, c); shown in higher magnification in (d, e, f); long sensilla with simple, terminal branches on the gaster (g) single example shown in greater magnification in (h).

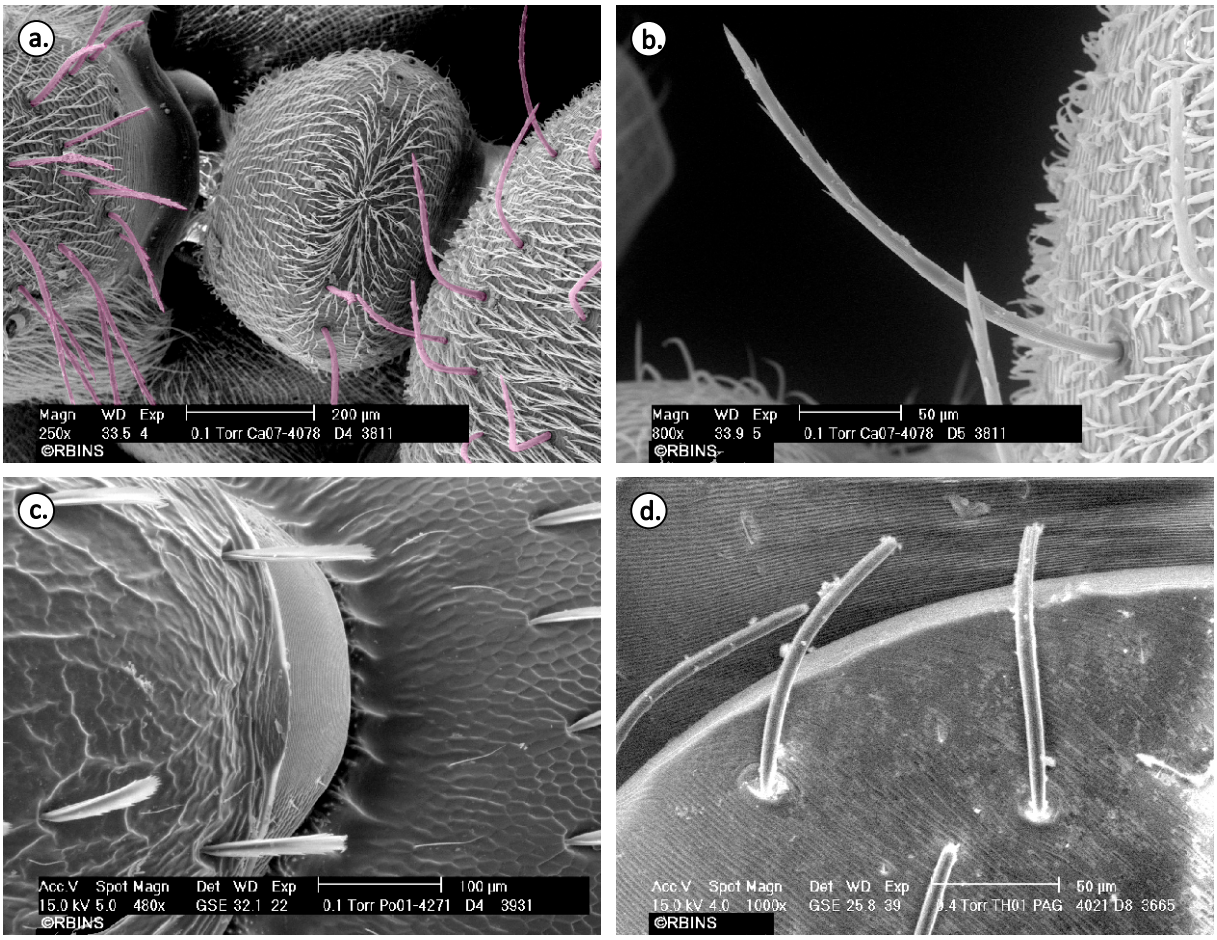

Figure 3.12. Species from RBINS database with branched sensilla. *Camponotus* sp. 07 mesosoma, petiole and gaster (a, b); *Pogonomyrmex cunicularius* petiole and gaster (c); *Thaumatomyrmex* sp. 01 (d).

Chapter 4

Miniaturisation of the antennal array

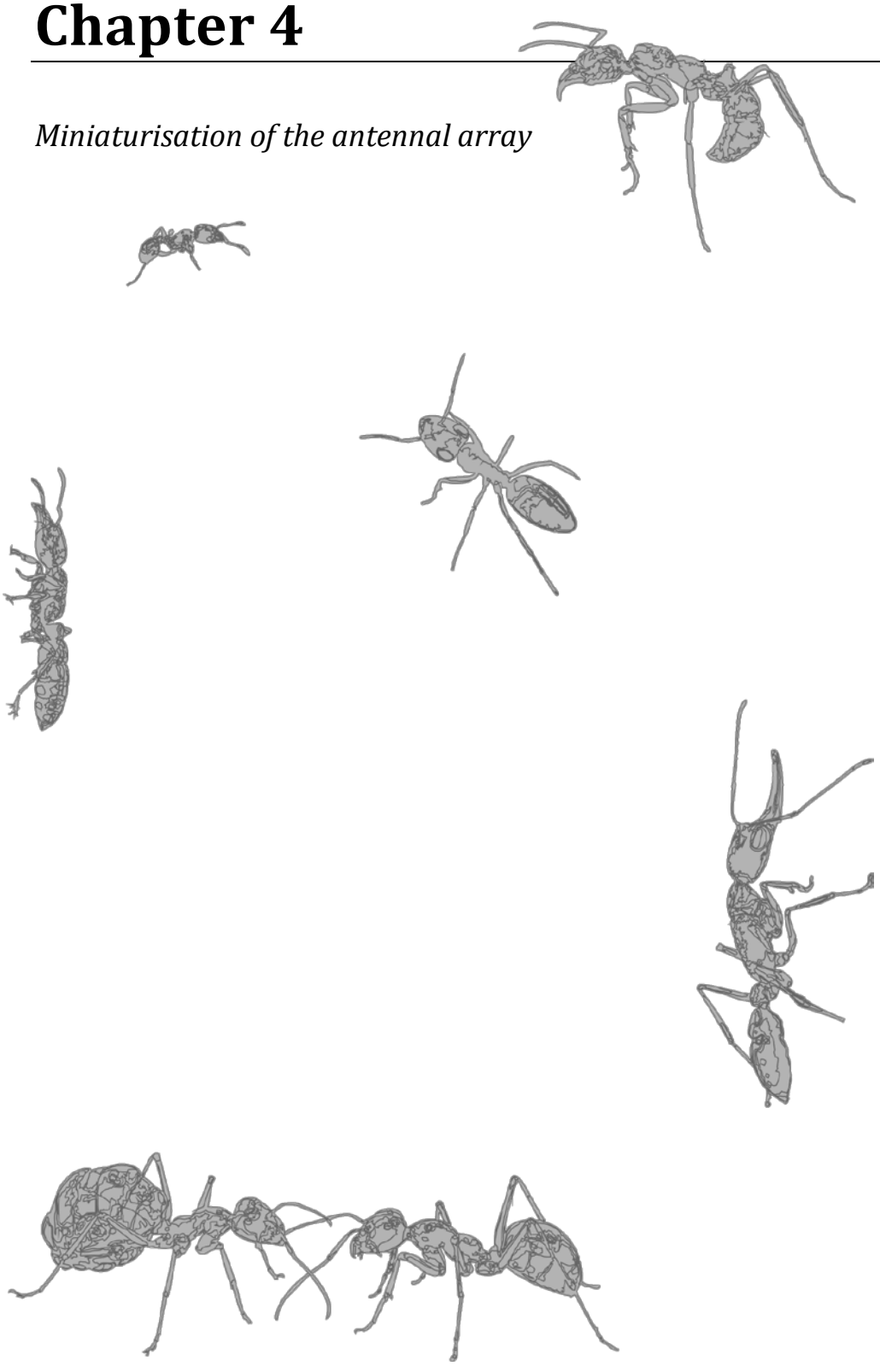

Chapter contents

This chapter represents the first large-scale, functional anatomy[3] survey of the antennal sensilla of Formicidae. As a consequence, there was no pre-existing framework for this kind of study. The development of methods for data collection and crafting of a context in which to interpret the results represented a large component of this thesis. In a sense, all the preceding chapters have laid the groundwork for this section from both a methodological and conceptual point of view. For the sake of succinctness, some level of familiarity with previous chapters will be assumed here (in particular content from **Chapter 1** and **Chapter 2**).

Images analysed in this chapter come from original SEM imagery (FRE), RBINS database (Leponce et al., 2008), AntWeb (www.antweb.org), and SEM images of four species collected for previous work (Ramirez-Esquivel, 2012). Full species lists and details of how and where data were used are included in the text and appendices. All measurements, analyses and writing were carried out by FRE with the following exceptions. Apical flagellomere area and volume estimates using spline interpolation were carried out by Caleb Ball. Measurements of antenna segment size in the tribe Attini were carried out by Barbara Ramirez-Esquivel. Specimen identification was carried out, in most cases, by Ajay Narendra.

The contents of this chapter are being prepared for publication as two separate manuscripts:

> **Ramirez-Esquivel, F., Zeil, J., Narendra, A., Miniaturisation of the Formicid antenna: why do small species have club antennae?**
>
> **Ramirez-Esquivel, F., Zeil, J., Narendra, A., Miniaturisation in ant chemosensilla: size, numbers and density.**

It is worth noting that the data collected for this chapter exceeds what could be presented here. The number of analyses also had to be limited by constraints on time and resources. This chapter represents a first attempt to understand the antennal array of ants in the context of miniaturisation

[3] One previous effort was made by Hashimoto (1990) with the intention of assessing sensilla anatomy as a potential taxonomic tool. Although the taxonomic coverage of this work is excellent, data on the size, numbers, types and organisation of the sensilla are less comprehensive.

and by no means answers every possible question. This will be an ongoing task that will, hopefully, be shared by future workers.

4.1. Introduction

Miniaturisation is the decrease of body size over an evolutionary time scale (Hanken and Wake, 1993). As a consequence the effects of miniaturisation are best studied using a comparative approach. Ants display a large variation in body size but also share many natural history traits across species, which facilitates comparative studies within this family. The miniaturisation of sensory systems is an interesting area as it encompasses different fields of study, from the physical properties of the stimuli to the morphological and neuroanatomical design of the receptors, to the impacts on the biology of a species. This chapter focuses on the morphology of the antennae and the chemosensory array, discussing the functional implications of anatomical changes in the context of miniaturisation.

The ant antennal array is an important sensory structure that functions as a complex interphase between an individual and its environment. The antenna is covered in a variety of sensilla, which function in different modalities (for a review see **Chapter 2**). This study will focus on three different types of chemosensilla: sensilla basiconica, trichodea and trichodea curvata, as chemoreception is of particular importance in the Formicidae due to their complex social habits (see **Chapters 2** and **3**).

Sensory systems are generally fine-tuned to suit an animal's ecological niche and sensory requirements. Despite the ecological diversity encompassed within the Formicidae, there are important commonalities shared by all subfamilies. Perhaps the most important of these is eusociality. This trait is by necessity associated with other important characteristics such as communication among nest-mates, nest-mate recognition, central place foraging, nest maintenance, etc. Additional important commonalities include a shared basic antennal architecture (i.e. three segmented, geniculate antennae) and the pedestrian habit of all worker ants. These ecological and anatomical consistencies across Formicidae facilitate comparative studies across this large taxonomic group.

Beyond ecology, body size plays a very important role in shaping sensory organ design. This is because many of the processes involved in sensing are size dependent; they cannot be scaled isometrically with body size without affecting function (see **Chapter 1**). This leads to a minimum functional size for sensory organs. These size limitations are particularly well understood in the case of visual systems. Visual units (ommatidia in the case of compound eyes) have well-established theoretical size limits

defined by factors such as the diffraction limit of lenses and neural noise (see **Chapter 1**). As animals become smaller their eyes must decrease in size as well. As compound eyes become smaller either the number of ommatidia may be reduced, leading to a drop in resolution, or the size of ommatidia may decrease, leading to a decline in sensitivity. However, the size of ommatidia may only be reduced so far without compromising function, at which point the only option is to reduce the number of ommatidia. These constraints may lead extremely small insects that rely on vision to favour bright environments (as small ommatidia have reduced sensitivity) and ecologies that do not require high visual resolution (e.g. pedestrian scavengers rather than active solitary visual hunters).

Unfortunately, the state of knowledge on the chemosensory biology in insects is not as advanced as our knowledge of visual systems. One big problem in this field is that the number of sensory units, sensilla, is not associated with resolution or sensitivity in a straightforward manner. This is because the number and types of chemoreceptors per sensillum may vary dramatically. However, some experiments have shown that there is a relationship between a decreased number of sensilla and a decrease in sensitivity (Chapman, 1982; Gill et al., 2013; Jayaweera and Barry, 2017; Spaethe et al., 2007). No studies to date appear to have assessed the relationship between the size of a sensillum and sensory function.

Chemosensilla consist of an outer cuticular peg with perforations that allow chemical cues to enter the lumen of the peg. Inside the peg there are dendritic endings of a variable number of chemosensory neurons. Housed in the membrane of these dendritic endings are chemoreceptors, which may be sensitive to a variety of chemical cues (d'Ettorre et al., 2017; Esslen and Kaissling, 1976; Kelber et al., 2006; Schneider and Steinbrecht, 1968; Slone et al., 2017). It is therefore, impossible to know from anatomy alone what chemical cues a species may be sensitive to. However, the number of chemoreceptors present seems to be dependent on the membrane surface area (Berg and Purcell, 1977). All things being equal, sensitivity should be related to the total sensory surface area, which may be approximated by the number of sensilla (and perhaps their size). The main factor unaccounted for here is that a species with a greater variety of chemoreceptors may be less sensitive to a given cue than a species with the same sensory surface area but fewer types of chemoreceptors (i.e. more copies of the same chemoreceptors).

Having outlined the limitations of anatomical studies, in this chapter I ask: If the association between reductions in body size, number of sensilla, and sensitivity are consistent, do small species have anatomical

modifications to maximise their access to sensory information? Does the size or density of sensilla play a role in this context?

Since we expect small ants to be constrained by the physical limits of chemical sensory physiology the main objective of this chapter is to attempt to identify potential adaptations that compensate for miniaturisation in the antennal array. However, because no large scale, comprehensive, comparative study on ant antennae has been carried out before, I first describe the overall range of variation. As discussed in the introductory chapter of this thesis, it is necessary to have a good understanding of the full range of variation in order to identify adaptations that are specific to miniaturisation.

Descriptions of the antennal array of individual species abound in the literature; unfortunately, the significant methodological differences across this literature mean that collating existing data is not appropriate. For example, different researchers have used different techniques to count the number of sensilla; length measurements of sensilla sometimes lack sample sizes (number of sensilla measured) and measures of variability (e.g. standard deviations); and even basic identification of sensilla may be contentious at times. While there are many excellent and thorough publications in this area, in most cases it remains difficult to carry out direct comparisons.

By using a consistent methodology this study aims to sample and carry out direct comparisons across a wide range of formicid species. This allows, for the first time, a quantitative description of the variability in size, numbers and distribution of chemosensilla across Formicidae. In addition, allometric patterns in gross antennal anatomy are analysed for the first time and the transition from filiform to club antennae is investigated. I added these latter analyses to the original aims since it became apparent over the course of this study that they were necessary to study the miniaturisation of the antennal array. Although the focus of this study is the identification of miniaturisation related adaptations, ecological and phylogenetic influences on the antennal array are considered throughout the analyses.

4.2. Methods

4.2.1. Specimen collection

Specimens were collected from various localities and by different workers into 70% ethanol. A full list of the species studied and collection details are given in the table below:

Table 4.1. Specimen collection details. Specimens were collected by AN: Ajay Narendra, CR: Chloé Raderschall, FRE: Fiorella Ramirez-Esquivel, FS: Franziska Schmitt, KC: Ken Cheng, PF: Pauline Fleischmann, NEL: Nicole E. Leitner, SW: Sara Wood.

Species	Location	Collected by
Amblyopone australis	Black Mt, ACT, Australia	AN
Camponotus consobrinus	ANU campus, ACT, Australia	FRE
Camponotus piliventris	ANU campus, ACT, Australia	FRE
Cataglyphis noda	Greece	FS and PF
Eciton hamatum	Barro Colorado Island, Panama	AN
Harpegnathos saltator	Shimoga, India	AN
Iridomyrmex calvus	ANU campus, ACT, Australia	FRE
Iridomyrmex purpureus	ANU campus, ACT, Australia	FRE
Lioponera singularis	Scotia, NSW, Australia	AN
Melophorus bagoti	Alice Springs, NT, Australia	KC
Meranoplus ferrugineus	ANU campus, ACT, Australia	FRE
Myrmecia croslandi	ANU campus, ACT, Australia	FRE
Myrmecia nigriceps	ANU campus, ACT, Australia	AN and SW
Myrmecia pyriformis	ANU campus, ACT, Australia	FRE
Myrmecia tarsata	ANU campus, ACT, Australia	AN and SW
Nothomyrmecia macrops	Poochera, SA, Australia	AN and FRE
Notoncus ectatommoides	ANU campus, ACT, Australia	FRE
Odontomachus simillimus	JCU campus, Townsville, Australia	AN
Oecophylla smaragdina	Townsville, Qld, Australia	AN
Ooceraea australis	ANU campus, ACT, Australia	AN
Opisthopsis pictus	Townsville, Qld, Australia	AN
Orectognathus clarki	Murramarang, NSW, Australia	AN
Paraparatrechina minitula	ANU campus, ACT, Australia	FRE
***Pheidole* sp.1**	ANU campus, ACT, Australia	FRE
Rhytidoponera metallica	ANU campus, ACT, Australia	FRE
***Technomyrmex* sp.1**	ANU campus, ACT, Australia	FRE
Temnothorax rugatulus	Santa Catalina Mt, Arizona, USA	NEL

4.2.2. Specimen preparation

The methods employed in this section match those used in **Chapter 2** (please refer to this section for full methods) with the following exceptions. Air dried samples were coated either with Au/Pd (60:40) or Au for 2 mins at 20 mA. Ant heads to be used for overview images were transferred, after coating, onto 12mm carbon tabs (ProSciTech) to provide a uniform black background.

4.2.3. Imaging and image analysis

Images of the dorsal surface of the apical segment were taken at a minimum magnification of x750 but most commonly x1.0-1.5k. Individual images were stitched to create a high resolution montage of the apical segment using Corel PHOTO-PAINT X6 (2012 Corel). All measurements were carried out using ImageJ 1.51i (Rusband, National Institutes of Health, USA), for details on how sensillum measurements were carried out see **Chapter 2** and **Figure 2.1**. Sensilla were counted using either the cell counter or multi-point functions of ImageJ. Maps were made using CorelDraw X6 (2012 Corel).

4.2.4. Size measurements

A number of body size measurements, both direct and indirect, are used in the ant literature. The relative advantages and disadvantages of these are reviewed in **Chapter 5**. However, there is no general consensus on the optimal measure or proxy for body size.

In the context of this study head width was selected as the optimal proxy for body size as it could be imaged simultaneously with antennae. Additionally, it was more robust to slight errors on the mounting angle of the specimen. Head width was measured directly above the eyes, from SEM images using ImageJ. Head length measurements were also recorded and found to be highly positively correlated within the sample (R^2=0.94).

A previous study on compound eye and sensilla indicated that specialised major workers had a reduced number of sensory units relative to their size (see Ramirez-Esquivel, 2012). This is thought to be a consequence of behavioural specialisation. As examining behavioural differences among castes was outside the scope of this study, specialised castes were excluded from the analyses. In the case of species with continuously varying body

size (without distinct morphologies) a large and a small worker were included wherever possible (e.g. *Myrmecia pyriformis*). In genera with very specialised workers such as *Atta* and *Cephalotes* major workers were excluded.

Allometry of antennomeres

Dataset

Results in this section come from a subset of the species examined in the main section of this chapter plus additional data gathered from SEM images from the online RBINS database (Leponce et al., 2008) and macrophotography images from AntWeb (www.antweb.org). For a full list of the species examined here see **Appendix 1**. The data used in this section were collected at a later date than the main dataset at which time the scapes were no longer available for measurement in many of the larger species. As a result there are few large specimens, however, general trends are still observable with this data set.

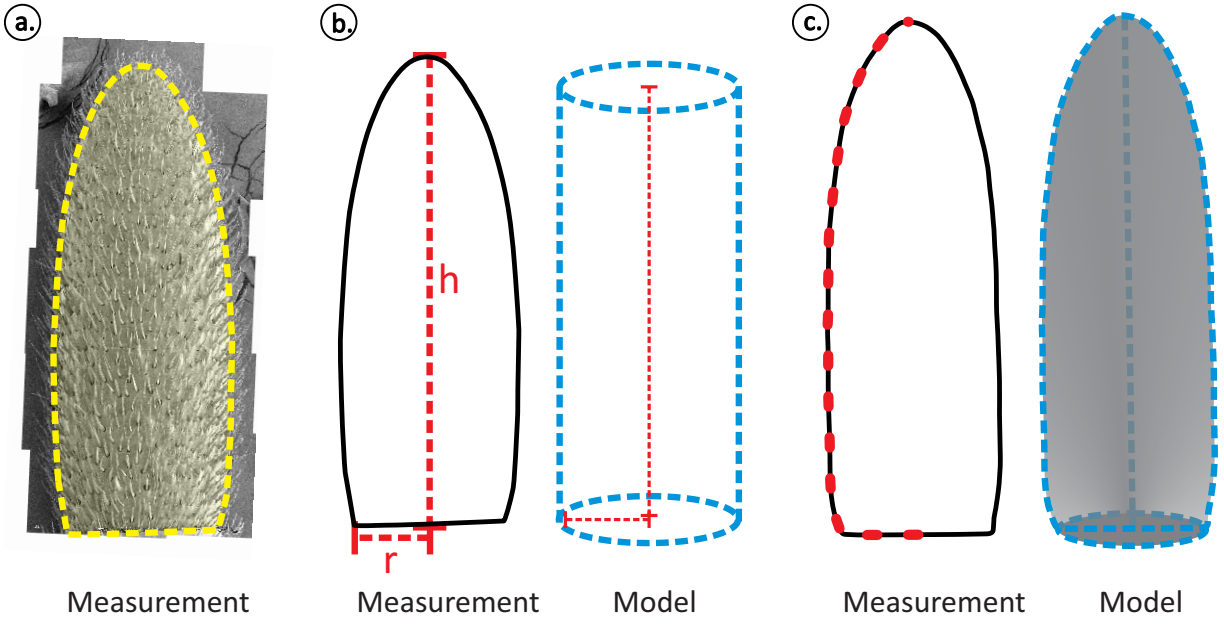

Figure 4.1. Methods of measuring and modelling the apical flagellomere. (a) Direct measurement of the visible dorsal surface (does not account for curvature). (b) Modelling as a perfect cylinder based on measurements of the height and radius. (c) Modelling based on the profile of the flagellomere.

4.2.5. Apical antennomere size

Measurements

Three size measurements were taken of the apical antennomere using high magnification SEM images of the dorsal surface of the antennomere (**Figure 4.1**). Firstly, two linear measurements were taken using the "straight line" tool of ImageJ: the total length (μm) and the base width (μm). A measure of surface area (μm²) was taken by tracing the visible area using the "freehand selection"; this measure did not take into account the effects of curvature. Volume was not directly measured in any specimens.

Size approximations

The total area and volume were coarsely approximated by modelling the apical antennomere as a cylinder using the real linear measurements described above. Area and volume were approximated as:

$$A = 2\pi rh$$
$$V = \pi r^2 h$$

Where r = ½ of the antennomere base width, and h = height of the antennomere. The top and bottom faces of the cylinder are excluded from the area calculations. This is because the bottom of the antennomere forms the joint with the next antennomere and bears no sensilla and the tip tapers so there is no large flat area at the tip of the antennomere.

A second approach attempted a more accurate estimate. Apical flagellomere shape was modelled by tracing the profile of the flagellomere from SEM montages of the dorsal surface. This was done using the "Multi-point" tool in ImageJ. Two sets of x, y-coordinates were exported in this manner, one for the left-hand side and one for the right. Using Mathematica 10.0 (Wolfram Research Inc., 2014) a cubic spline interpolation of the coordinates was constructed. The solid of revolution[4] of this interpolation was then used to generate an estimate of the area and volume of the flagellomere. This was done separately for the left and right profiles and outputs were then averaged.

[4] A solid object obtained by rotating a plane curve around a central axis.

4.2.6. Statistical analysis

Basic descriptive statistics and least squares regressions were carried out using Microsoft Excel 2010. Principal components analyses were computed using R (v. 3.2.2, The R Foundation for Statistical Computing) in conjunction with RStudio (v. 1.0.136, RStudio, Inc.). Outputs were assembled into completed figures using CorelDraw (2012 Corel).

4.2.7. Image post-processing and figure design

All figures were created using the Corel graphics suite (2012 Corel). Data images were edited only to improve the visibility of features of interest (i.e. contrast was adjusted where relevant). Some SEM images were colourised to highlight sensillum types by adding transparent colour layers over the original image. Line drawings were carried out by tracing SEM images.

For figures where information was conveyed exclusively through colour-codes, colour-blind safe schemes were selected using the online resource ColorBrewer 2.0 (Axis Maps LLC, 2009).

4.3. Results

SECTION SUMMARY

A large quantity of observational data was collected in this study. In order to present this in a manageable format this section will first discuss topics in the following order:

1. *Gross anatomy of the antenna: first in general and then with respect to miniaturisation.*
2. *Distribution, and scaling of peg length and numbers of the three focal chemosensilla (sensilla basiconica, trichodea, and trichodea curvata)*
3. *Exceptional species*
4. *Additional notes on fine scale morphology and other sensilla examined*

4.3.1. Gross anatomy of the antenna

Segmentation and joints

The general anatomy of the ant antenna is relatively stable across the ant phylogeny. All worker ants have funiculate, or elbowed, antennae comprised of three main segments the scape, pedicel and flagellum (see **Figure 4.2a**).

The most proximal segment is the scape. It articulates with the head at the torulus, a cuticular socket, where the end of the scape inserts. This end of the scape forms an extremely mobile ball and socket joint, which is covered in hair plate sensilla for proprioception (see **Figure 4.2c** and **e**). The distribution of these hair plate sensilla can vary from one species to another. Some genera seem to have well defined fields, e.g. *Myrmecia* and *Nothomyrmecia* seem to have three fields, dorsal, ventral and anterior (e.g. **Figure 4.2e**). While other genera, like *Oecophylla*, have a more homogeneous covering of hair plate sensilla.

The scape and pedicel articulate in a hinge-type joint, which is again equipped with hair plate sensilla (**Figure 4.2d**). The only intrinsic musculature in the antenna, the extensor and flexor muscles that operate this joint, are housed in the scape (see **Figure 4.2f**). The tendon insertion for the flexor muscle is often visible exteriorly (see **Figure 4.2d**).

The most distal segment is the flagellum. Although this segment is subdivided into several flagellomeres they are not true segments (developmentally) and do not possess true articulations with musculature (Snodgrass, 1984). However, some movement is possible as flagellomeres are joined with flexible cuticle (see **Appendix 7.2c**). Movement of the flagellum is indirectly mediated by the flexion and extension of the scape-pedicel joint, by the movement of the ball and socket joint of the scape-torulus and perhaps by changes in hydrostatic pressure (Ehmer and Gronenberg, 1997; Snodgrass, 1984).

A ring of campaniform sensilla around the distal border of the pedicel seem to monitor movements and any mechanical stresses they may impart on the cuticle at the pedicel-flagellum joint (see section "A special note on sensilla campaniformia" in **Chapter 3**, and Ehmer and Gronenberg, 1997). These sensilla can be difficult to observe as they do not display any sharp external edges (they appear fairly indistinct in SEMs). Long (approx. 100-300μm), putatively mechanoreceptive sensilla projecting from the distal border of an antennomere over the articulation with the next seem to be ubiquitous (see **Figure 4.2d**, blue). It is not clear if these are for proprioceptive purposes, to detect external forces or merely as some sort of guard to protect smaller sensilla from unwanted contact.

Antennomeres narrow proximally in such a way that they fit into each other (e.g. like a stack of tumblers, see **Appendix 7.2c**). At the base of each antennomere there is a narrow band of very short mechanoreceptors above the region of overlap with the next antennomere. Below this cuticular denticles can sometimes be observed (the antennomere has to be over-extended or separated from the antenna), these likely act to prevent overextension. There are no hair plate sensilla between antennomeres in the flagellum.

In worker ants the flagellum can contain from 3 to 11 flagellomeres (e.g. **Figure 4.3**). Although most species examined had antennae with 10 or 11 flagellomeres, their relative size varied quite dramatically. The size of flagellomeres is more homogeneous in larger species than in smaller ones. In many small species the apical flagellomeres can become enlarged giving rise to a clubbed antenna as opposed to the more uniform filiform type of larger species. Some species have a dramatically reduced number of antennomeres such as *Orectognathus clarki*.

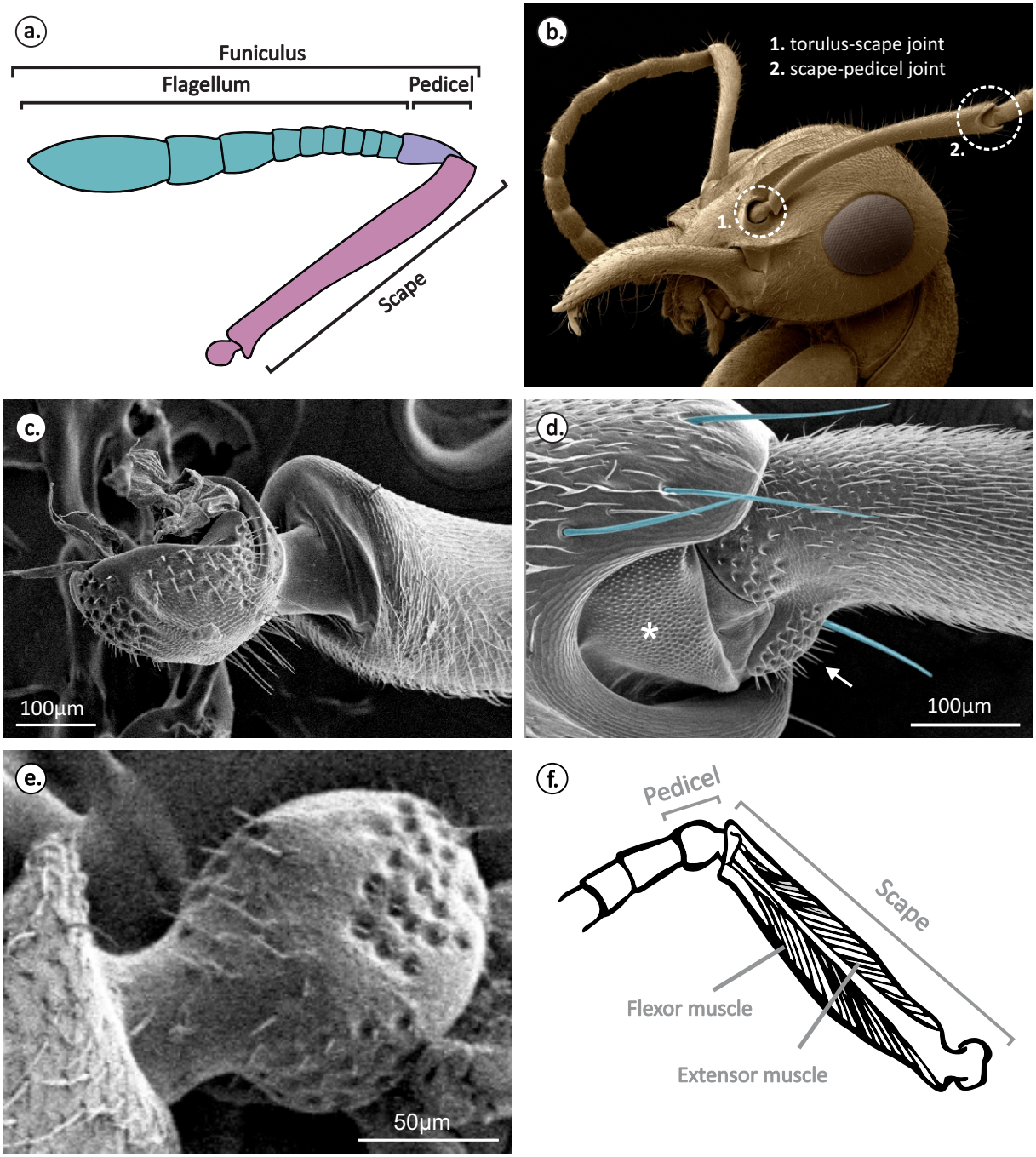

Figure 4.2. Antennal segmentation, joint types and proprioceptive bristles. (a) Colour-coded schematic of the three true segments of the ant antenna: flagellum, pedicel and scape (modified after Ramirez-Esquivel et al., 2017). (b) Colourised SEM of *Nothomyrmecia macrops* displaying the antennal joints with intrinsic musculature: 1. Torulus-scape joint = ball and socket joint, 2. Scape-pedicel joint = hinge joint. (c) The scape (detached from the torulus) showing hair plate sensilla (*Myrmecia pyriformis*). (d) The scape-pedicel joint showing the apodemal tendon insertion of the ventral pedicel muscle (*), hair plate sensilla (white arrow) and long mechanoreceptors (blue) projecting over the joint (*M. pyriformis*). (e) An example of hair plate sensilla fields (3 distinct groupings) on the head of the scape. (f) The only musculature within the antenna is housed in the scape (re-drawn from Snodgrass, 1984).

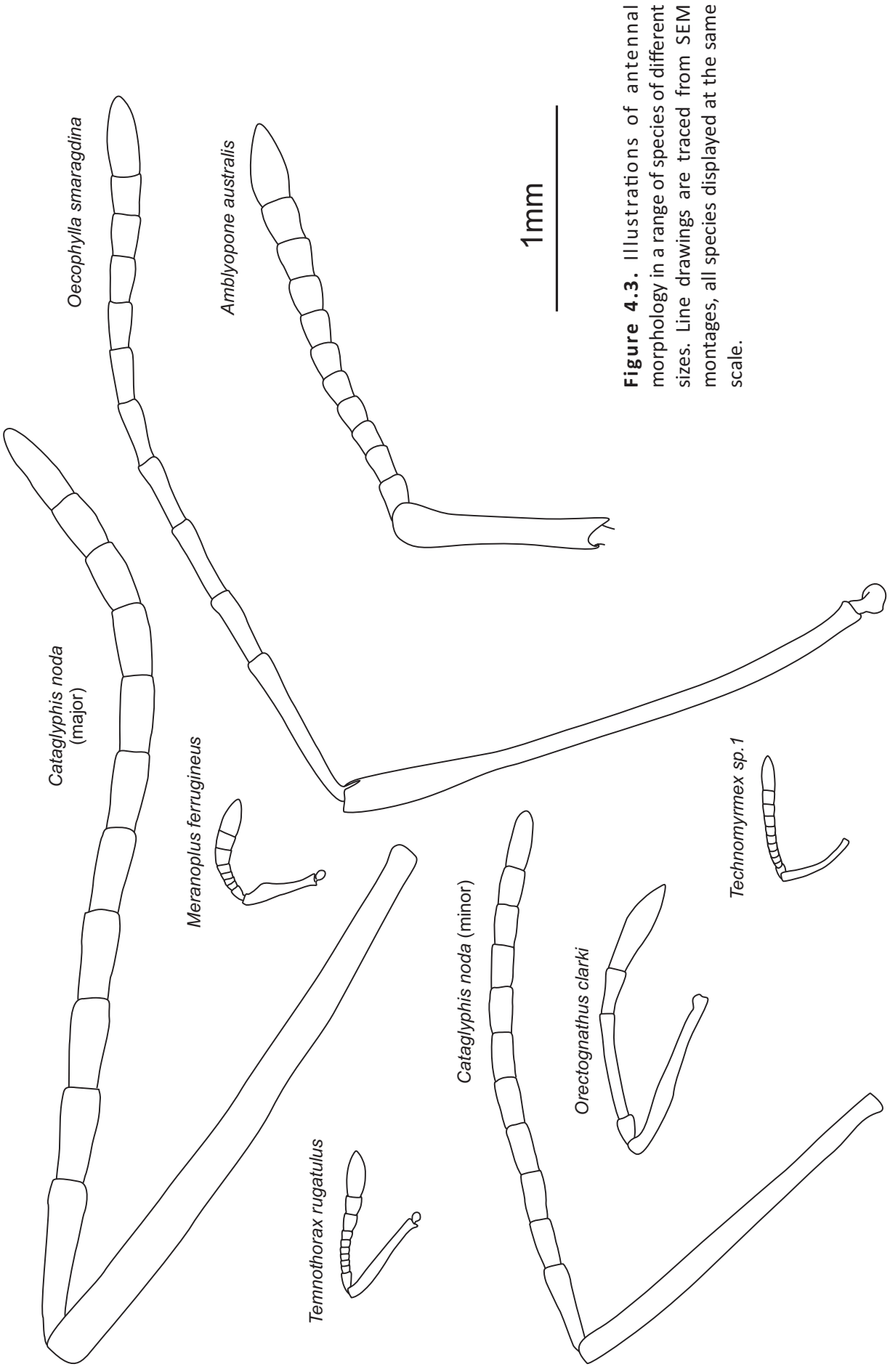

Figure 4.3. Illustrations of antennal morphology in a range of species of different sizes. Line drawings are traced from SEM montages, all species displayed at the same scale.

Allometry of the antennal segments and antennomeres

Allometry of the antennal segments

In order to study the scaling of the antenna relative to head width a number of potentially biologically relevant traits were measured. These consisted of:

- Head width (HW)
- Scape length (SL)
- Flagellum length (FL)
- Apical flagellomere length (AFL)
- Number of flagellomeres

In this section data obtained from original SEMs was supplemented using imagery from AntWeb (www.antweb.org) and RBINS (Leponce et al., 2008). High quality light microscopy images taken using the standard taxonomic angles (frontal view of the head, dorsal view of the body, and a lateral view of the body) were sufficiently detailed to collect these measurements. In this expanded dataset most Formicid subfamilies are represented and multiple species are included for the most diverse subfamilies; for a complete list of species analysed refer to **Appendix 1**.

To guide the analysis and interpretation of results, a principal components analysis (PCA) was carried out including all of the variables outlined above (**Figure 4.4**). PCA represents variables in n-dimensional space[5] and then projects them into a two-dimensional plot in a way that best represents the variability found in the dataset. In this case the first two principal components (the two axes or dimensions) represented the data well, 81% of the variability was explained (see axes weightings on **Figure 4.4**). The different variables are represented as vectors on the plot. The length of the vectors relative to the correlation circle (marked in maroon) indicates how well represented in 2D space that variable is (**Figure 4.4**); vectors that touch the correlation circle are perfectly represented. Vector angles can be loosely interpreted as follows: aligned vectors imply co-varying traits, vectors at 180° imply negatively correlated traits, orthogonal vectors imply non-correlated traits. Of course, the validity of these relationships depends on the degree of accuracy with which the 2D figure represents all the variables. This is because vectors that are seemingly aligned in 2D space may actually lie quite distant to one another in higher dimensional space.

[5] Where n = the number of variables or observations.

In this particular analysis plotting the first two principal components provided a good representation of the variation in the dataset (81% explained) and all vectors were well represented in two dimensions (see correlation circle, **Figure 4.4**). All the absolute measures of length of antennal parts seemed to co-vary to some degree with head width. This means that as head width increases scape, flagellum and apical flagellomere length all increased, although not necessarily in an isometric fashion. The ratio of FL/AFL was less closely co-varying with head width, while the ratio of FL/SL was not associated with head width. Similarly, the number of flagellomeres in the antenna did not closely co-vary with head width. Most species with few flagellomeres had small head widths but there was great variability in the head widths of species with higher numbers of flagellomeres. Unfortunately, categorical data such as subfamily and functional group classifications are not compatible with this kind of analysis.

The length of the whole antenna (scape + flagellum) exhibits a strong (R^2=0.81, n=113 species), positive, linear correlation with head width (see **Figure** 4.**5a**). This linear correlation predicts no consistent trend for antennae to be disproportionately long in either small or large species, although there were not many extremely large species in the dataset. This trend was corroborated by plotting size-corrected antennal length against head width (see **Figure** 4.**5b**). Some outliers can be observed in these plots (**Figure 4.5a** and **b**), notably *Leptomyrmex cnemidatus* (HW=1.26mm) has an antennal length over 3 times that predicted by the regression. *Leptomyrmex* ants are known spider mimics (Boudinot et al., 2016) and their elongated antennae are likely part of this adaptation (mimicking an extra pair of legs, see **Figure 4.6a**). The scape is so elongated in this genus that it is one of the main diagnostic features used for the taxonomic identification of *Leptomyrmex*.

Figure 4.4. Principal components analysis of antennal segments and antennomeres. Formicid sub-families are colour coded according the legend, number of species within each sub-family listed in brackets, coloured concave hulls or circles (for single representatives) surround individual species within each sub-family. Variables included are listed in the top legend. The length of vectors relative to the correlation circle (large, maroon circle) indicates how well represented that variable is in the 2D graph, vectors that reach the correlation circle are perfectly represented.

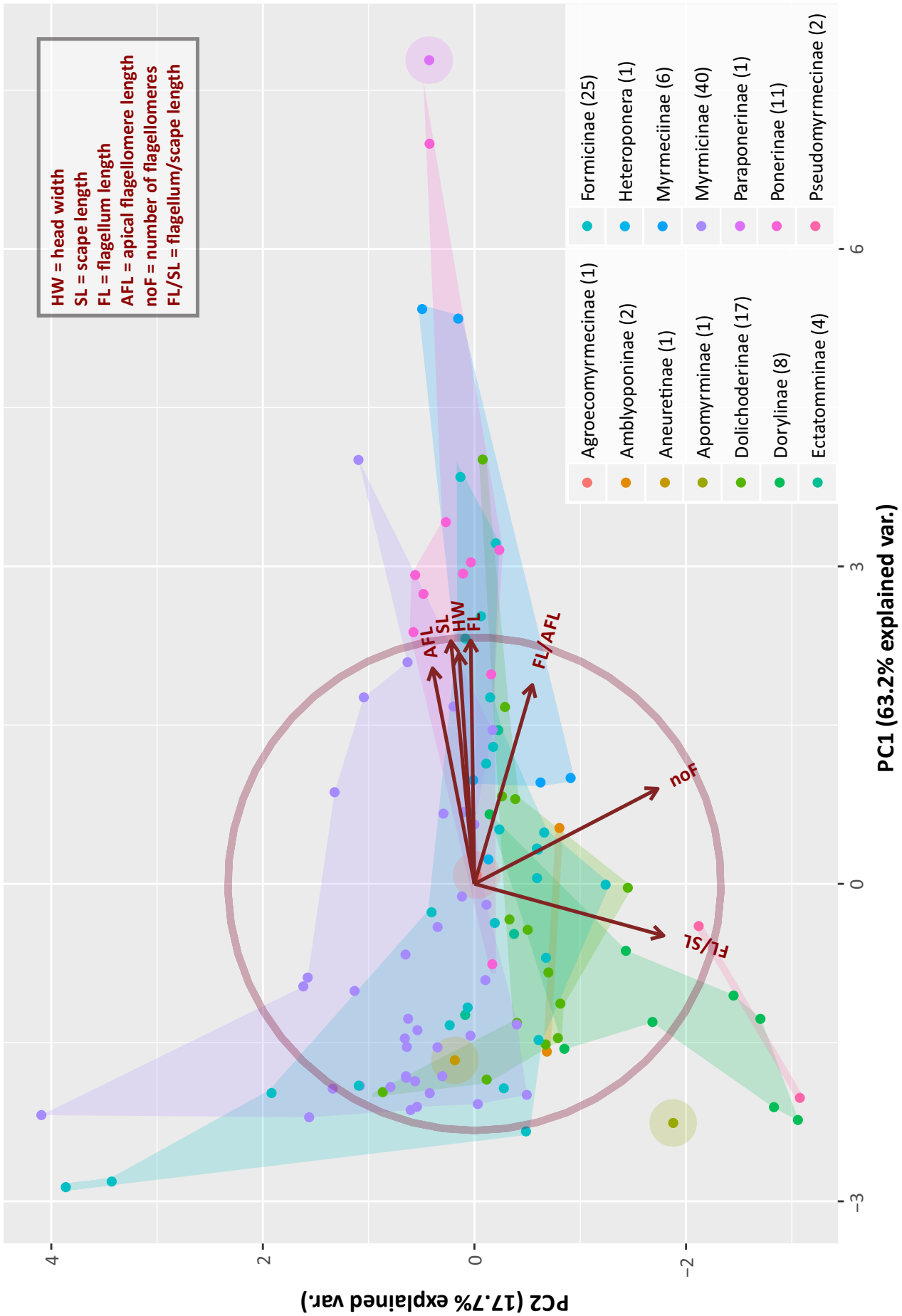
HW = head width
SL = scape length
FL = flagellum length
AFL = apical flagellomere length
noF = number of flagellomeres
FL/SL = flagellum/scape length
Formicinae (25)
Heteroponera (1)
Myrmeciinae (6)
Myrmicinae (40)
Paraponerinae (1)
Ponerinae (11)
Pseudomyrmecinae (2)
Agroecomyrmecinae (1)
Amblyoponinae (2)
Aneuretinae (1)
Apomyrminae (1)
Dolichoderinae (17)
Dorylinae (8)
Ectatomminae (4)
AFL
SL
HW
FL
FL/AFL
noF
FL/SL
PC1 (63.2% explained var.)
PC2 (17.7% explained var.)
−3
0
3
6
−2
0
2
4

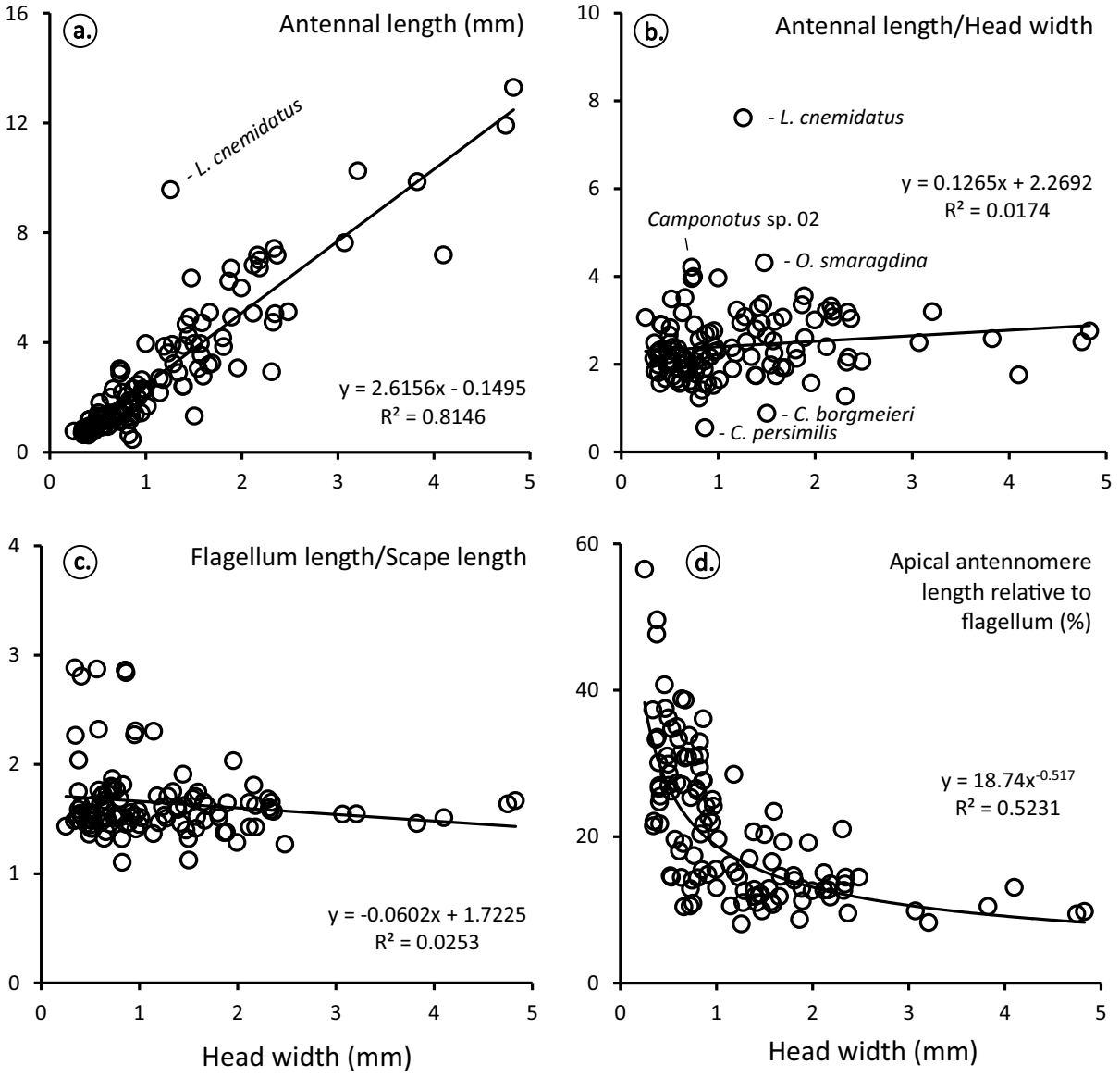

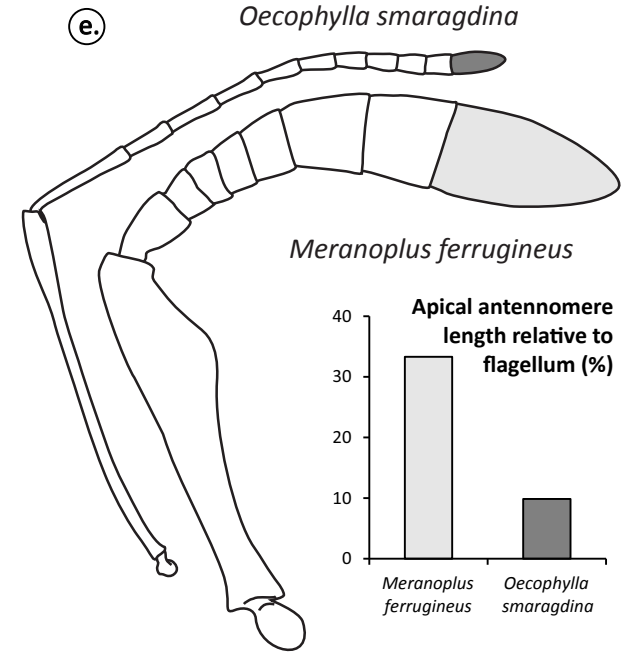

Figure 4.5. Scaling of different antennal parts with respect to head width (i.e. body size proxy). (a) The total antennal length (absolute length of scape+funiculus) has a very strong positive correlation with head width; (b) the relative antennal length (antennal length/head width) has no clear relationship with head width; (c) the ratio of flagellum to scape length has no clear relationship to head width; (d) the length of the apical antennomere relative to the total flagellum length (expressed as a percentage) has a moderately strong (R^2=0.56) power relationship with the head width; (e) a graphical illustration of the allometry described in panel (d): by scaling the antenna of *Meranoplus ferrugineus* (HW=0.6mm) by matching the scape length to that of *Oecophylla smaragdina* (HW=1.5mm) the different relative sizes of the apical antennomere can be directly compared.

The majority of species had antennae that measured on average 2.4 times the width of the head (standard deviation = 0.84, n = 119). There were more species that had disproportionately long antennae compared to species that had disproportionately short antennae. In particular there were three species that fell two standard deviations or more above the average, these were: *Leptomyrmex cnemidatus*, *Oecophylla smaragdina*, and *Camponotus* sp. 02. While we have already discussed the specialised ecology of *L. cnemidatus* the elongated antennae of *O. smaragdina* and *Camponotus* may also be associated with ecological specialisation but of a different kind. *O. smaragdina* is an arboreal specialist that builds elaborate leaf nests, in this case the elongation of the antennae may help to bridge gaps in the complex three dimensional crowns of trees. *Camponotus* sp. 02 is a carpenter ant, unfortunately there is no ecological information for this unnamed species, however, this genus is often associated with trees and aphid farming suggesting that their long antennae may also be driven by arboreal habits. The only species that had antennae two standard deviations or more below the average was *Cephalotes persimilis*; the next smallest relative antennal length was the congener *Cephalotes borgmeieri*. This makes some sense as *Cephalotes* ants have antennae that are adapted to tuck away in deep scrobes, specialised grooves on the head (**Figure 4.7** shows a similar adaptation in the genus *Meranoplus*).

The flagellum was on average about 1.7 times longer than the scape (standard deviation = 0.34, n = 115). There was no correlation between the ratio of flagellum to scape length and head width (see **Figure 4.5c**). There was a small group of outlying species (x > 2s.d.) that were characterised by having small head widths and a large ratio of flagellum to scape length. This group was comprised of:

- *Leptanilloides anae* (HW=0.34): 2.9 (+3.68 s.d.)
- *Pseudomyrmex acanthobius* (HW=0.57): 2.9 (+3.65 s.d.)
- *Lioponera aberrans* (HW=0.85): 2.9 (+3.62 s.d.)
- *Acanthostichus brevicornis* (HW=0.87): 2.8 (+3.55 s.d.)
- *Neivamyrmex carettei* (HW=0.41): 2.8 (+3.46 s.d.)
- *Ooceraea australis* (HW=0.58): 2.3 (+2.00 s.d.)

The majority of these species with short scapes have subterranean or leaf-litter habits and belong to the subfamily Dorylinae (see **Figure 4.8**). The exception here is *Pseudomyrmex* (Pseudomyrmecinae), which is arboreal. However, this genus exhibits a number of wasp-like traits (e.g. large eyes and sting) and a short scape is consistent with this. Additionally, these ants nest in hollow twigs and acacia thorns (i.e. constrained spaces) where

a short scape may be beneficial (see **Figure 4.6b**). These outliers are consistent with their relative position in the PCA plot at the negative extreme of the flagellum/scape length vector (**Figure 4.4**).

In some small species the workers have "club" antennae. In these species the apical antennomeres in the flagellum (usually 1-3 antennomeres) are enlarged and the remainder of the antennomeres are greatly reduced (e.g. **Figure 4.2a**). In most of the larger species the antennomeres are more evenly sized. In order to quantitatively describe this change in morphology the size of the apical antennomere relative to the whole flagellum can be compared. As species head width decreases the length of the apical antennomere makes up a greater proportion of the total flagellum length (see **Figure** 4.**5d**). In the most extreme example the apical antennomere represents 56% of the total flagellum length while in the majority of larger species the apical antennomere measures less than 20% of the total flagellum length. A graphical example of this disparity in scaling of the antennomeres is shown in **Figure 4.5e**, here the scape of *Oecophylla smaragdina* and *Meranoplus ferrugineus* have been matched in length. Since the scape has a very strong positive correlation with head width (R^2=0.90) matching the scape lengths is roughly equivalent to scaling both the antennae to how large they would be if both species were of the same body size, this allows a direct comparison of the changes in allometry. The relative enlargement of the apical antennomeres in *M. ferrugineus* becomes visually self-evident with this example.

The number of flagellomeres in the antenna was not consistently co-varying with head width. Most species with few antennomeres had small head widths but not all small species had few antennomeres (see **Figure 4.4**). The number of flagellomeres seemed to be greatly influenced by subfamily. Within the sample examined here only Myrmicinae, Formicinae and one species of Dolichoderinae had fewer than 10 flagellomeres. Of these Myrmicinae had slightly more species with a reduced number of flagellomeres. The species with the fewest flagellomeres (4) in this subfamily was *Microdaceton tanyspinosum*.

Figure 4.6. Species with extremely long or short scapes. (a) An example of a *Leptomyrmex* species with extraordinarily long scapes, which contribute to spider-mimicking behaviours by looking like an extra pair of legs (*L. nigriceps*, photographed by Richard Bajol). (b) Example of a *Pseudomyrmex* species with extremely short scapes, unlike other observed species with extremely short scapes this genus is not hypogaeic and does not belong to Dorylinae (*P. spinicola*, photographed by Alex Wild).

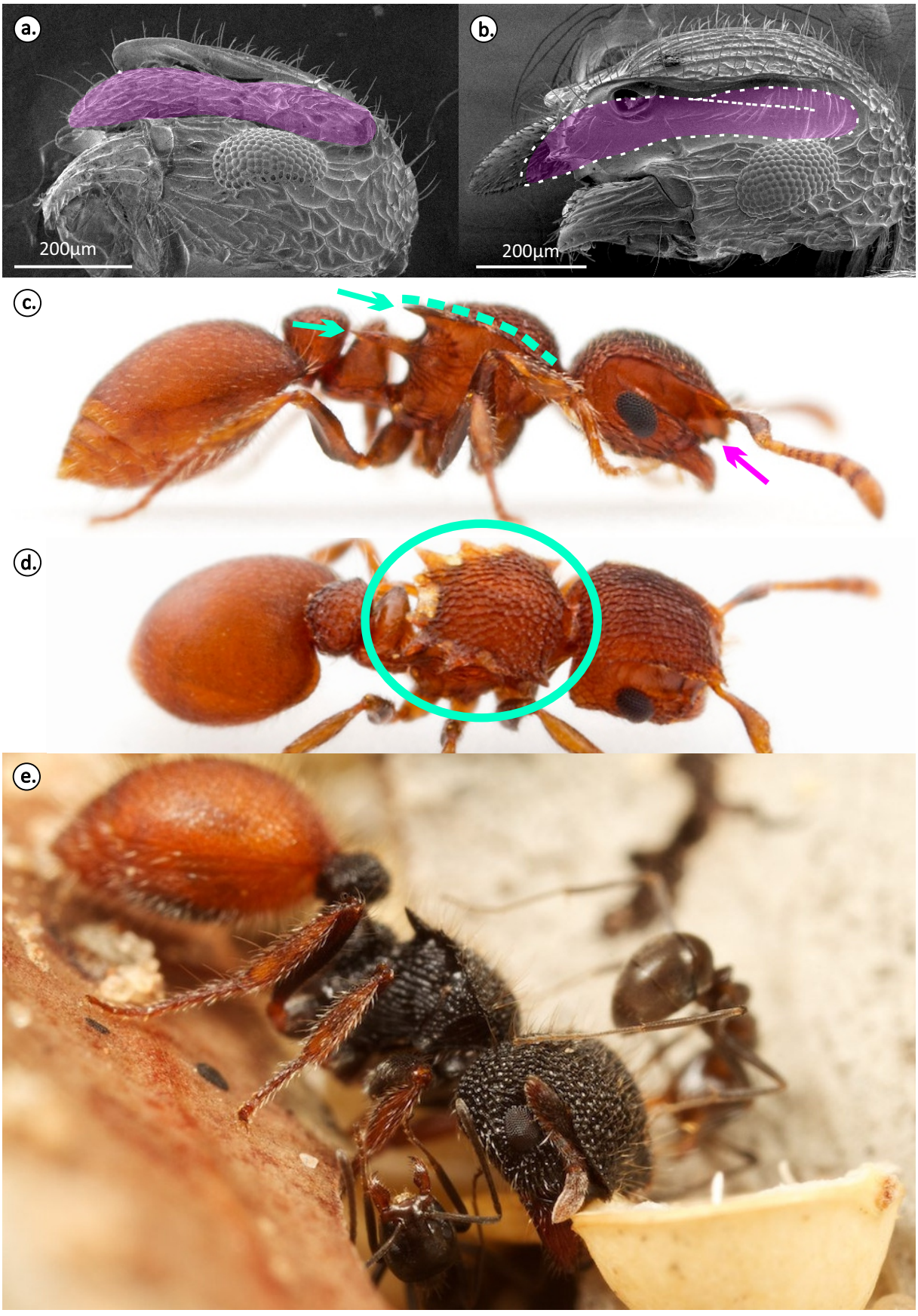

Figure 4.7. Examples of species with pronounced antennal scrobes. *Meranoplus ferrugineus* with: (a) antenna intact (pink) and (b) antenna removed to show the extent of the scrobe (the pink overlay shows where the antenna would be. (c, d) *Meranoplus* sp. showing defensive structures spines and premesonotal shield (green), antennal scrobe (pink), photographs by Alex Wild. (e) *Meranoplus* sp. retracting antennae for protection from attack by aggressive *Iridomyrmex* sp. (photographed by Ajay Narendra).

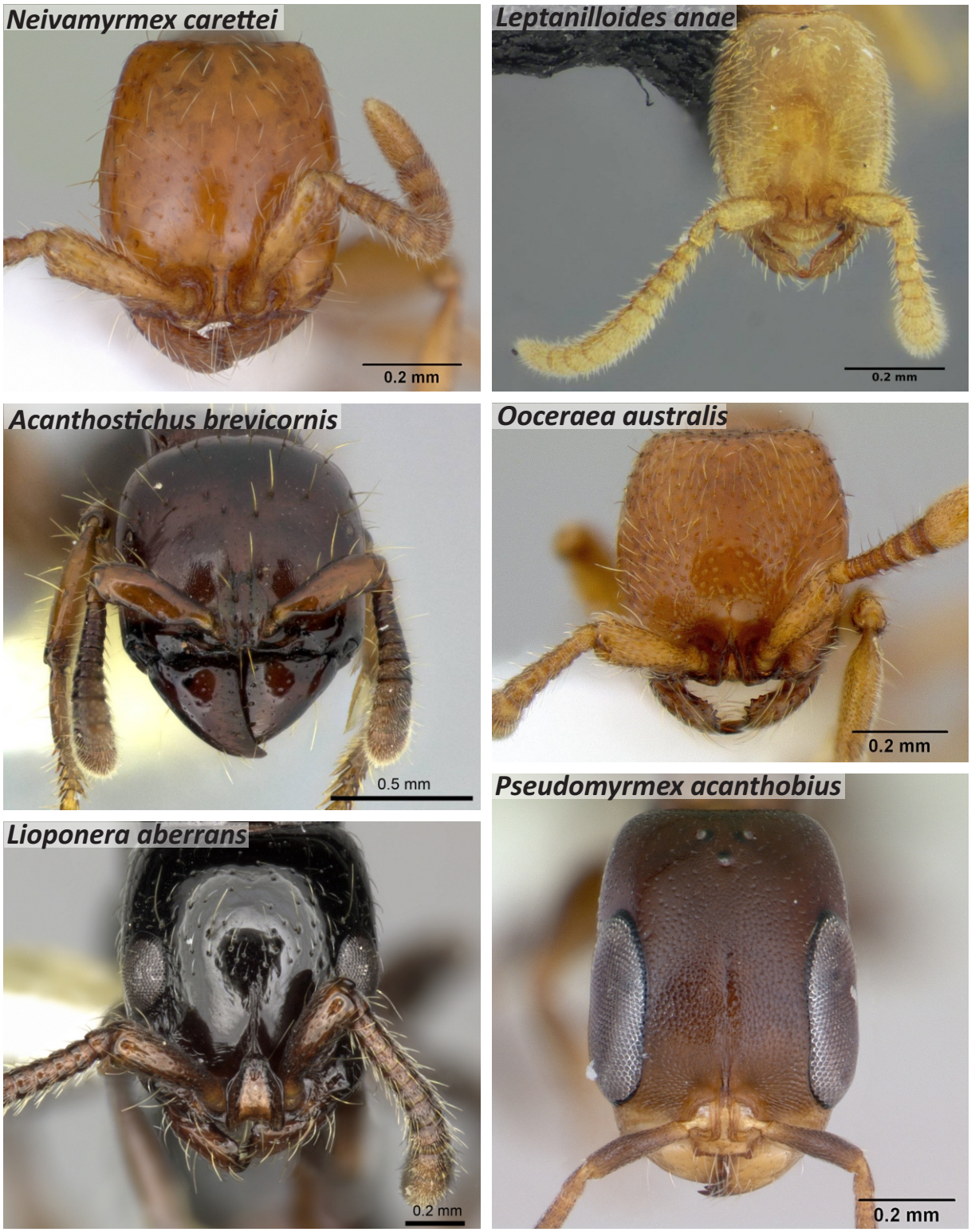

Figure 4.8. Species with extremely short scapes. All species in this group belong to the subfamily Dorylinae and are hypogaeic, with the exception of *Pseudomyrmex* (Pseudomyrmicinae). Note that the majority of these ants have greatly reduced eyes (*A. brevicornis*) or lack eyes (*N. care. ei*, *L. anae*, *C. edentatus*). All images from: AntWeb (www.antweb.org), except for *O. australis*: Atlas of Living Australia (www.ala.org.au)**.**

Allometry of the apical flagellomere

This section analysed original SEM data only (for full species list see **Table 4.2**). Apical flagellomere (AF) area was measured directly from SEM montages as the visible dorsal area and without taking curvature into account.

The AF length and surface area were positively linearly correlated with head width. *Eciton hamatum* was a clear outlier, (>2 s.d. above the mean, **Figure 4.9a**, cyan) despite being a moderately sized species. Removing this species from the regression substantially increases the strength of the correlation. Other species that had relatively long apical antennomeres were *Harpegnathos saltator* (**Figure 4.9a**, blue, +1.81 s.d.) and *Orectognathus clarki* (**Figure 4.9a**, green, +0.95, +0.73). However, both these species have long narrow apical antennomeres so their surface area is not relatively large (**Figure 4.9b**).

The area of the whole AF (not just dorsal surface) as well as the volume were approximated using two different models. The first approximation modelled the AF as a perfect cylinder with the top and bottom faces of the cylinder were excluded for area calculations. A second approach attempted a more accurate estimate by fitting a line to the flagellomere profile. The solid of revolution of this interpolation was then used to generate an estimate of the area and volume of the flagellomere.

Neither model showed the scaling pattern that would be expected from a series of geometrically similar objects (compare **Figure 4.10** to **Supplementary Figure 4.5**). In a series of regularly scaling cylinders the surface area would scale to the square of the linear measurement (in this case the head width or AF length) while the volume would scale to the cube. However, the AF does not scale regularly as small species tend to have club antennae while large species have filiform antennae (see **Figure 4.5d**). This morphological variation leads to a widening of the apical flagellomeres in small species. As a result the AF does not scale with the patterns expected for geometrically similar bodies. Although there is considerable variability around the lines of best fit, the variation in shape of the AF in species of different sizes seems to result in an area to volume ratio (A:vol) that is more uniform across small and large species than would be expected if the AF shape were constant (compare **Figure 4.10e** and **f** to **Supplementary Figure 4.5**). If the apical flagellomere scaled isometrically we would expect A:vol to scale with an exponent of -1 (**Supplementary Figure 4.5**).

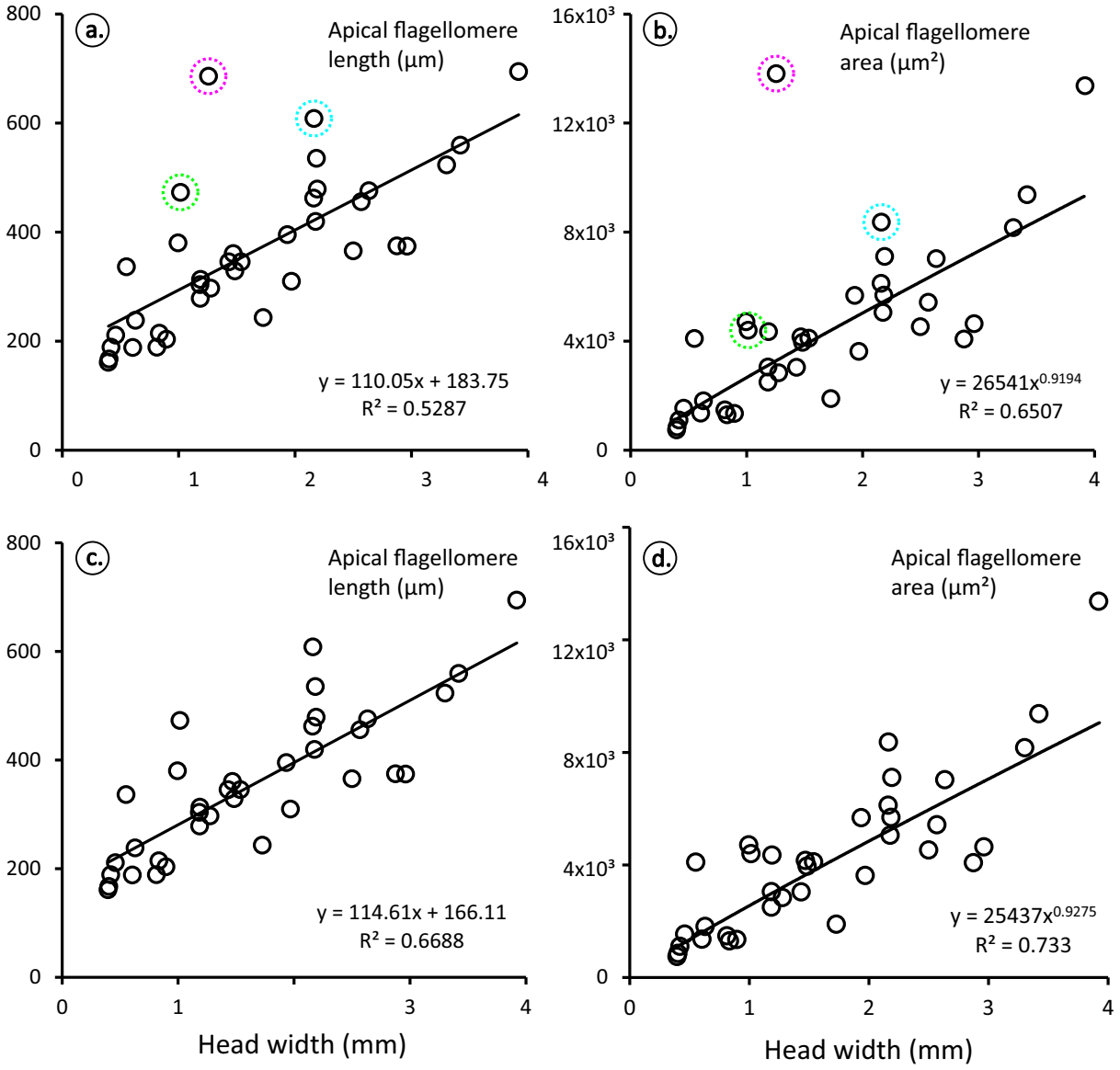

Figure 4.9. Scaling of the apical flagellomere relative to head width. (a) Apical flagellomere length (µm) vs head width, *Eciton hamatum* workers (>2 s.d. above the mean) highlighted with dotted cyan line, also highlighted are *Harpegnathos saltator* (blue) and *Orectognathos clarki* (green); (c) *E. hamatum* removed. (b) Apical flagellomere area (µm²), measured as dorsal surface area, vs head width, Eciton hamatum workers (>2 s.d. above the mean) highlighted with dotted cyan line; (d) *E. hamatum* removed.

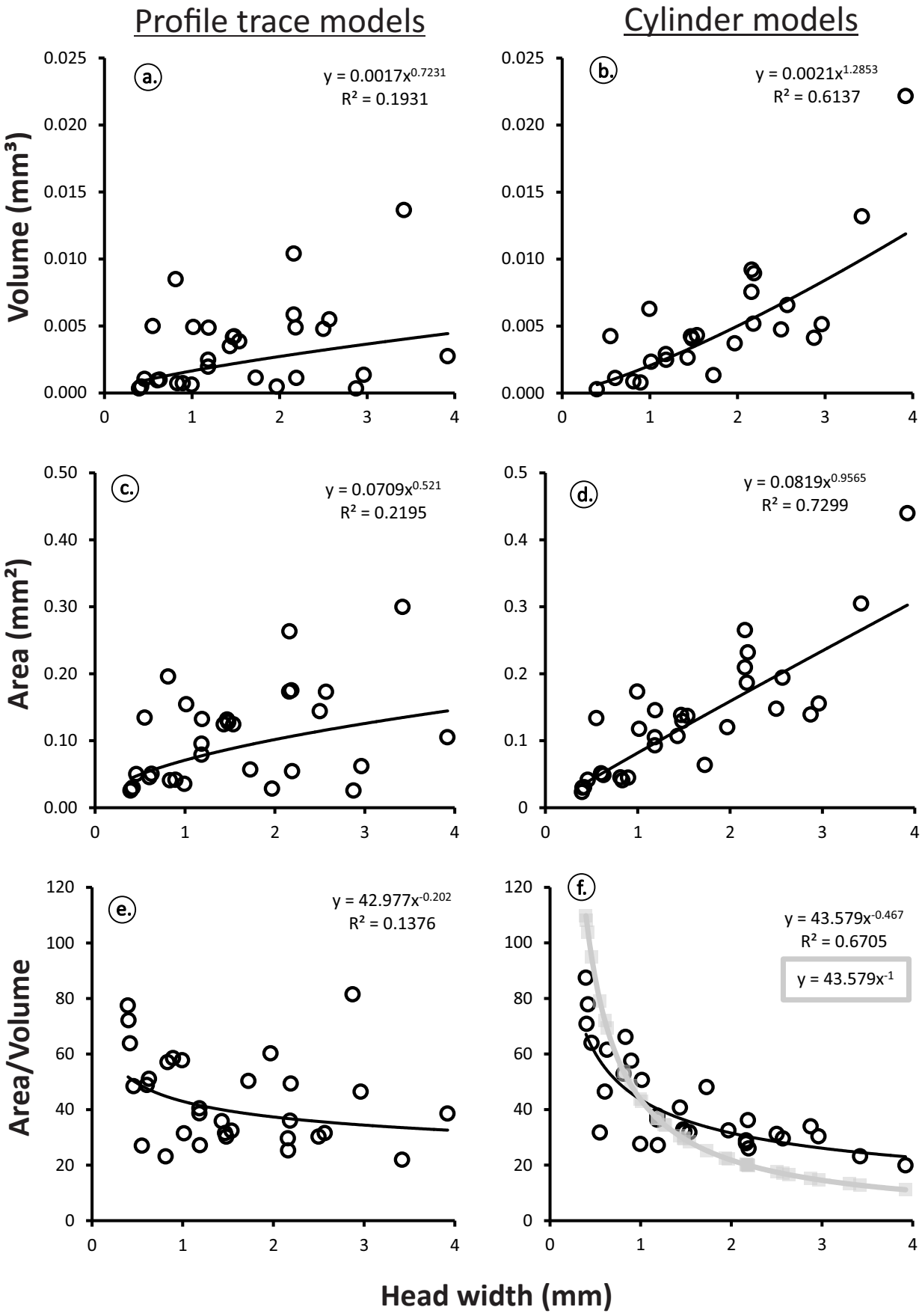

Figure 4.10. Two models for estimating the area and volume of apical flagellomere area and volume. (a, c, e) Left-hand column presents data obtained by tracing the curvature of the flagellomere and integrating areas and volumes (see Methods). (b, d, f) Right-hand column approximates areas and volumes by modelling the apical flagellomere as a cylinder (see Methods). (f) Light grey curve represents the area to volume ratio scaling that would be expected if flagellomeres were geometrically similar (i.e. scaled isometrically).

4.3.2. Antennal sensilla

Species examined

Analyses were carried out using original data from 28 species listed below (**Table 4.2**), unless explicitly stated. Sample size varied among species; originally a sample size of 5 specimens per species was the aim. However, this proved to be too time consuming, so as data collection continued the sample size was dropped to 1 to maximise the taxonomic coverage. To maintain consistency and prevent certain species from having too much weighting in models sample sizes were equalized as follows. In cases of strongly polymorphic species a small and a large specimen were included (wherever possible), if there was a particularly strong range of variation an intermediately sized worker was also included so that such species had a maximum of 3 representative specimens included in regressions. In cases where multiple specimens for a monomorphic species were examined the results were averaged across specimens so that a single value was included for such species. The exact details of the number of specimens and castes included in analyses are listed below:

Table 4.2. Information on species included in comparative study (21 genera). Functional group classification and notes on biology according to Brown (2000). When multiple castes have been included in the analysis these will consist of: 2 = minor and major, 3 = minor, media and major. The total number of specimens studied is indicated by "n", totals are given on the bottom row.

Species	Sub-family	Biology	Functional group	Castes in analysis	n
Amblyopone australis	Amblyoponinae	Predators, esp. of Chilopoda	C	1	1
Iridomyrmex calvus	Dolichoderinae	Generalized foragers	DD	1	3
Iridomyrmex purpureus	Dolichoderinae	Generalized foragers	DD	1	5
***Technomyrmex* species 1**	Dolichoderinae	Generalized foragers	O	1	1
Ooceraea australis	Dorylinae	Army ants, predators of other ants	C, SP(c)	1	1
Lioponera singularis	Dorylinae	Army ants, predators of other ants	C, SP(c)	1	2
Eciton hamatum	Dorylinae	Army ants, predators of other ants	TCS	1	2
Rhytidoponera metallica	Ectatomminae	Generalized predators	O	1	1
Camponotus consobrinus	Formicinae	Generalized foragers	SC	2	2

Camponotus piliventris	Formicinae	Generalized foragers	SC	1	2
Cataglyphis noda	Formicinae	Scavengers	HCS	3	3
Melophorus bagoti	Formicinae	Nest in the ground	HCS	2	2
Melophorus hirsutus	Formicinae	Nest in the ground	HCS	2	2
Notoncus ectatommoides	Formicinae	Generalized foragers	CCS	1	2
Oecophylla smaragdina	Formicinae	Predator, tend homopterans, arboreal	TCS	1	3
Opisthopsis pictus	Formicinae	Generalized foragers	SC	1	1
Paraparatrechina minitula	Formicinae	Generalized foragers	O	1	2
Myrmecia croslandi	Myrmeciinae	Generalized predators	SP	1	5
Myrmecia nigriceps	Myrmeciinae	Generalized predators	SP	2	2
Myrmecia pyriformis	Myrmeciinae	Generalized predators	SP	2	6[6]
Myrmecia tarsata	Myrmeciinae	Generalized predators	SP	1	1
Nothomyrmecia macrops	Myrmeciinae	Nocturnal predators	SP	1	7
Temnothorax rugatulus	Myrmecinae	Generalized foragers and parasites	CCS, TCS	1	5[7]
Meranoplus ferrugineus	Myrmicinae	Seed harvesters and general foragers	HCS	1	3
Orectognathus clarki	Myrmicinae	Predators	SP	1	2
***Pheidole* species 1**	Myrmicinae	Many seed harvesters, many omnivorous	GM	2	6
Harpegnathos saltator	Ponerinae	Predators	SP	1	1
Odontomachus simillimus	Ponerinae	Predators	O, ?SP	1	1
28	**8**			**36**	**72**

Species sampled were not necessarily distributed in a way that reflected the real world diversity contributions of each subfamily but adequate coverage of subfamilies was achieved (see **Figure 4.11**). The main peculiarity of the sample used in this study is the inclusion of several *Myrmecia* species, a fairly specialised ant, which however covers a large range of body sizes.

[6] For full dataset see **Chapter 2.**

[7] For full dataset see **Chapter 3**

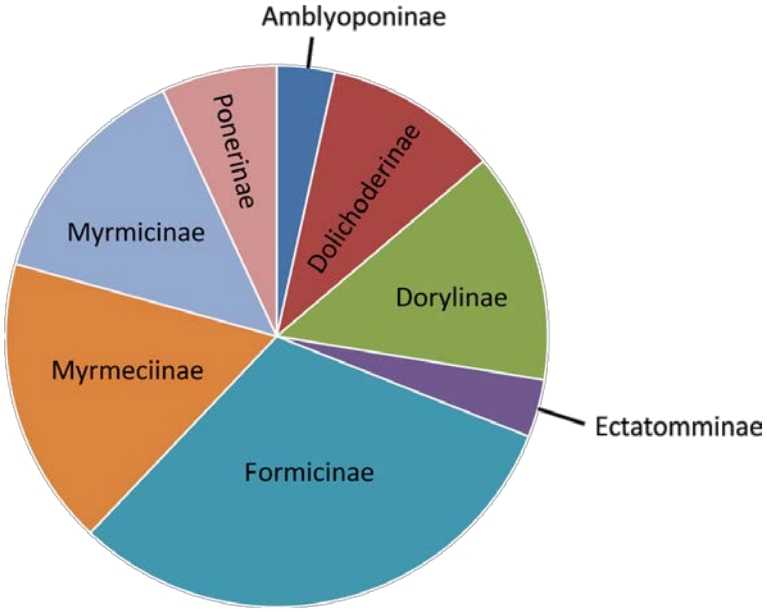

Figure 4.11. Relative contribution of each subfamily towards the dataset. Note that these do not reflect real world diversity contributions of each sub-family. The sub-family Myrmeciinae is particularly over-represented in this sample.

Focal chemosensilla

This section focuses on the effects of scaling body size (measured by proxy using head width) on three chemosensilla. These three types are sensilla basiconica, trichodea and trichodea curvata (hereafter referred to as curvata for brevity). These sensilla were readily identified across species despite some degree of variability in their morphology. **Figure 4.12** provides an overview on the appearance of the three sensilla and how they were measured. Throughout this chapter, as in previous chapters, the three sensilla are represented in figures with a shape and colour-code that is kept as consistent as possible (see **Figure 4.12**).

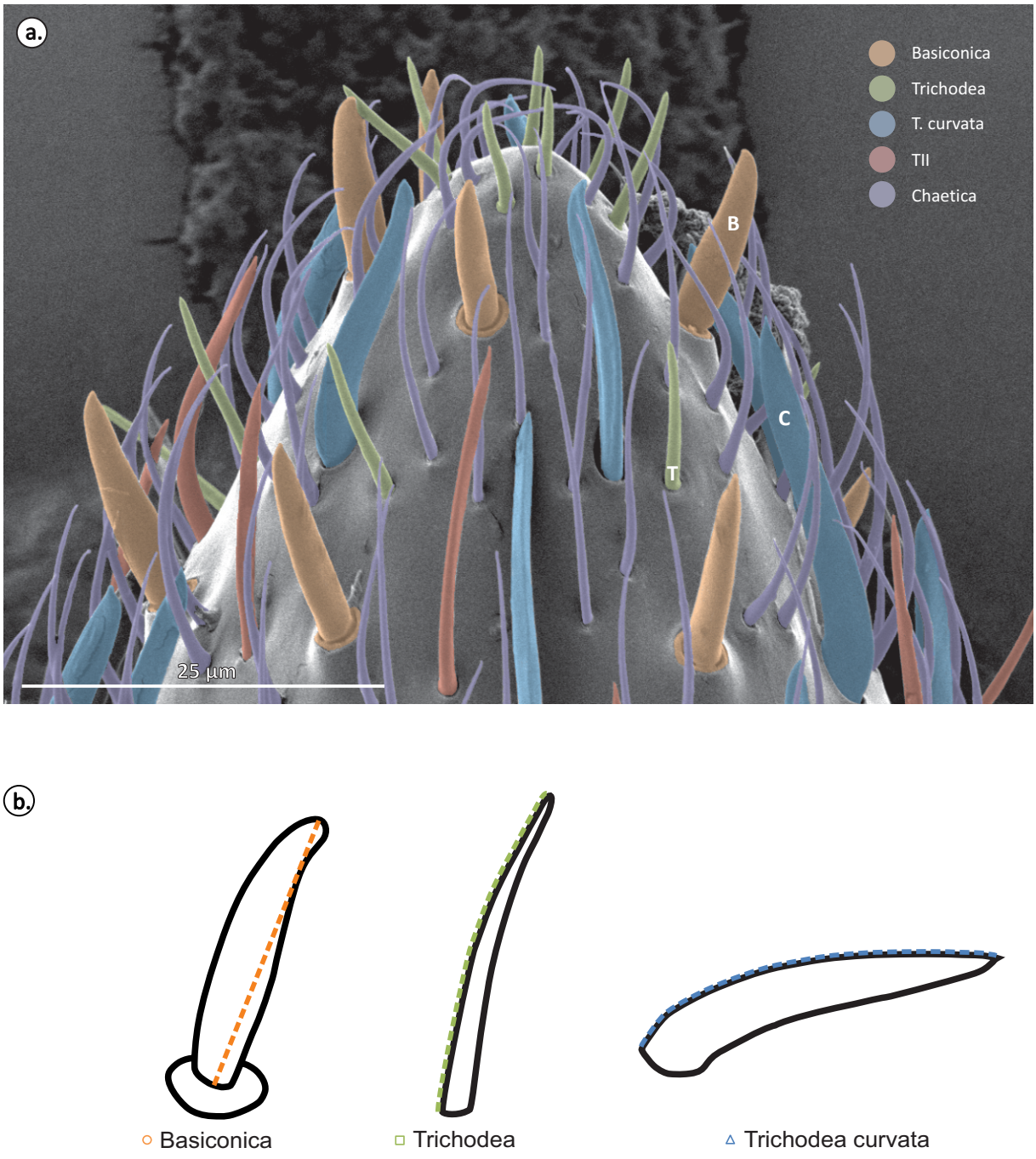

Figure 4.12. Sensillum types. (a) Colourised SEM of the most common filiform sensillum types on the ant antenna. (b) Illustration of focal chemosensillum types and examples of length measurements for each type.

Distribution

The vast majority of species studied retained the characteristic distributions of sensilla observed in previous chapters (**Chapter 2** – *M. pyriformis*, **Chapter 3** – *T. rugatulus*). Sensilla basiconica and trichodea tended to occur in pairs throughout the apical antennomere except at the tip where there were only sensilla trichodea and chaetica (see **Figure 4.13**). In some cases there was some bias towards one side or the other (generally the medial side) or towards the tip. This was not the case with sensilla curvata. Sensilla curvata occurred throughout the antennomere except at the tip. Some species had chemosensilla "dead zones" usually along one of the sides on the proximal end of the antennomere, for instance *A. australis, O. clarki* and *E. hamatum.*

Beyond this "dead zone" *E. hamatum* was also unique in a number of ways. This army ant had disproportionately large antennae (including AF, see **Figure 4.9a** and **b**, **Figure 4.13**) and extremely short sensilla curvata in large quantities. These dominated the greater part of the dorsal surface of the apical flagellomere while sensilla basiconica and trichodea were clustered around the proximo-medial margins. The lateral margins were dominated by long mechanoreceptors (not shown). Despite these peculiarities this species was not omitted from this series of analyses.

Ooceraea australis and *Lioponera singularis* was another pair of unusual species. However, in this case these species have been omitted from analyses on sensillum numbers and distribution but not from analyses on sensillum size. This is because the distribution of sensilla on the apical flagellomeres of these two species differs significantly from those of most other species. These species will be discussed in more detail later on.

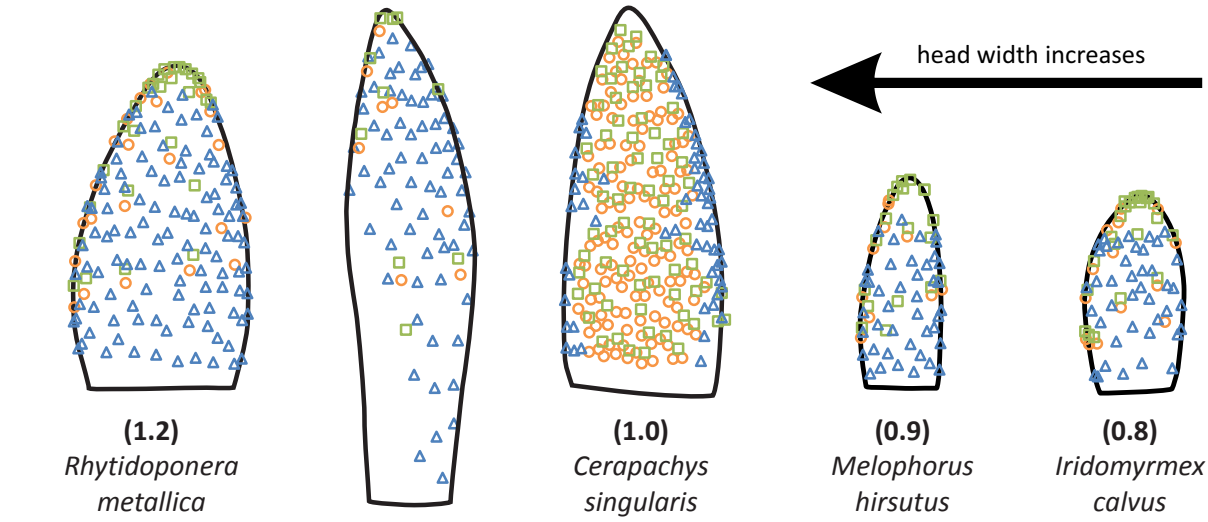
head width increases
(1.2)
Rhytidoponera metallica
(1.1)
Orectognathus clarki
(1.0)
Cerapachys singularis
(0.9)
Melophorus hirsutus
(0.8)
Iridomyrmex calvus

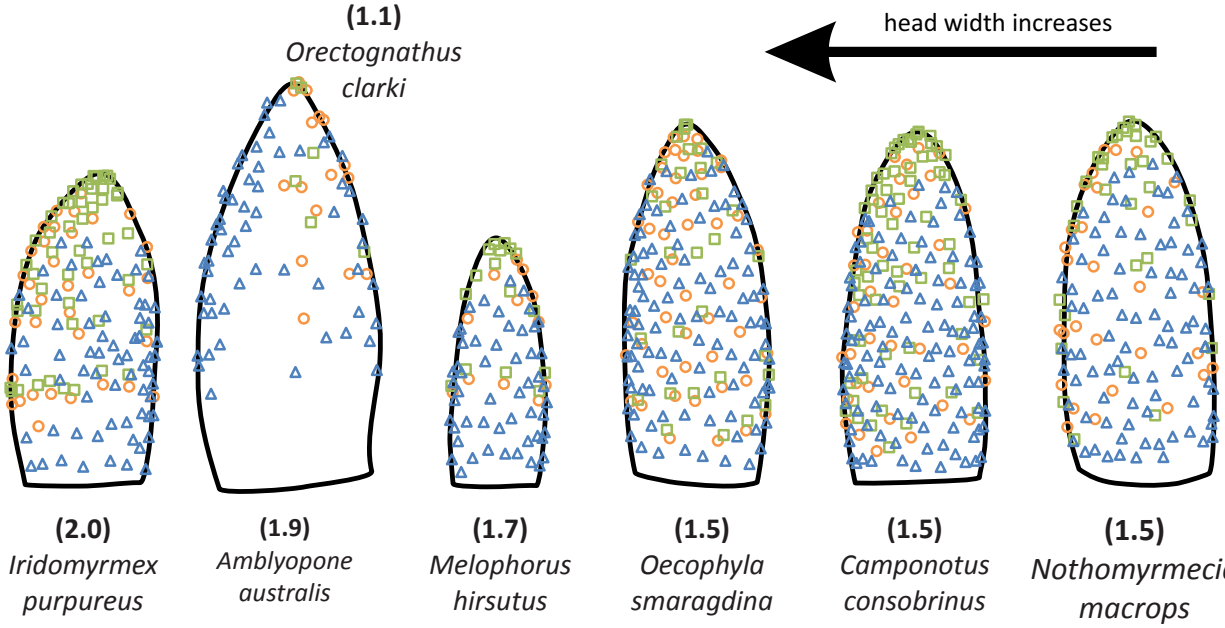
head width increases
(2.0)
Iridomyrmex purpureus
(1.9)
Amblyopone australis
(1.7)
Melophorus hirsutus
(1.5)
Oecophyla smaragdina
(1.5)
Camponotus consobrinus
(1.5)
Nothomyrmecia macrops

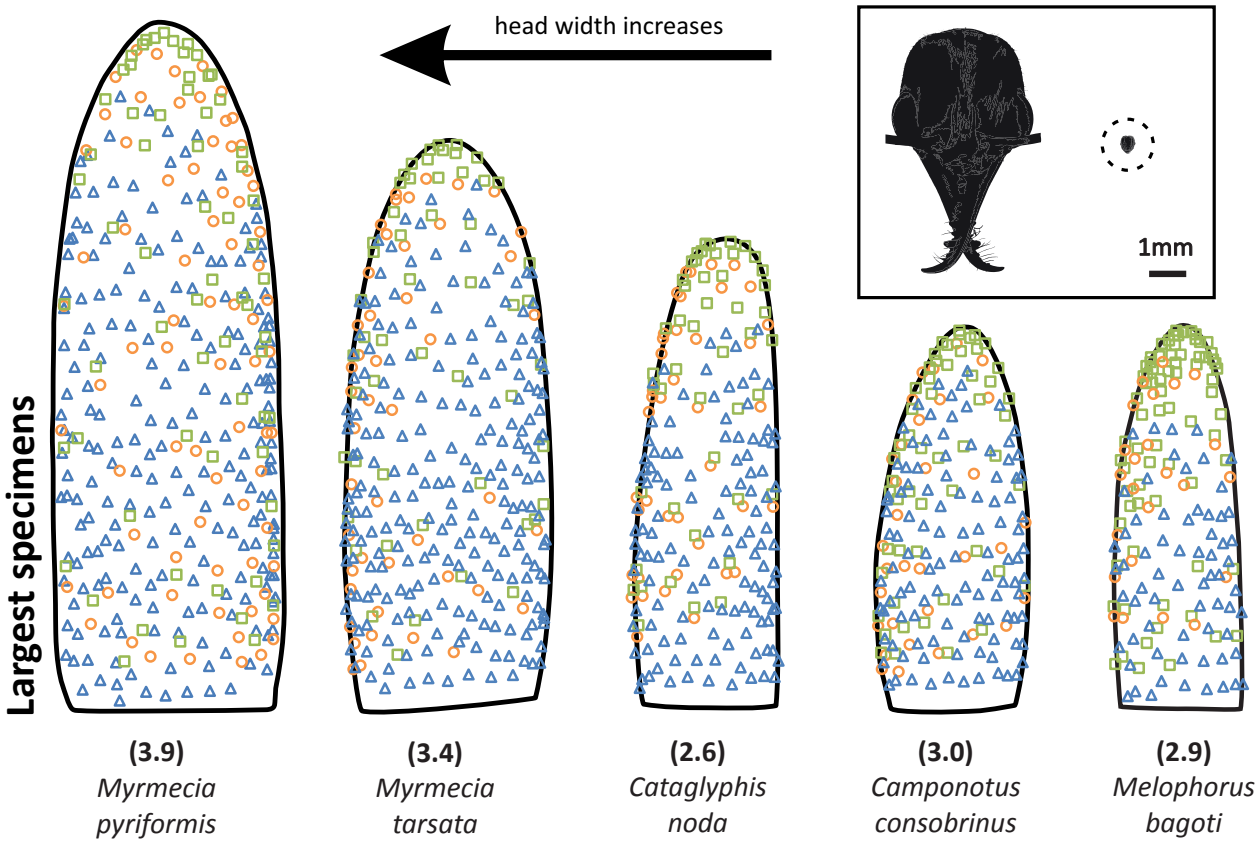
Largest specimens
head width increases
1mm
(3.9)
Myrmecia pyriformis
(3.4)
Myrmecia tarsata
(2.6)
Cataglyphis noda
(3.0)
Camponotus consobrinus
(2.9)
Melophorus bagoti

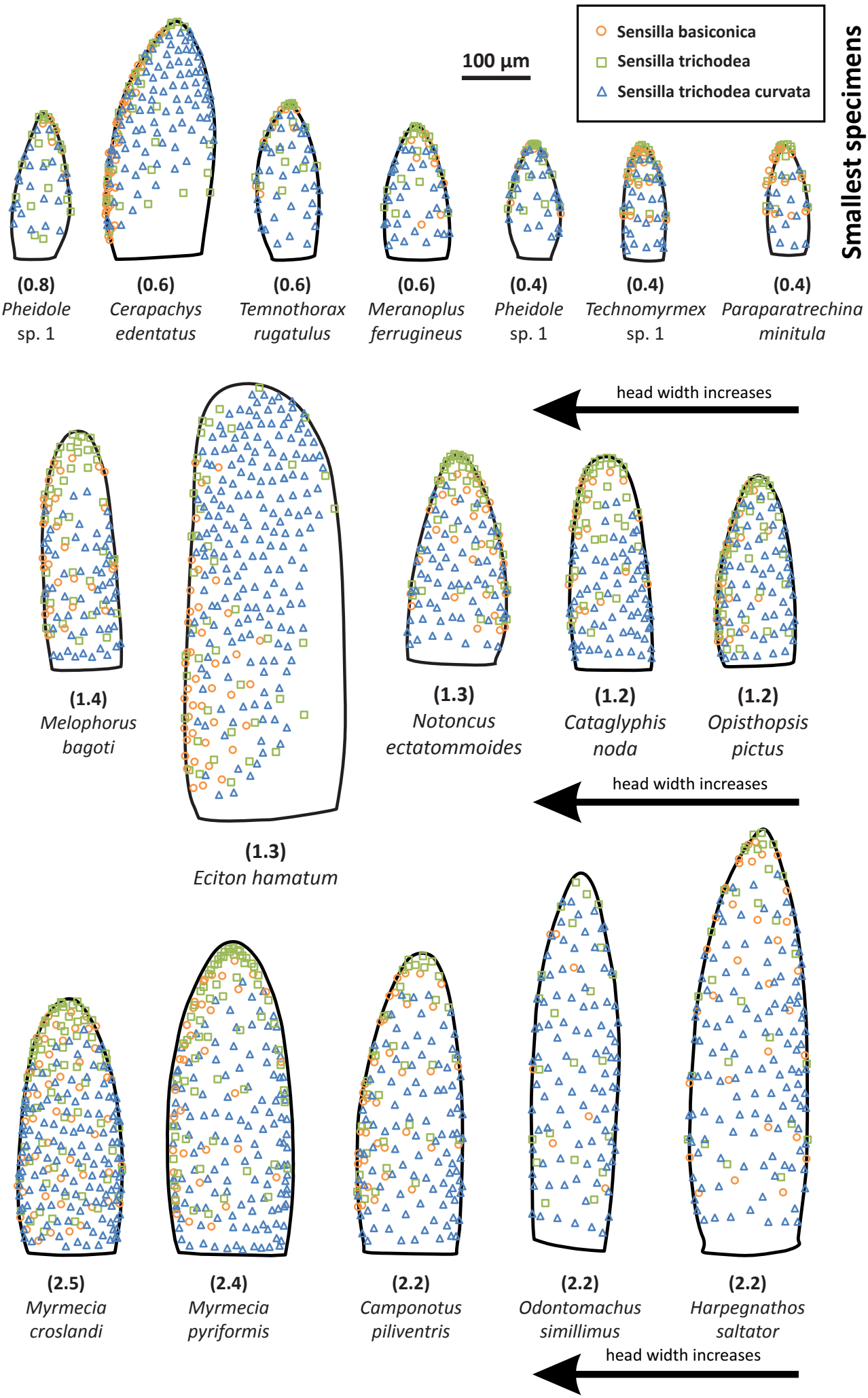
Sensilla basiconica
Sensilla trichodea
Sensilla trichodea curvata
100 µm
Smallest specimens
(0.8)
Pheidole sp. 1
(0.6)
Cerapachys edentatus
(0.6)
Temnothorax rugatulus
(0.6)
Meranoplus ferrugineus
(0.4)
Pheidole sp. 1
(0.4)
Technomyrmex sp. 1
(0.4)
Paraparatrechina minitula
head width increases
(1.4)
Melophorus bagoti
(1.3)
Eciton hamatum
(1.3)
Notoncus ectatommoides
(1.2)
Cataglyphis noda
(1.2)
Opisthopsis pictus
head width increases
(2.5)
Myrmecia croslandi
(2.4)
Myrmecia pyriformis
(2.2)
Camponotus piliventris
(2.2)
Odontomachus simillimus
(2.2)
Harpegnathos saltator
head width increases

Figure 4.13. Distribution of sensilla basiconica, trichodea and trichodea curvata over the apical antennomere of the study species. All antennomeres are displayed at the same scale at a magnification of x1250 times. Additionally all antennomers have been organised such that right=lateral and left=medial. The head width (in mm) of the mapped specimen is indicated in brackets next to the species name. The inset gives a graphical representation of the range of specimen sizes studied, comparing the head of the largest species (*Myrmecia pyriformis*) to that of one of the smallest (*Pheidole* sp.1).

Size and abundance of sensilla

Data overview – Principal components analysis (PCA)

Initial analyses on the size and numbers of the three focal chemosensilla were guided by PCA analysis (see **Figure 4.14**). The outcomes of which will be discussed first. Co-varying traits were then further explored using bi-variate least squares regressions (**Figures 4.15 and 4.16**). The outcomes of these latter analyses are discussed in the following sections.

The PCA included the following variables:

- **Head width (mm):** acts as a proxy for body size. Head size is additionally a relevant measure as it is the appendage bearing segment and houses the processing centre for sensory input, the brain.
- **Apical flagellomere area (μm):** gives some indication of the available sensory surface.
- **Numbers of sensilla** basiconica (B), trichodea (T) and trichodea curvata (C): there's evidence to suggest that larger insects tend to have more sensilla (Ramirez-Esquivel et al., 2014)
- **Median peg[8] length (μm):** median was chosen as a measure of central tendency as length was extremely variable (mean is more susceptible to outliers), there is very little information on the scaling of peg size in the literature
- **Peg length standard deviation (μm):** as a measure of variability (increased variability is sometimes associated with miniaturisation, see **Chapter 1**)

[8] Peg=external cuticular element of the sensillum

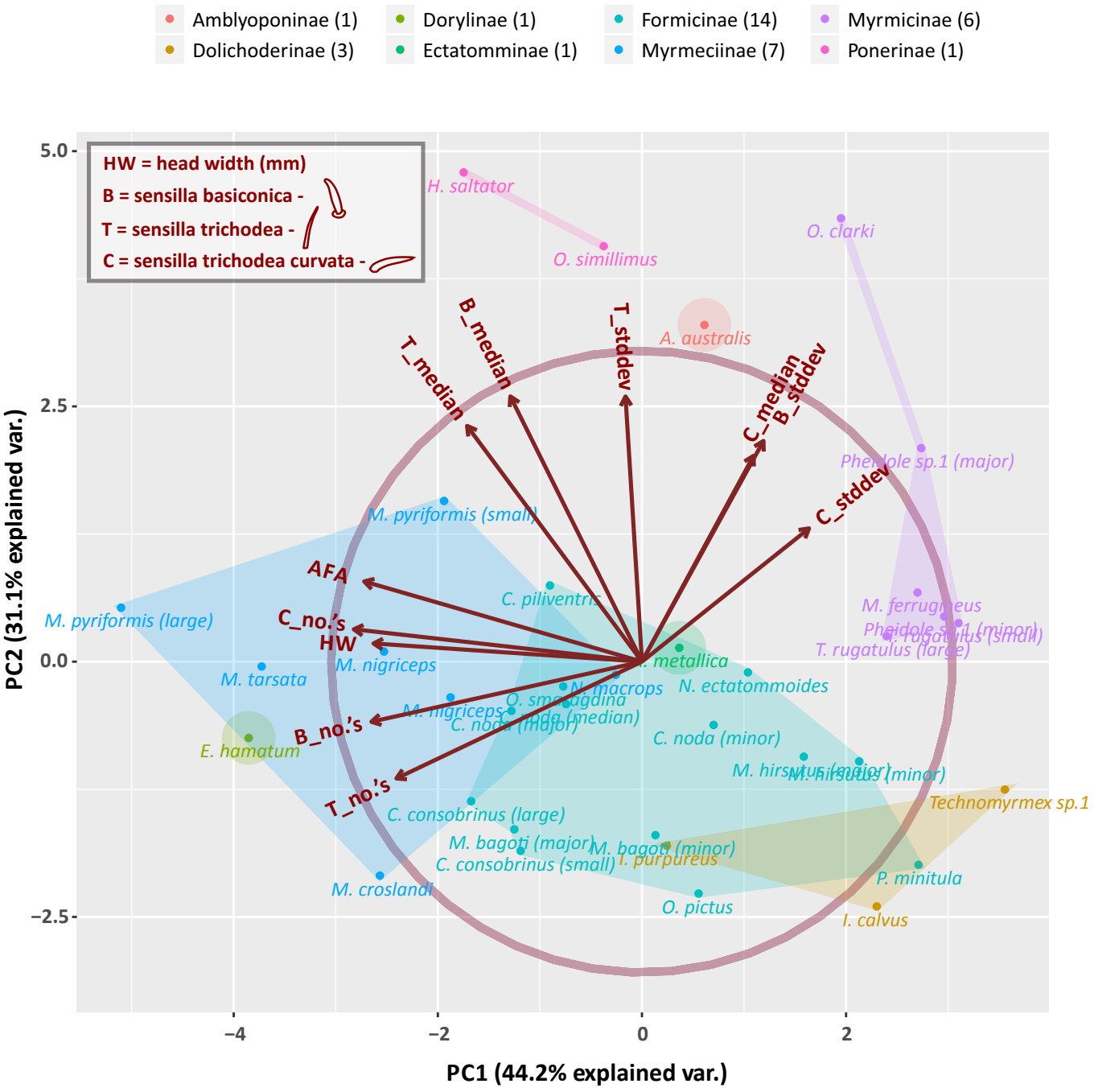

Figure 4.14. Principal components analysis of chemosensilla characteristics. Sensillum names abbreviated as: sensilla basiconica (B), trichodea (T), trichodea curvata (C). Variables included: HW = head width in mm, median = median sensillum length (µm), stddev = standard deviation of sensillum length (µm), no.'s = number of sensilla per dorsal surface of apical antennomere of each specimen. Each subfamily is colour-coded as indicated in the key (top), additionally the number of representatives is indicated in brackets next to the subfamily name. In the plot each subfamily is surrounded by convex hulls, single representatives of a sub-family are surrounded by a circle to indicate that there are no more species in that grouping. The length of vectors relative to the correlation circle (large, maroon circle) indicates how well represented that variable is in the 2D graph, vectors that reach the correlation circle are perfectly represented.

Data points were additionally colour-coded by subfamily to get a qualitative impression of the impact of phylogenetic position.

The first two principal components of the PCA captured 75.3% of the variability in the dataset. The output indicated some variables closely co-varied while others were more loosely associated. The variables seem to be loosely segregated into two adjacent quadrants, one containing head width, apical flagellomere area, and sensillum numbers, the other containing all measures of sensillum length (median and standard deviation for sensilla basiconica, trichodea, and curvata).

Within the first quadrant the number of sensilla curvata is the most closely associated with head width while the numbers of sensilla basiconica and trichodea are less closely associated with head width. Apical flagellomere area is most closely associated with head width and sensilla curvata numbers but does not co-vary exactly with head width. This is consistent with trends observed in the previous section, the apical flagellomere does not scale isometrically but tends to be relatively larger in small species (there is additionally considerable variation in the relative size of the AF).

The second quadrant contains sensillum length measures (median and standard deviation). The distribution of variables indicates that the length of sensilla basiconica and trichodea may be very loosely associated with head width at best. In contrast, the vectors representing the sensilla curvata length and those representing the length standard deviation for all sensilla are found at roughly 90-120° to the head width. This indicates that the length of sensilla curvata and the degree of variability in the length of sensilla are not associated with head width (and by extension with body size) or are weakly negatively correlated.

Some interesting trends can be observed in the way in which subfamilies group in the PCA plot (**Figure 4.14**). As the head width vector aligns quite closely with the x-axis we can interpret horizontal variation as approximating size. The distribution of points in the y-axis is roughly indicative of variation of sensillum length and length variability. With this in mind there seems to be an association between Myrmeciinae, Formicinae and Dolichoderinae. Although Myrmeciinae and Dolichoderinae don't directly overlap these three subfamilies seem to vary along a similar dimension where most of the segregation occurs along the y-axis. This indicates that these three subfamilies could scale in a similar fashion. Ectatomminae also overlaps with Formicinae but with only one representative it is difficult to say whether the rest of this subfamily would

form part of this grouping. All these subfamilies are phylogenetically grouped together in the so called "formicoid clade" (Ward, 2007).

In contrast, Ponerinae, Amblyoponinae, and Myrmicinae seem very distinct on the plot compared to the grouping discussed above. Ponerinae and Amblyoponinae in particular are very distinct in their y-values, these are specialist ants (generally predatory) and are placed together in a "poneroid clade" (Ward, 2007). Myrmicinae on the other hand fall within the "formicoid clade" and curiously display the widest range of variation along the y-axis. Unfortunately, patterns of overlap between these three subfamilies could not be more clearly resolved here due to small sample size.

To further define the patterns of scaling observed in the PCA each sensillum was analysed independently. The results of these analyses are presented in **Figure 4.15** (across Formicidae comparison) and **Figure 4.16** (subfamilies colour coded and outliers labelled) and are discussed below. Additionally, qualitative information on distribution patterns was collected by mapping the three sensilla on the dorsal surface of the apical antennomere (see **Figure 4.13**).

Sensilla basiconica

Sensilla basiconica were on average 20µm long (±6.6µm standard deviation, n=29 species). The species with the shortest median sensilla basiconica was *Technomyrmex* sp.1 (9µm, n=8 sensilla), while the species with the longest was *Harpegnathos saltator* (41µm, n=24 sensilla). There was a very weak trend (R^2=0.21) for larger species to have longer sensilla (see **Figure 4.15a**). However, some species deviated (longer or shorter) from the expected values for their head width and this seemed to be related to subfamily (**Figure 4.16a**). A number of species were notable for their very long sensilla (>2 s.d.):

- *Harpegnathos saltator* (HW=2.16mm): 41µm, Ponerinae
- *Amblyopone australis* (1.94): 34µm, Amblyoponinae
- *Odontomachus simillimus* (2.18): 33µm, Ponerinae

This is consistent with the marked segregation of the ponerine and ambyoponine ants in the PCA.

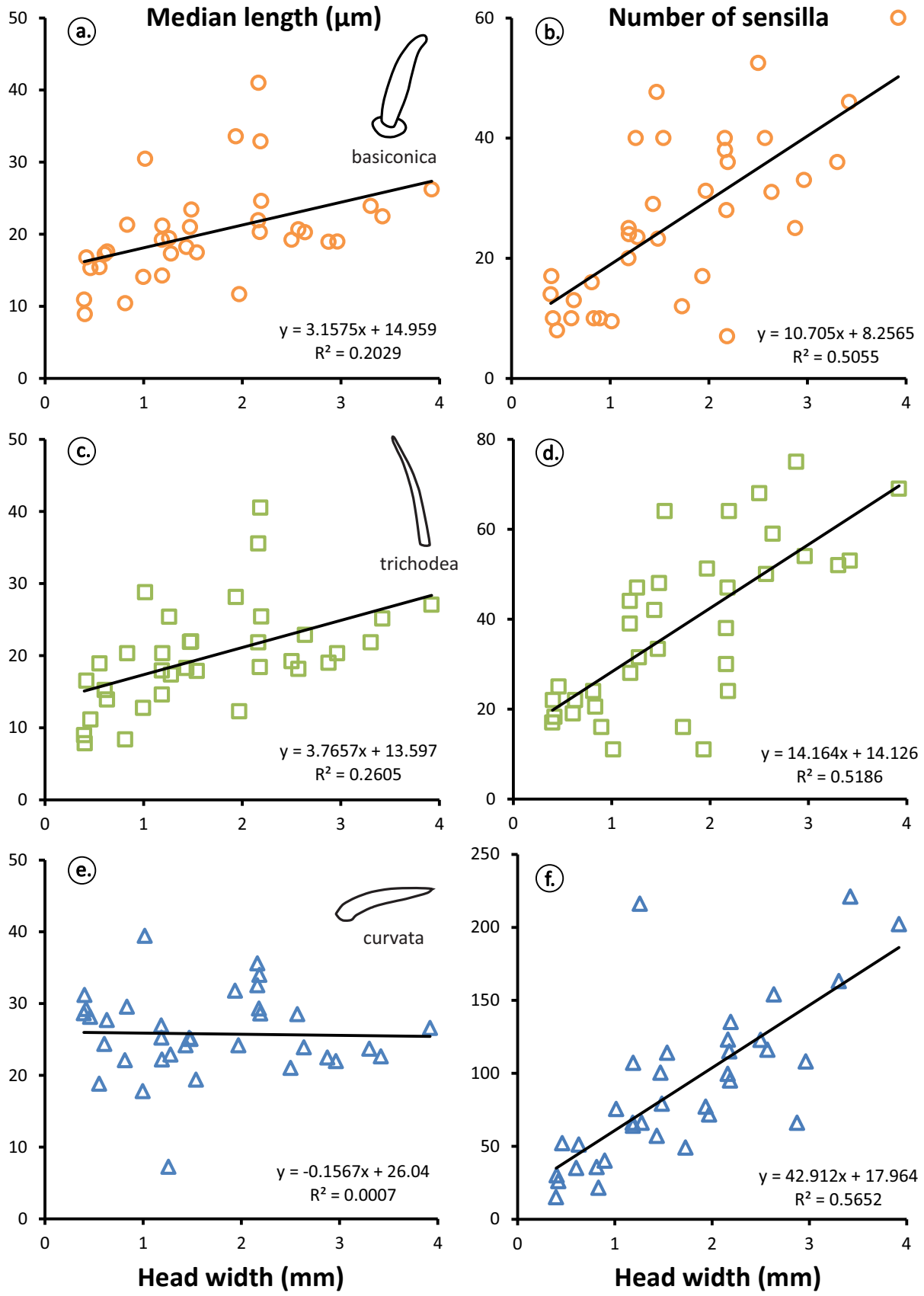

Figure 4.15. Scaling of length and abundance of sensilla basiconica, trichodea and trichodea curvata. The first column of scatter plots contains information on the median length of three chemosensilla across different species while the second column plots the abundance of the same three types. Orange circles = sensilla basiconica (a, b); green squares = sensilla trichodea (c, d); blue triangles = sensilla trichodea curvata (e, f).

Although no species had sensilla that were 2 s.d. shorter than the average there was a small group of species with comparatively short sensilla including:

- *Technomyrmex* sp. (0.40): 8.9µm (-1.7 s.d.), Dolichoderinae
- *Iridomyrmex calvus* (0.81): 10µm (-1.4 s.d.), Dolichoderinae
- *Paraparatrechina minitula* (0.40): 10.9µm (-1.4 s.d.), Formicinae
- *Iridomyrmex purpureus* (1.97): 12µm (-1.3 s.d.), Dolichoderinae

The abundance of sensilla basiconica varied from 7 (*O. simillimus*, Ponerinae) to 60 (*M. pyriformis*, Myrmeciinae) sensilla per apical antennomere. There was a positive linear correlation between head width and the number of sensilla basiconica (R^2=0.51, see **Figure 4.15b**) although there were some notable exceptions to this trend.

The only outlier (±2 s.d.) was:

- *Myrmecia pyriformis* (3.92): 60 sensilla (+2.4 s.d.), Myrmeciinae

Closely followed by:

- *Myrmecia croslandi* (2.50): 53 sensilla (+1.9 s.d.), Myrmeciinae

The species with the highest abundances of sensilla basiconica belonged to Myrmeciinae (see **Figure 4.16**), this subfamily contained the largest specimens.

Some species had unexpectedly low abundances of sensilla basiconica based on their head widths. Based on the regression derived in **Figure 4.15b**, *O. simillimus* (HW=2.18mm) would be expected to have about 32 sensilla basiconica as opposed to 7. Similarly, the regression grossly overestimates (by 50-120%) the abundance of sensilla basiconica in most species with a head width below 1mm.

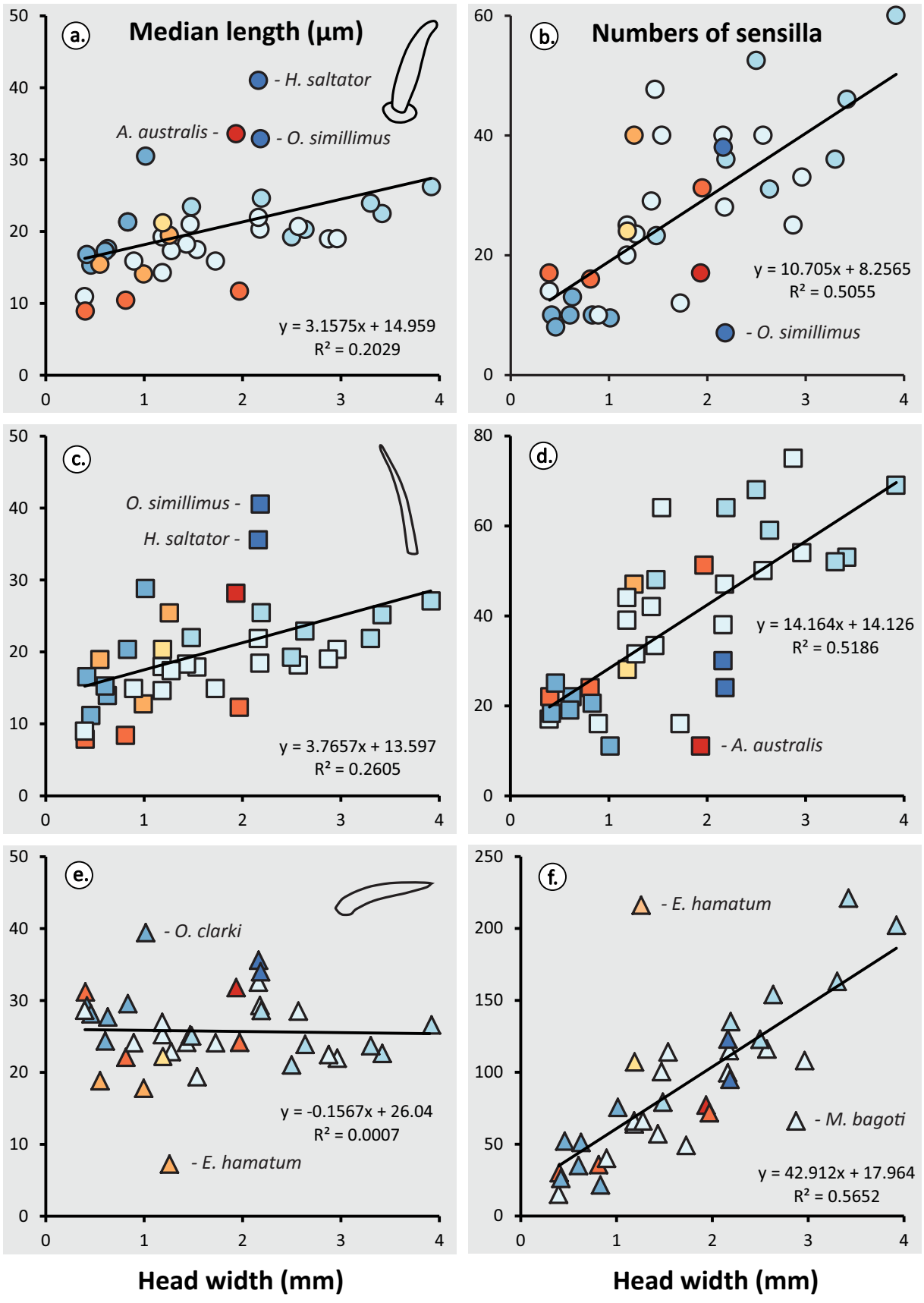

Amblyoponinae (1)
Dorylinae (3)
Formicinae (14)
Myrmicinae (6)
Dolichoderinae (3)
Ectatomminae (1)
Myrmeciinae (7)
Ponerinae (2)

Figure 4.16. Scaling of peg length and abundance of sensilla basiconica, trichodea and trichodea curvata with respect to head width. This figure contains the same data as the preceding plate except here data points are colour-coded by subfamily (see key, number of species included in brackets). The first column of scatter plots contains information on the median length of three chemosensilla across different species while the second column plots the abundance of the same three types. Circles = sensilla basiconica (a, b); squares = sensilla trichodea (c, d); Triangles = sensilla trichodea curvata (e, f). Colour scheme generated using ColorBrewer 2.0 (Axis Maps LLC, 2009; colour blind safe).

Sensilla trichodea

Sensilla trichodea were on average 20µm long (±6.9µm standard deviation, n=29 species). *Technomyrmex* sp.1 had the shortest sensilla trichodea (8µm, n=15 sensilla) while *O. simillimus* had the longest (41µm, n=9 sensilla). Like in basiconica there was a tendency for species with a larger head width to have longer sensilla (R^2=0.26, see **Figure 4.15c**). Both of the ponerine species examined, *O. simillimus* (2.18) and *H. saltator* (2.16), had unexpectedly long sensilla trichodea, not just for their head width but relative to every other species studied (+3.0 s.d. and +2.3 s.d. respectively).

There was a positive, linear correlation between head width and number of sensilla trichodea (R^2=0.52, see **Figure 4.15d**). Sensilla trichodea were generally more abundant than sensilla basiconica and ranged from 11 in *O. clarki* and *A. australis* (-1.5 s.d.) to 75 in *M. bagoti* (+2.0 s.d.).

Sensilla trichodea curvata

Sensilla trichodea curvata were the longest of the three chemosensilla studied. They were on average 26µm (±5.6µm s.d., n=29 species). The majority of species had sensilla that varied in length from 18 to 34µm. The sensillum length did not scale with head width and is fairly consistent across species. However, there were some exceptions, *O. clarki* had the longest sensilla trichodea curvata at 40µm (+2.4 s.d.) while *E. hamatum* had by far the shortest at 7µm (-3.3 s.d.). These extremely short sensilla look markedly different from the sensilla curvata in any other species (see **Figure 4.18**), the next shortest sensilla curvata were 18µm (*L. singularis*). However, the shape and pattern of pores is consistent with the sensilla curvata of other species (**Figure 4.18a**).

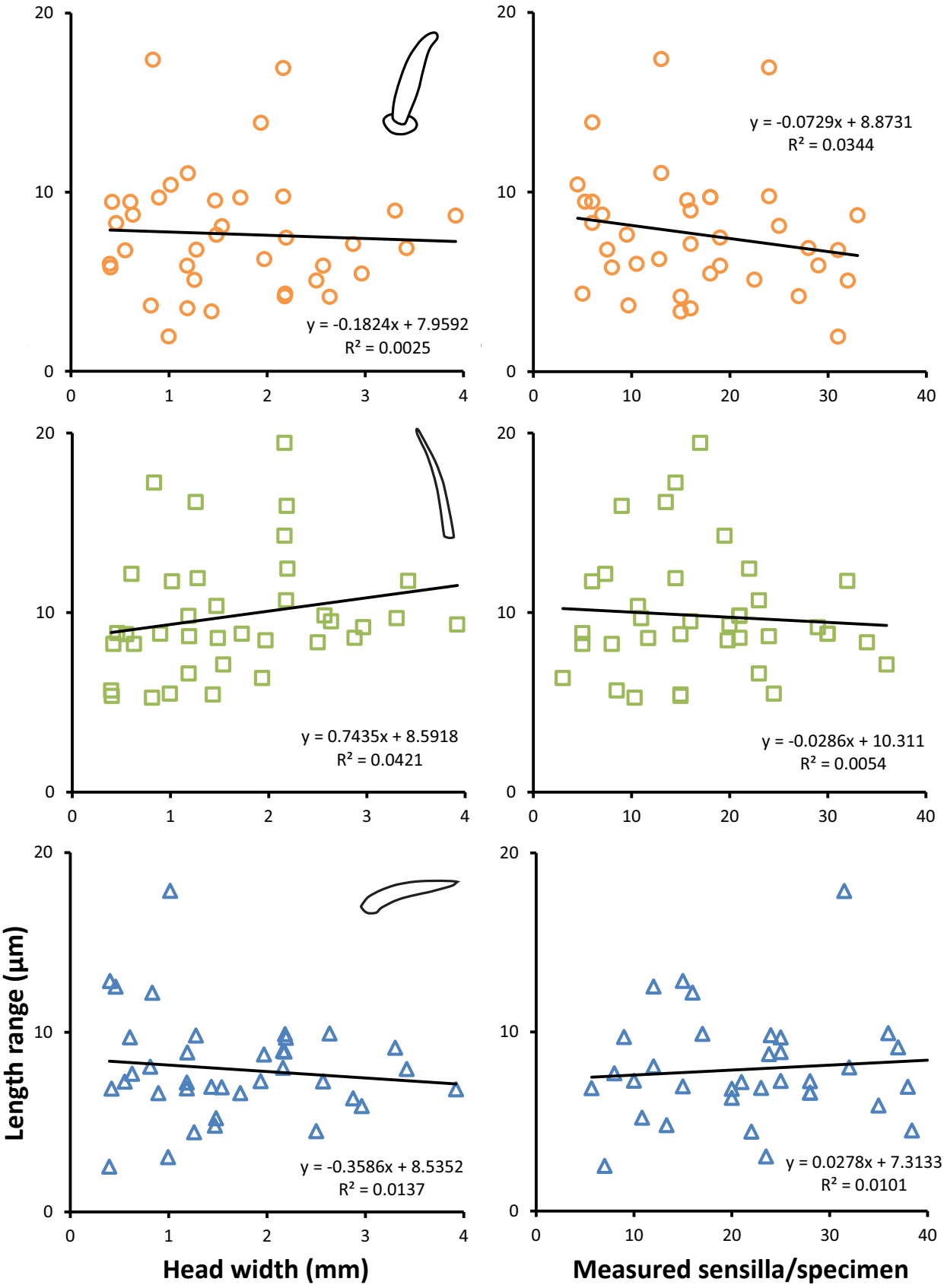

Figure 4.17. Variability (range) of chemosensillum length across species. Length range of the three studied chemosensilla (basiconica = orange circles, trichodea = green squares, trichodea curvata = blue triangles) relative to head width (left column) and relative to the number of sensilla measured per specimen (right column).

The number of sensilla curvata scales positively with head width (R^2=0.57). There were three outlying species (±2.0 s.d. or more):

- *Myrmecia tarsata* (3.42): 221 sensilla (+2.4 s.d.), Myrmeciinae
- *Eciton hamatum* (1.26): 216 sensilla (+2.3 s.d.), Dorylinae
- *Myrmecia pyriformis* (3.92): 202 sensilla (+2.1 s.d.), Myrmeciinae

While the Myrmeciinae were among the largest species examined, therefore leading to high sensillum abundances, *E. hamatum* was a medium sized relative to other species. The observed sensilla curvata abundance in this latter species differed from the predicted value (based on the regression) by 200%, making this species stand out from all other studied species (see **Figure 4.16f**).

Sensillum length variability

In previous sections sensillum length was discussed in terms of median lengths. However, the degree of variability in sensillum length was not constant across species (see **Figure 4.17**). This is of interest because increased variability in certain anatomical features has been associated with miniaturisation (see **Chapter 1**).

On average the ranges in sensillum length were 7.7µm in basiconica (±3.4, 29 species), 9.9µm in trichodea (±3.4, 29 species), 7.9µm in trichodea curvata (±2.9, 29 species). The most variable species had ranges of 17.4µm (range = max – min, basiconica, *Pheidole* sp.1, n=13 sensilla), 19.5µm (trichodea, *H. saltator*, n=17), 17.9µm (trichodea curvata, *O. clarki*, n=32). The most stable species had ranges as small as 1.9µm (basiconica, *Lioponera singularis*, n=31), 5.3µm (trichodea, *I. calvus*, n=10), 2.5µm (trichodea curvata, *P. minitula*, n=7). There was no relationship between sensillum length variability (range) and head width (see **Figure 4.17**, left hand column).

In previous sections standard deviation has been used as a measure of variability as this is considered a more robust measure. However, standard deviation calculation incorporates sample size. Depending on the specimen the number of sensilla measured varied enormously. In each specimen as many sensilla as possible were measured to avoid bias (sensillum length may vary according to location on the antennomere (Ramirez-Esquivel, 2012)). Larger specimens had more measurable sensilla. As a consequence, the variability in sample size among species of different sizes might have been a cause for concern here. Using range as a measure of variability

allows for the independent analysis of the sampling effects. Plotting sample size versus sensillum range showed no correlation between sample size and sensillum length variability (see **Figure 4.17**, right hand column).

Density

The total number of chemosensilla increased with head width across all species (**Figure 4.18a**). The number of chemosensilla per unit area, however, had a weak (R^2=0.35) negative correlation to head width (**Figure 4.18b**). Consequently, smaller species tended to have a higher density of chemosensilla. A power regression provided the best fit for the data, however, the predictive power of this regression is quite poor. Addition of further data to the regression is likely to result in changes to this equation.

Species with the lowest density (sensilla/mm^2) included:

- *Amblyopone australis* (1.94mm) – 1850 (Amblyoninae)
- *Orectognathus clarki* (1.02mm) – 2183 (Myrmicinae)
- *Odontomachus simillimus* (2.18mm) – 2217 (Ponerinae)
- *Harpegnathos saltator* (2.16mm) – 2284 (Ponerinae)
- *Myrmecia pyriformis* (3.92mm) – 2477 (Myrmeciinae)

Of these *M. pyriformis* is the only species that is well described by the regression and therefore the low density may be attributed to its large size. In the case of the other species the low density of chemosensilla may be attributable to their phylogeny and ecology.

In contrast three of the four species with high chemosensillum density were extremely small and well described by the regression. This group included:

- *Technomyrmex* sp. (0.40mm) – 8077 (Dolichoderinae)
- *Paraparatrechina minitula* (0.40mm) – 6206 (Formicinae)
- *Temnothorax rugatulus* (0.46mm) – 5533 (Myrmicinae)
- *Myrmecia croslandi* (2.50mm) – 5374 (Myrmeciinae)

Although, *M. croslandi* is not small in absolute terms, it is the smallest *Myrmecia* species examined. It may thus be considered to fit well with this trend of increasing density with decreasing size in the context of within genus scaling.

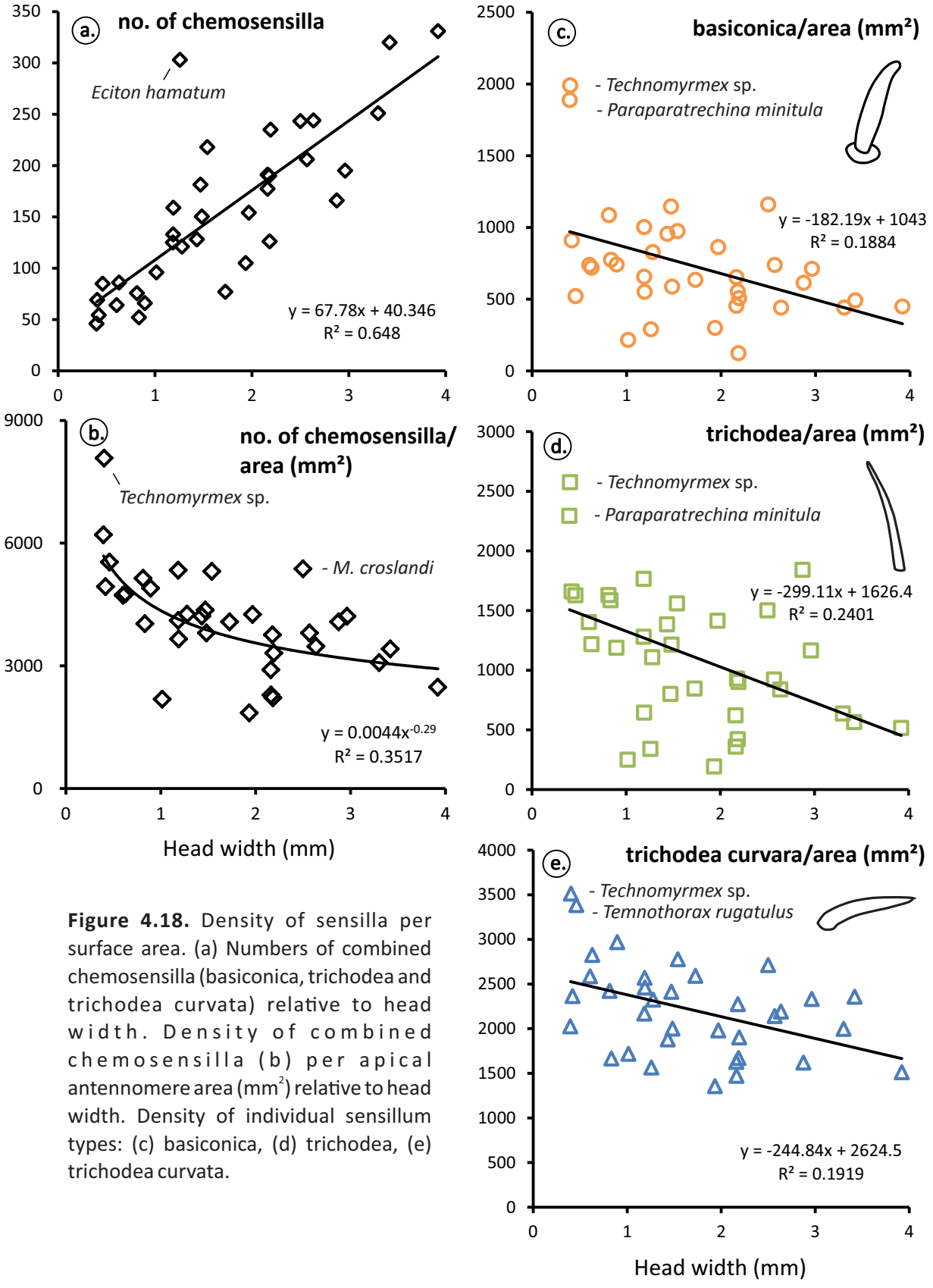

Figure 4.18. Density of sensilla per surface area. (a) Numbers of combined chemosensilla (basiconica, trichodea and trichodea curvata) relative to head width. Density of combined chemosensilla (b) per apical antennomere area (mm^2) relative to head width. Density of individual sensillum types: (c) basiconica, (d) trichodea, (e) trichodea curvata.

In terms of individual sensillum types some rough comparisons can be made across the three different types of sensilla. For instance, sensilla basiconica and trichodea density scale similarly with a similar pattern of sharp outliers (**Figure 4.18c** and **d**). Meanwhile sensilla curvata scaling looks a bit different (**Figure 4.18e**), here there is a more consistent degree of variability around the regression for all head widths (less sharply outlying species).

4.3.3. Exceptional species

In some special cases there were species that stood out significantly from the observed general patterns. Some examples such as the extremely long antennae of *Leptomyrmex* (see **Figure 4.6**), have already been discussed in previous sections. Some additional species with unusual characteristics are discussed below; of particular interest as extremely unusual examples are *Ooceraea australis*, *Lioponera singularis* and *Eciton hamatum*.

Ooceraea australis and Lioponera singularis

In most species there was a fairly homogeneous mixture of the three chemosensillum types on the dorsal flagellomere (**Figure 4.13**) while in both of these Dorylinae species sensilla basiconica and trichodea were segregated from sensilla curvata. Sensilla basiconica and trichodea occupied the medio-ventral aspect of the apical flagellomere while sensilla curvata was found on the latero-dorsal surface (see **Figure 4.19**). The dorso-ventral distribution of sensilla was only thoroughly studied in *Myrmecia pyriformis* (**Chapter 2**) and *Temnothorax rugatulus* (**Chapter 3**). However, the segregation of sensillum types in these two species was marked enough to make it difficult to compare these species with the rest of the dataset so they were excluded from analyses of sensillum numbers and density. The peg lengths were incorporated into analyses and did not particularly stand out.

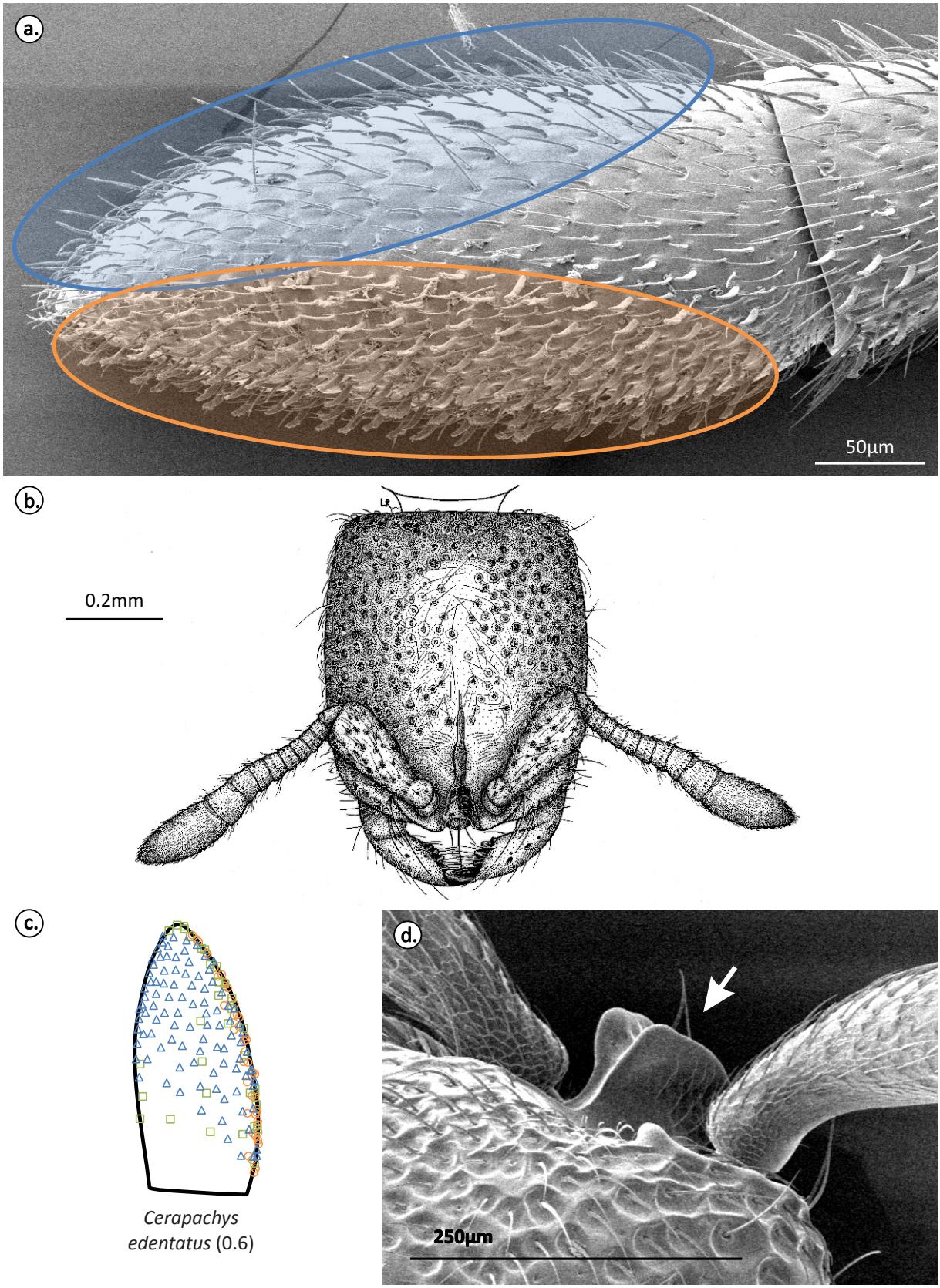

Figure 4.19. *Ooceraea australis* antennae are uniquely organised. (a) The chemosensilla of the apical antennomere are dorso-ventrally segregated: sensilla basiconica and trichodea (orange) are primarily located on the ventro-medial side while sensilla curvata (blue) are on the dorso-lateral side. (b) Illustration of *O.* australis (drawn by Ladina Ribi), note the short scape. (c) Apical antennomere map (dorsal left antenna), basiconica (orange circles), trichodea (green squares), trichodea curvata (blue triangle). (d) SEM of the antennal attachment and antennifer (white arrow) in the closely related *Lioponera singularis*.

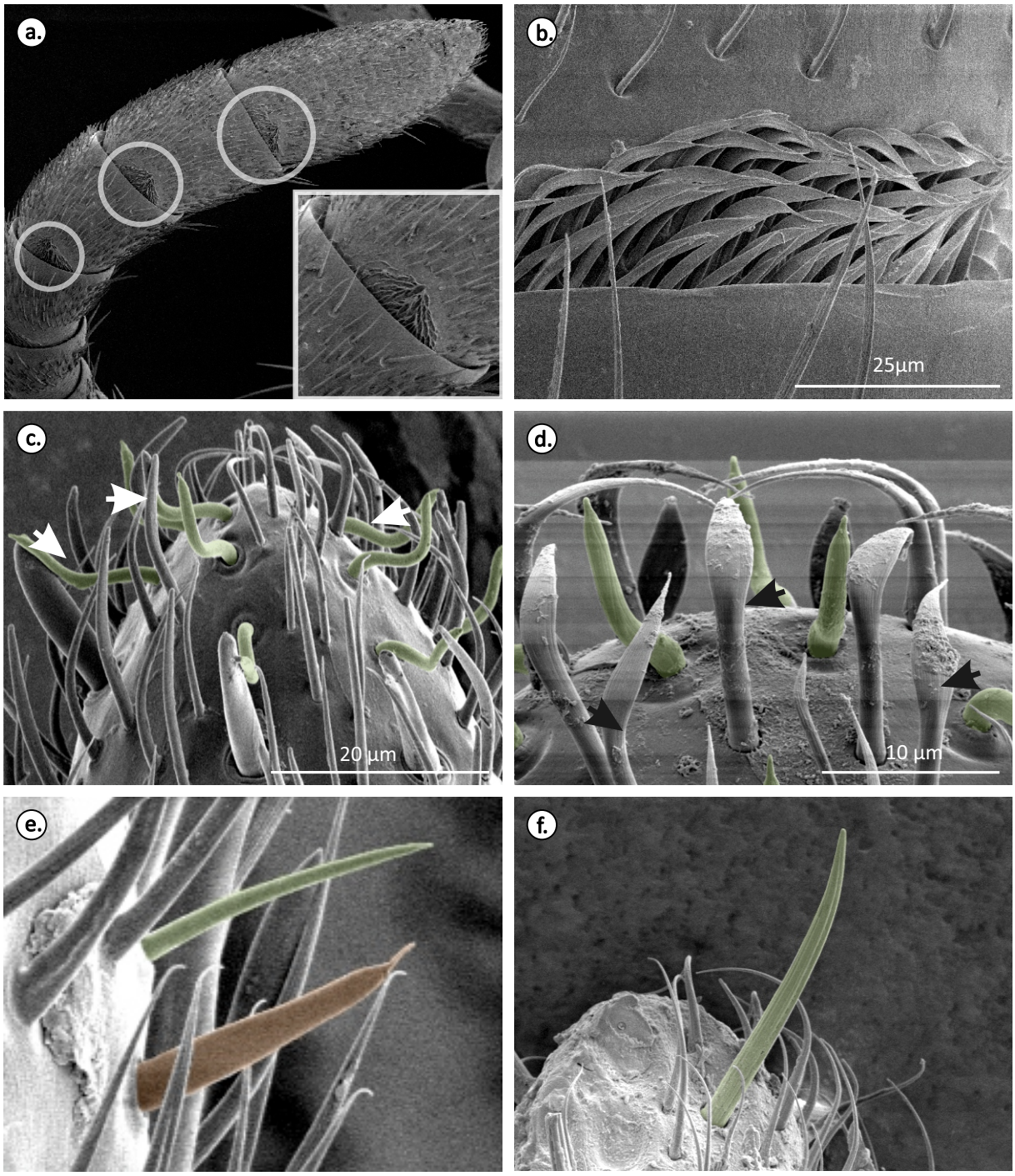

Figure 4.20. Examples of some peculiar sensilla. (a-b) Peculiar sensilla found between flagellomeres in *Cerapachys edentatus*. (c) An example of 'curly' sensilla trichodea (green) on the tip of the antenna of *Melophorus hirsutus* and unusual blunt-tipped sensilla (white arrows); (d) curly sensilla trichodea and unusual sensilla (all uncolourised sensilla, black arrows) with flattened and bent ends on the tip of *Cataglyphis noda* (sensilla trichodea colourised in green). (e) Unusual sensillum basiconicum (orange) with an elongated tip in *Technomyrmex* sp.1. (f) *Odontomachus simillimus* unusually long trichodea (green).

Another peculiarity of this genus was their very short scapes. These resulted in the antennae being held very close to the mandibles when folded (see **Figure 4.19**). In addition both species had quite pronounced antennifers (**Figure 4.19d**) that seem to limit the range of motion of the scape. Based on observations of the anatomy and the way the antennae are held in dead specimens it looks as if the mobility of the antenna may be somewhat limited in *Ooceraea* and *Lioponera* compared to that of other species. These observations would need to be corroborated using behavioural observations. However, this in conjunction with the odd segregation of chemosensillum types, point to the interesting possibility that the organisation of the sensillar array is shaped by the pattern of antennal movement through 3D space.

Lastly, another peculiar feature of *Ooceraea australis* were the unusual sensilla recorded between flagellomeres. Although there were no hair plate sensilla or other proprioceptive sensilla between flagellomeres in the case of *Ooceraea australis* small fields of unusual sensilla have been observed between flagellomeres (see **Figure 4.20a** and **b**). Given their location a proprioceptive function would seem logical, however, their morphology is quite different from other proprioceptors. These sensilla are bilaterally flattened, shaped like a broad sabre and are found in dense groupings in the lateral side of the antenna only.

Eciton hamatum

Eciton hamatum had remarkable antennae compared to other species of ant. The antennae themselves were greatly thickened and rivalled those of the largest species examined in size (see **Figure 4.13** and **Figure 4.21**).

The sensilla curvata were extremely short (see **Figure 4.21a** and **b**). The peg was additionally contained within a slight depression on the antennal surface. This may serve to protect sensilla curvata from breakage in the highly cluttered and densely populated environments that army ants operate in. Apart from being extremely short these sensilla were prodigiously numerous (compare **Figure 4.21c** to **4.20d**). An alternative theory may be that, shortening the sensillum peg may mitigate the effects of boundary layers around the antenna and improve airflow and delivery of chemical stimuli. This could be particularly critical during the raiding behaviours these ants are notorious for.

Melophorus

Two species in this genus were examined, a smaller species *M. hirsutus* (collected in Canberra, Australia) and a larger species *M. bagoti* (collected in Alice Springs, Australia). This genus is known for its thermophilic habits. Most species inhabit hot dry climates and are active during the hottest part of the day when other ants have retired to their nests. These two species had a peculiar form of 'curly' sensilla trichodea at the tip of the apical flagellomeres (see **Figure 4.20c** and **d**). It is not clear whether these curly sensilla have any functional significance but the coiled shape may be more resistant to mechanical breakage caused by antennating hard substrates such as dry clay soils common in *Melophorus* habitats. Additionally, unusual thickened, blunt-tipped sensilla were observed around these curly sensilla (see **Figure 4.20c**, white arrows). It is not clear whether these are distinct types of sensilla or if it they are modified forms of the usual sensilla chaetica that typically surround sensilla trichodea at the tip of the flagellomere.

Cataglyphis noda

Cataglyphis noda is another thermophilic genus that inhabits arid climates. This species exhibited pronounced 'curly' sensilla trichodea similar to those seen in *Melophorus* species (see **Figure 4.20d**). In addition there were unusual sensilla associated with sensilla trichodea at the tip of the flagellomere, similar to the situation in *Melophorus*. The morphology of these sensilla was quite different though. The unidentified sensilla had dorso-ventrally flattened tips ends and ended in a sharp tip (see **Figure 4.20d**, black arrows).

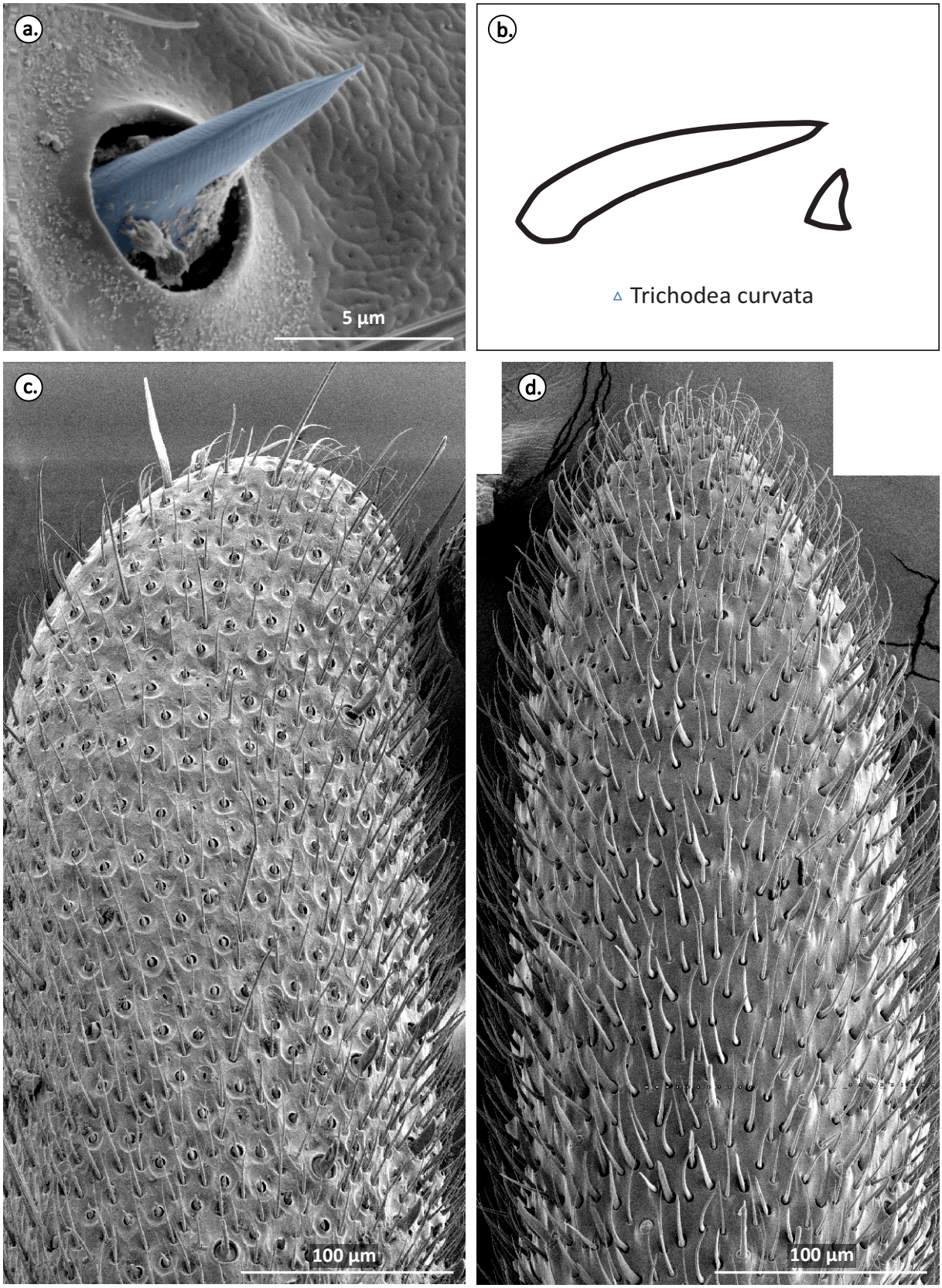

Figure 4.21. Short sensilla trichodea curvata in *Eciton hamatum*. (a) *Eciton hamatum* sensilla trichodea curvata (colourised blue, note that there is some contamination on the sensillum peg - not colourised). (b) Schematic comparing a "typical" sensilla trichodea curvata (*M. pyriformis*) and that of an *E. hamatum* specimen, drawing to scale. Scale matched comparison of the apical flagellomere of (c) *E. hamatum* and (d) *M. pyriformis.*

4.3.4. Additional notes on the antennal array

Fine scale morphology

On the whole the three focal chemosensilla were easily identified in all species. That is not to say that there was no variation in sensilla anatomy across species (for some examples see **Figure 4.22** and **Figure 4.23**). This variation, however, was not thoroughly documented here. This is because whole antennae were imaged using a Hitachi S-4300 SE/N scanning electron microscope. Imaging single sensilla requires high magnification imaging with a field emission gun better suited to biological specimens to avoid charging artefacts or damage to the sample. In previous chapters this was done using a Zeiss UltraPlus FESEM but this is a separate imaging process with its own technical requirements and settings. Some notable morphological variations were observable even at relatively low magnification imaging. This included the short sensilla curvata of *E. hamatum* and the "curly" sensilla trichodea of *Melophorus* and *Cataglyphis* (see **Figure 4.21a** and **Figure 4.20c-d**, discussed in greater detail above).

Some extremely small species exhibited some morphological peculiarities. For example, *Technomyrmex* sp. 1 had sensilla basiconica that terminated on a thin, elongated tip (e.g. **Figure 4.20c**). As seen in at least one species: *Pheidole* sp.1 (see **Figure 4.22e** and **j**), small species may also have a different pattern of pores on sensilla basiconica although this was not thoroughly investigated. This may potentially indicate that there were fewer dendritic endings within the sensilla of smaller species. Although, exhaustive superfine scale morphological studies of the sensilla were outside the scope of this chapter, the observed variations may point to interesting changes in the underlying ultrastructure of sensilla in very small ants.

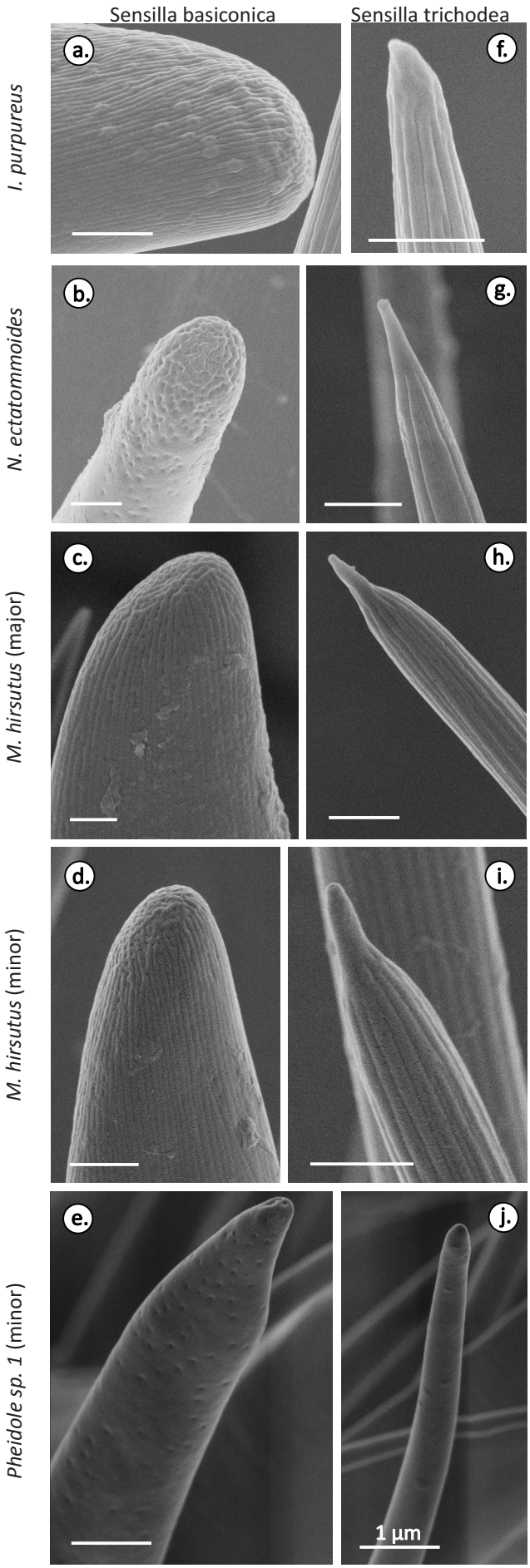

Figure 4.22. High magnification images of the tips of paired sensilla. (a-e) Sensilla basiconica and (f-j) sensilla trichodea showing the different patterns of striation and pores in five of the six studied animals. No images of *Pheidole sp. 1* major workers were available. All scale bars = 1µm. Modified from Ramirez-Esquivel (2012).

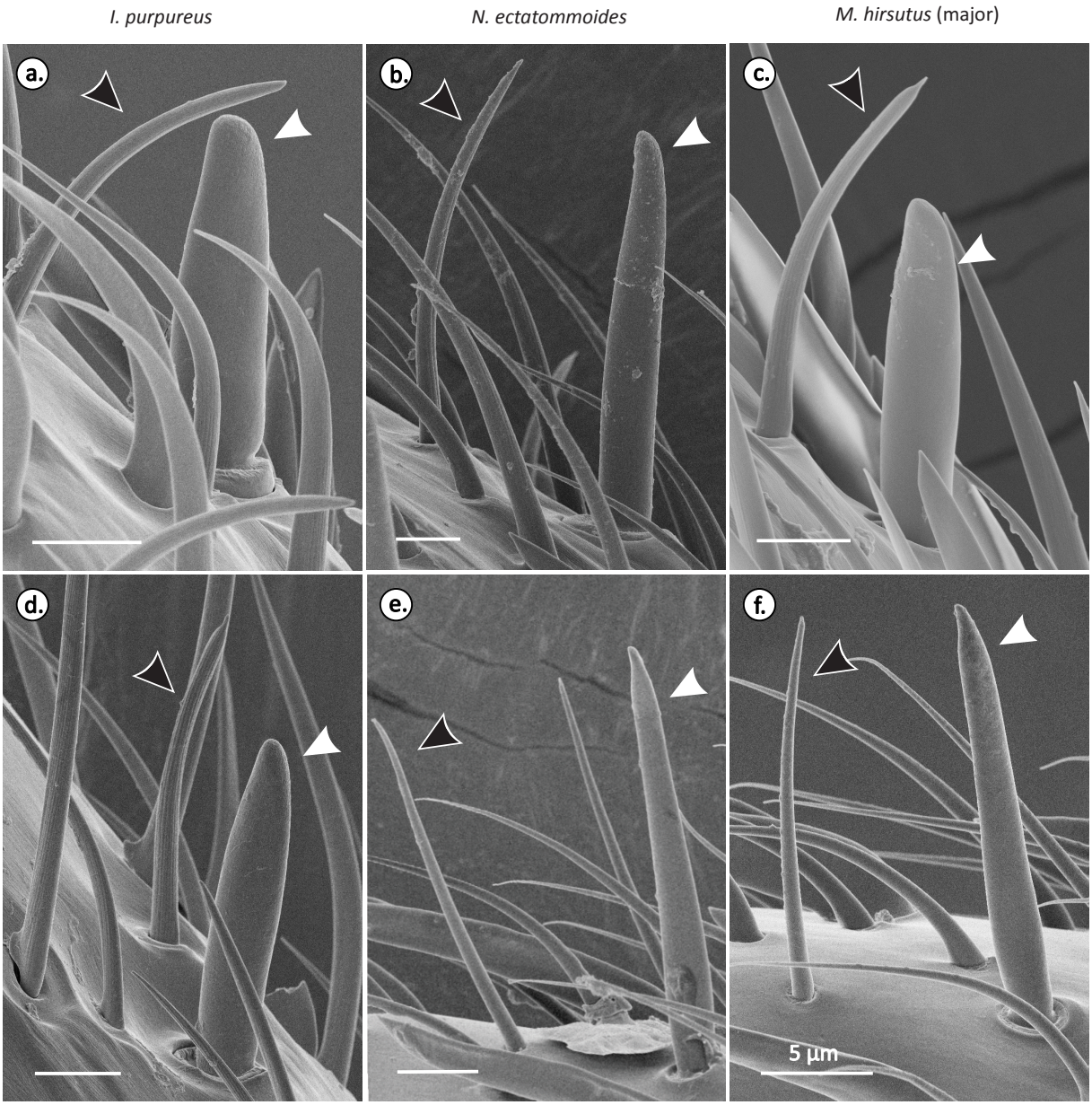

Figure 4.23. Examples of variation in the morphology of sensilla basiconica (white arrows) and sensilla trichodea (black arrows). All scale bars = 5µm. Modified from Ramirez-Esquivel (2012).

Other sensillum types

There was generally a great consistency of types of sensilla and general distribution patterns across most species studied. In addition to the three focal chemosensilla the full complement of sensillum types described in **Chapter 2** (sensilla coeloconica, coelocapitular, ampullacea, chaetica and TII) was present in most species. However, pore sensilla, in particular sensilla coelocapitular and coeloconica were not visible in some specimens but this is more likely due to their low natural abundance than to their actual absence. In the case of sensilla coeloconica, a tendency to cluster in fields, which may wrap around the side to the ventrum is probably also responsible. TII sensilla were also not identifiable in some species but this may be due to a lack of strong distinguishing features and insufficient image quality. Additionally, there were some rare species with sensilla that could not be assigned to any known types. This included some blunt tipped sensilla around the apex of the apical flagellomere in *Melophorus* species and the flattened sensilla observed in the same location on *Cataglyphis* (see previous section). These sensilla may be an unusual form of filiform mechanoreceptor or an undescribed type of sensillum. In general it was extremely unusual to see sensilla that could not be identified.

4.4. Discussion

SECTION SUMMARY

This discussion will follow a similar structure of the results section with some additional topics covered:

1. *Gross anatomy of the antenna: first in general and then with respect to miniaturisation.*
2. *Distribution, and scaling of peg length and numbers of the three focal chemosensilla*
3. *Exceptional species*
4. *Sensillum, cell, and genome size*
5. *The functional significance of the apical flagellomere*
6. *Conclusions and future directions*

Some parts of this discussion will consider ecologically driven adaptations, methodological considerations, and other topics that represent a departure from the main area of interest, miniaturisation. To maintain a cohesive narrative these sections have been placed in cutaway boxes such as this one and may be read independently.

4.4.1. Miniaturisation of antennae

> *"For every type of animal there is a most convenient size, and a large change in size inevitably carries with it a change of form."*
>
> (Haldane, 1926)

I carried out a large-scale comparative study of antennal allometry including 120 species and found that certain variables tend to be associated with ecology while others may be at least partly related to body size. Although all ants have geniculate (elbowed) antennae (see **Figure 4.2a**), the number, shape and size of flagellomeres varied. The length of the scape, the ratio of funiculus to scape and the relative total length of the antenna compared to the body varied widely. Specialised ecological traits such as defensive adaptations and arboreal habits seem to be the main drivers in determining these variables. However, a transition from club to filiform antennae was to some extent correlated with body size (**Figure 4.5d**). This *"change in form"* is interesting because it may allow some small species to compensate for the rapid decrease of volume to surface area that accompanies decreasing body size.

This section is devoted to the anatomy of the antenna itself. It first discusses ecologically driven adaptations and then focuses on miniaturisation related adaptations.

Adaptive antennae length

Antennal length and proportions are likely to have important functional implications for how an ant uses her antennae. Factors such as range of movement, total functional chemoreceptive area of the antenna, and the volume of air a set of antennae can probe, will be at least partially dependent on the particular dimensions and relative proportions of the antenna. In this chapter I examined a number of antennal allometries (see **Figure 4.5** and **Supp. Fig. 4.4**). The majority of these variables, including antennal length, antennal length to head width ratio, and flagellum to scape length ratio did not reveal any special adaptations around the smallest species (**Figure 4.5d** will be discussed separately in the next section). However, some outlying species exhibited ecologically driven adaptations.

The idea that antennal dimensions reflect on the ecology of taxa is not entirely new. A study by Dlusskiy (1983) proposed that the ratio between the scape and the total antennal length may be a relevant measure of sociality in Hymenoptera. Certain ratios within Hymenoptera permit antennation of objects carried in the mandibles whereas others do not. For example parasitic forms such as scoliids, velvet ants and solitary betilids are unable to antennate the contents of their mandibles (Dlusskiy, 1983). Social insects must be capable of delicately manipulating objects in their mandibles such as brood items (eggs, larvae, pupae), nest mates (e.g. carrying during migrations, ejecting sick or dead workers) and monitoring them with their antennae. These types of antenation allow them to determine the developmental state of a larva, the health of a queen or the presence of intruders all of which are vital for colony fitness.

However, all ants are eusocial so such pronounced differences in antennal anatomy as described by Dlusskiy (1983) were not expected. One major difference between ants and other hymenoptera is that all workers are pedestrian. Furthermore, different species walk along very different substrates depending on their ecology.

Some environments may be more cluttered than others and this is likely to be relevant for the design of slender organs designed to probe the surrounding environment, such as antennae. Species inhabiting open spaces may be driven to gain as much information as possible by making their antennae longer, while species in cluttered environments such as the leaf litter may prefer to keep their antennae shorter for protection against mechanical damage. Furthermore, while Dlusskiy focussed on the differences between social and non-social species other ecological factors and interspecies interactions may be important in shaping optimal antennal design.

In the results section I gave *Leptomyrmex* as an instance of ecologically driven elongation of the antennae. This particular case is a bit special because this genus specialises in mimicking spiders to deter unwanted confrontations (Boudinot et al., 2016). Thus the elongation of the antennae is likely to contribute to this adaptation by mimicking an extra pair of legs. Unfortunately, data on the sensillum array of this particular genus was not collected so any potential impacts of this elongation on the chemosensory array could not be examined more closely. Luckily, *Oecophylla smaragdina* has similarly long antennae and sensillum information is available for this species. This allows us to examine whether ecologically driven elongation has any impacts on the sensilla of the apical flagellomere.

O. smaragdina is a relatively well studied arboreal species with complex social behaviours. Despite having extra long antennae *O. smaragdina* does not have more chemosensilla or an increased apical flagellomere surface area (see **Figure 4.24a** and **b**) and the size of the apical flagellomere is consistent with that of species of similar head width (accurately predicted by the regression, see **Supp. Fig. 4.4d**). Like in *L. cnemidatus* the extra length in the antennae comes, primarily from an elongated scape and pedicel, and to a lesser extent from some of the proximal flagellomeres.

The extra length of *O. smaragdina* antenna seems to be an ecological adaptation for their arboreal habitat. Longer antennae may assist with searching for neighbouring surfaces in the complex 3D structure of the tree canopy (see **Figure 4.24c** and **d**). Additionally, *Oecophylla* species build leaf nests constructed by workers by bringing leaves together using worker chains and binding them using silk (Cole and Jones, 1948). Long antennae would help to find nest-mates across a gap during this chain building behaviour.

In contrast to this arboreal species a number of hypogaeic species

with extremely short antennae were also described in the results (see **Figure 4.8**). In this case shortening of the antennae was most marked in the scape and is most likely a protective measure. Short antennae may be more easily folded close to the head for protection in cramped spaces.

Another interesting example of short antennae is that of *Meranoplus*. This genus is not hypogaeic but it is characterised by their elaborate defensive structures (see **Figure 4.7**) such as pronounced scrobes capable of enveloping the entire antenna and promesonotal shields (Andersen, 2006). Despite this difference the antennae are again primarily shortened through a reduction in the scape (about half the predicted length for a species of its size) and to a lesser degree through a shortening of the proximal flagellomeres (data not shown). Species in this genus are generally timid generalist or granivorous ants. When disturbed many species retract their antennae into the scrobes, curl up into a foetal position and "play dead". *Meranoplus ferrugineus*, the species examined in this study, was observed in the field being harassed by smaller species of *Iridomyrmex* (personal observation). In the light of this ecological information it seems likely that the disproportionately short antennae of *M. ferrugineus* (see **Figure 4.7**) is a result of its defensive adaptations and not related to sensory considerations or caused by miniaturisation. This hypothesis is supported by the fact that despite the overall shortening of the antenna the number of chemosensilla on the apical flagellomere are not reduced and the flagellomere is not shortened (data not shown).

In conclusion, most of the antennal allometries examined did not reveal miniaturisation-related adaptations but some species exhibited ecologically driven adaptations (**Figure 4.5a-c**). Changes in the ratio of antennal length to head width or flagellum to scape length were not correlated with changes in head width (see **Figure 4.5b** and **c**). Since head width is a proxy for body size, we can disregard these allometric relationships in the context of miniaturisation-related adaptations. Ecologically driven shortening or lengthening of the antennae was mostly driven by shortening or lengthening of the scape and pedicel and did not affect the number of sensilla in the apical flagellomere. In contrast, the ratio of apical flagellomere to total flagellum length (**Figure 4.5d**) does change markedly with changing head width. This is discussed in detail directly below.

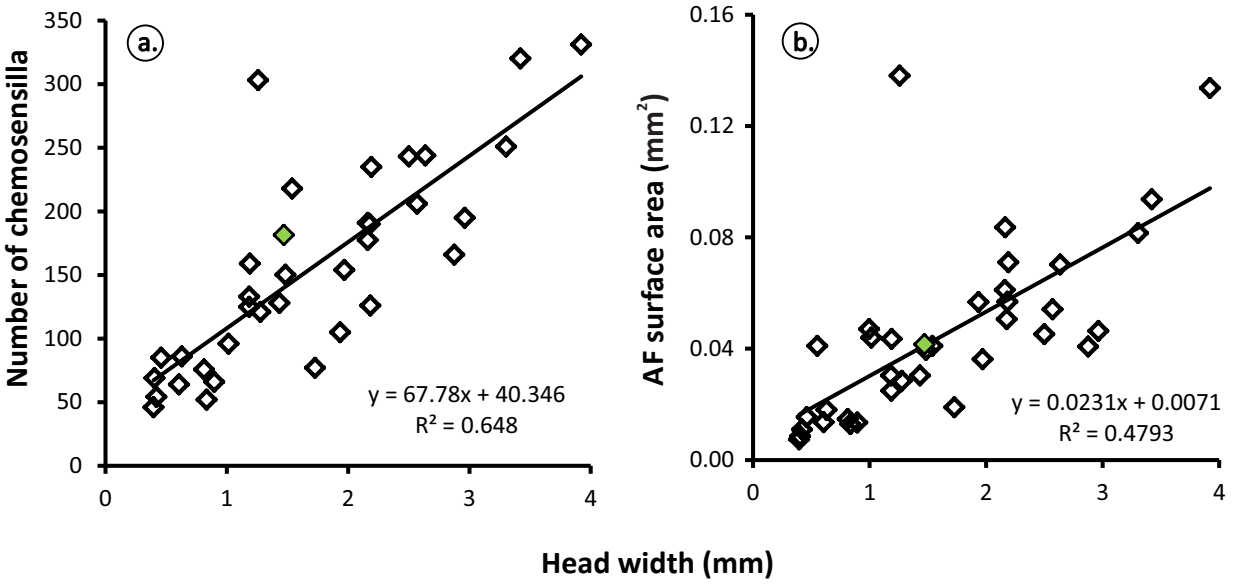

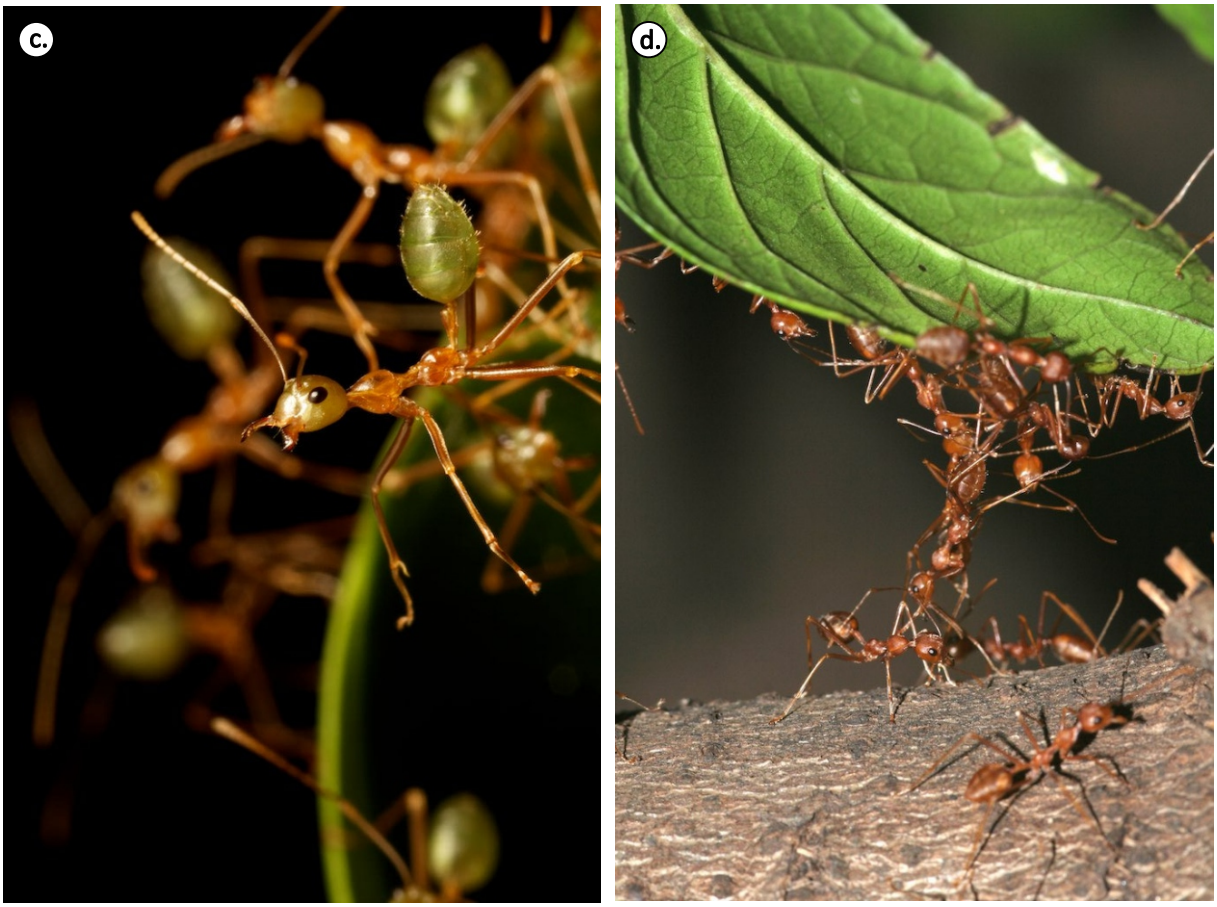

Figure 4.24. Despite the extra long antennae *O. smaragdina* (green diamonds) does not have extra sensilla or any difference in the density of chemoreceptive sensilla. (a) Absolute numbers of sensilla (B+T+C); (b) surface area of the apical flagellomere (mm^2). (c, d) Photographs of *O. smaragdina* workers bridging a gap in the canopy, note that the antennae are outstretched as workers search for neighbouring nest mates and surfaces (photographs by Ajay Narendra).

Miniaturisation and shape of the flagella

Club antennae in the smallest species

There was a significant trend for smaller species to have an apical flagellomere that was relatively large and which made up a much greater proportion of the total flagellomere length (see **Figure 4.5d**). This was accompanied by a dramatic reduction in the size of proximal flagellomeres and sometimes by a reduction in the number of flagellomeres. This suite of traits results in the so-called "club" antennae of smaller species. Although this term might seem evocative of a distinct morphotype, my dataset shows a continuous variation from filliform to club antennae. The most drastic examples of apical flagellomere enlargement occurred in species with a head width of less than 1mm.

Enlargement of the apical flagellomere concurrent with a decrease in body size seems to be an adaptation to miniaturisation. One potential explanation for the adaptive usefulness of this trait is that the enlargement of the flagellomere facilitates a constant relationship between the surface area and volume of the flagellomere. As a body becomes smaller its volume decreases at a faster rate than its surface area, as the former scales to the cube and the latter to the square (for detailed discussion of this see **Chapter 1**). A disproportionately large flagellomere may mitigate this effect. Maintaining an adequate surface area to volume ratio (A:vol) is important for many biological processes (see **Chapter 1**).

Why is volume important?

There are three important practical considerations when thinking about the volume requirements of an antenna as a metabolically active sensory organ (Schneider, 1964). Sensilla require haemolymph supply, gas exchange, and neural innervation (see **Figure 4.25a** and **b**). Haemolymph flow to the antennae is facilitated by a circulatory organ and a single vessel per antenna which terminates in a single pore at the apical antennomere (Matus and Pass, 1999). This circulatory organ is an ampulla consisting of elastic connective tissue without any musculature; pulsation is believed to be achieved indirectly through contraction of the pharynx dilator muscles. Oxygen arrives at the antennae through antennal tracheae (most likely a single unbranched trachea for each antenna) which project from the frontal cerebro-optic air-sac, this is in turn fed by the cervical trachea which connect to spiracles in the thorax (Kristensen, 1984;

Tonapi, 1959). Lastly, sensory information is conveyed to the brain via the antennal nerve (**Figure 4.25c-d**). All sensory information exits the antenna and is directed to specific brain regions. Olfactory information is generally first routed to the antennal lobe (**Figure 4.25e**) while gustatory information is generally directed along multiple pathways (Strausfeld, 2012). In addition, the internal aspect of sensilla can be quite elaborate comprising not only sensory neurons (of variable numbers) but also accessory cells (**Figure 4.25d**, red arrow), which assist in the proper function of the sensillum. An antenna must therefore have sufficient volume to accommodate all these structures: a trachea, nerves, sensillum accessory cells, and some minimum volume of haemolymph.

So do all small species have club antennae?

Not all small species had relatively enlarged apical flagellomeres. Enlargement of the apical flagellomere above approx. 20% of the total flagellum length was only observed in small species (see **Figure 4.5d**). The most dramatic examples were seen in species with a head width below 1mm. However, below this threshold there was a large variation in the relative size of the apical flagellomere. Some species did not exhibit an enlargement (AFL<20%) while others showed an extreme enlargement (AFL=57%).

In order to investigate this variability, let us examine species with HW<1mm sorted by subfamily (**Figure 4.26a** and **Table 4.3**). This subsample includes four subfamilies with multiple representatives with HW<1mm, these are Formicinae, Myrmicinae, Dolichoderinae, and Dorylinae. Species in Myrmicinae tended to have the greater enlargement of the apical flagellomere in general and were among the species with the greatest enlargements overall. The species with the greatest observed enlargement belonged to Formicinae but some of the larger species (HW>0.5mm) in this subfamily did not have enlarged AFs at all (<20%). Dorylinae species had only somewhat enlarged AFs (22-28%) with one species attaining a greater enlargement (35%). Dolichoderinae species had very little or no enlargement of the AF (10-27%).

Table 4.3. Apical flagellomere length (AFL) relative to flagellum length (expressed as a percentage) in different ant subfamilies with extremely small species. Size is measured in mm using head width (HW) as a proxy for body length.

	HW - range	Average AFL	AFL std dev	n (species)
Dolichoderinae	0.40-0.96	17.7%	5.8%	13
Dorylinae	0.34-0.96	25.8%	4.9%	7
Formicinae	0.25-0.91	26.5%	13.7%	13
Myrmicinae	0.34-0.97	31.9%	6.6%	27

These observations seem to indicate that phylogeny as well as body size plays a role in determining the relative size of the apical flagellomere. Some subfamilies exhibited a greater degree of apical flagellomere enlargement than others. The degree of enlargement was, to some extent, characteristic for each subfamily; there was little deviation from the subfamily average AF relative length (**Table 4.3**). Formicinae was unique in this respect in that it had a standard deviation that was about double that of other subfamilies (see **Table 4.3**). Beyond the degree of enlargement the scaling pattern of the AF length seemed to be characteristic for individual subfamilies (**Figure 4.26a**). Fitting correlation curves to individual subfamilies generally returned stronger R^2 values than for the pooled sample (compare lines of best fit and R^2 values in **Figure 4.26a**). At this point, it is not clear why some subfamilies scale more strongly than others.

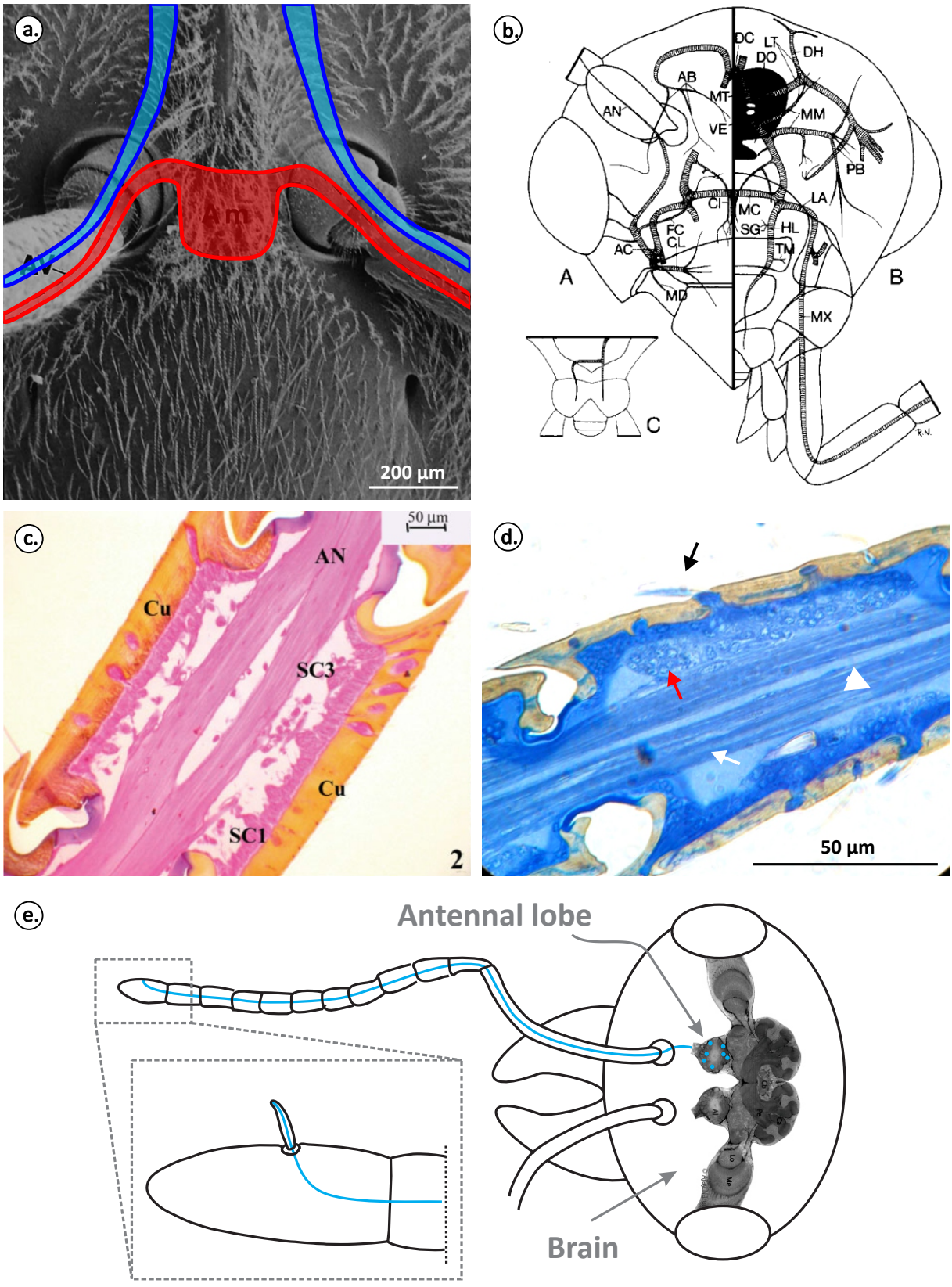

Figure 4.25. Antennal infrastructure. (a) Frontal view of an ant head showing the location of the ampulla (pulsatile organ) and antennal vessel and antennal trachea access (modified from Matus and Pass, 1999). (b) Tracheal organisation on the hymenoptera head (reproduced from Kristensen, 1984). (c) Antennal nerve (AN) within the antenna of the large *Dinoponera lucida* (reproduced from Marques-Silva et al., 2006). (d) Internal aspect of the antenna in the smaller *Notoncus ectatommoides* showing the antennal nerve (white arrow), sensilla curvata on the surface (black arrow) with underlying neuron and accessory cell bodies seen as granular material (red arrow). (e) Illustration of the neural connection between sensilla and the antennal lobe in the brain (modified from Chapter 8).

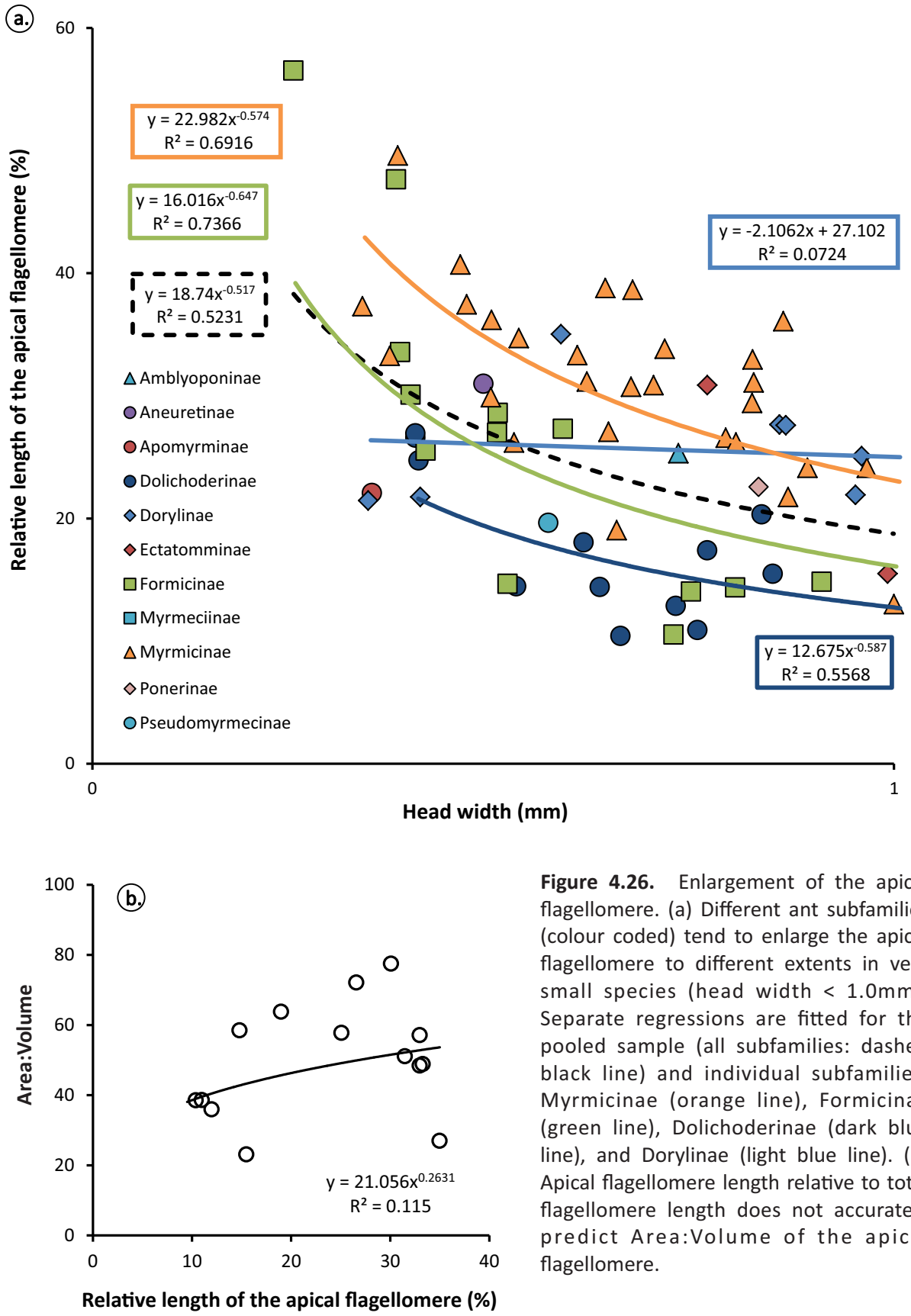

Figure 4.26. Enlargement of the apical flagellomere. (a) Different ant subfamilies (colour coded) tend to enlarge the apical flagellomere to different extents in very small species (head width < 1.0mm). Separate regressions are fitted for the pooled sample (all subfamilies: dashed black line) and individual subfamilies: Myrmicinae (orange line), Formicinae (green line), Dolichoderinae (dark blue line), and Dorylinae (light blue line). (b) Apical flagellomere length relative to total flagellomere length does not accurately predict Area:Volume of the apical flagellomere.

A note on describing club antennae

In this chapter I use the length of the apical flagellomere relative to total flagellum length to define antennal morphology. An antenna with an AFL>20% of total flagellum length is categorised as a club antenna, while an antenna with AFL<20% is categorised as a filiform antenna. This categorisation is based on the available measurements (i.e. length was the only measure available; width area and volume could not be measured in this study) and the observed distributions of relative apical flagellomere length (see **Figure 4.5d**, note the rapid scaling of relative AFL above 20% in the smallest ants). This categorisation was only meant as a guideline based on the available information and is by no means an exhaustive morphological description. A more exhaustive description of the whole flagellum is necessary to describe the shape changes that accompany the transition from club to filiform antennae. One aspect of club antennae that has not been discussed here is how flagellomere numbers change and if all club antennae have a reduced number of flagellomeres. Measurements of all the flagellomeres and flagellomere numbers are need to better describe shape changes in the flagellum of small ants.

Do club antennae help small ants to maintain a certain area:volume?

My results indicated that species with club antennae (i.e. AFL>20%) did not necessarily have a greater internal volume per unit of surface area than species with filiform antennae (i.e. AFL<20%; see **Figure 4.26b**). Unfortunately, data on the area to volume ratio and relative enlargement of the AFL were only available for very few species. As a result, this question cannot be conclusively answered at this time.

Another factor of interest, which could not be adequately addressed with the data collected, was how the flagellum thickness changed with decreasing body size. There was some indication that smaller species had relatively thicker flagella (see **Figure 4.5e**). Unfortunately, flagellum width was only measured at the base of the apical flagellomere, which tended to be enlarged. As a result it is not possible to closely examine the scaling of the flagellum width. However, it is likely that there is a minimum flagellum width dictated by the minimum lumen volume and cuticle thickness.

Flagellomere shape is quite complex and variable, the models and measurements employed in this chapter can only serve as a first approximation. More accurate methods are required to determine the exact

relationship between surface area and volume in small ant species relative to their larger counterparts.

Methods of modelling the AF surface area and volume

Both of the methods used to model the AF (cylinder and profile trace models) produced outputs that scaled with much smaller exponents than expected. If the flagellomere scaled isometrically, the area would be expected to scale to the square and the volume to the cube (see **Figure 1.2**). Instead the four models predicted a much slower increase in the area to volume ratio (**Figure 4.10a-d**). The fitted lines do not resemble those expected because the apical flagellomeres of different species do not form a series of geometrically similar objects. In other words the shape of the apical flagellomere is changing with body size.

This change in flagellomere shape generates variability in the A:vol observed across species (**Figure 4.10e** and **f**). The degree of variability differs quite drastically between the two models as the way in which they approximate shape is quite different. Although the profile trace model estimates shape more realistically there is still a margin of error associated with this method. Unfortunately, this error margin cannot be quantified without direct volume and area measurements for comparison. Furthermore, without error estimations it is not possible to say exactly how realistic my estimates of A:vol scaling are. However, what is clear from these models is that changing the shape of the apical flagellomere can be used as a tactic to tune the A:vol.

More accurate area and volume estimates might be made using alternative techniques. For example, resin embedded antennae could be used to obtain serial sections, which can be used to reconstruct area and volume (e.g. see methods in: Quesada et al., 2011). Alternatively, the antennae may be cleared (e.g. with a 10% KOH solution), mounting in a liquid medium and imaged using a confocal microscope. The cuticle autofluorescence should provide sufficient contrast for this kind of imaging. It is unfortunate that it would not be possible to image antennae that have been used for SEM imaging in this way as the metal coating would render the

antennomere opaque to confocal illumination. Furthermore, even if the order of the techniques was reversed it would be difficult to use the same antenna for both studying the sensilla and measuring the area and volume as the clearing process is likely to damage the fragile sensilla. The best alternative would be to use one antenna to examine the external surface and the other to examine the internal anatomy. Although there is some right/left variation within individuals this seems like the best solution.

Why have club antennae?

What functional advantages are there to club antennae? Although it is not possible to tell at this point whether club antennae maximise volume there are other aspects of this antennal morphology to consider. For instance, if club antennae do indeed maximise volume in order to accommodate sensillar equipment they would be expected to have more sensilla. However, small species (HW<1mm) with pronounced club antennae seem to only have chemosensilla on distal flagellomeres (e.g. Ramirez-Esquivel et al., 2017). As a result club antennae are likely to lead to a decrease in the total number of chemosensilla.

A comparison between two species of similar size and disparate antennal morphology supports this hypothesis. A small worker of *Temnothorax rugatulus* (HW=0.46mm) has a club antenna and a total of 85 chemosensilla (sensilla basiconica+trichodea+curvata, over the whole antenna), while *Technomyrmex* sp.1 (HW=0.40mm) has a filiform antenna and a total of 142 chemosensilla (the shape of the whole antenna for these two species is illustrated in **Figure 4.3**). While *T. rugatulus* has sensilla in 3 out of 9 flagellomeres, *Technomyrmex* sp.1 has chemosensilla in 9 out of 10 flagellomeres. This example indicates that club antennae do not lead to an increase in the total number of chemosensilla. Although this is a single example and more data is necessary to address this question in full, it suggests an alternative hypothesis to explain the adaptive value of antennal shape. Club antennae may not be shaped by evolutionary pressure to maximise chemoperception but instead may represent an energy saving strategy by restricting sensilla to one flagellomere.

Sensory systems, from the peripheral structures to the central processing centres of the brain, are metabolically expensive to maintain and

miniature species are under particular pressure to mitigate these costs (see **Chapter 1**). Club antennae may be a form of simplified antennal array that has arisen in order to minimise metabolic cost. Concentrating chemosensilla on the apical flagellomeres may facilitate adequate provisioning of haemolymph and gas exchange to the sensilla as the antennal trachea and haemolymph vessel terminate at the tip of the antenna (Kristensen, 1984; Matus and Pass, 1999; Tonapi, 1959).

It is possible that species with club antennae may prioritise other sensory modalities such as vision (e.g. Groothuis and Smid, 2017; Stöckl et al., 2016) or that the costs associated with maintaining elaborate antennae outweigh the benefits. Miniaturisation may have led to behavioural simplification or ecological shifts that result in a decrease in the quality and/or quantity of the chemosensory input required.

Flagellomere numbers

Flagellum anatomy varied not only in the relative proportions of flagellomeres but also in the number of flagellomeres present in any given species (see **Figure 4.4**). Although flagellomeres are not true segments (developmentally) they do result in compartmentalisation of the antenna by introducing constrictions along its length. Excessive compartmentalisation may make it difficult to accommodate antennal infrastructure such as nerve tracts, trachea and haemolymph. One might think that this variability is a non-functional trait of certain genera in certain subfamilies. Flagellomere numbers are in fact used in some taxonomic keys. However, the fact that reduced flagellomere numbers was a trait exclusive to small species suggests otherwise. In this study all species with less than 10 flagellomeres had a head width smaller than 1.0mm. One problem with this idea is that not all small species have reduced numbers of flagellomeres. However, this could be due to the evolutionary trajectory of a species, rather than a lack of adaptive benefit. Reduction in flagellomere number may be a combination of adaptive pressure and evolutionary time for that pressure to manifest physiological change.

Cuticular thickness

Another subject that may interest future studies is the scaling of cuticular thickness. There are a variety of reasons why the exoskeleton may not scale isometrically with body size. If small ants do indeed possess

disproportionately thick cuticle club antennae may help to cope with a decreasing antennal lumen. One reason why secreting an extremely thin cuticle may be challenging is that the exoskeleton has fairly complex structure with a number of layers that perform different roles. There is an obvious limit to the miniaturisation of tissues, which is the number of cell layers. No tissue can be thinner than the thickness of a monolayer. In order to move past this limit, some very small insects may reduce the number of distinct layers in the dermis (p. 233, Polilov, 2016).

While isometric scaling of the cuticle may be adaptive in terms of preserving an adequate internal volume, this may be complicated by changes in the properties of the cuticle as its thickness decreases. For example, mechanical strength and permeability (for desiccation protection) are intrinsic properties of a material and are linked to the absolute thickness of the cuticle. These concerns may be addressed by small species with behavioural adaptations such as inhabiting moister niches and increasing mechanical strength (by thickening the cuticle) only around critical areas such as around articulations.

4.4.2. Miniaturisation of sensillum arrays: Functional interpretation of results

What aspects of ant chemoreception can be revealed by studying the external anatomy of the antenna? In ant compound eyes the sensory units can be quantified by observing the external anatomy of the eye and counting the facet numbers (although there are some complicating factors such as neural pooling). Unfortunately, the situation in chemoreception is not so simple. Each chemosensillum may contain a variable number of sensory neurons with a variety of chemoreceptors in their membranes. As a result, studying the antennal anatomy gives an incomplete sense of the degree of elaboration of an antennal array. Having said that, the complexity of the ant antennal array far outstrips the resources dedicated to studying it. A start must be made somewhere and the outside is as good a place as any.

Organisation

Although a dramatic reduction in body size can disrupt the signalling systems that mediate development in the embryo we find no evidence of such changes in ants. In **Chapter 1** the example of the minute scydmaenid beetle larvae (*Cephennium* and relatives) was discussed. Here the

arrangement of setae on the dorsal surface, which is usually highly regular, becomes random and setae occur in great numbers across the body surface. This is thought to be the result of a signalling breakdown in the minute species (Minelli, 2003). Another interesting example given by this author is that of the slit sense organs or slit sensilla in spiders. In most spider genera these cuticular mechanoreceptors are organised in an extremely consistent fashion (Pringle, 1955), however, in the minute *Comaroma simonii* this organisation breaks down (Kropf, 1997). Minelli (2003) compares this loss of regularity in a spider to the perfect regularity of similar organs in the historically minute arachnids, the mites (Acari).

The data from this study did not reveal any obvious differences in the organisation of antennal sensilla (see **Figure 4.13**). This may indicate that the taxa examined have an evolutionary history of small body size that is long enough to ensure an adequate adaptation of embryological signalling systems; or perhaps that miniaturisation in this clade has not reached a point at which signalling systems are disturbed at all. At this point it is impossible to tell without further research.

Size (length)

Sensillum length did not scale strongly with head width across Formicidae as a whole. There was a very weak positive linear relationship in the case of sensilla basiconica (R^2=0.20) and trichodea (R^2=0.26) while there was no relationship in the case of sensilla curvata (R^2<0.01). However, there seems to be a strong phylogenetic effect on the length of sensilla (see **Figure 4.16**, left hand column). Plotting within subfamily comparisons may identify a much stronger effect in the case of sensilla basiconica and trichodea (but not curvata). In fact, plotting a within subfamily scaling comparison of sensilla basiconica for Formicinae (n=14), the subfamily with most representatives in this study, improves the regression to R^2=0.45. The sensilla basiconica and trichodea of some subfamilies seem to scale in a similar fashion while others do not. For example Formicinae, Myrmeciinae, and Dolichoderinae seem to scale more or less continuously, i.e. with a similar exponent (recall their overlapping distributions in the PCA, **Figure 4.14**), while Ponerinae sensilla are extremely long compared to every other subfamily.

It is not clear why there should be an effect of head width on sensillum length in sensilla basiconica and trichodea but not in sensilla curvata. The difference in scaling effects may be somehow linked to differences in the volatility of target odours for these different sensillum types. While not

much is know about sensilla trichodea, sensilla curvata is associated with the perception of volatile alarm pheromones (Dumpert, 1972a), while sensilla basiconica is known to detect heavy cuticular hydrocarbons (Ozaki et al., 2005; Slone et al., 2017). Why these differences should lead to differences in peg length variability is not known at present. However, the remarkable consistency in the length of sensilla curvata across Formicidae is quite puzzling and worth further investigation. Studying differences in internal ultrastructure among chemosensilla may be enlightening.

Sensillum length was extremely variable within individuals. Although increased variability is a trait associated with miniaturisation (see **Chapter 1**), in this case there was no increased variability associated with the smallest ants (see **Figure 4.17**). It is not clear what produces this variability and what underlying changes may accompany changes in peg length. Studying internal anatomy and organisation of neuron cell bodies and dendrites may reveal whether longer sensilla may, for example, increase sensitivity by providing more sensory area. There is some indication that variability in sensillum length may be involved in the efficient packing of sensilla across the antenna. In the case of *Pheidole* ants the length of sensilla decreased with proximity to the tip of the apical flagellomere, which is the area of greatest sensillum density (Ramirez-Esquivel, 2012). Since volume is extremely limited at the tip of the antenna relative to surface area (due to the tapering tip) this may imply that shorter sensilla have fewer underlying cells and take up less volume.

Although for the most part there was no interaction between the length and the number of sensilla (data not shown) there were a few interesting exceptions. In a very few, select, species there was a weak interaction between the size and the numbers of sensilla. That is, in *Eciton hamatum* there was a dramatic shrinking of the peg length of sensilla curvata concurrent with a large increase in the numbers of this sensillum. In *Orectognathus clarki*, the opposite was true and a large increase in peg length was accompanied by a decrease in the numbers of sensilla. It is unclear whether there is any functional significance to this observation.

Numbers

The number of chemosensilla present in the smallest species was dramatically reduced (7-15%) compared to that of the larger species. What does such a large drop in chemosensillum numbers mean for small species? Decreases in the number of sensilla may indicate a decrease in sensitivity, a shrinking in odour space or both. Sensillum numbers do not equate to

chemosensory neuron numbers. However, we should still expect that the sheer drop in sensillum numbers observed between the largest and the smallest species is accompanied by an equally dramatic difference in sensory neurons. Previous studies have associated a decrease in sensillum numbers with a decrease in sensitivity, often measured as latency to detection or changes in detection thresholds (Chapman, 1982; Gill et al., 2013; Jayaweera and Barry, 2017; Spaethe et al., 2007). It stands to reason then that there must be functional costs to a decrease in the number of sensilla.

Size was not the only factor influencing sensillum numbers. Certain species with specialised ecologies stood out even within their subfamilies. These included specialised predatory species such as *Odontomachus simillimus* and *Amblyopone australis*, which had reduced numbers of sensilla basiconica and trichodea. Not all predatory ants displayed this reduction in chemosensilla though; *Myrmecia* species for example (known as active visual predators), had some of the greatest numbers of sensilla. Interestingly, sensilla curvata did not show as much variation in abundance as the other chemosensilla. The one notable exception here was *Eciton hamatum*, which exhibited an extreme increase in the number of sensilla curvata.

The number of sensilla seems to scale linearly with body size. Although there is some variation around the line of best fit, probably due to ecologically driven adaptations, there was no sign that scaling patterns changed in smaller species (see **Figure 4.16**, right hand column). This might indicate that a lower limit for sensillum numbers has not been reached in this sample. However, some previous intraspecific studies have found positive linear correlations between body size and the number of sensilla, including a study of the minute fairy wasp *Trichogramma evanescens* (Ramirez-Esquivel et al., 2014; Spaethe et al., 2007; van der Woude and Smid, 2015). Regardless of the scaling pattern, small species exhibited a dramatic reduction in total chemosensillum numbers. This must have functional consequences for their chemosensory competence. Whether this manifests itself in a reduction in sensitivity, odour space, the ability to discriminate between odours, or some combination of these it is not possible to say at this point.

Density

In this study small species were found to have the densest arrays (**Figure 4.18b-e**). In the most extreme instance (*Technomyrmex* sp.) the

chemosensilla were more than twice as dense as in larger specimens (8077 compared to 3000-4000 sensilla/mm^2). Closer packing of the sensilla may serve as a compensatory mechanism to maximise the number of sensilla. Denser packing of organs has been observed previously in some miniature species (e.g. Beutel and Haas, 1998). Unfortunately, at this time we do not know whether the absolute density of all sensilla (not just chemosensilla) is increased in small species. If the sensilla are more densely packed in general (i.e. there is no reduction in the number of mechanosensory sensilla in small species), this could have interesting consequences for small species.

Increasing the packing density of sensilla will eventually lead to a decrease in the leakiness of the sensillum array (Koehl, 2001b). In order for an animal with a dense array to maintain a similar rate of flow to that experienced by less dense arrays the speed of antennal movement will have to increase. This is because increasing the sensillum density leads to a decrease in Reynolds numbers, a measure of the ratio of inertial to viscous forces, and a thickening of the boundary layer. If compensatory behaviours such as waving antennae faster do not take place this will lead to a transition towards diffusion driven odour transport and there will be a much slower turn over in odour molecules (Koehl, 2001a).

Small animals may not need to accelerate antennal movements if they operate at a slower temporal scale or a sufficiently small spatial scale. Small animals tend to operate at smaller ranges (Kaspari and Weiser, 1999) but while some very small species (<2mm) are slow walking, many are not. Additionally, odour dispersal at very small spatial scales may in any case be dominated by diffusion due to the formation of boundary layers around surfaces. The thickness of this boundary layer will be dependent on the structure of the surface and the speed of flow overhead.

Slow walking small species may not be able to move fast and far enough to escape the effects of boundary layers. In this scenario it may be beneficial for very small species to transition from a dependence on volatile odours to a greater reliance on contact chemoreception. However, we do not find support for this hypothesis in the current dataset, except for a slightly more dramatic scaling in sensilla curvata (the smallest species has 7% of the abundance observed in the largest species) than in sensilla basiconica (12%).

Unfortunately, most research in this area has been carried out on fast moving insects such as bees and moths, which mostly locomote through flight, or in aquatic crustaceans (e.g. Koehl, 2001a; Koehl, 2001b;

Schneider et al., 1998a; Schneider et al., 1998b). Although it is interesting to speculate, physical interactions at microscales are difficult to intuit and further work is required to establish the true nature of air flow around these miniature arrays. Thought provoking work along these lines already exists and techniques have already been developed to examine these kinds of interactions such as particle image velocimetry (Beebe et al., 2002; Casas et al., 2010; Koehl, 2001a; Reiten et al., 2017). Future work investigating the effects of sensillum array density in very small insects using this kind of approach seems promising.

Exceptions, outliers, or specialists?

"allometry sweeps all interesting variability under the rug"

(Calder, 1984)

Although the purpose of this study was to identify miniaturisation specific adaptations and establish scaling trends other interesting observations were made along the way. Throughout this chapter I tried to point out interesting ecologically driven adaptations rather than "sweeping them under the rug". Indeed some interesting results in the analysis of sensilla variability came from studying ecologically unusual species rather than tiny species. For example, *Eciton hamatum* with their tiny sensilla curvata and hugely enlarged antennae stood out much more dramatically than the smallest species examined. Although it would be easy to disregard exceptional species as a bit of nuisance that interferes with general scaling patterns these special cases are precisely what makes studying antennal arrays so fascinating.

While allometry provides a baseline from which we can compare interesting novel adaptations, at the same time ecological adaptations can obscure or outweigh the influence of scaling trends in some cases. For instance, protecting the antennae can outweigh maximising sensory area or reach of the antenna. This is seen in hypogaeic species (especially in Dorylinae) and in species with specialised scrobes that allow the antennae to be folded away in case of attack (e.g. *Meranoplus*, Myrmicinae, and *Cephalotes*, Formicidae).

Some subfamilies had very distinct antennal arrays, which may

have been shaped by their specialised ecological habits. These included the Dorylinae (army ants) and Ponerinae (specialist visual predators). Although not many species were available for study (two genera for each sub-family) the specimens that were examined fell so outside the norm that it seems likely there is something special about these groups. This may be due to their specialised ecologies and their phylogenetic relationship to some of the more prevalent and diverse groups such as Myrmicinae. Interestingly, the bull ants (Myrmeciinae) considered unusual ants with many wasp-like primitive traits had antennal arrays that were quite consistent with the scaling patterns and morphology observed in most other species. Future studies could focus at the subfamily level, to minimise the effects of ecology and phylogeny. Such work could examine the impacts of factors such as antennal movements and predatory vs. generalist habits on the design of antennal arrays.

4.4.3. Miniaturisation: Traits of interest

Sensillum, cell, and genome size

The smallest ant sensilla observed in this study were smaller than the sensilla of some of the smallest known hymenoptera (Chalcidoidea, and in particular Mymaridae and Trichogrammatidae)(Polilov, 2015). The shortest sensilla in this study belonged to:

- Basiconica: *Paraparatrechina minitula* – 7.6µm
- Trichodea: *Technomyrmex* sp. – 6.4µm
- Curvata: *Eciton hamatum* (short morphotype) – 4.5µm
  Ooceraea australis (regular morphotype) – 15.4µm

By comparison the sensilla of some chalcid wasps are given in the table below (see **Table 4.5**). Unfortunately, the sensillum types in this family are a bit different so it is difficult to make direct comparisons. However, placoid sensilla are known volatile chemosensilla, like sensilla curvata, in non-formicid Hymenoptera.

Table 4.4. Sensillum length (µm) in a selection of Chalcidoidea, modified from Polilov (2016). For reference, the smallest ant species examined in this chapter had a body length of 1700µm.

	Megaphragma mymaripenne	***Trichogramma australicum***	***Trichogramma dendrolimi***	***Pteromalus puparum***	***Pteromalus cerealellae***
Body length (µm)	220	500	600	2600	2000
Chaetoid	11.72	23.16	19.69	21.4	48
Trichoid (type 1)	13.41	8.52	11.93	36	88.9
Placoid	29.64	38.83	–	39.4	112.8

The difference in body size between the smallest ant species studied here and *Megaphragma mymaripenne* was in the order of 6.8 fold (see **Figure 4.27**). Fairy wasps are the smallest described insects, as a result they are under intense pressure to miniaturise every aspect of their biology. They have very few sensilla per antenna and the length of sensilla is often comparable to the length of the antennomere (e.g. van der Woude and Smid, 2015). The fact that the smallest observed ant sensilla are smaller or comparable to fairy wasp sensilla indicates that it may not be possible for sensilla to become much smaller than the minima reported here.

Could genome size affect sensilla?

We expect genome size to affect the miniaturisation of the antennal arrays as sensilla are formed by a finite number of cells. In the introductory chapter of this thesis, I explored a wide range of considerations including the interaction between genome size and cell size, and potential knock on effects on the macro scale (e.g. organ and body size, structural complexity, etc.). Since sensilla have a finite cell number the size of their cells is likely to impact on their underlying "volume footprint" and perhaps even on the size of the sensillum peg.

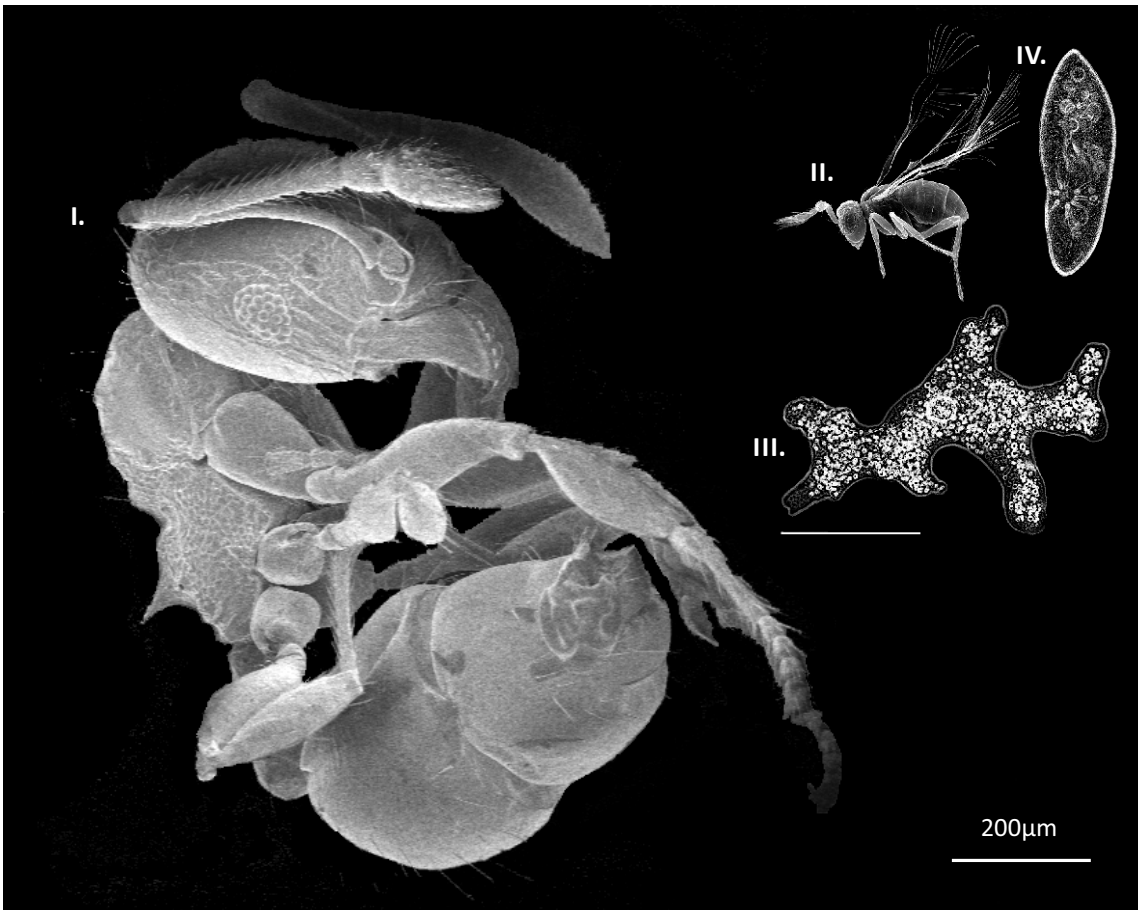

Figure 4.27. Miniaturisation in ants and fairy wasps. Size comparison of one of the smallest species in the dataset (I.) *Pheidole* sp.1 (SEM by FRE) to the fairy wasp (II.) *Megaphragma mymaripenne* and some unicellular organisms: (III.) *Amoeba proteus* and (IV.) *Paramecium caudatum* (modified from Polilov, 2015), figure to scale.

Since cell sizes have not been reviewed in this context, we must rely on the information on the genome size of ants and other hymenoptera which is available. The association between cell and genome size is due to species with extremely large genomes being unable to reduce cell size beyond a lower limit (see **Chapter 1**). So while cell size may vary irrespective of genome size in different tissue types, there is lower limit on cell size due to genome size. A small genome is a considered to be a requirement (or preadaptation) for miniaturisation which maintains tissue complexity (see **Chapter 1**)

The smallest Formicid genomes (C-value: 0.18) are comparable to Trichogrammatid genomes (C-value: 0.18-0.25) (data downloaded from: Gregory, 2001). This indicates that some ant species should be capable of a similar degree of sensillum miniaturisation as Trichogrammatidae. Given that Trichogrammatid wasps are among the smallest known insects this may indicate that the minimum peg size observed here is representative of the minimum physical limit for sensilla.

There is a range of genome sizes across ant species (see **Figure 4.28**), it is thought that some ant species have undergone a doubling or tripling of their genomes (Tsutsui et al., 2008). It may be of interest to see if differences in genome size are reflected in differences in the sensillar array. One interesting observation is that the subfamily Ponerinae has some of the largest genome sizes in Formicidae (Tsutsui et al., 2008) as well as some of the longest chemosensilla which often occurred in low numbers (see **Figure 4.16**). Unfortunately there is little overlap between species surveyed in currently available genome data and the species surveyed in this study.

The functional significance of the apical flagellomere: Concentrating sensilla at the tip

Although this chapter did not systematically quantify the change in sensilla across the entire flagellum, there is substantial evidence to indicate that in ants the number of chemosensilla dramatically decreases proximally (e.g. Dumpert, 1972b; Mysore et al., 2010; Nakanishi et al., 2009; Ramirez-Esquivel et al., 2017; Renthal et al., 2003). One potential interpretation of this organisation may be linked to the way ants use their antennae.

Ants actively antennate surfaces and probe volumes of air. Concentrating chemosensilla distally may help to probe large volumes of air in an efficient fashion. The geniculate antenna design gives the tip of the antenna the greatest range of motion. When the pedicel-scape joint is extended the tip of the antenna reaches the furthest distance from the body to probe surrounding areas but when the joint is flexed the tip of the antenna can situated to examine proximal odours (e.g. from brood or prey held at the mandibles). This means that rather than having more sensilla evenly distributed along the antenna for sampling proximal and distal cues the sensilla can be concentrated in one location and brought to the cue as needed. Additionally, being effectively at the end of a lever the apical antennomeres will also experience the greatest acceleration. This may be important to overcome boundary layer effects and refresh the 'parcels' of air that the antenna can sample.

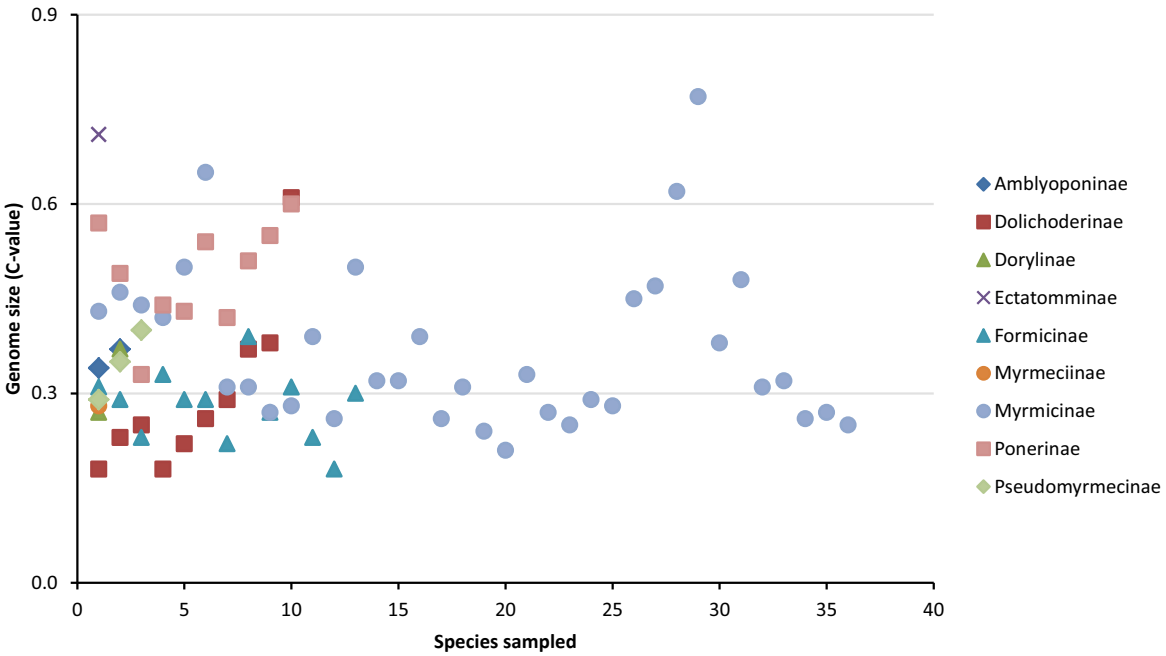

Figure 4.28. Genome size across Formicid subfamilies. Some subfamilies have been more thoroughly sampled than others. Data downloaded from: Gregory (2001), [Accessed: 31/05/17].

The relative size of air volumes able to be probed by smaller species is likely to be comparable to those in larger species (total antennal length relative to head width does not decrease with decreasing head width). However, the absolute size is much smaller. This is important because, as discussed in **Chapter 1**, airflow and odour transport does not scale in a consistent fashion. At lower Reynolds numbers the effects of boundary layers and diffusion dominate, and so, small, walking ants may need to move their antennae faster to overcome boundary layer effects.

Although the focus of this thesis is on miniaturisation, it is important not to forget the role of ecology in shaping sensory systems. Interesting examples of this principle are acute zones in compound eyes. These are shaped by the particular characteristics of visual stimuli relevant to an animal's ecology. For instance, the facet array of fiddler crabs have acute zones that are optimised to detect fast vertical movement across the horizon, ideal for detecting aerial predators (Zeil and Hemmi, 2006). A nice quote from this body of work reminds us that the design of a sensory system reflects the context in which it evolved:

> *"Studying vision in fiddler crabs reminds us that vision has a topography, that it is context-dependent and pragmatic and that there are perceptual limits to what animals can know and therefore care about."* – (Zeil and Hemmi, 2006)

The same principles must necessarily apply to the organisation of the ant antenna. Although here I attempt to interpret antennal morphology within the framework of miniaturisation, it is possible that some of the anatomical features of small antennal arrays are a reflection of ecological pressures rather than size. There is still much we do not know about how ants use their antennae (e.g. patterns of antennal movements), and what they require from their chemosensory input. As our knowledge in this area deepens it should become possible to identify how particular features of the antennal array reflect an animal's ecology and context in much the same way that it is already possible to do this with visual arrays. This should make it easier to identify miniaturisation specific adaptations.

In this study one potential example of sensory topography such as described above can be found in the exceptional organisation of the antennae of *Ooceraea australis* and *Lioponera singularis*. In these two genera putative contact chemosensilla are found almost exclusively on the ventro-medial surface of the antenna. In contrast, volatile chemosensilla are found on the dorso-lateral aspect of the antenna (see **Figure 4.19**).

This may reflect a strongly segregated chemical landscape where non-volatiles of interest are found exclusively in the mandibles or directly in front of the head while volatiles are lateral external cues. However, it is not clear why this chemosensillum segregation should occur in *Ooceraea australis* and *Lioponera singularis* but not in other ant genera. Hypogaeic habits and a lack of reliance on visual input (*O. australis* has no externally visible eyes but *L. singularis* does) may provide the propitious conditions for this kind of topography. Future work could focus on hypogaeic species to see if this pattern persists.

4.5. Conclusions and future directions

This chapter examined the effects of decreasing body size on the antennal array of chemosensilla. Species examined had head widths (body size proxy) spanning an order of magnitude from the smallest (HW=0.4mm) to the largest species (HW=3.9mm). Decreasing size was accompanied with a reduction in the numbers of chemosensilla, a shortening of the peg in two of the three types of chemosensilla examined, and an increase in density of chemosensilla. The pattern of distribution for different sensillum types across the apical flagellomere did not change with decreasing body size.

The numbers of chemosensilla scaled linearly with head width. This scaling pattern has also been observed in intraspecific comparisons within hymenoptera (Spaethe et al., 2007; van der Woude and Smid, 2015). At this point it is important to remember that the number of chemosensilla is not necessarily equivalent to the number of chemosensory neurons. The true scaling patterns of the chemosensory array may differ from what is observed here if the number of chemosensory neurons housed by each sensillum varies significantly from one species to the next.

The length of sensilla varied with head width in two of the three studied chemosensilla. Sensilla basiconica and trichodea scaled linearly with head width although scaling patterns differed for different subfamilies. Ultrastructural studies of the internal anatomy of sensilla are needed to establish whether these differences in sensillum length are accompanied by an increase in sensory area (e.g. area of the dendritic ending exposed to stimuli) or if longer sensilla are larger and can accommodate more chemosensory neurons.

Chemosensillum density increased in smaller species. This chapter examined only chemosensory sensilla, future studies may examine whether this increase in density is consistent across all sensillum types or

if absolute sensillum density is constant and increases in chemosensilla are accompanied by decreases in, say, filiform mechanoreceptors. It would be interesting to determine whether the absolute density of arrays changes with decreasing body size as this determines the 'leakiness' of an array (i.e. how air flows around the sensilla) (e.g. Koehl, 2001b). This is an important characteristic of a sensory array as it shapes, among other things, its temporal resolution properties (Schneider et al., 1998a; Schneider et al., 1998b).

Antennal morphology changed with decreasing size. Small species displayed a relative enlargement of the apical flagellomere, especially in species with a head width < 1mm. Although this was originally thought to maximise the volume available for the necessary support structures that sensilla require, my data did not provide conclusive evidence for this. A relative enlargement of the apical flagellomere length did not necessarily lead to a surface area to volume ratio resembling that of larger species. However, apical flagellomeres had complex three-dimensional shapes that could only be roughly estimated here. Future studies may be able to attribute functional consequences to the relative enlargement of the apical flagellomere through direct measurement of area and volume of the antenna (e.g. through serial semi-thin sections).

Some small species had a reduced number of flagellomeres. This may eliminate excessive compartmentalisation in extremely small antennae. Future studies may use phylogenetic analyses to establish whether this is a derived trait in species with a longer evolutionary history of miniaturisation. The reduction of flagellomere numbers could represent an instance of oligomerisation (or simplification) of the antennal anatomy in miniature species.

While there were strong general scaling patterns, differences in phylogeny and ecology gave rise to outliers. Species tended to cluster within subfamily groups and while some subfamilies seemed to scale according to similar principles others did not. Ponerinae, Amblyoponinae and Dorylinae were particularly striking examples of subfamilies with distinct scaling patterns. This is perhaps not surprising as these subfamilies contain species that specialise in somewhat unusual ecologies such as active predation and raiding (aggressive group predation). The strong phylogenetic and/or ecological signal in the data made it difficult to derive allometry curves that accurately described the scaling of the antennae for all of Formicidae. Comparing the antennal arrays within subfamilies or other lower taxonomic groupings will result in allometric curves with a stronger predictive power.

Antennae are sensory organs that furnish their bearers with information that is crucial for individual and nest level fitness. Therefore, it stands to reason that these organs would be fine-tuned to the particular sensory requirements necessary for particular ecological niches. Previous studies on other hymenopteran groups suggest that differences in sensillum size, density and distribution may be associated with ecological differences such as prey type (Polidori et al., 2012; Polidori and Nieves-Aldrey, 2014). The evolutionary trajectories of lineages and the degree of ecological diversity within a clade will determine how cohesive a group might be. My results indicate that species within the so called poneroid clade are quite distinct from species in the formicoid clade (Ward, 2007), while species within the formicoid clade are scale in a comparable manner with the exception of the dorylomorphs (e.g. *Eciton*, *Lioponera*, and *Ooceraea*).

The anatomy of the ant antennae is exquisitely nuanced and varied. Having established the main trends in chemosensillum scaling there are now pressing questions about the underlying ultrastructure and physiological properties and how these relate to external anatomy left to address. The question of how chemosensory competence (e.g. sensitivity, odour discrimination, and size of the odour space) scales with diminishing body size (and the accompanying reduction in number and size of sensilla) is an open question that can only be answered through the multidisciplinary study of this complex system.

4.6. Reference list

Andersen, A.N., 2006. A systematic review of Australian species of the myrmecine ant genus *Meranoplus* F. Smith, 1853 (Hymenoptera: Formicidae). Myrmecologische Nachrichten 8, 157-170.

Beebe, D.J., Mensing, G.A., Walker, G.M., 2002. Physics and applications of microfluidics in biology. Annual review of biomedical engineering 4, 261-286.

Berg, H.C., Purcell, E.M., 1977. Physics of chemoreception. Biophysical Journal 20, 193-219.

Beutel, R., Haas, A., 1998. Larval head morphology of *Hydroscapha natans* (Coleoptera, Myxophaga) with reference to miniaturization and the systematic position of Hydroscaphidae. Zoomorphology 118, 103-116.

Boudinot, B.E., Probst, R.S., Brandao, C.R.F., Feitosa, R.M., Ward, P.S., 2016. Out of the Neotropics: newly discovered relictual species sheds light on the biogeographical history of spider ants (*Leptomyrmex*, Dolichoderinae, Formicidae). Systematic Entomology 41, 658-671.

Brown, W.L.J., 2000. Diversity of Ants, In: Agosti, D.M., Alonso, J.D., Schultz, L.E., Ted, R. (Eds.), Ants: Standard Methods for Measuring and Monitoring Biodiversity.

Calder, W.A., 1984. Size, function, and life history. Courier Corporation, Cambridge.

Casas, J., Steinmann, T., Krijnen, G., 2010. Why do insects have such a high density of flow-sensing hairs? Insights from the hydromechanics of biomimetic MEMS sensors. Journal of The Royal Society Interface 7, 1487-1495.

Chapman, R., 1982. Chemoreception: the significance of receptor numbers. Advances in Insect Physiology 16.

Cole, A., Jones, J., 1948. A Study of the Weaver Ant, *Oecophylla smaragdina* (Fab.). American Midland Naturalist, 641-651.

d'Ettorre, P., Deisig, N., Sandoz, J.-C., 2017. Decoding ants' olfactory system sheds light on the evolution of social communication. Proceedings of the National Academy of Sciences, 201711075.

Dlusskiy, G., 1983. A new family of upper Cretaceous Hymenoptera: An "intermediate link" between the ants and the scolioids.

Dumpert, K., 1972a. Alarmstoffrezeptoren auf der Antenne von *Lasius fuliginosus* (Latr.)(Hymenoptera, Formicidae). Journal of Comparative Physiology A 76, 403-425.

Dumpert, K., 1972b. Bau und Verteilung der Sensillen auf der Antennengeißel von *Lasius fuliginosus* (Latr.)(Hymenoptera, Formicidae). Zoomorphology 73, 95-116.

Ehmer, B., Gronenberg, W., 1997. Proprioceptors and fast antennal reflexes in the ant *Odontomachus* (Formicidae, Ponerinae). Cell and Tissue Research 290, 153-165.

Esslen, J., Kaissling, K.-E., 1976. Zahl und Verteilung antennaler Sensillen bei der Honigbiene (*Apis mellifera* L.). Zoomorphologie 83, 227-251.

Gill, K.P., van Wilgenburg, E., Macmillan, D.L., Elgar, M.A., 2013. Density of antennal sensilla influences efficacy of communication in a social insect. The American naturalist 182, 834-840.

Gregory, T.R., 2001. Animal genome size database. TR Gregory.

Groothuis, J., Smid, H.M., 2017. *Nasonia* parasitic wasps escape from Haller's rule by diphasic, partially isometric brain-body size scaling and selective neuropil adaptations. Brain, Behavior and Evolution.

Hackmann, A., Delacave, H., Robinson, A., Labonte, D., Federle, W., 2015. Functional morphology and efficiency of the antenna cleaner in *Camponotus rufifemur* ants. Open Science 2, 150129.

Haldane, J.B.S., 1926. On being the right size. Harper's Monthly Magazine 152, 424-427.

Hanken, J., Wake, D.B., 1993. Miniaturization of body size: organismal consequences and evolutionary significance. Annual Review of Ecology and Systematics 24, 501-519.

Jayaweera, A., Barry, K.L., 2017. Male antenna morphology and its effect on scramble competition in false garden mantids. The Science of Nature 104, 75.

Kaspari, M., Weiser, M., 1999. The size–grain hypothesis and interspecific scaling in ants. Functional Ecology 13, 530-538.

Kelber, C., Rössler, W., Kleineidam, C.J., 2006. Multiple olfactory receptor neurons and their axonal projections in the antennal lobe of the honeybee *Apis mellifera*. Journal of Comparative Neurology 496, 395-405.

Koehl, M., 2001a. Transitions in function at low Reynolds number: hair-bearing animal appendages. Mathematical methods in the applied sciences 24, 1523-1532.

Koehl, M.A.R., 2001b. Fluid dynamics of animal appendages that capture molecules: arthropod olfactory antennae, In: Fauci, L.J., Gueron, S. (Eds.), Computational Modeling in Biological Fluid Dynamics. Springer Verlag, New York.

Kristensen, N.P., 1984. Respiratory system of the primitive moth *Micropterix calthella* (Linnaeus)(Lepidoptera: Micropterigidae). International Journal of Insect Morphology and Embryology 13, 137-156.

Kropf, C., 1997. Slit sense organs of *Comaroma simonii* Bertkau: a morphological atlas (Araneae, Anapidae), Proceedings of the 17th European Colloquium of Arachnology, Edinburgh, pp. 151-159.

Leponce, M., Delsinne, T., Laurent, Y., Cillis, J., Bachy, I., Heughebaert, A., Desmet, P., Youdjou, N., 2008. RBINS Ant eMuseum: Paraguay Collection. Royal Belgian Institute of Natural Sciences.

Matus, S., Pass, G., 1999. Antennal circulatory organ of *Apis mellifera* L.(Hymenoptera: Apidae) and other Hymenoptera: functional morphology and phylogenetic aspects. International Journal of Insect Morphology and Embryology 28, 97-109.

Minelli, A., 2003. The Development of Animal Form: Ontogeny, Morphology, and Evolution. Cambridge University Press.

Mysore, K., Shyamala, B.V., Rodrigues, V., 2010. Morphological and developmental analysis of peripheral antennal chemosensory sensilla and central olfactory glomeruli in worker castes of *Camponotus compressus* (Fabricius, 1787). Arthropod Structure & Development 39, 310-321.

Nakanishi, A., Nishino, H., Watanabe, H., Yokohari, F., Nishikawa, M., 2009. Sex-specific antennal sensory system in the ant *Camponotus japonicus*: structure and distribution of sensilla on the flagellum. Cell and Tissue Research 338, 79-97.

Ozaki, M., Wada-Katsumata, A., Fujikawa, K., Iwasaki, M., Yokohari, F., Satoji, Y., Nisimura, T., Yamaoka, R., 2005. Ant nestmate and non-nestmate discrimination by a chemosensory sensillum. Science's STKE 309, 311.

Polidori, C., García, A.J., Nieves-Aldrey, J.L., 2012. Antennal sensillar equipment in closely related predatory wasp species (Hymenoptera: Philanthinae) hunting for different prey types. Comptes rendus biologies 335, 279-291.

Polidori, C., Nieves-Aldrey, J.L., 2014. Diverse filters to sense: great variability of antennal morphology and sensillar equipment in gall-wasps (Hymenoptera: Cynipidae). PloS one 9, e101843.

Polilov, A.A., 2015. Small is beautiful: features of the smallest insects and limits to miniaturization. Annual Review of Entomology 60, 103-121.

Polilov, A.A., 2016. At the Size Limit: Effects of Miniaturization in Insects. Springer.

Pringle, J., 1955. The function of the lyriform organs of arachnids. Journal of Experimental Biology 32, 270-278.

Quesada, R., Triana, E., Vargas, G., Douglass, J.K., Seid, M.A., Niven, J.E., Eberhard, W.G., Wcislo, W.T., 2011. The allometry of CNS size and consequences of miniaturization in orb-weaving and cleptoparasitic spiders. Arthropod Structure & Development 40, 521-529.

Ramirez-Esquivel, F., 2012. From large to small, from day to night: The sensory costs of miniaturisation in ants, Evolution, Ecology and Genetics. The Australian National University, Canberra p. 46.

Ramirez-Esquivel, F., Leitner, N.E., Zeil, J., Narendra, A., 2017. The sensory arrays of the ant, *Temnothorax rugatulus*. Arthropod Structure & Development 46, 552-563.

Ramirez-Esquivel, F., Zeil, J., Narendra, A., 2014. The antennal sensory array of the nocturnal bull ant *Myrmecia pyriformis*. Arthropod Structure & Development 43, 543-558.

Reiten, I., Uslu, F.E., Fore, S., Pelgrims, R., Ringers, C., Verdugo, C.D., Hoffman, M., Lal, P., Kawakami, K., Pekkan, K., 2017. Motile-cilia-mediated flow improves sensitivity and temporal resolution of olfactory computations. Current Biology 27, 166-174.

Renthal, R., Velasquez, D., Olmos, D., Hampton, J., Wergin, W.P., 2003. Structure and distribution of antennal sensilla of the red imported fire ant. Micron 34, 405-413.

Schneider, D., 1964. Insect antennae. Annual Review of Entomology 9, 103-122.

Schneider, D., Steinbrecht, R.A., 1968. Checklist of insect olfactory sensilla, Symposia of the Zoological Society London, pp. 279-297.

Schneider, R., Lanzen, J., Moore, P., 1998a. Boundary-layer effect on chemical signal movement near the antennae of the sphinx moth, *Manduca sexta*: temporal filters for olfaction. Journal of Comparative Physiology A 182, 287-298.

Schneider, R.W., Price, B.A., Moore, P.A., 1998b. Antennal morphology as a physical filter of olfaction: temporal tuning of the antennae of the honeybee, *Apis mellifera*. Journal of Insect Physiology 44, 677-684.

Slone, J.D., Pask, G.M., Ferguson, S.T., Millar, J.G., Berger, S.L., Reinberg, D., Liebig, J., Ray, A., Zwiebel, L.J., 2017. Functional characterization of odorant receptors in the ponerine ant, *Harpegnathos saltator*. Proceedings of the National Academy of Sciences, 201704647.

Snodgrass, R.E., 1984. Anatomy of the Honey Bee. Cornell University Press.

Spaethe, J., Brockmann, A., Halbig, C., Tautz, J., 2007. Size determines antennal sensitivity and behavioral threshold to odors in bumblebee workers. Naturwissenschaften 94, 733-739.

Stöckl, A., Heinze, S., Charalabidis, A., El Jundi, B., Warrant, E., Kelber, A., 2016. Differential investment in visual and olfactory brain areas reflects behavioural choices in hawk moths. Scientific Reports 6.

Strausfeld, N.J., 2012. Atlas of an Insect Brain. Springer Science & Business Media.

Tonapi, G., 1959. A note on the respiratory system of the male of *Dorylus labiatus* Shuck, Proceedings of the Indian Academy of Sciences-Section B. Springer, pp. 87-93.

Tsutsui, N.D., Suarez, A.V., Spagna, J.C., Johnston, J.S., 2008. The evolution of genome size in ants. BMC Evolutionary Biology 8, 64.

van der Woude, E., Smid, H.M., 2015. How to escape from Haller's rule: olfactory system complexity in small and large *Trichogramma evanescens* parasitic wasps. Journal of Comparative Neurology 524, 1876-1891.

Ward, P.S., 2007. Phylogeny, classification, and species-level taxonomy of ants (Hymenoptera: Formicidae). Zootaxa 1668, 549-563.

Zeil, J., Hemmi, J.M., 2006. The visual ecology of fiddler crabs. Journal of Comparative Physiology A 192, 1-25.

4.7. Appendices

4.7.1. Appendix 1 – Species analysed for "Allometry of antennomeres"

Supplementary Table 4.1. List of species examined for "Allometry of antennomeres" section. "No." column gives number code used in PCA plot. "Image source" describes source for raw data (SEM images) for that species.

Species	DATA	Sub-family	HW	ID
Ankylomyrma coronacantha	AntWeb	Agroecomyrmecinae	1.18	1
Adetomyrma bressleri	AntWeb	Amblyoponinae	0.73	2
Amblyopone australis	Fiorella	Amblyoponinae	1.96	3
Aneuretus simoni	AntWeb	Aneuretinae	0.49	4
Apomyrma stygia	AntWeb	Apomyrminae	0.35	5
Azteca brevicornis	AntWeb	Dolichoderinae	0.84	6
Doleromyrma sp	AntWeb	Dolichoderinae	0.53	7
Dolichoderus angusticornis	AntWeb	Dolichoderinae	1.39	8
Dorymyrmex antillanus	AntWeb	Dolichoderinae	0.63	9
Forelius brasiliensis	AntWeb	Dolichoderinae	0.76	10
Iridomyrmex agilis	AntWeb	Dolichoderinae	1.28	11
Leptomyrmex cnemidatus	AntWeb	Dolichoderinae	1.26	12
Tapinoma kinburni	AntWeb	Dolichoderinae	0.41	13
Turneria arbusta	AntWeb	Dolichoderinae	0.61	14
Iridomyrmex calvus	Fiorella	Dolichoderinae	1.89	15
Technomyrmex sp.	Fiorella	Dolichoderinae	0.40	16
Azteca sp. 01	RBINS	Dolichoderinae	0.77	17
Dorymyrmex exsanguis	RBINS	Dolichoderinae	0.73	18
Gracilidris pombero	RBINS	Dolichoderinae	0.66	19
Acanthostichus brevicornis	AntWeb	Dorylinae	0.87	20
Cylindromyrmex striatus	AntWeb	Dorylinae	0.95	21
Labidus coecus	AntWeb	Dorylinae	2.31	22
Leptanilloides anae	AntWeb	Dorylinae	0.34	23
Lioponera aberrans	AntWeb	Dorylinae	0.86	24
Ooceraea australis	Fiorella	Dorylinae	0.58	25
Lioponera singularis	Fiorella	Dorylinae	0.96	26
Neivamyrmex carettei	RBINS	Dorylinae	0.41	27
Ectatomma edentatum	AntWeb	Ectatomminae	1.46	28
Gnamptogenys acuminata	AntWeb	Ectatomminae	0.99	29
Rhytidoponera haeckeli	AntWeb	Ectatomminae	1.19	30
Gnamptogenys regularis	RBINS	Ectatomminae	0.77	31

Anoplolepis tenella	AntWeb	Formicinae	0.75	32
Calomyrmex albertisi	AntWeb	Formicinae	2.32	33
Camponotus aberrans	AntWeb	Formicinae	1.80	34
Formica adamsi whymperi	AntWeb	Formicinae	1.23	35
Gigantiops detructor	AntWeb	Formicinae	1.86	36
Melophorus hirsutus	AntWeb	Formicinae	1.29	37
Tapinolepis tumidula	AntWeb	Formicinae	0.42	38
Teratomyrmex greavesi	AntWeb	Formicinae	0.80	39
Cataglyphis noda	Fiorella	Formicinae	2.37	40
Cataglyphis noda	Fiorella	Formicinae	3.07	41
Cataglyphis noda	Fiorella	Formicinae	1.42	42
Melophorus hirsutus	Fiorella	Formicinae	1.65	43
Melophorus hirsutus	Fiorella	Formicinae	1.54	44
Melophorus hirsutus	Fiorella	Formicinae	0.91	45
Notoncus ectatommoides	Fiorella	Formicinae	1.34	46
Oecophylla smaragdina	Fiorella	Formicinae	1.47	47
Paraparatrechina minitula	Fiorella	Formicinae	0.40	48
Brachymyrmex luedervaldti	RBINS	Formicinae	0.51	49
Camponotus sp. 02	RBINS	Formicinae	0.73	50
Myrmelachista sp. 01	RBINS	Formicinae	0.38	51
Paratrechina sp. 02	RBINS	Formicinae	0.52	52
Pheidole sp. 01	RBINS	Formicinae	0.51	53
Pheidole sp. 02	RBINS	Formicinae	0.59	54
Strumigenys sp. 02	RBINS	Formicinae	0.38	55
Strumigenys sp. 04	RBINS	Formicinae	0.25	56
Acanthoponera mucronata	AntWeb	Heteroponera	1.60	57
Myrmecia clarki	AntWeb	Myrmeciinae	1.81	58
Myrmecia nigriceps	AntWeb	Myrmeciinae	3.21	59
Nothomyrmecia macrops	AntWeb	Myrmeciinae	1.57	60
Myrmecia pyriformis	Fiorella	Myrmeciinae	3.83	61
Nothomyrmecia macrops	Fiorella	Myrmeciinae	1.45	62
Acanthomyrmex ferox	AntWeb	Myrmicinae	1.14	63
Acromyrmex coronatus	AntWeb	Myrmicinae	0.87	64
Aphaenogaster floridana	AntWeb	Myrmicinae	1.00	65
Atta columbica	AntWeb	Myrmicinae	4.10	66
Atta texana	AntWeb	Myrmicinae	2.12	67
Baracidris sitra	AntWeb	Myrmicinae	0.38	68
Cardiocondyla emeryi	AntWeb	Myrmicinae	0.34	69
Carebara concinna	AntWeb	Myrmicinae	0.46	70
Epelysidris brocha	AntWeb	Myrmicinae	0.50	71
Eutretramorium mocquerysi	AntWeb	Myrmicinae	1.69	72
Formicoxenus quebecencis	AntWeb	Myrmicinae	0.53	73

Harpagoxenus canadensis	AntWeb	Myrmicinae	0.89	74
Leptothorax calderoni	AntWeb	Myrmicinae	0.79	75
Liomyrmex gestroi	AntWeb	Myrmicinae	0.80	76
Meranoplus pulcher	AntWeb	Myrmicinae	0.64	77
Messor cephalotes	AntWeb	Myrmicinae	2.48	78
Microdaceton tanyspinosum	AntWeb	Myrmicinae	0.64	79
Mycetarotes parallelus	AntWeb	Myrmicinae	0.83	80
Nesomyrmex anduzei	AntWeb	Myrmicinae	0.97	81
Novomessor albisetosus	AntWeb	Myrmicinae	1.59	82
Ocymyrmex zekhem	AntWeb	Myrmicinae	1.67	83
Podomyrma basalis	AntWeb	Myrmicinae	1.38	84
Meranoplus ferrugineus	Fiorella	Myrmicinae	0.61	85
Pheidole sp.2	Fiorella	Myrmicinae	0.65	86
Acromyrmex sp. 01	RBINS	Myrmicinae	1.50	87
Cephalotes borgmeieri	RBINS	Myrmicinae	1.50	88
Crematogaster crinosa	RBINS	Myrmicinae	0.62	89
Crematogaster quadriformis	RBINS	Myrmicinae	0.82	90
Cyphomyrmex sp. 01	RBINS	Myrmicinae	0.67	91
Leptothorax sp. 01	RBINS	Myrmicinae	0.70	92
Leptothorax sp. 02	RBINS	Myrmicinae	0.67	93
Mycetophylax sp. 03	RBINS	Myrmicinae	0.50	94
Oxyepoecus rastratus	RBINS	Myrmicinae	0.47	95
Pogonomyrmex cunicularius	RBINS	Myrmicinae	1.58	96
Pogonomyrmex naegelli	RBINS	Myrmicinae	1.02	97
Rogeria sp. 02	RBINS	Myrmicinae	0.71	98
Wasmannia auropunctata	RBINS	Myrmicinae	0.53	99
Wasmannia sp. 01	RBINS	Myrmicinae	0.37	100
Paraponera clavata	AntWeb	Paraponerinae	4.83	101
Anochetus agilis	AntWeb	Ponerinae	1.99	102
Diacamma aequale	AntWeb	Ponerinae	1.89	103
Dinoponera australis	AntWeb	Ponerinae	4.75	104
Harpegnathos saltator	AntWeb	Ponerinae	2.12	105
Megaponera analis	AntWeb	Ponerinae	2.34	106
Odontoponera denticulata	AntWeb	Ponerinae	2.34	107
Harpegnathos saltator	Fiorella	Ponerinae	2.16	108
Odontomachus simillimus	Fiorella	Ponerinae	2.18	109
Odontomachus simillimus	Fiorella	Ponerinae	2.18	110
Anochetus neglectus	RBINS	Ponerinae	0.92	111
Pseudomyrmex acanthobius (duckei?)	RBINS	Pseudomyrmecinae	0.57	112
Pseudomyrmex denticollis	RBINS	Pseudomyrmecinae	1.15	113

4.7.2. Appendix 2 – Imaging times

In order to provide some guidelines for future investigators some imaging times are given in association with specimen size. This also gives some impression of the sampling effort required for small specimens relative to larger ones.

Over the course of my PhD I spent a total of 119 hours at the SEM. The maximum number of images acquired during a 3.5 hour session was about 100 images. Adjusting settings, locating and identifying specimens, saving and labelling image files and exchanging specimens all take significant amounts of time which must be accounted for when planning sessions. Additionally, once images are acquired they must be processed and analysed, another very time consuming process.

Supplementary Table 4.2. Imaging times for the apical segments of different species at a range of magnifications. Time required per specimen is a conservative estimate based on the image acquisition time alone, i.e. raster scan time for each image (approximately 40 seconds), this does not include the time taken to save and label images, navigate the specimen stub or exchange samples.

Species	Magnification	Size of area (μm^2)	Images in montage	Time (mins)
Amblyopone australis	X900	56768	9	6.0
Camponotus consobrinus **(major)**	X1.2k	46329	13	8.7
Camponotus consobrinus **(minor)**	X1.0k	41042	11	7.3
Camponotus piliventris	X1.2k	55423	14	9.3
Cataglyphis noda **(major)**	X800	54192	8	5.3
Cataglyphis noda **(median)**	X1.0k	50544	11	7.3
Cataglyphis noda **(minor)**	X1.2k	30426	9	6.0
Eciton hamatum	X700	147477	13	8.7
Harpegnathos saltator	X1.0k	83620	17	11.3
Iridomyrmex calvus	X1.2k	13703	7	4.7
Iridomyrmex purpureus	X800	34731	7	4.7
Lioponera singularis	X1.0k	46060	10	6.7
Melophorus bagoti	X1.0k	30342	8	5.3
Meranoplus ferrugineus	X1.2k	13274	6	4.0
Myrmecia croslandi	X800	45415	7	4.7
Myrmecia nigriceps	X1.0k	91991	13	8.7
Myrmecia pyriformis **(major)**	X800	114660	15	10.0
Myrmecia pyriformis **(minor)**	X1.5k	66989	29	19.3
Myrmecia tarsata	X800	93703	13	8.7
Odontomachus simillimus	X1.0k	56841	15	10.0
Oecophylla smaragdina	X1.2	40436	13	8.7

Ooceraea australis	X1.2k	40969	19	12.7
Opisthopsis pictus	X1.5k	24915	9	6.0
Orectognathus clarki	X1.0	46926	9	6.0
Paraparatrechina minitula	X1.5k	7668	5	3.3
***Pheidole* sp.1**	X1.2k	12988	7	4.7
Rhytidoponera metallica	X1.5k	43480	19	12.7
***Technomyrmex* sp.1**	X1.2k	8542	3	2.0
Temnothorax rugatulus	X1.2k	12659	6	4.0

4.7.3. Appendix 3 – Imaging and preparation artefacts

Notes on SEM interpretation: Contamination, preparation and imaging artefacts

SEM specimen preparation in this chapter was optimised for maximising throughput. In order to facilitate this, specimens were not fixed in aldehyde or osmium tetroxide but rather partially dehydrated in 70% ethanol and then air dried. In the vast majority of cases this was not problematic. However, in some cases some sensilla exhibited shrinkage or collapse. This was most common in early preparations where specimens were directly dehydrated in 100% ethanol. Gradual dehydration or critical point drying should prevent this kind of artefact. Very small specimens were also more prone to shrinkage, whether this was due to these specimens having thinner cuticle or whether the ethanol penetrated faster leading to a more sudden dehydration is not known. Signs of shrinkage were very obvious in all specimens as chemosensilla pegs are hollow and tend to either collapse at the tip or become bilaterally flattened if incorrectly dehydrated (see **Supp. Fig. 3**).

Dirt and contamination are a common problem in SEM imaging. Although I trialled various protocols for cleaning specimens (including sonication for various times and intensities, soap and saline solution) they all resulted in damage to the sensilla. Some workers resort to using newly eclosed adults for SEM imaging to avoid contamination. Unfortunately, that was not an option here. Whenever possible specimens were collected live and kept in a clean container where there was ample opportunity for self-preening. Ants have sophisticated antennal comb structures that allow them to remove particulates from their sensilla (Hackmann et al., 2015). This proved to be

the most efficient method of maximising the probability that a specimen would be as clean as possible. Many specimens were still dirty to some extent but it was rare to find a specimen that was dirty to the extent that sensilla could not be identified.

Charging is a common problem with biological specimens. Coating and imaging under low accelerating voltages help to ameliorate the effects of charging but it is difficult to completely eliminate charging on a specimen. Imaging at low accelerating voltages and at greater working distances can help to reduce charging but also reduces the resolution of the image obtained. For this reason, microscopists will toe the line to find ideal imaging conditions for a specimen. Readjustments may also be necessary when moving from one part of the specimen to the next. Identifying the effects of charging is therefore, more important than avoiding them altogether. These can include, areas of extreme brightness or banding in the image, apparent "bending" of structures and damage to the specimen (see **Supp .Fig. 3** for examples).

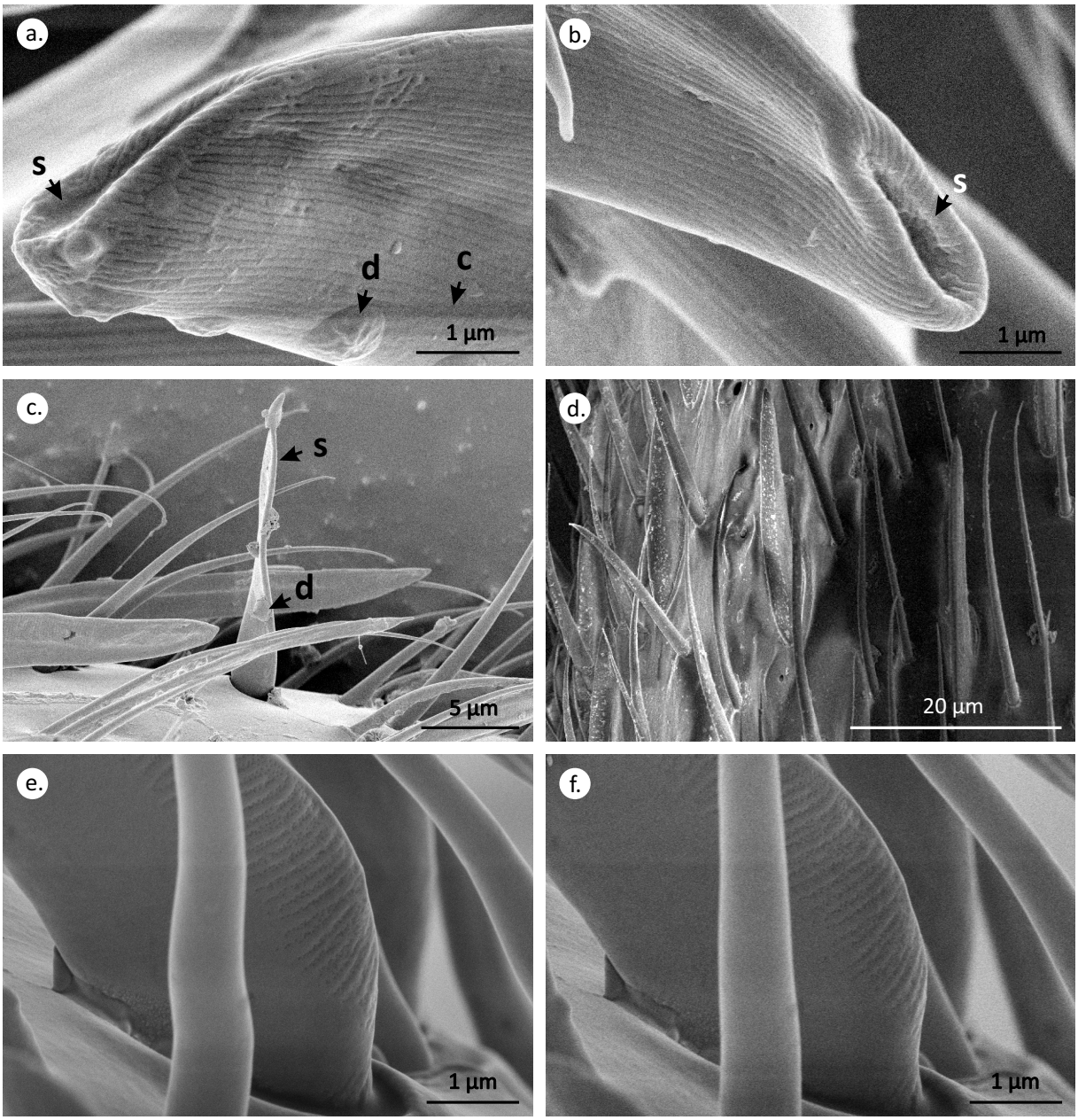

Supplementary Figure 4.3. Examples of sample preparation and imaging artefacts. (a) Collapsed tip of sensillum basiconicum due to shrinkage **s**, dirt on the sensillum **d** and some charging **c**; (b) collapse sensillum tip and sides; (c) billaterally flattened sensillum due to shrinkage; (d) charging effects (chiaroscuro like effect) in *Opisthopsis pictus* antenna; (e) charging effects "bent" sensillum (f) same location with less charging.

4.7.4. Appendix 4 – Scaling graphs

Supplementary Figure 4.4. Scaling of the head and antenna with respect to head width. Measured using images from AntWeb (www.antweb.org), RBINS database (Leponce et al., 2008) and original imagery (see **Supplementary Table 4.1** for full species list).

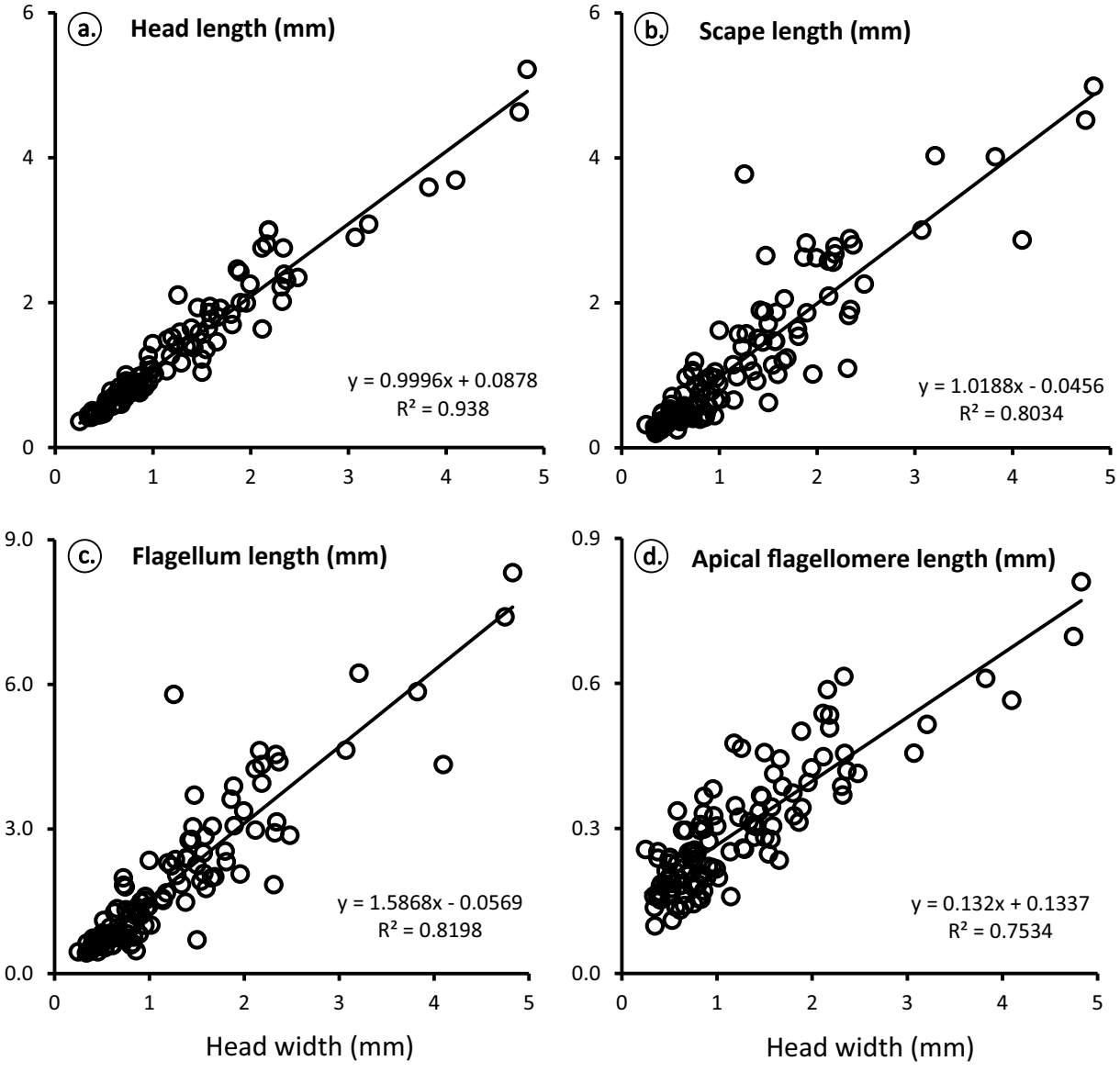

Supplementary Figure 4.4. Scaling of the head and antenna with respect to head width. Measured using images from AntWeb (www.antweb.org), RBINS database (Leponce et al., 2008) and original imagery (see Supplementary Table 1 for full species list).

4.7.5. Appendix 5 – Scaling of geometrically similar cylinders

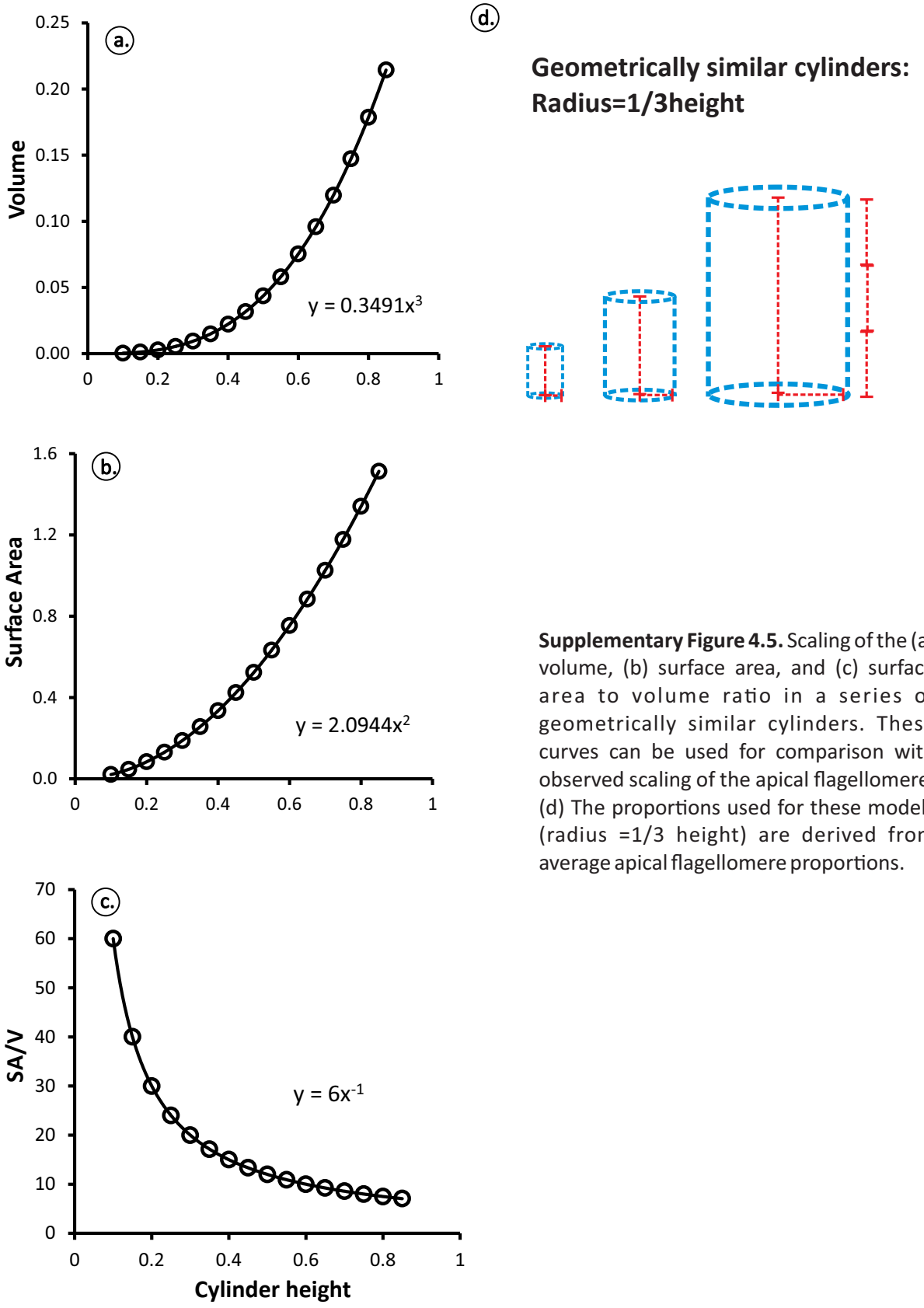

Supplementary Figure 4.5. Scaling of the (a) volume, (b) surface area, and (c) surface area to volume ratio in a series of geometrically similar cylinders. These curves can be used for comparison with observed scaling of the apical flagellomere. (d) The proportions used for these models (radius =1/3 height) are derived from average apical flagellomere proportions.

Chapter 5

Describing body size variation in ants

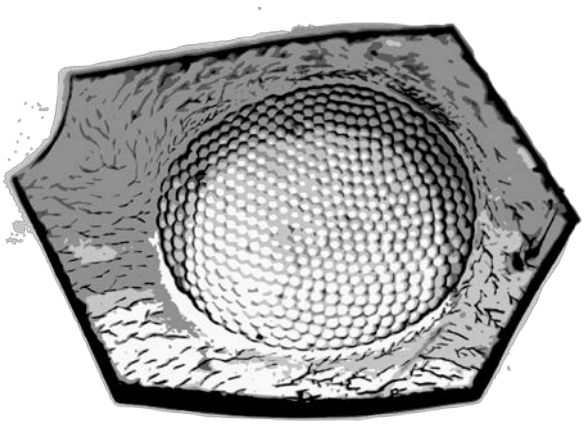

Chapter contents

This chapter represents an attempt to come to grips with body size variation in ants. Good examples of thorough descriptions of intraspecific body size variation exist throughout the ant literature. Unfortunately, these studies tend to focus on a narrow range of species and it remains unclear how much variability one might expect to find in other, less well-studied, species. This in turn makes it difficult to determine an appropriate sample size for comparative studies. In particular, the question arises whether monomorphic species are truly monomorphic. How much variation is expected from a monomorphic population?

In this chapter I cover three main topics. Firstly, I briefly review the literature and terminology used to describe ant species with different worker body size variability. Secondly, I examine the advantages and disadvantages of different methods used to measure body size. And thirdly, I attempt to quantify body size and sensory system variability in one putatively monomorphic ant species, *Iridomyrmex purpureus*.

5.1. Introduction

In previous chapters we identified significant variability in the size of ant workers and in the elaboration of their sensory systems. This was not unexpected in the highly polymorphic *Myrmecia pyriformis* workers, but was perhaps surprising in the purportedly monomorphic ant *Temnothorax rugatulus*. Reading through the ant literature, one can get the misleading impression that the lines between monomorphism and polymorphism are stark. That is, one gets the impression that the differences between species where all workers are of equal body size and those where they vary significantly is self-evident and simple. Using terminology such as monomorphic and polymorphic is convenient but by describing populations in such absolute terms subtle yet important differences in populations can be overlooked.

5.1.1. How much variation is there?

Some of the more commonly studied genera in Formicidae are polymorphic (e.g. *Atta*, *Solenopsis*, *Camponotus*, *Formica* (Fraser et al., 2000; Gouws et al., 2011; Tschinkel et al., 2003; Wilson, 1953)). It is likely that as a result of this trend we have more adequate tools to describe polymorphism than we do to describe monomorphism. Indeed, "polymorphic" is an umbrella term to describe a number of different, well-described conditions. Polymorphism can mean that there are distinct, non-overlapping, size castes (such as in many leaf cutter ants) or it can refer to a continuous variation in body size.

There are two main ways in which these two different types of anatomical polymorphism have been examined. Firstly, the frequency of different body sizes can be plotted to obtain a population frequency histogram. Theoretically, species with distinct castes will exhibit bi- or polymodal distributions, while species with continuous body size variation will have unimodal distributions (e.g. **Figure 5.1a**)(pp.307-314 Hölldobler and Wilson, 1990; Wilson, 1953). However, in many cases the largest caste performs specialised tasks and is metabolically expensive to produce (e.g. Porter and Tschinkel, 1986; Wetterer, 1999). As a result there can be very few individuals in this size category, making it difficult to capture size categories using frequency histograms (see **Figure 5.1c**). Additionally, the age and size of the colony can significantly alter the worker size distribution, generally skewing towards more small workers in younger colonies (e.g. Tschinkel, 1988; Wetterer, 1999).

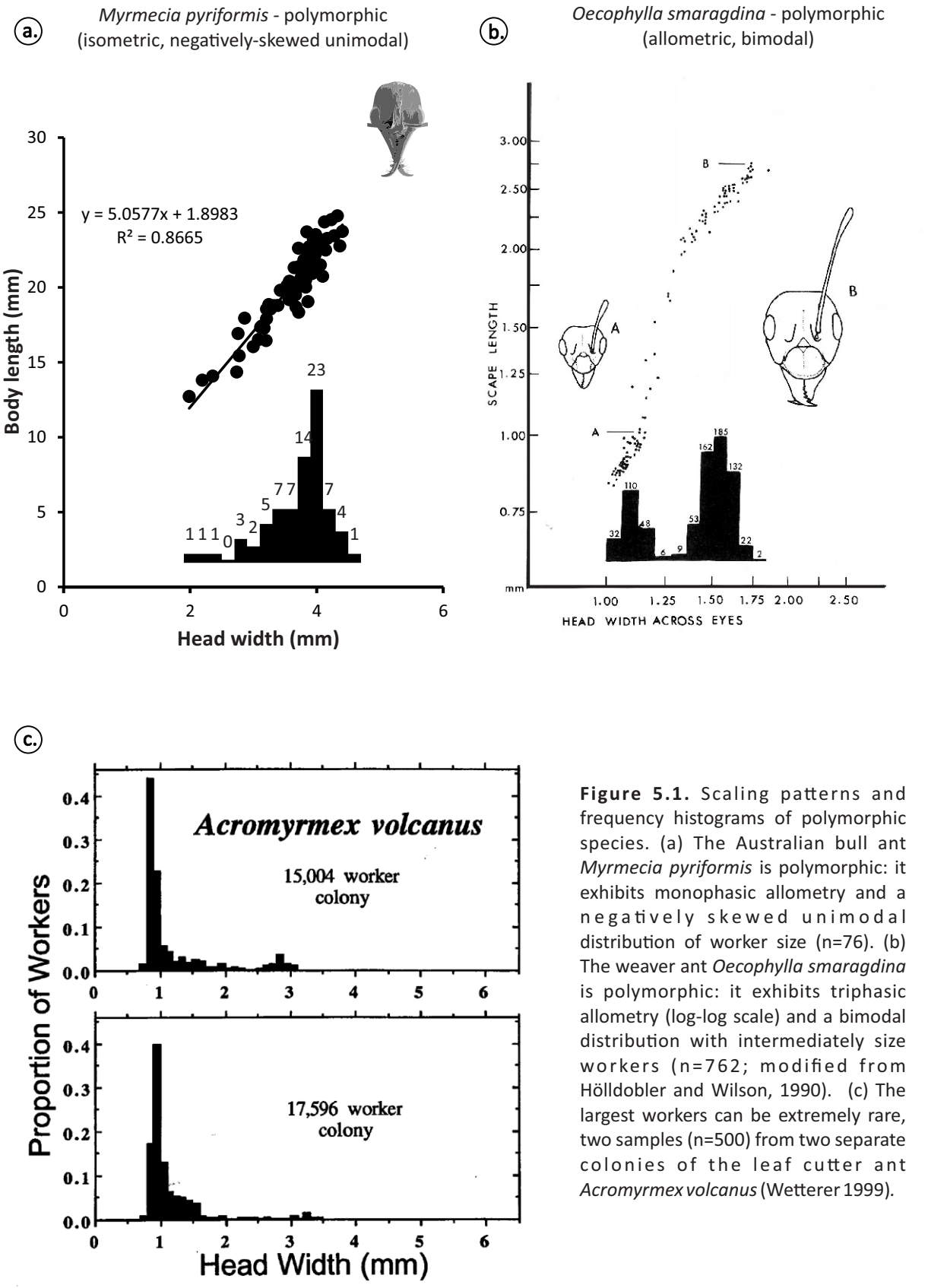

Figure 5.1. Scaling patterns and frequency histograms of polymorphic species. (a) The Australian bull ant *Myrmecia pyriformis* is polymorphic: it exhibits monophasic allometry and a negatively skewed unimodal distribution of worker size (n=76). (b) The weaver ant *Oecophylla smaragdina* is polymorphic: it exhibits triphasic allometry (log-log scale) and a bimodal distribution with intermediately size workers (n=762; modified from Hölldobler and Wilson, 1990). (c) The largest workers can be extremely rare, two samples (n=500) from two separate colonies of the leaf cutter ant *Acromyrmex volcanus* (Wetterer 1999).

A different way of examining worker size is to examine the allometry of different morphs. This is generally done by plotting two linear measures of size against one another; for example body length against head width (Tschinkel, 1988), head width against scape length (e.g. Fraser et al., 2000; Wilson, 1953) or head length vs femur length (e.g. Kaspari and Weiser, 1999). In species with distinct castes, increasing body size is often accompanied by allometric rather isometric scaling of the head. This is probably because the largest caste is often specialised in activities such as leaf cutting (e.g. *Atta*), seed milling (e.g. *Pheidole*) or nest guarding (e.g. *Cephalotes*). These activities require excessively large heads either to accommodate additional mandibular musculature or to block the nest entrance (see **Figure 5.2**). Examining individual workers using this approach permits a more detailed description of the kind of polymorphism present. If the scaling of all workers can be described using the same allometric exponent, then the species can be said to exhibit monophasic allometry. This is the kind of polymorphism observed in *M. pyriformis*, the species examined in **Chapter 2** (see **Figure 2.1a**). If there is a scaling discontinuity and different castes scale under different allometric exponents then species may exhibit diphasic or triphasic allometry. This is the case with *Oecophylla smaragdina* (see **Figure 5.1b**).

Despite these different ways of describing castes and polymorphism, it is rare to find distinct, non-overlapping size castes. Often it is more relevant to consider size in conjunction with behavioural specialisations and this is how minor and major castes may be assigned in some cases. In many instances it may not be possible to clearly categorise all workers due to the presence of intermediate body sizes which do not clearly belong to one size category or another. These kinds of subtleties make rigid categorisation difficult, but at least there are frameworks to describe different kinds of polymorphism. When it comes to monomorphic species the problem can be more difficult. There is no standard percentage variability around the mean that delineates the boundary between "normal" variability and polymorphism.

The vast majority of ant species are presumed to be monomorphic (Hölldobler and Wilson, 1990; Tschinkel et al., 2003; Wilson, 1953). But what does monomorphism mean? How much variation and what patterns of variation are expected to be exhibited by worker populations of monomorphic species? Hölldobler and Wilson define monomorphism in their landmark monograph as follows:

> *"The workers of the normal mature colony display isometry (with a log-log curve slope of approximately 1.0) and very limited size*

> *variability. A plot of their size-frequency distribution is symmetrical and has only a single mode. In other words the properties of variation are not basically different from those in a typical random collection for non-social insects. The worker castes of most ant genera and species are monomorphic. Also, within the majority of genera and higher taxonomic groups monomorphism is evidently the primitive state."* – (p.310 Hölldobler and Wilson, 1990)

Although this seems like a very thorough and clear definition in theory, there are a few difficulties with the way the term is applied in practice. Firstly, there is no discrete difference between monomorphic and polymorphic, instead there is a continuous variation in variability ranging from absolute monomorphism, through various kinds of polymorphism, to complete dimorphism (Wilson, 1953). This makes it unclear how much size variability is permitted when labelling species as monomorphic. Secondly, generating allometry curves and size frequency distributions is labour intensive, requiring large sample sizes, and therefore are not available for every studied species. As a shortcut, species are sometimes assumed to be monomorphic if size variation or distinct castes are not visually obvious (e.g. *Temnothorax rugatulus*, see **Chapter 3**). Unfortunately, this can lead to body size variability being sometimes overlooked. Lastly, in Hölldobler and Wilson's (1990) definition, the size distributions of monomorphic species are compared to those of populations of non-social insects. However, such populations are not necessarily normally distributed. Gouws et al. (2011) examined the frequency distributions of species from different insect orders and found that although many were normally distributed, it was not uncommon to find skewed distributions (particularly positively skewed).

Differences in body size are difficult to quantify because size is not the simple measure we might think it is. Changes in size are very often accompanied by changes in shape. Shape changes are difficult to capture as they may affect different body parts differently through the differential allocation of resources to different imaginal discs during development (Stern and Emlen, 1999; Wilson, 1953). In ants, worker size variability is shaped by a host of factors including genetic variability, number of queens present, colony age and nutrition, seasonal effects, and developmental conditions during larval development (Goodisman and Ross, 1996; Porter, 1988; Porter and Tschinkel, 1986; Rissing, 1987; Schwander et al., 2005; Tschinkel, 1998). The complex interactions among these influential factors are difficult to unravel, but this should not dispel our interest in body size variability.

Why is size variation important?

The size distributions of colonies can have a significant impact on the success of the colony (e.g. Billick and Carter, 2007; Tschinkel, 1988; Yang et al., 2004). Differences in size can have wide ranging effects on a variety of factors from locomotion and the way an animal moves through its environment (Espadaler and Gómez, 2001; Kaspari and Weiser, 1999), to how species interact with plant species (Chamberlain and Holland, 2009), to neurobiological characteristics such as brain size (Chittka and Niven, 2009). Size differences, even relatively small ones (Groothuis and Smid, 2017; Ramirez-Esquivel et al., 2017; van der Woude and Smid, 2015), can lead to variability of the sensory systems of individuals (Kelber et al., 2010; Perl and Niven, 2016b; Ramirez-Esquivel et al., 2014; Spaethe et al., 2007; Spaethe and Chittka, 2003). This kind of variability is particularly interesting as it has the potential to generate intranidal differences in sensory thresholds and behaviours, which can potentially underlie task allocation and social organisation (Charbonneau and Dornhaus, 2015).

5.1.2. How do we measure size?

An additional challenge for the study of body size in ants is how to measure body size. Should weight or linear measurements be used? Should wet or dry specimens be used? What linear measurement is most representative of body size? There are many methods of measuring size, all with their advantages and disadvantages, and it can be difficult to determine what the best way of describing size is for a particular study.

Weight measurements

Weight may be measured in dry or wet specimens. This is advantageous in that a specimen's weight can be quickly and easily measured. However, as a measurement of size neither wet-weight nor dry-weight are particularly reliable as insect weight can vary significantly without changes to the size of body parts (Tschinkel et al., 2003). Ants in particular do not moult so changes in nutrition are not reflected by changes in the size of the exoskeleton. The gaster may become distended after a large meal but the size of its cuticular plates (sclerites) will not change (only the soft integument will reversibly expand). Ants can store large quantities of liquid food in the crop (an extreme example of this is the specialised replete caste found in some species, although these workers do not forage or leave the nest), which make up a significant portion of their total

weight. As a rough estimate, foraging studies on honeybees show that foragers habitually carry 30-40% of their body mass in nectar (Feuerbacher et al., 2003). As a result wet weight can be significantly biased by satiety. A worker that has recently ingested liquid (e.g. honeydew) will be heavier than a worker that has not fed (Skinner, 1980). This can be counteracted to some extent by drying specimens. However, dry weight can be biased by the nutritional state of the worker, the amount of energy stored in the body as fat, and the solid component of liquid food (sugar crystals)(MacKay, 1985; Skinner, 1980). Consequently, weight measurements, although convenient, are not an ideal measure of ant size.

Figure 5.2. Major castes with enlarged heads specialised in (a) leaf cutting *Atta colombica*, (b) seed milling *Pheidole* sp., and (c) nest defence *Cephalotes rohweri*, minor worker (d) included for comparison. All photographs by Ajay Narendra.

Linear measurements

Linear measurements tend to be favoured in the ant literature. This may partly be due to their applicability to museum specimens, which are generally pinned and therefore not suited to weighing. Instead, preserved specimens may be photographed at various angles (generally using a dissecting microscope or, increasingly, a multi-focus imaging setup) and measured digitally using software such as ImageJ 1.51i (Rusband, National Institutes of Health, USA). Provided the specimens are correctly mounted and appropriate equipment is used, linear measurements can be very accurate and repeatable (see **Figure 5.3** for examples of common linear measures).

The most obvious linear size measurement is body length. However, this can be hard to measure in preserved specimens where abdominal segments may shrink during drying or the whole specimen may curl. Additionally, measuring body length may not always be the most practical option. For example, in the case of this thesis, having a body part that can be used as a proxy for whole body size can save a lot of time and effort. As long as the body part is small enough it can be mounted together with the antennae and the two can be examined together using the same technique. This not only saves time but, keeps the antenna sample physically associated with a measure of body size. This is important as it is difficult to label specimens on SEM stubs, especially in a way that they can be identified both inside and outside the SEM column (the stubs are very small and regular ink is generally not visible under EM illumination).

There are a few different linear measurements in common use that may be used as a proxy for body size. However, it is not clear how accurately they reflect the size of the specimen or if the measured body part scales isometrically across a variety of species. This is particularly important for intraspecific comparative studies. Here I examine the relationship between body length and the following proxies: head width, head length, Webber's length, hind femur length, scape length (see **Figure 5.3**). At this point measuring body weight, may seem like a simpler solution. However, there are problems associated with this method as well. Here, I trial the use of dry specimen weight as a measure of size, in the relatively large species *Iridomyrmex purpureus*.

1. Whole ant anatomy

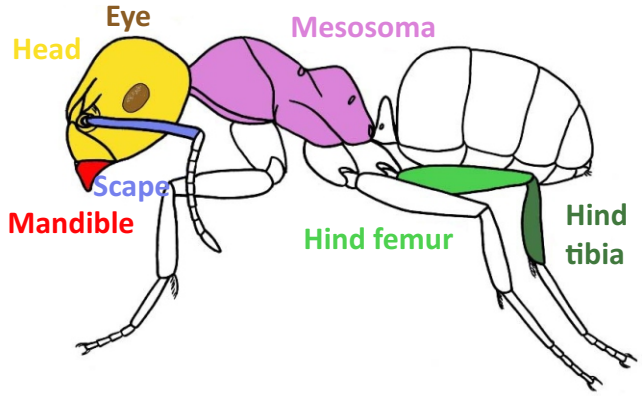

2. Head width measures: head width across the eyes (a-b) are preferred

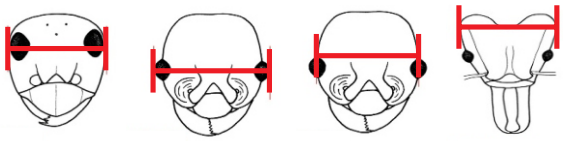

a) across eyes **b)** across eyes / maximum **c)** above eyes **d)** maximum

3. (a) Head length (red line) and (b) clypeus length (blue line)

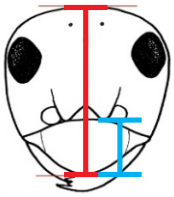

Head length is the maximum longitudinal length from the most anterior part of the clypeus to the posterior cephalic margin, in full face view

4. Mandible length

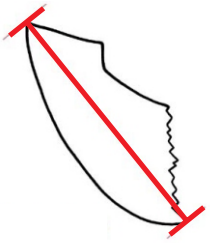

5. Hind femur length

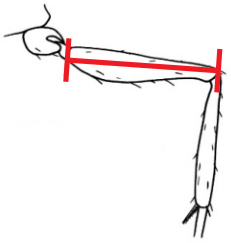

6. Scape length

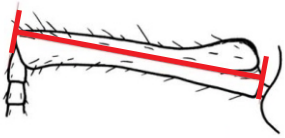

7. Weber's length

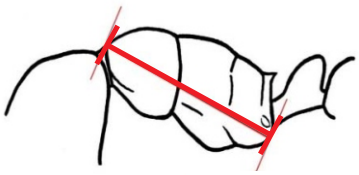

8. Pronotum width

9. Inter-ocular distance

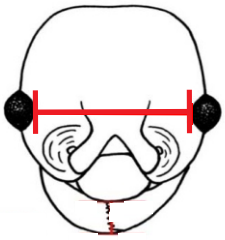

10. Eye width

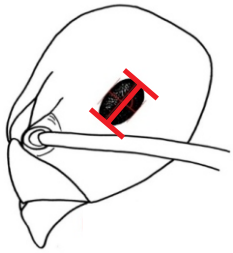

11. Whole body length

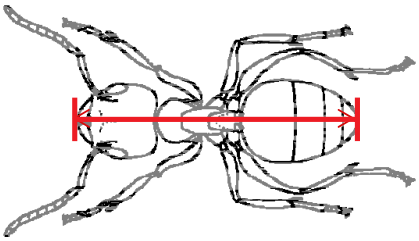

Measured from tip of mandibles to tip of gaster, with the ant in an extended position.

Figure 5.3. Some common linear measurements modified from measurement guidelines for GLAD database (Parr et al., in review).

Instrument accuracy

Compared to similar studies in vertebrates, ant studies face the additional challenge of measuring very small specimens. Beside the difficulty in manipulating specimens, this size limitation imposes a much harsher constraint on the accuracy of the instruments used to measure specimens. Where ordinary rulers, callipers or balances may suffice for large animals, devices with smaller error margins must be used to measure ants. Light and EM microscopy may be used to take linear measurements and precision microbalances may be used to weigh specimens. It is important to take into account the size of the error margin relative to the quantity being measured.

5.1.3. How much do sensory systems vary?

We know from a number of comparative studies that the elaboration of sensory systems varies with body size among workers within a colony (e.g. Kelber et al., 2010; Perl and Niven, 2016a; Ramirez-Esquivel et al., 2017; Ramirez-Esquivel et al., 2014; Spaethe et al., 2007; Spaethe and Chittka, 2003). Furthermore, there is evidence that these differences have functional consequences for the sensory competence of workers, which in turn has impacts on behaviour (Kelber et al., 2010; Spaethe et al., 2007; Spaethe and Chittka, 2003). In most cases, changes in sensory system elaboration has been studied in species with relatively large body size variation among workers (e.g. leaf-cutter ants, wood ants, bumble bees and bull ants). Unfortunately, there is very little known about the degree of variation present in monomorphic or less markedly polymorphic species. This is of interest for two reasons:

1. Sensory system descriptions for a species are often based on a limited sample of individuals. It would be interesting to know how much variation might be expected to exist in the sensory organs of monomorphic species. This would help to select suitable sample sizes, when appropriate, or to at least highlight the possibility of variability. Different sensory systems in different monomorphic species may vary to different degrees so no absolute value may be placed on variability. However the answer to the basic question of whether sensory systems in monomorphic species vary at all is not clear.
2. Given the potential role of sensory system elaboration on task allocation and self-organisation in social insects (Charbonneau and Dornhaus, 2015) it would be interesting to consider how much

variation might be found in sensory systems of monomorphic species and most importantly how this variability might translate into functional differences in sensory competence.

Here I use a very simple measure of sensory system elaboration, facet numbers, to record the degree of variability in a single monomorphic species of ant, *Iridomyrmex purpureus*. Needless to say this is not intended to be a thorough investigation of this question, but a small contribution towards highlighting that there are in fact differences among so called monomorphic workers.

5.2. Methods

5.2.1. Cross-species comparison of body size proxies

A large dataset of ant morphometric measurements was downloaded from the GLAD database (Parr et al., in review). This database included a number of different measurements, for the purpose of this study six measurements were selected: head width, head length, hind femur length, scape length, Weber's length, and body length. Details on the measuring protocols downloaded from the database are included in **Figure 5.3** (additional instructions for contributors are included in **Appendix 5.1**). These data were used to generate least-square linear regressions in Microsoft Excel (Microsoft 2010).

5.2.2. Within species body size variability: *I. purpureus*

Study species

The Australian meat ant, *Iridomyrmex purpureus*, was selected for this study. This species is easy to collect in large numbers as it is an extremely common, dominant species, which builds large, populous and conspicuous pebble mounds (Greenaway, 1981; Greenslade, 1976). Worker size variability is not apparent upon visual inspection and previous samples of workers found limited variability in the head width of workers (**Chapter 4**, Ramirez-Esquivel, 2012).

Extranidal workers were collected from around the nest mound at three separate locations in Canberra, Australia in March of 2016. The Australian National University field station (35°16'51.5"S, 149°06'43.9"E), the Australian War Memorial (ANZAC parade, 35°17'01.6"S, 149°08'44.2"E), and the Mount Majura nature reserve (35°14'47.3"S, 149°10'21.5"E) which borders residential suburbs (see **Figure 5.4**). Approximately 100 workers were collected from each colony directly into 70% ethanol.

Body-size measurements

Weight

Ants of each colony were spread out in large petri dishes where they were individually screened for missing appendages, incomplete specimens were discarded. Specimens were then dried at 50°C (DSK Electron microscope oven TD-700) for a minimum of eight days. After drying, ants were weighed with a Mettler – Toledo XP205 balance with an accuracy of ±0.015mg (Mettler – Toledo Ltd, Greifensee, Switzerland). To ensure complete drying, a subset of specimens were weighed every few days until two consistent (±0.2 mg) readings were obtained. All specimens from all nests were weighed (n=300, 3 nests), given an individual identifier and stored in labelled Eppendorf tubes.

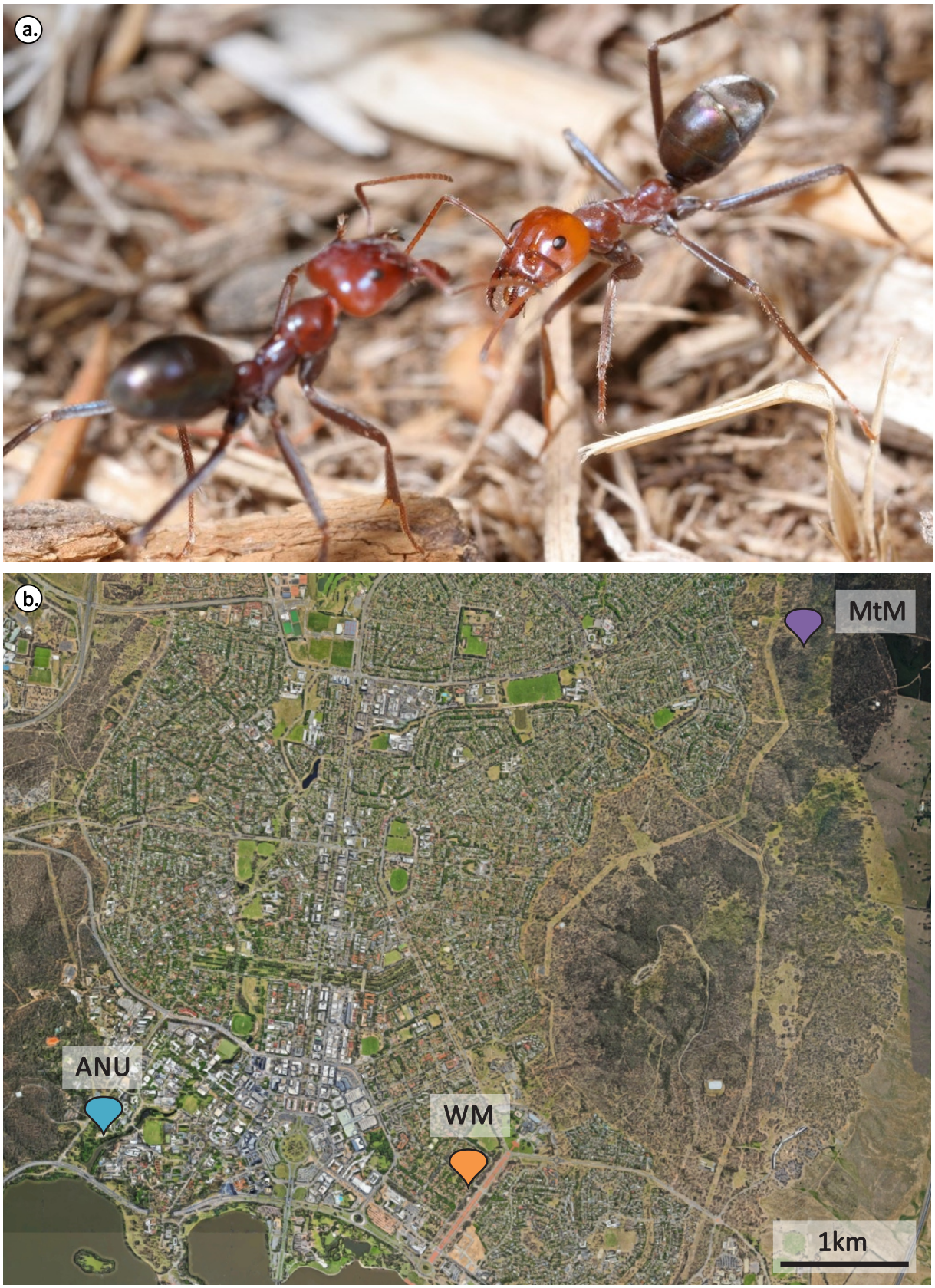

Figure 5.4. Study species and collection sites. (a) Two *Iridomyrmex purpureus* workers antennate each other (photographed in Canberra by Ajay Narendra). (b) Ants were collected from three locations: the Australian National University field station (ANU), the Australian War Memorial (WM), and from the Mount Majura (MtM) nature reserve bordering the suburb of Hackett (satellite imagery from Google Maps).

Head width and femur length

The head (all specimens) and right pro-leg (Mt Majura specimens only) were removed and mounted on labelled glass slides using dental wax. Slides were then photographed under a dissecting microscope (Olympus SZX9, Nikon DS-Fi1). Head width (n=300, 3 nests) and femur length (n=100, 1 nest) measurements were taken from digital images using ImageJ 1.45s (Rusband, National Institutes of Health, USA). Head width was measured immediately above the eyes, and femur length and head length were measured as per **Figure 5.3**.

Facet counts

After body size measurements were taken the compound eyes were imaged using one of two different techniques outlined below. All images were post-processed in the same manner. Facets were counted using the "Multi-point" tool in ImageJ 1.51i (Rusband, National Institutes of Health, USA).

Nail polish replicas

Nail polish replicas of the compound eye were mounted on glass slides and photographed (for full methods see **Chapter 7** and Ribi et al., 1989) using a Leica compound microscope (DM2500). In cases where replicas were not perfectly flat, Z-stacking was used to obtain fully focussed images. Focus stacking was done using Zerene Stacker (Version 1.04, Zerene Systems, LLC).

SEM

Specimens were mounted on aluminium stubs using carbon tape and sputter coated with gold (for full methods see **Chapter 2** or **Chapter 7**).

5.3. Results and Discussion

5.3.1. How do we measure size? – Linear measurements in a cross-species comparison of body size proxies (GLAD data)

The sub-set of data that I used contained 86 genera, sometimes with multiple species and specimens per genus, sometimes a single species, rarely a single specimen. In total there were 2,229 specimens, not all specimens had data for all the relevant traits so subsets of this sample were used for some of the regressions. Samples sizes are stated on a case by case basis on the figures.

Commonly used proxies for body size were plotted against body length (**Figure 5.5** and **Figure 5.6**). Weber's length was the most highly correlated with body length (R^2=0.88). However, most other proxies were also highly correlated with body length: head length (R^2=0.85), pronotum width (R^2=0.85), head width (R^2=0.82). Any of these proxies predict body length adequately.

The only proxy that had a markedly worse predictive power was hind femur length (R^2=0.76). Small species were reasonably well described by femur length but species with a body length greater than about 6.0mm were not. This was reflected in a marked increase in the absolute value of residuals (residual = observed value – value predicted by the correlation curve) with increasing body length (data not shown).

The body lengths of medium sized specimens were the most poorly predicted by the proxies. Specimens that had a body length of approximately 5-12mm had the highest and lowest residuals observed (data not shown). Within this range, *Camponotus*, *Acromyrmex* and *Formica* were the genera most commonly over or under estimated by the different proxies. All of these genera have workers with very variable body size (Perl and Niven, 2016a; Wetterer, 1999; Wheeler, 1991). This leads me to conclude that proxies struggle to predict body size across Formicidae when highly polymorphic species are included in data sets (lower level groupings such as tribes or genera may not encounter this problem). Polymorphic species generate body size variability through allometric growth (Wilson, 1953) and this interferes with the predictive power of proxies. If highly polymorphic species must be included in a comparative study, selecting specimens that are not of extreme size (not the smallest or

the very largest) might avoid complications. These kinds of specimens are more likely to scale in a similar fashion to specimens of less variable species than workers that belong to highly specialised castes (e.g. large soldiers). A similar approach has been taken by previous studies, excluding major workers from analyses in dimorphic species (Espadaler and Gómez, 2001; Kaspari and Weiser, 1999). Closer analysis of polymorphic species in this dataset may reveal a better way to treat these species in the context of comparative studies.

The regressions plotted in this chapter assessed proxies for large scale comparative studies across Formicidae. Comparisons within lower taxonomic groupings such as subfamilies, tribes or genera may find that some proxies are more accurate than others within specific taxonomic groupings (for example see: Tschinkel et al., 2003).

5.3.2. Body size and facet number variation: *I. purpureus*

Weight

Weight and head width measurements were collected for approximately 100 specimens from each colony examined. Weight was more closely correlated to head width in some colonies than in others (see **Figure 5.7**). I found no correlation in the ANU sample (R^2=0.01) and only a weak correlation in the WM sample (R^2=0.21) but there was a moderate correlation in the MtM sample (R^2=0.50). Pooling all observations resulted in an extremely weak correlation (R^2=0.11). Worker weight is therefore not a reliable measure of worker size.

The difference in worker weight variability was somewhat surprising. The ANU sample had by far the largest residuals with some workers weighing more than twice their expected weight (as predicted by the line of best fit). This may be due to differences in collection times. Specimens collected at the start of, say, the morning foraging bout, might be more uniform in weight than specimens collected later in the foraging bout which may be laden or unladen. Unfortunately, collection times for the different samples were not recorded.

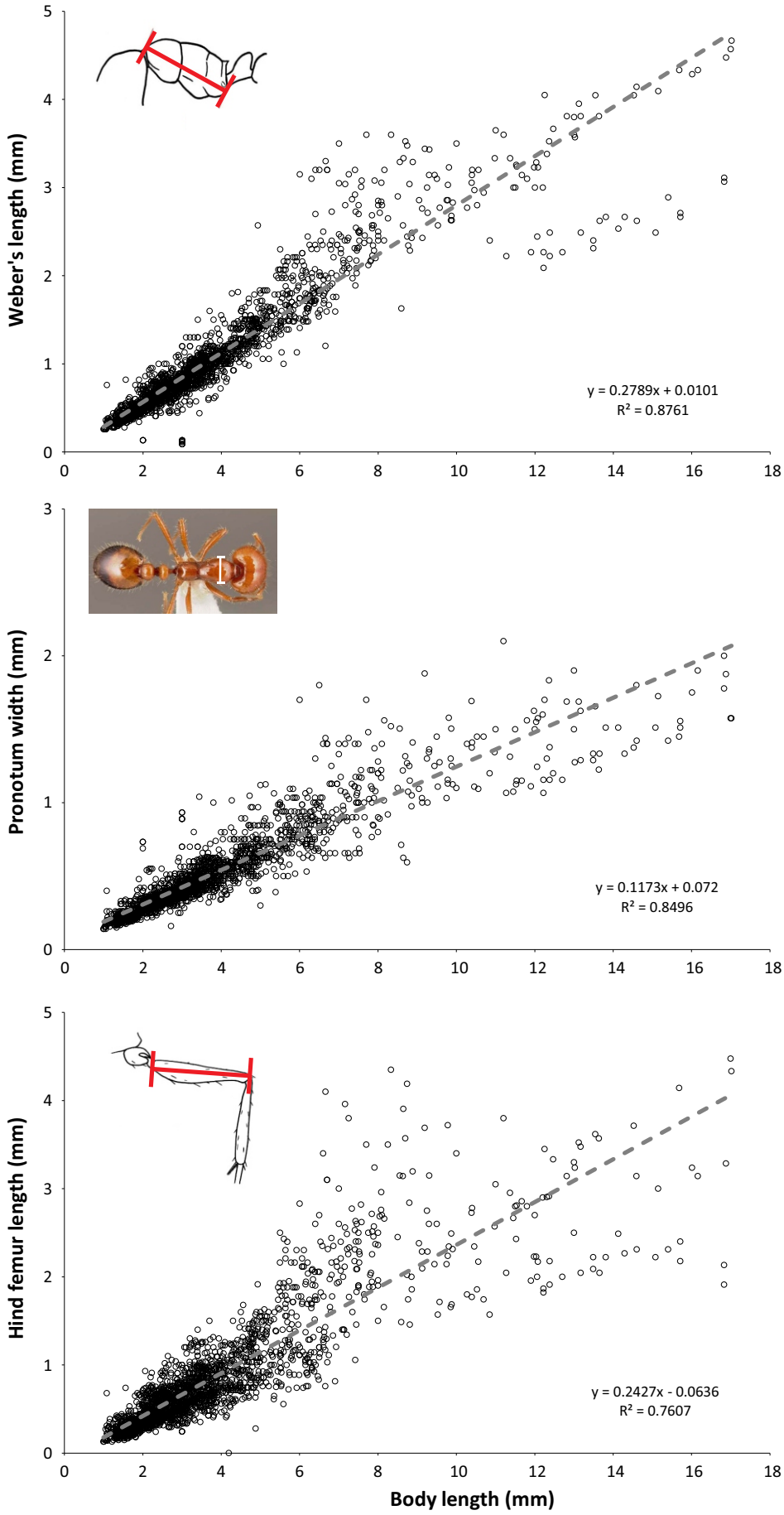

Figure 5.5. Linear regressions of different commonly used body size proxies including Weber's length (diagonal mesosoma length), pronotum width and hind femur length. Data from GLAD database (Parr et al., in review).

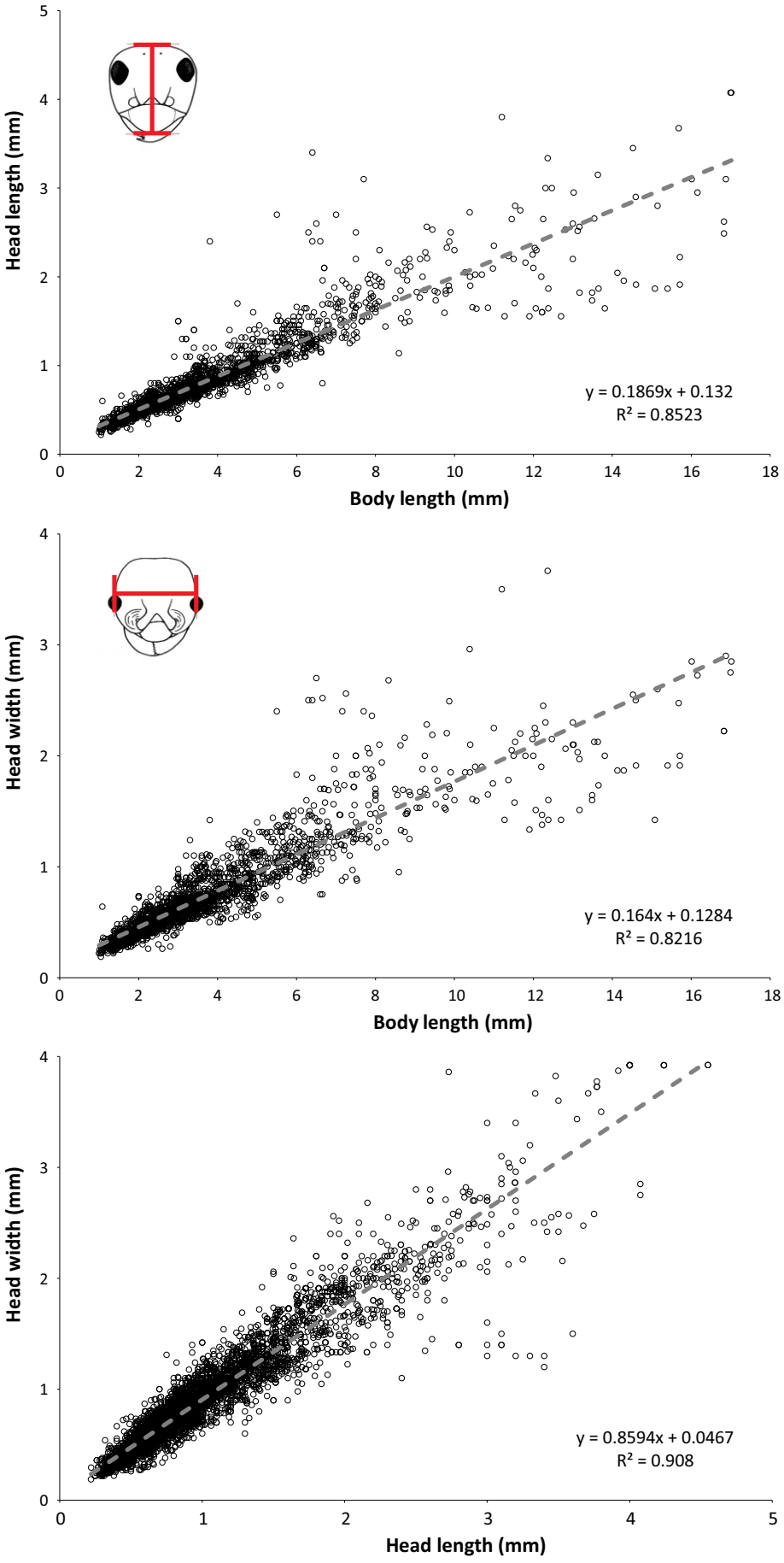

Figure 5.6. Linear regressions of different commonly used body size proxies: head length and head width. Data from GLAD database (Parr et al., in review).

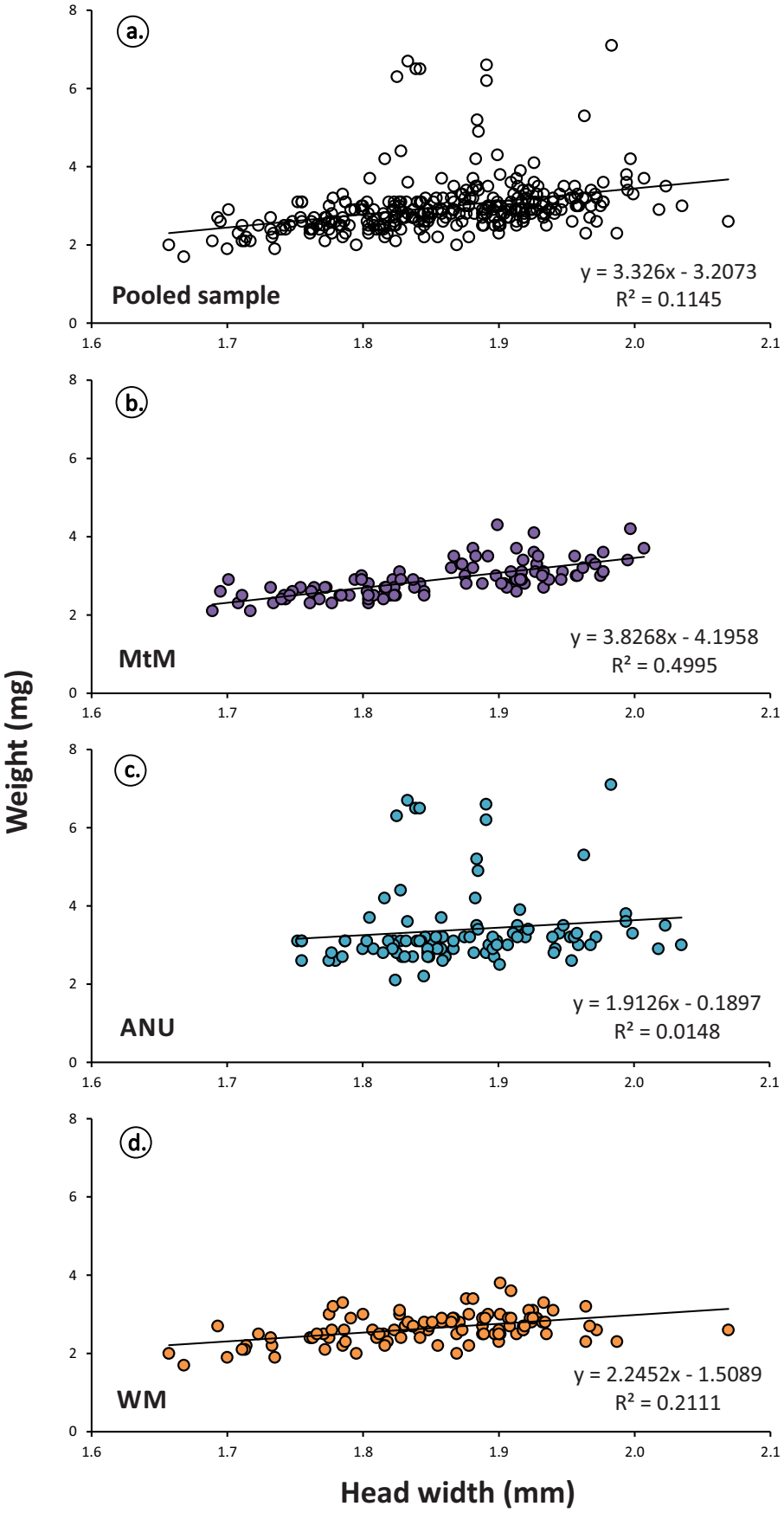

Figure 5.7. Scaling of worker weight with head width for: (a) pooled sample, and for individual colonies (b) Mount Majura (MtM), (c) Australian National University (ANU), (d) War Memorial (WM).

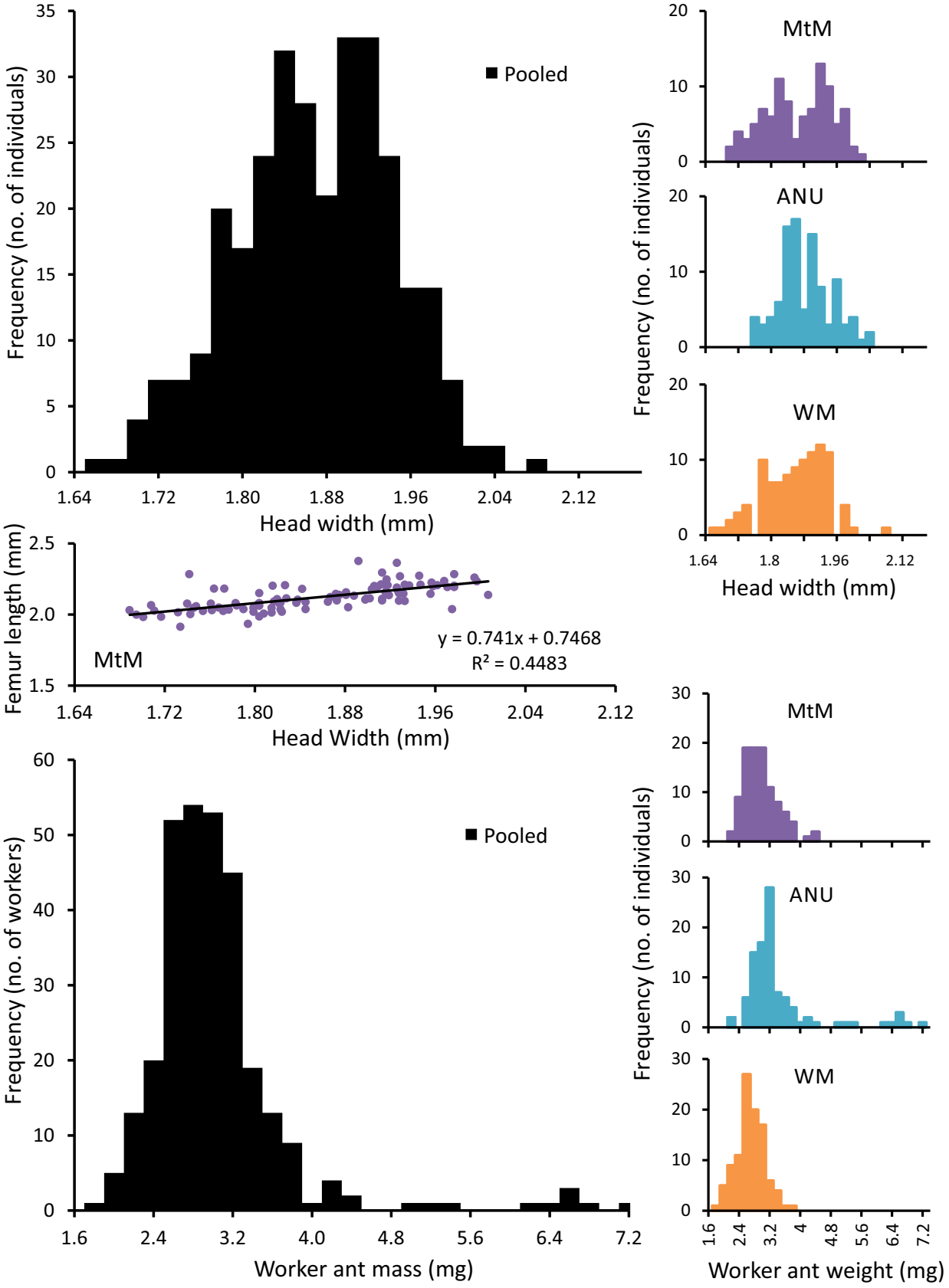

Figure 5.8. *Iridomyrmex purpureus* worker head width (top) and weight (bottom) distribution of the three studied colonies. Pooled data distributions are given in black, individual colony distributions are given in colour on the right. Femur length scaling with head width is additionally measured in the MtM sample (scatter plot).

Head width

Worker body size was measured by proxy using head width (**Figure 5.8**). Pooling size data from the three sampled colonies (n= 301) returned an average head width of 1.86mm ±0.08 (standard deviation). The minimum observed head width was 1.66mm while the maximum was 2.07mm, both of these extremes represented about a 10% increase or decrease relative to the average (i.e. about 20% variability around the mean). This seems like a fairly small degree of variability, but in order to investigate whether there was any evidence of caste differentiation the scaling of two linear body size measurements was studied for signs of allometry. Femur length was measured in workers of the MtM sample as an additional linear measure of size. Plotting femur length against head width revealed a linear relationship (n=99, R^2=0.45, **Figure 5.8**). This suggests that workers scale in an isometric fashion.

Frequency histograms of head width at the different sites looked very distinct. The WM site showed a gradual increase in the number of workers as head width increase with a sharp drop in frequency at HW=1.96mm. Workers at MtM seem to be bimodally distributed with peaks at HW=1.82 and 1.92mm. Lastly, ANU seems to have a normal distribution which appears almost perfectly symmetrical. The pooled distribution still retains a central minimum (at HW=1.88mm), which implies bimodality. It is not possible to say from these data whether a bigger sample may eliminate this minimum or not. Frequency histograms of weight exhibited completely different distributions to head width. Pooled weight was very narrowly distributed (87% of the data fell within 1 standard deviation of the average, as opposed to 69% in head width) with a long positive tail, which is mainly driven by heavy workers in the ANU sample. This demonstrates that choosing an appropriate measure of size is vitally important. Different measures will result in different distributions.

Differences among nests

At this stage, differences in frequency distributions among nests cannot be explained. One possibility is that they may be generated by differences in genetic diversity in the different colonies. *I. purpureus* colonies may be founded by a single queen or multiple, unrelated queens (Carew et al., 1997; Hölldobler and Carlin, 1985). As a result the genetic variability of different colonies could be quite

disparate.

Colony age and resource availability is also known to affect worker size distributions in other species (Porter and Tschinkel, 1986; Tschinkel, 1988). Young colonies and resource limited colonies are known to produce smaller workers and a smaller range of worker body sizes (Porter and Tschinkel, 1986; Tschinkel, 1988). Lastly, as discussed previously, the presence or absence of very heavy workers (>4.0mg) in different colonies may be driven by differences in collection times. Workers collected later during a foraging bout are more likely to be heavier.

In conclusion, although the different nests sampled seem to differ quite significantly in their frequency distributions, the moderate degree of body size variation (approx.. 20%) in conjunction with the lack of allometric scaling suggests that this species is monomorphic or weakly polymorphic.

5.3.3. How much do sensory systems vary?

Facet numbers in *I. purpureus* varied from 442 to 555 and scaled weakly with head width (see **Figure 5.9**). The strength of the correlation between head width and facet number varied among the different nests with the ANU having an extremely weak correlation (R^2=0.12, n=46), while MtM and WM had moderate correlations (MtM: R^2=0.45, n=42; WM: R^2=0.36, n=30). Pooled data exhibited a weak association between head width and facet numbers (**Figure 5.9b**). The slope and intersect of the regression lines also varied among colonies (see **Figure 5.9a**). This is consistent with a previous study on the polymorphic species *Formica rufa* (Perl and Niven, 2016a). These results indicate that monomorphic species are subject to similar types of intraspecific variation as compared to those observed in polymorphic species.

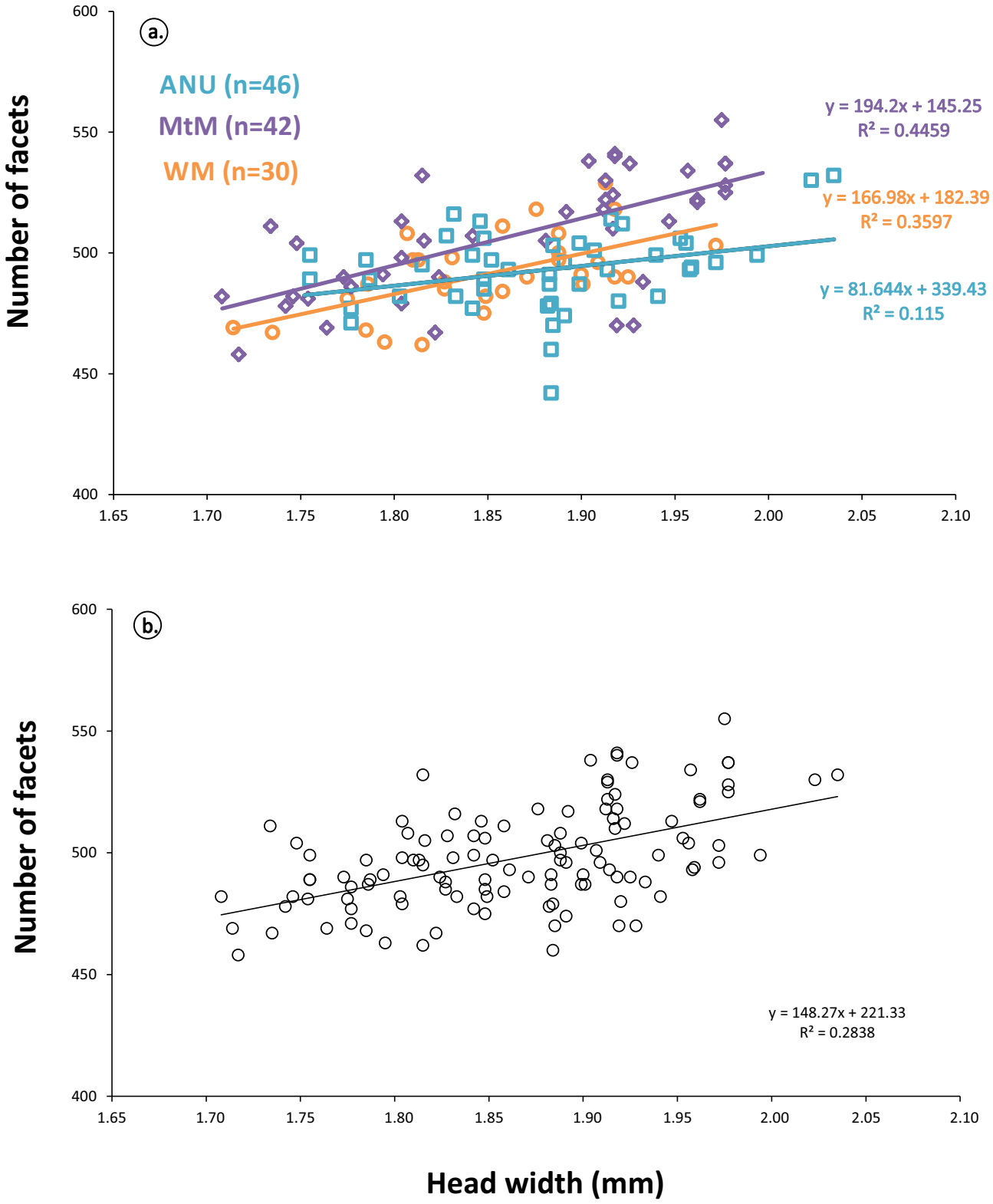

Figure 5.9. Scaling of facet numbers with head width in three separate colonies (a) and in the pooled sample (b). Data include facet counts from both SEM images and nail polish replicas.

Facet counting techniques

Two different techniques were used to count facets in this chapter: cornea replica and SEM imaging. Cornea replicas can be used to take additional measurements such as facet and eye areas although they are much more time consuming to prepare. SEM imaging permitted much faster data acquisition, but because of perspective foreshortening it is not possible to take additional measurements using these images. Ideally other aspects of facet array variability, such as interommatidial angles and facet diameters, should be quantified using method such as described by Douglass and Wehling (2016). This kind of data would allow us to make more meaningful statements about the functional implications of facet array variability.

I. purpureus is known to use visual cues to navigate (Card et al., 2016). A difference in over 100 facets, representing a 25% increase, from the smallest to the largest worker seems like a sizeable difference in facet numbers. Such a difference may give rise to variation in the visual resolution of workers but further data are necessary to say whether this is the case or not. However, the exact functional implications of differences in visual resolution can only be ascertained through behavioural studies.

Although it is not possible to give a functional interpretation of these results at this time, comparing this dataset with facet numbers in other species helps to put these results into perspective. For this purpose I collected facet numbers from the literature and from my own work (see **Figure 5.10**, sources listed in **Appendix 5.1**). This results in a large spread of facet numbers, as species with different ecologies have vastly differing visual requirements (see **Figure 5.11** for examples of differences in compound eye investment across ant species), for example genera of predatory ants with solitary foragers such as *Myrmecia, Harpegnathos* and *Gigantiops* have high visual acuity (see **Figure 5.10a**).

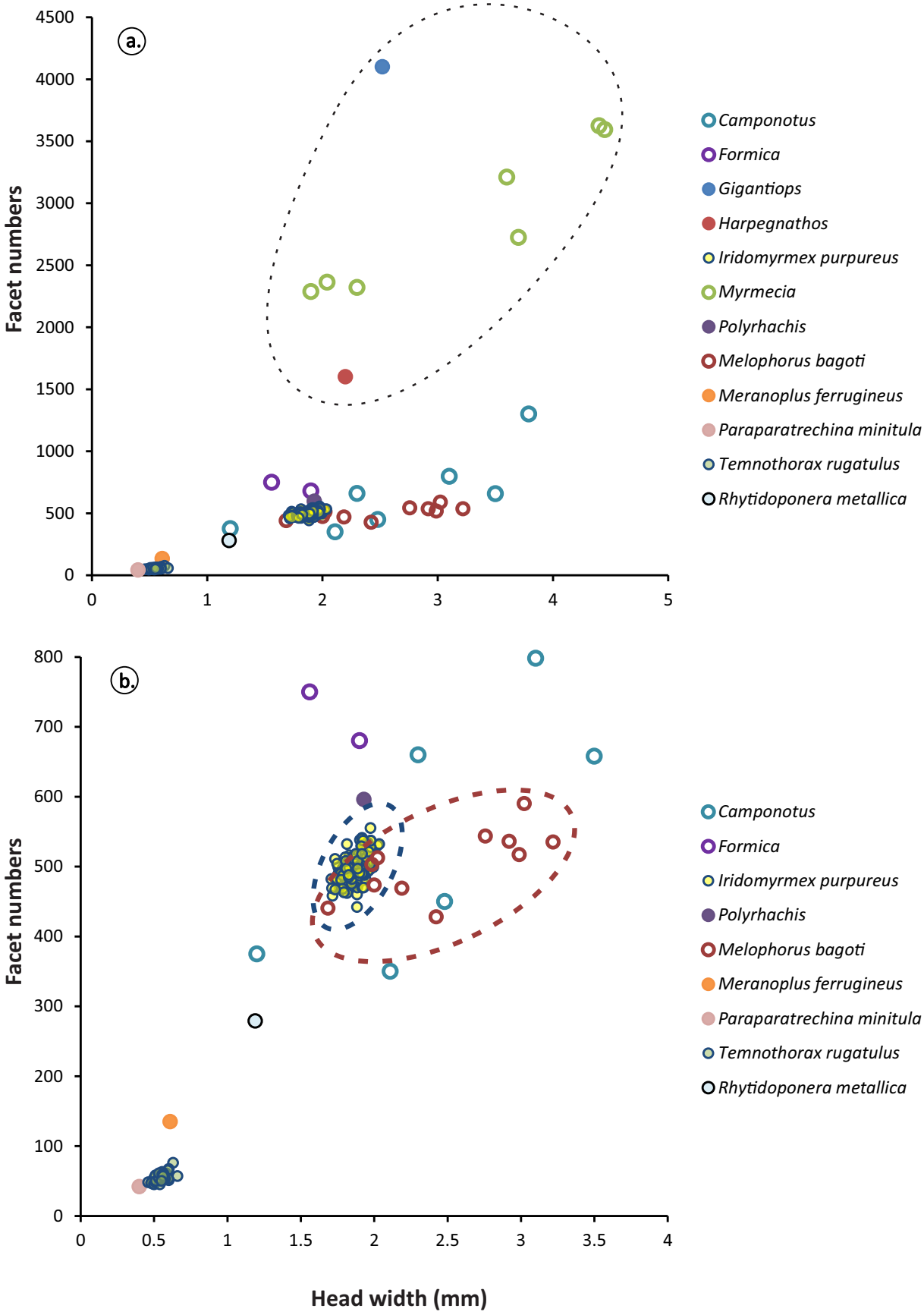

Figure 5.10. Facet numbers across ant species. Where more than one species is included per genus only the genus name is given (for full list of species and data sources see Appendix 1). (a) All collated data, species with high visual acuity are circled in black. (b) Species with fewer than 1000 facets; *Melophorus bagoti* specimens are circled in red, *Iridomyrmex purpureus* specimens circled in blue.

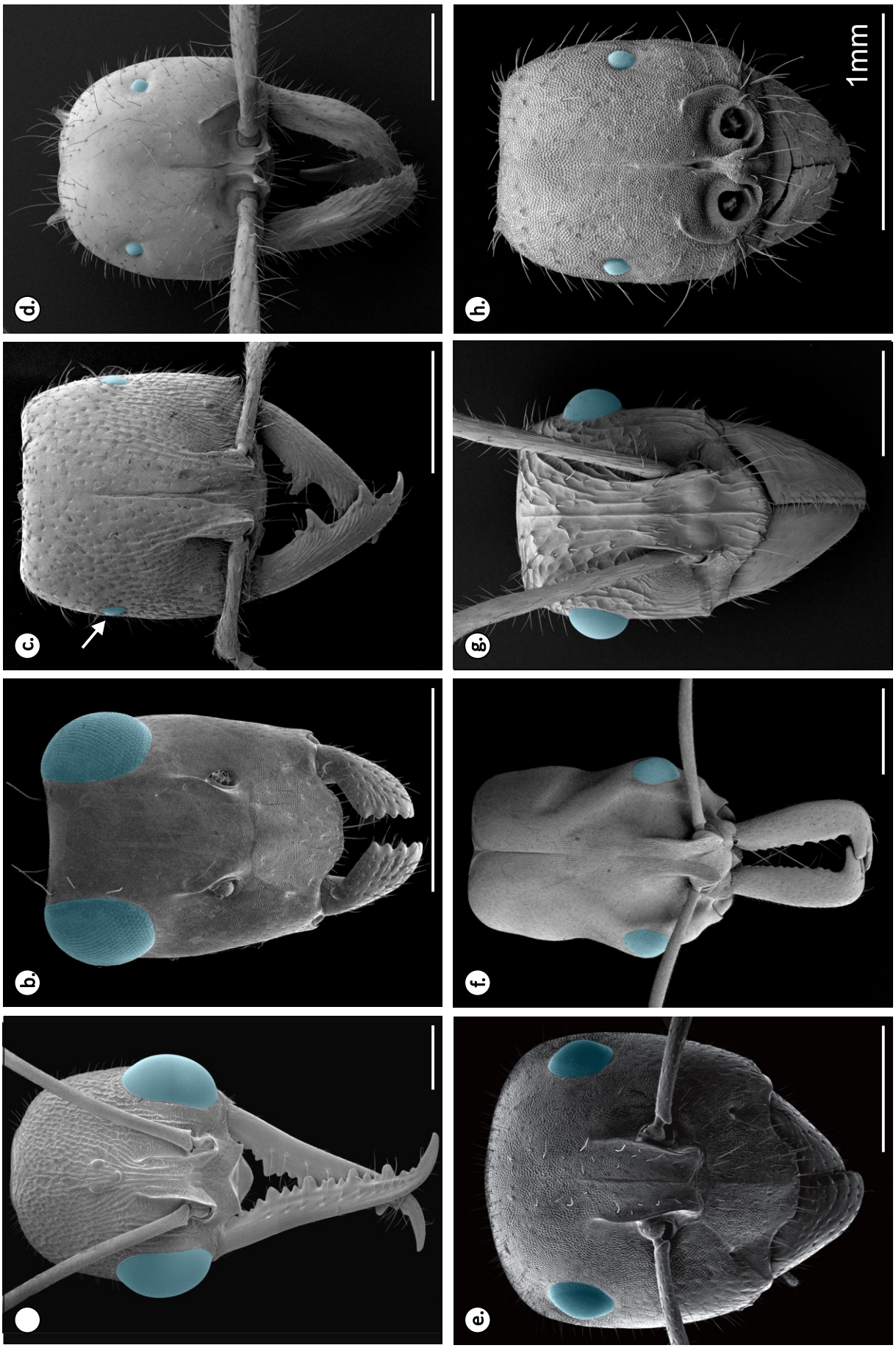

Figure 5.11. Compound eye diversity in ants. (a) *Myrmecia nigriceps*; (b) *Opisthopsis pictus*; (c) *Amblyopone australis*; (d) *Eciton hamatum* (major); (e) *Camponotus piliventris*; (f) *Odontomachus simillimus*; (g) *Ectatomma tuberculatum*; (h) *Eciton hamatum* (minor). All scale bars = 1mm.

To make a more meaningful comparison, let us concentrate on ants with fewer than a 1000 facets (see **Figure 5.10b**). *Melophorus bagoti* is a good candidate for comparing facet number variability as this species is active in bright conditions like *I. purpureus* (Greenaway, 1981; Schwarz et al., 2011). Furthermore, *M. bagoti* is of a similar size to *I. purpureus* but polymorphic (Schwarz et al., 2011), which permits an interesting comparison of facet number variability. Workers of *M. bagoti* in this sample had head widths varying from 1.7mm to 3.2mm, which is approximately 4.7 times more variability in head width than I observed in *I. purpureus* (1.7 to 2.0mm). However, the facet numbers of both species had a very similar range of variability:

- *I. purpureus*: 555 – 442 = 113
- *M. bagoti*: 590 – 428 = 162

This demonstrates that, not only the patterns, but also the degree of variability in facet numbers can be comparable in monomorphic (or weakly polymorphic species) and markedly polymorphic species.

5.4. Conclusions

Size is not the simple measure we generally think it is. Allometry, nutritional state, and variability in developmental conditions all contribute to creating variation in shape, corpulence, and the size of different body parts. Measuring size and describing population variability is a non-trivial exercise and we should be aware of the complexities underlying our classification systems (monomorphic, polymorphic, etc.). It is incorrect to assume that worker ants are uniform because superficially we cannot see differences. It remains a challenge to assess how this variability translates into differences in agility, speed, sensory thresholds and consequently into different task specialisations.

5.5. References

Billick, I., Carter, C., 2007. Testing the importance of the distribution of worker sizes to colony performance in the ant species *Formica obscuripes* Forel. Insectes Sociaux 54, 113-117.

Card, A., McDermott, C., Narendra, A., 2016. Multiple orientation cues in an Australian trunk-trail-forming ant, *Iridomyrmex purpureus*. Australian Journal of Zoology 64, 227-232.

Carew, M., Tay, W., Crozier, R., 1997. Polygyny via unrelated queens indicated by mitochondrial DNA variation in the Australian meat ant *Iridomyrmex purpureus*. Insectes Sociaux 44, 7-14.

Chamberlain, S., Holland, J., 2009. Body size predicts degree in ant–plant mutualistic networks. Functional Ecology 23, 196-202.

Charbonneau, D., Dornhaus, A., 2015. When doing nothing is something. How task allocation strategies compromise between flexibility, efficiency, and inactive agents. Journal of Bioeconomics 17, 217-242.

Chittka, L., Niven, J., 2009. Are bigger brains better? Current Biology 19, R995-R1008.

Douglass, J.K., Wehling, M.F., 2016. Rapid mapping of compound eye visual sampling parameters with FACETS, a highly automated wide-field goniometer. Journal of Comparative Physiology A 202, 839-851.

Espadaler, X., Gómez, C., 2001. Formicine ants comply with the size-grain hypothesis. Functional Ecology 15, 136-138.

Feuerbacher, E., Fewell, J.H., Roberts, S.P., Smith, E.F., Harrison, J.F., 2003. Effects of load type (pollen or nectar) and load mass on hovering metabolic rate and mechanical power output in the honey bee *Apis mellifera*. Journal of Experimental Biology 206, 1855-1865.

Fraser, V.S., Kaufmann, B., Oldroyd, B.P., Crozier, R.H., 2000. Genetic influence on caste in the ant *Camponotus consobrinus*. Behavioral Ecology and Sociobiology 47, 188-194.

Goodisman, M.A.D., Ross, K.G., 1996. Relationship of queen number and worker size in polygyne colonies of the fire ant *Solenopsis invicta*. Insectes Sociaux 43, 303-307.

Gouws, E.J., Gaston, K.J., Chown, S.L., 2011. Intraspecific body size frequency distributions of insects. PloS one 6, e16606.

Greenaway, P., 1981. Temperature limits to trailing activity in the australian arid-zone meat ant *Iridomyrmex purpureus* form *viridiaeneus*. Australian Journal of Zoology 29, 621-630.

Greenslade, P., 1976. The meat ant *Iridomyrmex purpureus* (Hymenoptera: Formicidae) as a dominant member of ant communities. Austral Entomology 15, 237-240.

Groothuis, J., Smid, H.M., 2017. *Nasonia* parasitic wasps escape from Haller's rule by diphasic, partially isometric brain-body size scaling and selective neuropil adaptations. Brain, Behavior and Evolution.

Hölldobler, B., Carlin, N.F., 1985. Colony founding, queen dominance and oligogyny in the Australian meat ant *Iridomyrmex purpureus*. Behavioral Ecology and Sociobiology 18, 45-58.

Hölldobler, B., Wilson, E.O., 1990. The Ants. The Belknap Press of Harvard University Press, Cambridge, Massachusetts.

Kaspari, M., Weiser, M., 1999. The size–grain hypothesis and interspecific scaling in ants. Functional Ecology 13, 530-538.

Kelber, C., Rössler, W., Kleineidam, C.J., 2010. Phenotypic plasticity in number of glomeruli and sensory innervation of the antennal lobe in leaf-cutting ant workers (*A. vollenweideri*). Developmental neurobiology 70, 222-234.

MacKay, W.P., 1985. A comparison of the energy budgets of three species of *Pogonomyrmex* harvester ants (Hymenoptera: Formicidae). Oecologia 66, 484-494.

Narendra, A., Kamhi, J.F., Ogawa, Y., 2017. Moving in dim light: behavioral and visual adaptations in nocturnal ants. Integrative and Comparative Biology.

Parr, C.L., Dunn, R.R., Sanders, N.J., Weiser, M.D.P., M., Fitzpatrick, M.C., Arnan, X., Baccaro, F., Bishop, T.R., Brandão, C.R.F., Chick, L., Donoso, D.A., Fayle, T.M., Gómez, C., Grossman, B., Munyai, T.C., Pacheco, R., Retana, J., Sagata, K., Silva, R.R., Tista, M., Vasconcelos, H., Yates, M., Gibb, H., in review. The GLobal Ants trait Database (GLAD): a new database on the geography of ant traits (Hymenoptera: Formicidae)

Perl, C.D., Niven, J.E., 2016a. Colony-level differences in the scaling rules governing wood ant compound eye structure. Scientific Reports 6, 24204.

Perl, C.D., Niven, J.E., 2016b. Differential scaling within an insect compound eye. Biology Letters 12, 20160042.

Porter, S.D., 1988. Impact of temperature on colony growth and developmental rates of the ant, *Solenopsis invicta*. Journal of insect physiology 34, 1127-1133.

Porter, S.D., Tschinkel, W.R., 1986. Adaptive value of nanitic workers in newly founded red imported fire ant colonies (Hymenoptera: Formicidae). Annals of the Entomological Society of America 79, 723-726.

Ramirez-Esquivel, F., 2012. From large to small, from day to night: The sensory costs of miniaturisation in ants, Evolution, Ecology and Genetics. The Australian National University, Canberra p. 46.

Ramirez-Esquivel, F., Leitner, N.E., Zeil, J., Narendra, A., 2017. The sensory arrays of the ant, *Temnothorax rugatulus*. Arthropod Structure & Development 46, 552-563.

Ramirez-Esquivel, F., Zeil, J., Narendra, A., 2014. The antennal sensory array of the nocturnal bull ant *Myrmecia pyriformis*. Arthropod Structure & Development 43, 543-558.

Ribi, A., Engels, E., Engels, W., 1989. Sex and caste specific eye structures in stingless bees and honeybees (Hymenoptera: Trigonidae, Apidae). Entomologia Generalis 14, 233-242.

Rissing, S.W., 1987. Annual cycles in worker size of the seed-harvester ant *Veromessor pergandei* (Hymenoptera: Formicidae). Behavioral Ecology and Sociobiology 20, 117-124.

Schwander, T., Rosset, H., Chapuisat, M., 2005. Division of labour and worker size polymorphism in ant colonies: the impact of social and genetic factors. Behavioral Ecology and Sociobiology 59, 215-221.

Schwarz, S., Narendra, A., Zeil, J., 2011. The properties of the visual system in the Australian desert ant *Melophorus bagoti*. Arthropod Structure & Development 40, 128-134.

Skinner, G., 1980. The feeding habits of the wood-ant, *Formica rufa* (Hymenoptera: Formicidae), in limestone woodland in north-west England. The Journal of Animal Ecology, 417-433.

Spaethe, J., Brockmann, A., Halbig, C., Tautz, J., 2007. Size determines antennal sensitivity and behavioral threshold to odors in bumblebee workers. Naturwissenschaften 94, 733-739.

Spaethe, J., Chittka, L., 2003. Interindividual variation of eye optics and single object resolution in bumblebees. Journal of Experimental Biology 206, 3447-3453.

Stern, D.L., Emlen, D.J., 1999. The developmental basis for allometry in insects. Development 126, 1091-1101.

Tschinkel, W.R., 1988. Colony growth and the ontogeny of worker polymorphism in the fire ant, *Solenopsis invicta*. Behavioral Ecology and Sociobiology 22, 103-115.

Tschinkel, W.R., 1998. Sociometry and sociogenesis of colonies of the harvester ant, *Pogonomyrmex badius*: worker characteristics in relation to colony size and season. Insectes Sociaux 45, 385-410.

Tschinkel, W.R., Mikheyev, A.S., Storz, S.R., 2003. Allometry of workers of the fire ant, *Solenopsis invicta*. Journal of Insect Science 3, 2.

van der Woude, E., Smid, H.M., 2015. How to escape from Haller's rule: olfactory system complexity in small and large *Trichogramma evanescens* parasitic wasps. Journal of Comparative Neurology 524, 1876-1891.

Wetterer, J.K., 1999. The ecology and evolution of worker size-distribution in leaf-cutting ants (Hymenoptera: Formicidae). Sociobiology 34, 119-144.

Wheeler, D.E., 1991. The developmental basis of worker caste polymorphism in ants. American Naturalist 138, 1218-1238.

Wilson, E.O., 1953. The origin and evolution of polymorphism in ants. The Quarterly Review of Biology 28, 136-156.

Yang, A.S., Martin, C.H., Nijhout, H.F., 2004. Geographic variation of caste structure among ant populations. Current Biology 14, 514-519.

5.6. Appendices

5.6.1. Appendix 1

These are the guidelines (**Figure 5.3**) on measuring the traits relevant to this chapter that contributors to the GLAD database must follow as given on the download date 14/07/17 (Parr et al., in review):

In order to maintain consistency among trait data, we recommend that contributors provide data using the protocols in the following pages. We provide a list of traits used in the database and priority for measurement and diagrams of the measurements requested. However, we also accept data collected in other ways if appropriate documentation is supplied.

We recommend that, if possible:

1. Six specimens are measured for monomorphic species (termed workers) and for majors (soldiers) and minors (workers) of dimorphic species and that ten specimens are measured for polymorphic species (workers)
2. Specimens are measured while dry –mounted
3. Data are entered on our standard Traits data entry sheets (see link)
4. Accompanying Source, Locality and Assemblage data are provided (see link to data sheets)

The following line drawings are by Melanie Tista, except S11, which was contributed by Elena Angulo. All photographic ant images were extracted from AntWeb (https://www.antweb.org/).

5.6.2. Appendix 2

Species	Author/Publication
Camponotus consobrinus	(Narendra et al., 2017)[9]
Camponotus detritus	(Narendra et al., 2017)
Camponotus irritans	(Narendra et al., 2017)
Camponotus ligniperda	(Narendra et al., 2017)
Camponotus pennsylvanicus	(Narendra et al., 2017)
Camponotus sericeiventris	(Narendra et al., 2017)
Cataglyphis bagoti	(Schwarz et al., 2011) and SS personal communication
Formica integroides	(Narendra et al., 2017)
Formica polyctena	(Narendra et al., 2017)
Gigantiops destructor	(Narendra et al., 2017)
Harpegnathos saltator	(Narendra et al., 2017)
Iridomyrmex purpureus	Present study.
Melophorus bagoti	(Narendra et al., 2017)
Meranoplus ferrugineus	Ramirez-Esquivel (unpublished data)
Myrmecia croslandi	(Narendra et al., 2017)
Myrmecia desertorum	(Narendra et al., 2017)
Myrmecia nigriceps	(Narendra et al., 2017)
Myrmecia piliventris	(Narendra et al., 2017)
Myrmecia pyriformis	(Narendra et al., 2017)
Myrmecia tarsata	(Narendra et al., 2017)
Paraparatrechina minitula	Ramirez-Esquivel (unpublished data)
Polyrachis sokolova	(Narendra et al., 2017)
Rhytidoponera metallica	Ramirez-Esquivel (unpublished data)
Temnothorax rugatulus	(Ramirez-Esquivel et al., 2017)

[9] This publication collates facet numbers from other authors, please see references within.

Chapter 6 – Thesis conclusions

Concluding remarks on miniaturisation

Conclusions

Miniaturisation is an intriguing topic. On the one hand, decreasing body size seems like a perfectly ordinary thing. Animals come in all sorts of sizes and we ourselves experience fairly dramatic changes in size over the course of our lifetimes. Why then, should the study of miniaturisation be such a captivating topic? The answer to this question might be that although we think of size as a simple measurable characteristic it is in fact the complete opposite; a large change in body size implies much more than a simple up or down-scaling of the existing components. It affects just about every aspect of an animal's biology and can lead to novel adaptations and unexpected interactions between biological systems.

Size is a complex trait. A large change in body size may dramatically affect the basic biological building blocks (e.g. genome and cell size), it may require a rearrangement of organs or a simplification of structures. It may also completely re-define the way in which an animal interacts with its environment, from the other species it interacts with (its ecological niche) to how it is affected by the laws of physics (e.g. how it moves). As a consequence of all this, a very small animal may inhabit the same world we do but the way it perceives and interacts with said world can be radically different from our own lived experience. Analysing the biological design challenges and limitations that small animals face is extremely engaging because it not only reveals much about the fundamentals of life but also because it unveils a foreign world that is all around us.

The things that make miniaturisation fascinating conversely also make it extremely challenging to study. Miniaturisation is a complex trait that should ideally be approached from a multidisciplinary perspective. The introductory chapter of this thesis attempted to give an overview of the breadth of topics that may need to be considered in the study of miniaturisation. I carried this breadth of perspective forward into the later chapters in my discussion and interpretation of results. Unfortunately, in research breadth and depth of study tend to be at odds with one another. As a general rule, I attempted to be as thorough as possible in my data collection and address each research question in great depth. As a result broader considerations were often not pursued experimentally but discussed theoretically. In doing so it was my hope to maintain a broad perspective without compromising the quality of my work by spreading myself too thinly across different topics and techniques. I believe this approach has been successful in two capacities. Firstly, the breadth of literature reviewed in my introductory chapter and discussed throughout

provides a comprehensive, multidisciplinary theoretical framework from which to approach the study and interpretation of traits associated with miniaturisation. Although miniaturisation reviews currently exist they generally focus on fairly narrow topics or disciplines. My approach is so far unique in synthesising theories and findings from disparate fields into a unified framework. Secondly, I have compiled here an unprecedented wealth of anatomical data that gives us the first thorough description of antennal scaling in ants. This first anatomical study has yielded a range of interesting and sometimes unexpected results.

My findings indicate that the antennal sensillum array is highly conserved across subfamilies with the same types of sensillum observed in most species with very few exceptions (e.g. *Eciton*). This contrasts with the dizzying array of external sensillum morphologies displayed on the antennal arrays of higher taxonomic groupings (e.g. Lepidoptera, Coleoptera, etc.). Even within the Hymenoptera sensillum diversity makes it difficult to compare different families. This makes the Formicidae an ideal study group.

I found that the number of sensilla scaled with size but that the size of sensillum pegs could not be accurately predicted by body size. However it was interesting to note that the size of sensillum pegs varied greatly within individuals. It remains to be seen whether external peg length is a reflection of any functionally significant difference among sensilla (e.g. number of neurons or extent of dendritic endings). Unexpectedly, I found some indication that the shape of the antenna itself may be of interest to the study of miniaturisation. The continuous gradient I observed from filiform to club shaped antennae may be indicative of an adaptation for maximising the volume of the antennal lumen in very small species.

The design constraints operating on the sensory sensilla need to be better understood to make more meaningful conclusions on the functional implications of the scaling trends observed in this thesis. Factors such as the impact of sensillum density on sensillum function (e.g. array 'leakiness' and antennation speeds) and the relationship between sensillum size and number of underlying chemosensory neurons need to be further investigated. Additionally, direct measurements of antennal area and volume should also shed some light on the scaling patterns of the antenna as whole and whether shape changes can ameliorate surface area:volume constraints.

One aspect that has clearly stood out from studying the scaling patterns of sensillum arrays across Formicidae is the strong effect that phylogeny and

ecology play on shaping the anatomy of the antennal sensory array. This will need to be taken into account in future studies. Examining lower taxonomic groupings (such as a single subfamily or tribe) with little variation in the ecology of different species may prove fruitful in establishing a better understanding of scaling patterns.

One problem I did not expect to find when I first started was that measuring body-size should be as difficult as it is. Firstly, the numerous linear measurements used to estimate body-size in the ant literature can be quite confusing. I am grateful that I was able to generate and access data to make sense of different size measurements for myself (I thank Heloise Gibb for making GLAD data available to me; Parr et al., in review). Secondly, the degree of variation that I observed within monomorphic species was much greater than I expected. It is extremely difficult to establish what should constitute a 'normal' level of variation and perhaps this is a misguided idea in any case. Variability is likely to depend on a host of phylogenetic, genetic and developmental factors that may well change from one colony to the next let alone from one species to another. Nevertheless, I have found this question of intraspecific variation fascinating. A greater awareness of this kind of nuance may be key to understanding behavioural variation among workers.

Another key focus of this thesis was the study of sensory systems. Their study holds a particular appeal because sensory information fundamentally shapes how an animal interacts with the world it inhabits. The sensory organs underpin behaviours by determining what information an animal has about its surroundings. From our perspective antennae are particularly interesting because they are quite different from vertebrate sensors in that they are quite mobile and endowed with a variety of different types of sensors. There is no sensor in a human that is quite analogous to an antenna; we cannot extend an arm away from our bodies to smell a potential food (although we can touch it and know about its temperature and moisture). We know relatively little about the design principles of antennae and their study has lagged behind our understanding of vision for some time.

Chemoreception in particular is challenging to understand. This is probably due to a number of factors. Chemical cues diffuse through the environment according to much more complex patterns than light or sound. Additionally the technology available to measure chemical cues/smells is nowhere near as sophisticated as analogous tools available to measure light and sound. Lastly, our understanding of chemical senses may be influenced by how we, as humans, perceive chemical cues (see Sela

and Sobel, 2010) The ways in which humans process olfactory input in the brain seem to make it difficult for us to consciously attend to this sense. This may make it difficult for us to think and reason about odours in the same way that we do about light and sound. An interesting thought experiment is to try to describe an image or a sound to someone else as compared to a smell. While we have many words to describe the properties of light and sound it can be challenging to communicate a smell or flavour without referring to a food or a plant with similar properties.

Studying chemoreception remains a complex task from any given perspective. Our assumptions about how this sense functions are constantly being challenged by new evidence emerging from integrative insect studies. Some surprising results from the recent literature include evidence for modulation of sensitivity to odour cues throughout the lifetime of an ant (Ghaninia et al., 2017), differential responses to the same odour cues based on odour concentration (Hallem and Carlson, 2006), and the presence of response interactions between different chemoreceptive neurons within the same sensillum (Hallem and Carlson, 2006). Even the basic delineation between gustation and olfaction seems to be questioned in the recent literature (Joseph and Carlson, 2015). We appear to still have a limited understanding of the design principles of this complex sense and of the selective pressures that have led to its diverse manifestations.

Reference list

Ghaninia, M., Haight, K., Berger, S.L., Reinberg, D., Zwiebel, L.J., Ray, A., Liebig, J., 2017. Chemosensory sensitivity reflects reproductive status in the ant *Harpegnathos saltator*. Scientific Reports 7, 3732.

Hallem, E.A., Carlson, J.R., 2006. Coding of odors by a receptor repertoire. Cell 125, 143-160.

Joseph, R.M., Carlson, J.R., 2015. *Drosophila* chemoreceptors: a molecular interface between the chemical world and the brain. Trends in Genetics 31, 683-695.

Parr, C.L., Dunn, R.R., Sanders, N.J., Weiser, M.D.P., M., Fitzpatrick, M.C., Arnan, X., Baccaro, F., Bishop, T.R., Brandão, C.R.F., Chick, L., Donoso, D.A., Fayle, T.M., Gómez, C., Grossman, B., Munyai, T.C., Pacheco, R., Retana, J., Sagata, K., Silva, R.R., Tista, M., Vasconcelos, H., Yates, M., Gibb, H., in review. The GLobal Ants trait Database (GLAD): a new database on the geography of ant traits (Hymenoptera: Formicidae).

Sela, L., Sobel, N., 2010. Human olfaction: a constant state of change-blindness. Experimental brain research 205, 13-29.

Chapter 7 – Methods Appendix

Techniques for Investigating the Ant Visual System Anatomy

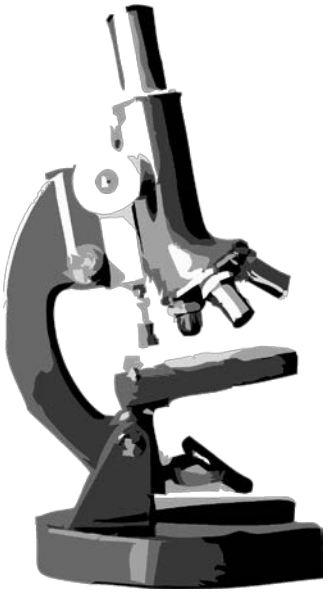

Chapter contents

Throughout the course of my PhD I used a variety of microscopic techniques to investigate the anatomy of ant eyes and antennae. This chapter describes many of these techniques in detail and is intended to provide guidance for future students and researchers in this area. The chapter is written with a focus on studying eye anatomy, though most of these techniques can be adapted to study antennae as well.

The contents of this chapter are based on the following publication:

> **Fiorella Ramirez-Esquivel, Willi Ribi, Ajay Narendra (in press) Techniques to Investigate the Anatomy of the Ant Visual System. JoVE**

It differs from the original in editorial details only and in the addition of an Appendix with examples of microscopic techniques adapted for use with antennae.

Author contributions:
Manuscript concept and planning: FRE, WR, AN; first draft: FRE; figure design: FRE; raw images: FRE, WR, AN; critical review of the manuscript: FRE, WR, AN. This chapter reviews established methods in the field of insect microscopy.

7.1. Introduction

Vision is an important sensory modality for most animals. Vision is especially crucial in the context of navigation for pinpointing goals, establishing and adhering to routes, and obtaining compass information (Wehner, 2003; Zeil, 2012). Insects detect visual information using a pair of compound eyes and, sometimes, one to three dorsally-placed simple eyes called ocelli (Fent and Wehner, 1985; Taylor et al., 2016; Warrant and Dacke, 2016).

The eyes of ants are of particular interest because, while ants are wonderfully diverse, they conserve some key characteristics across species. Despite dramatic variation in anatomy, size, and ecology, the vast majority of species are eusocial and live in colonies; as a result, different species face similar visual challenges in terms of navigating back and forth between a central place and resources. Across ants, the same basic eye bauplan can be observed in animals ranging from 0.5–26 mm in body length, from exclusively diurnal to strictly nocturnal species, and from slow walking subterranean to leaping visual predators (Ali et al., 1992; Bulova et al., 2016; Hölldobler and Wilson, 1990; Narendra et al., 2010; Weiser and Kaspari, 2006). Each of these staggering differences in ecology and behaviour give rise to innumerable permutations of the same basic eye structures to suit different environments, lifestyles, and body-sizes (Moser et al., 2004; Narendra et al., 2011). Consequently, studying the visual ecology of ants provides a veritable treasure trove of possibilities to the determined investigator.

Understanding the visual system of insects is essential for gaining an insight into their behavioural capabilities. This is apparent from integrative studies which nicely combine anatomy with ecology and behaviour to a great success in select insect groups (e.g. Dacke et al., 2003; Greiner et al., 2004; Stöckl et al., 2016; Warrant et al., 2004; Zeil, 1983). Though the field of ant navigation and ant behaviour in general has been quite successful, very little emphasis has been placed on ant vision outside of a few select species. Here, we will elaborate on the techniques involved in investigating eye design of ants. While we will focus on ants, these techniques can also be applied, with slight modifications, to other insects.

7.2. Protocol

7.2.1. Specimen Preparation

Note: It is necessary to first understand the relative location of the compound eye and ocelli to each other and on the head. This can be achieved by acquiring images of the dorsal view of the head. For this, we recommend processing samples either for photomicrography or using scanning electron microscopy (SEM) techniques. Below are the steps involved for both processes.

i.i. Specimen Collection

i.i.i. Collect and store specimens directly into 70% ethanol. Collect different castes whenever possible.

i.i.ii. Label specimens with time, date, place and any other relevant observations (e.g. collected while foraging, mating aggregation, nesting inside a twig, etc.)

i.i.iii. Collect enough specimens to have multiple replicates in each treatment.

i.ii. Photomicrography and Z-Stacking

i.ii.i. Air dry specimens and mount them on triangular point cards using water soluble glue, and then on an insect pin. For details see Lattke (2000).

i.ii.ii. Image using a high magnification stereomicroscope with a Z-stepper motor and a colour camera.

i.ii.iii. Use a diffuser to achieve uniform lighting for specimens.

i.ii.iv. Capture images at different focal planes and save images in a lossless file format (such as tiff) and focus stack them using commercially available software.

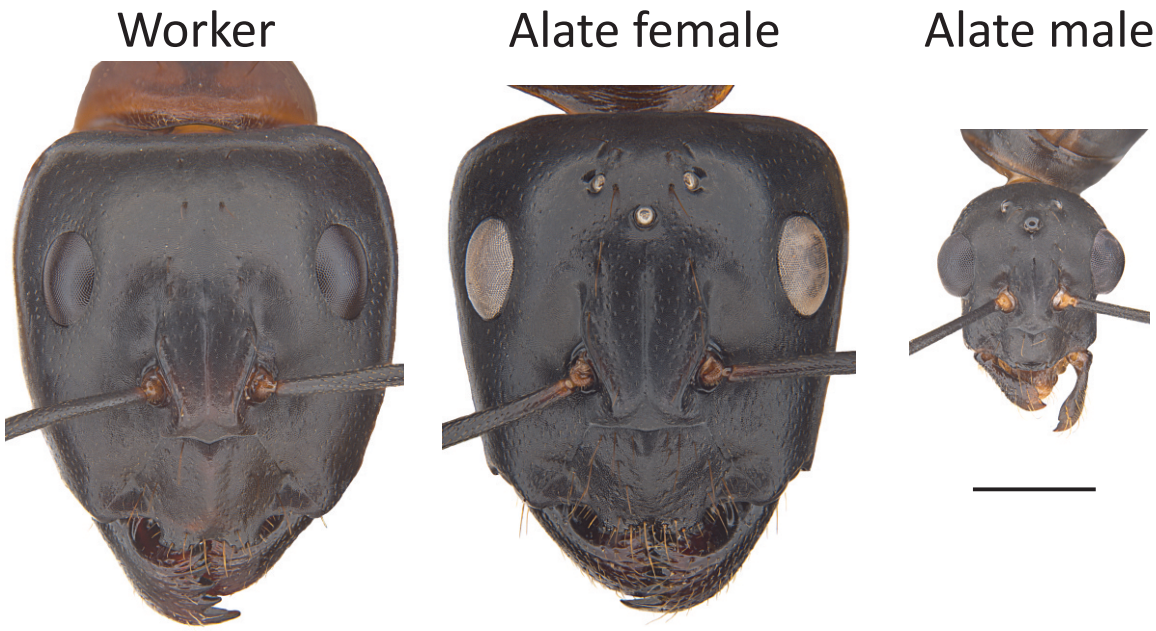

Figure 7.1. Z-stack photomicrographs of the three castes of the Australian sugar ant, *Camponotus consobrinus*. This provides an overview of the layout of the visual system in all three castes. Adapted from Narendra et al. (2016b). Scale bar = 1 mm.

i.iii. Scanning Electron Microscopy (SEM)

Note: Thoroughly clean all tools and surfaces with ethanol to avoid contamination of the specimen with dust and other particulates.

i.iii.i. Dehydrate specimens in ethanol overnight and air dry in a Petri dish.

i.iii.ii. Use a sharp razor blade to separate the head from the remainder of the body.

i.iii.iii. Mount the head at the required viewing angle (e.g. dorsal facing up) on aluminium stubs using conductive carbon tape or tabs. Cut the carbon tape into thin strips and fold it to support the head capsule.

i.iii.iv. Use a sputter coater to apply gold to the surface of the specimen for 2 min. at 20 mA with a rotary stage. The time and current may need to be adjusted depending on the instrument.

i.iii.v. Transfer specimens to a new aluminium stub with fresh carbon tape or tabs.

Note: The uncoated carbon will provide a black background but transferring specimens can damage the gold coating.

i.iii.vi. Check that the specimen orientation is still correct using a dissecting microscope and adjust as necessary with a pair of fine forceps or similar tool. Take care not to scratch the gold coating; handle as little as possible.

i.iii.vii. Load specimens onto the SEM stub holder, making note of the position of stubs and specimens relative to each other.

Note: Some SEMs are equipped with a stage camera but many are not and it can be difficult to locate small specimens at high magnification.

i.iii.viii. Image the specimens. Use a low accelerating voltage to avoid charging and a small aperture for good depth of field.

Note: Settings are best optimized in consultation with a technician specialized in the particular instrument being used.

7.2.2. Quantifying Facet Numbers and Diameters

ii.i. Cornea replicas

ii.i.i. Use ants preserved in ethanol or mounted on a pin for this purpose (step 1.1.1).

ii.i.ii. Mount the animal on an insect pin or on plasticine. If the head is relatively large, the remaining body parts can be removed.

ii.i.iii. Use an insect pin or a fine toothpick to pick up a small drop of fast-drying colourless nail polish and quickly spread it over the eye. Ensure the pin does not scratch the eye. The nail polish should cover the entire eye and part of the surrounding head capsule.

Note: It is important that the nail polish be of relatively uniform thickness across the eye.

ii.i.iv. Leave the nail polish to set at room temperature.

ii.i.v. Once it is fully set, use a fine insect pin to gently lift the replica from the head capsule surrounding the eye.

ii.i.vi. Use a fine pair of clean forceps to lift the replica, grasping the part of the replica that covers the head and not the eye.

ii.i.vii. Be mindful of the orientation of the eye: the anterior, posterior, dorsal, and ventral region.

ii.i.viii. Place the replica on a glass slide. Use a razor blade to trim the replica by carefully removing excess material around the eye. Use a needle or a pair of forceps to prevent the replica from moving.

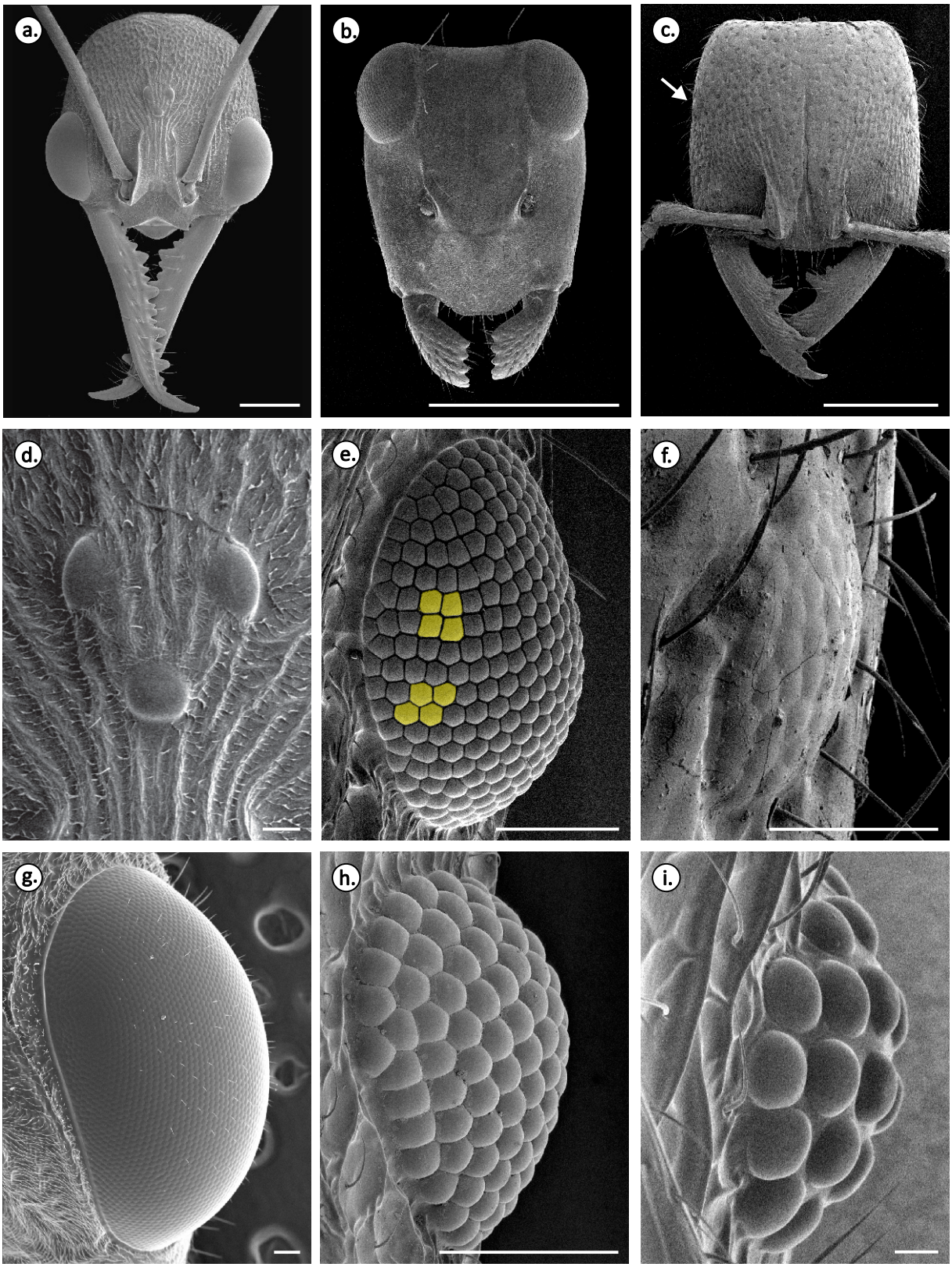

Figure 7.2. Scanning electron micrographs of the ant visual system demonstrating the imaging capabilities of this technique. Top row shows different eye positions and eye sizes in: (a) *Myrmecia nigriceps*; (b) *Opisthopsis pictus*; and (c) *Amblyopone australis* (note the very small eyes, white arrow). Images acquired at high magnification showing: (d) the three simple eyes in workers of *Myrmecia nigriceps;* different sized compound eye in (e) *Rhytidoponera metallica* (note the different shaped ommatidia in different regions of the compound eye in yellow), (f) *Amblyopone australis*, (g) *Myrmecia pyriformis,* (h) *Orectognathus clarki*, and (i) *Pheidole* species. Scale bars = 1 mm (A–C), 100 µm (D–H), 10 µm (I).

ii.i.ix. If the eye is very convex, use a razor blade to make 3–4 fine partial radial incisions around the edge to help 'flatten' the replica. If the eye is relatively 'flat', there is no need to make such incisions.

ii.i.x. Place a cover slip gently on the eye replica, recording the orientation of the replica on the slide. Do not apply pressure as this can eliminate the corneal impression on the nail polish.

ii.i.xi. Seal the coverslip using a very small amount of nail polish on each of the four corners. If the nail polish flows between the cover slip and glass slides it will damage the replica.

ii.i.xii. Image the slide on a compound microscope.

Note: If only some facets are in focus, then this suggests the eye replica is not flat enough – discard and start again from step ii.i.iii.

ii.i.xiii. Import the image into freely available programs (such as ImageJ or Fiji) where the number of ommatidia and size of each ommatidia can be measured.

Note: This method can be used to prepare replicas of ocelli, too. Since each ocellus has a single lens, we recommend keeping all the ocelli together in one replica.

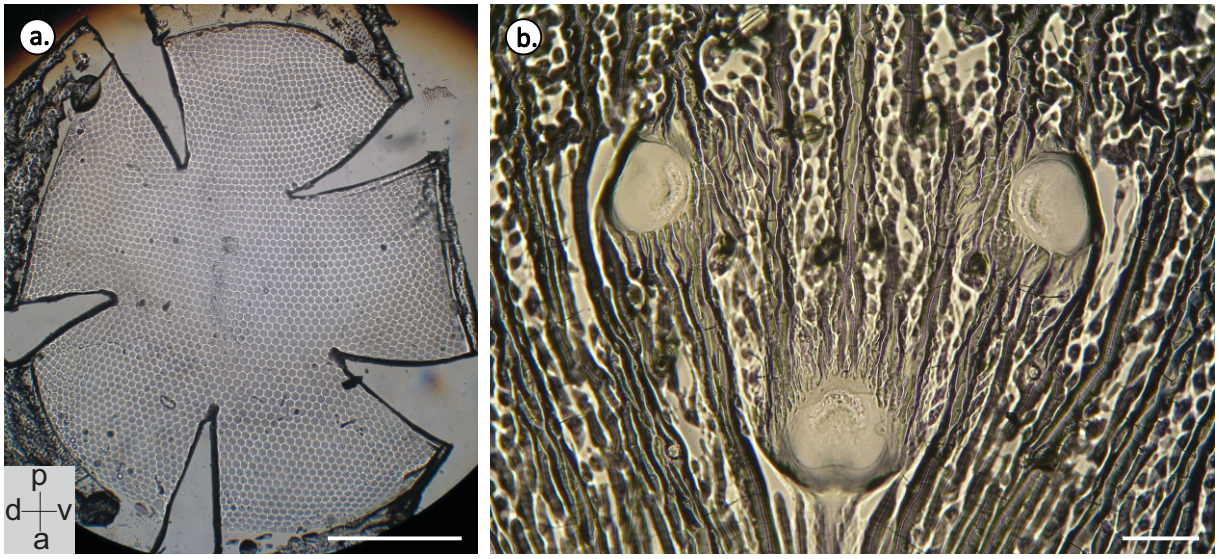

Figure 7.3. Cornea replicas of ant eye and ocelli. (a) Replica of the compound eye of a worker of *Myrmecia nigriceps*. The convex replica was flattened by making incisions. The inset indicates posterior (p) – anterior (a) and dorsal (d) – ventral (v) axes (b) Replica of the ocelli of worker of *Myrmecia tarsata*. Scale bars = 0.5 mm (a), 10 µm (b).

7.2.3. Analysing the Structure of the Eye

Note: To study the anatomy of the eye requires, in most cases, two complementary techniques of light microscopy (LM) and transition electron microscopy (TEM). The initial processing stages require similar techniques for both LM and TEM. Differences in the procedures for the two techniques begin from the sectioning stage onwards. Processing samples requires the use of hazardous chemicals that must be handled with care and discarded responsibly. Use personal protective equipment, work in a fume hood, always read the safety data sheets (SDS), and carry out risk assessments before starting.

iii.i. Dissection

iii.i.i. Anaesthetize specimens by cooling or by exposure to gaseous CO_2.

iii.i.i.i. CO_2 anaesthesia is very fast (generally taking effect in under 1 min) and care should be taken to avoid overexposure as this may result in the death of the specimen. If using dry ice pellets (solid CO_2), avoid direct contact with specimens as this can cause cold burns.

iii.i.i.ii. Cold anaesthesia is slower to take effect; 4°C is sufficiently cold, and lower temperatures are not recommended. Establish an appropriate cooling time for the species. Large or cold resistant ants, such as bull ants, may require >10 min to become fully immobilized, while smaller species may only need 1–2 min. Excessive cooling will kill the specimen (avoid direct contact with ice). Specimens should preferably be held in small, foam-stoppered, plastic containers and placed in an icebox where they can be observed rather than in an electric refrigerator or freezer.

iii.i.ii. Place specimen on a Petri dish, and adjust for viewing under a dissecting microscope. Working quickly is important to preserve anaesthesia and to avoid degeneration of the tissue once incisions are made (this can happen within seconds).

iii.i.iii. Remove antennae with forceps. If working with a stinging insect, it is advisable to amputate the gaster first to avoid being stung.

iii.i.iv. Remove the mouthparts using a sharp razor blade; forceps may be used to hold the specimen down. Cut through the anterior part of the eye (large specimens) or as close to the eyes as possible (small specimens) without tugging on the brain as this may tear out the retina.

iii.i.v. Prepare to open the head capsule. Angle the specimen so that the site of the first incision is pointing up; this may be done either

under the dissecting microscope while holding the specimen in forceps or under visual control while holding the specimen between the thumb and fore finger.

iii.i.vi. Make a transverse incision through the head to remove the ventral portion of the head; part of the ventral eye may be removed in large species to improve fixation and infiltration. The head should still be attached to the body at this point.

iii.i.vii. Sever the head capsule from the body by making a coronal incision just posterior to the compound eye.

iii.i.viii. Place the dissected head capsule with the compound eyes in ice cold fixative: 2.5% glutaraldehyde and 2% paraformaldehyde in phosphate buffer (pH 7.2–7.5).

Caution: Fixative is corrosive and toxic; wear appropriate protection and work in a fume hood.

Note: It is important to work quickly to arrest neural tissue degeneration. The dissection should be completed in 2 min or less (efficient dissection may require some practice).

Note: If the eye needs to be adapted to bright or dark conditions, then first expose the animals to the required light condition for a few hours. Carry out the dissections in the respective light conditions. Dissections can be carried out under red lights to simulate darkness.

iii.ii. Specimen processing

iii.ii.i. Keep the specimens in the fixative at room temperature with motion on an orbital shaker, for 2 h. Large specimens may require longer fixation times.

iii.ii.ii. Remove the fixative and dispose of it appropriately. Wash specimens in room temperature phosphate buffer (3 times, 5 min each) on the shaker.

Note: The phosphate buffer comprises of 8 g NaCl, 0.2 g KCl, 1.44 g Na_2HPO_4, and 0.244 g KH_2PO_4 in 1 L of distilled H_2O (pH 7.2).

iii.ii.iii. Remove the phosphate buffer and add 2% OsO_4. Place the specimen jar on the shaker in the fume hood for 1–2 h. This is a post-fixation step to fix fats and provide contrast for TEM.

Note: Osmium fixation times are subject to specimen size; as a rough rule of thumb, calculate 1 h of fixation per 1 mm^3.

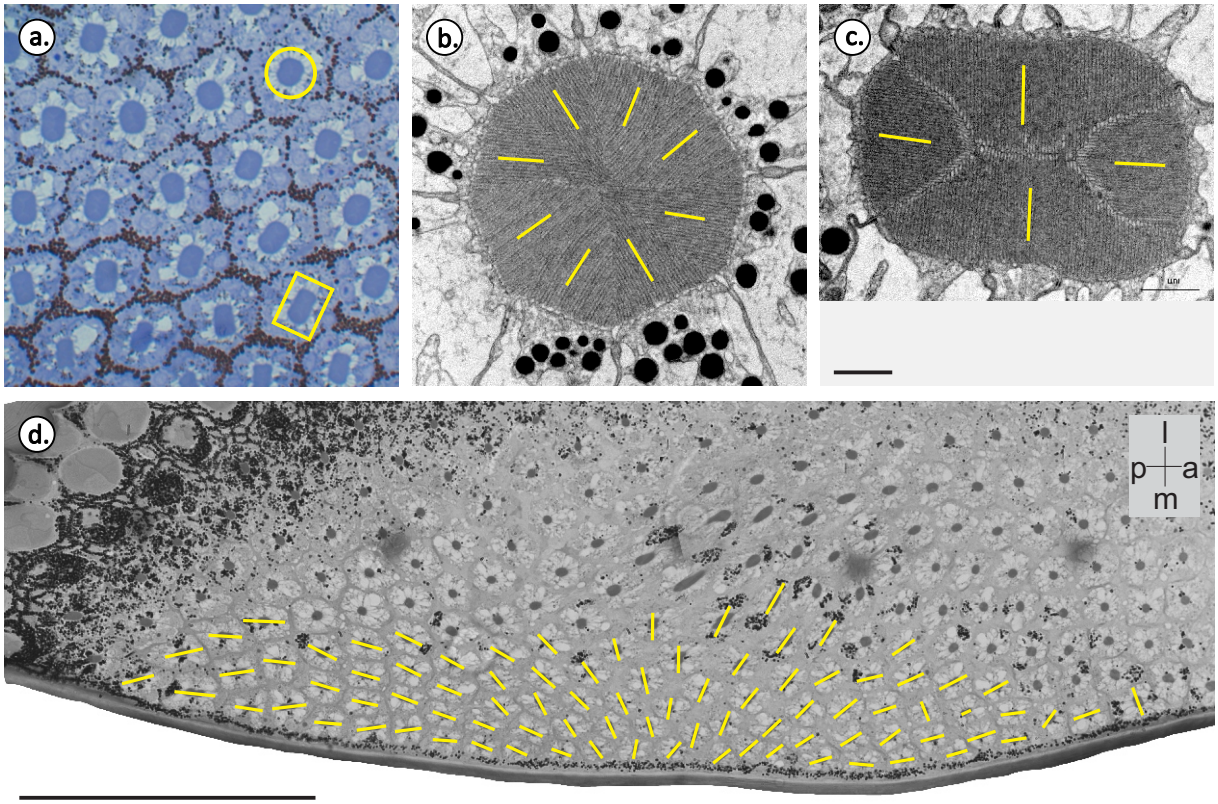

Figure 7.4. LM and EM images of rhabdom cross-sections. (a) Cross section of distal rhabdoms in *Myrmecia nigriceps* stained in toluidine blue can be used distinguish rhabdoms that are circular or rectangular in shape. Transmission electron micrographs show: (b) multiple orientations of microvilli in the circular rhabdom and (c) microvilli oriented in two opposite directions in the rectangular shaped rhabdom. (d) Using light microscopy, the long axis of the rectangular rhabdoms are mapped to show a fan-like organisation in the dorsal region of the eye in a queen of *Camponotus consobrinus*; inset indicates posterior (p) - anterior (a) and lateral (l) - medial (m) axes. Panel D adapted from Narendra et al. (2016b). Scale bars = 10 µm (a), 1 µm (b-c), 100 µm (d).

iii.ii.iv. Remove the osmium solution and dispose of it appropriately. Wash specimens in room temperature buffer (3 times, 5 min each) on the shaker.

iii.ii.v. Dehydrate the specimens by placing them in increasing concentrations of ethanol or acetone; for example, 50, 70, 80, and 95% for 10 min each and finally 100% (2 times, 15 min each). Place the specimens on the shaker between solution changes.

Note: If necessary, specimens may be stored in 70% ethanol overnight.

iii.ii.vi. Drain the ethanol and add 100% acetone. Leave it for 20 min on the shaker (skip this step if dehydrating the specimen in acetone). Replace with fresh acetone and leave for a further 20 min.

iii.ii.vii. Infiltrate the tissue with resin using the following ratios of acetone to resin: 2:1 (3 h), 1:1 (overnight), 1:2 (4 h), and pure resin (overnight). At each step leave specimens on the shaker inside the fume hood, and seal the container for all but the last two steps.

Note: Resin is too viscous to be drained, so specimens must be moved to a new disposable container at each step.

iii.ii.viii. Prepare blocks to mount the samples. Blocks can be custom made by cutting acrylic glass into small rectangular blocks (1.5 x 0.5 x 0.3cm). Blocks can also be made by pouring epoxy resin (there are many commercial kits available) into a silicon mould and then cure it in the oven for 12–14 h at 60°C.

Caution: Uncured (liquid) resin is carcinogenic and should be returned to the oven until fully hardened.

iii.ii.ix. Place the block vertically in the mould. Carefully take the specimens from the liquid resin, allow excess resin to drain, and place the specimen on the top of the block. A small amount of additional resin can be used to bind the specimen to the block.

iii.ii.x. Label the block. Print the paper labels and embed it in the block or attach it to a block face.

iii.ii.xi. Keep the mould with the embedded blocks in the oven for 12–14 h at 60°C.

iii.ii.xii. Store the specimen block in a clean envelope. This can be stored in this manner over several months to years.

iii.ii.xiii. Leave the used containers, dirty gloves, and other contaminated equipment in the fume hood to allow acetone to evaporate completely (minimum 12 h).

iii.ii.xiv. Cure resin in the oven before discarding disposable equipment or scraping resin off other items such as forceps.

iii.iii. Sectioning

iii.iii.i. Observe the block under the dissecting microscope to ensure that the specimen orientation is appropriate for the sectioning plane.

iii.iii.ii. If the orientation is not appropriate, use a jeweller's saw to cut out the specimen and re-orient using fragments of set resin and fresh resin to re-seat the specimen. The head may also be split into two halves to section the two eyes separately. Cure resin again before proceeding.

iii.iii.iii. Mount the block on the removable microtome chuck. Remove the chuck and place on holder.

iii.iii.iv. Trim the resin block using a razor blade under the dissecting microscope.

Caution: Do not do this when the chuck is mounted on the microtome arm as it can jolt the arm and damage the bearings.

iii.iii.v. Remount the chuck onto the microtome arm and angle the specimen.

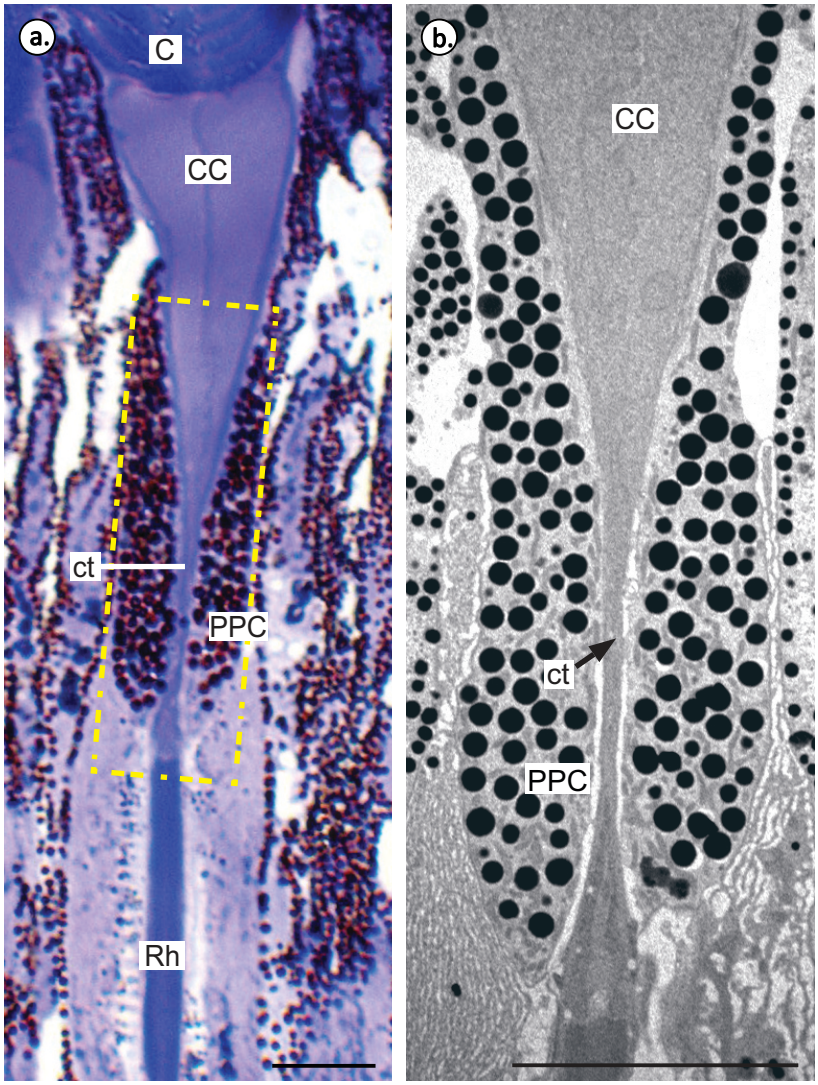

Figure 7.5. LM and electron microscopy images of an ommatidium in a light-adapted eye of *Myrmecia tarsata*. (a) Longitudinal section of an ommatidium showing the cornea (C), crystalline cone (CC), cone tract (ct), rhabdom (Rh) and primary pigment cells (PPC). (b) Dashed rectangular box in panel A from a different section viewed under a TEM to quantify the narrow width of the cone tract. Adapted from Narendra et al. (2016). Scale bars = 10 µm.

iii.iii.vi. Mount the knife on the holder at the appropriate angle (0° for glass knives, see manufacturer's instructions for diamond knives).

Note: Glass knives can be made cheaply with a glass knife maker but must be replaced periodically as they lose their edge; high quality diamond knives can be purchased but are expensive, require special care, and are not suitable for beginners.

iii.iii.vii. Fill the knife boat with distilled water using a syringe fitted with a filter (0.45 μm pore size).

iii.iii.viii. Fill the boat until the water level reaches the edge of the knife; the meniscus may be convex in other areas of the boat.

iii.iii.ix. Drain the boat until the meniscus is very slightly concave but still reaches the edge of the knife. The water level can be adjusted at any point, but always add/remove water away from the edge of the knife.

iii.iii.x. Carefully bring the knife towards the specimen and align the block to the knife. This is best done slowly, periodically checking the proximity of the knife through the eyepiece and from the side.

Note: Check the instrument handbook for specific instructions as instruments vary.

iii.iii.xi. Set the section thickness on the microtome. Selecting the correct thickness will be dependent on specimen size, region of interest and the kind of knife being used.

iii.iii.xii. If using a glass knife, select a higher setting (e.g. 4 μm) if a lot of material must be cut away before reaching the area of interest. If a diamond knife is being used or if the specimen is very small, 1–2 μm may be more appropriate.

iii.iii.xiii. Start the "cutting" (cranking the microtome wheel) when the knife is close but not yet cutting into the specimen to perform the last part of the approach. Sections should start appearing within a few rotations; if not, stop and very carefully bring the knife a little closer.

iii.iii.xiv. Adjust the section collecting thickness (1 μm for semi-thin sections) when approaching the region of interest.

iii.iii.xv. Collect any sections using an eyelash tool.

Note: Eyelash tools can be made with an eyelash mounted onto a thin stick with nail polish.

iii.iii.xvi. If a lot of material must be removed, allow the sections to accumulate and remove en masse by removing the knife and flushing it out with water. If using a glass knife, this may be an appropriate time to change to a fresh section of the knife or to a new knife.

iii.iii.xvii. Place a series of small droplets of distilled water on a slide using a Pasteur pipette or ideally, the filter equipped syringe.

iii.iii.xviii. Carefully float the collected section from the eyelash tool onto the water droplet.

iii.iii.xix. Collect sections like this until it is appropriate to check the depth of sectioning.

Note: Although it can be tedious, it is always best to check often.

iii.iii.xx. Place the slide on a hotplate set to 60°C. Allow all the water to evaporate and the section to adhere to the slide.

iii.iii.xxi. Dye sections with toluidine blue for 10–60 s (staining time will vary with section thickness). Dispense the dye with a syringe equipped with a filter (as above).

iii.iii.xxii. Place a drop of the dye on one end of the slide and spread it using the side of the needle without touching or scraping the sections. Place the slide on the hotplate until a gold rim appears around the edge of the dye drop.

iii.iii.xxiii. Rinse the slide by spraying it with distilled water in a wash bottle and place it on the hot plate to dry it.

iii.iii.xxiv. Check under the compound microscope and image them.

iii.iii.xxv. Repeat until region of interest is reached.

iii.iii.xxvi. For ultra-thin sections: set the cutting thickness between 40–60 nm to collect TEM sections.

iii.iii.xxvii. Cut about 3–5 sections and check thickness using an interference colour chart. Sections should reflect light grey when viewed at an angle.

Note: Chloroform fumes can be pipetted over sections to relax any creases. This is most relevant to experienced users and beginners need not worry. Too much chloroform released too close to the section can damage sections.

iii.iii.xxviii. Pick up a Formvar-coated, copper, slot grid held with forceps with the Formvar side up. Be careful not to puncture the Formvar coating.

iii.iii.xxix. Dip the grid into the boat edgeways and away from the sections, then bring the grid up parallel to the surface under the sections. If necessary use the eyelash tool to guide the sections over the grid.

iii.iii.xxx. Carefully dab around the tip of the forceps with filter paper to soak up water trapped between the arms. If this is not done, water tension can pull the grid up between the arms or make it stick to one side; this can result in contamination or mechanical damage.

iii.iii.xxxi. Carefully remove excess water from the grid itself by standing the grid edgeways on filter paper.

iii.iii.xxii. Place the grid in a grid holder.

iii.iii.xxxiii. Repeat until enough sections have been collected.

iii.iii.xxxiv. Semi-thin sections can be imaged directly with any compound microscope equipped with a camera. Immersion oil can be placed directly onto the sections. Slides should be stored in a slide box to prevent discolouration.

iv. Staining Ultra-thin Sections for TEM Contrast

Note: The following steps should be carried out under cover as the dyes are light and CO_2 sensitive. Furthermore, EM dyes use heavy metals to produce contrast and are therefore hazardous substances. Appropriate care must be taken when handling these stains.

iv.i. Cover a few large Petri dishes with aluminium foil to block light. Work under these for the following steps. Partially uncover them to allow working space as needed, but place the covers back on as soon as possible.

iv.ii. Cut a piece of wax film and carefully place five droplets of 6% saturated uranyl acetate on it using a Pasteur pipette.

iv.ii.i. To prepare the solution, mix 2 g uranyl acetate with 100 mL 50% methanol in distilled water and filter the solution before using. The solution cannot be stored and should be made fresh each time (Ribi, 1987).

iv.iii. Carefully pick up the TEM grids with forceps and balance on top of dye droplets with the section side down. Leave for 25 min.

iv.iv. Rinse grids individually by rapidly dipping them in and out of distilled water; progress through four separate vials of distilled water.

iv.v. Place five droplets of lead citrate on a fresh piece of film. Arrange a few NaOH pellets around the dye droplets (this absorbs atmospheric CO_2 to prevent precipitation of lead carbonate).

iv.v.i. To make the lead citrate solution, prepare bi-distilled water by boiling distilled water for 0.5 h. Allow the water to cool then in a sealable container, add 0.3 g lead citrate to 100 mL of the bi-distilled water. Add 1 mL 10 M NaOH, seal the container tightly, and shake until dissolved (Ribi, 1987).

iv.vi. Place the grids on the dye drops as described in 4.3 and cover. Stain for 5 min.

iv.vii. Rinse in distilled water as before by dipping the grids in and out of distilled water 20 times. Progress through three vessels of distilled water.

iv.viii. Soak up excess water with filter paper and allow the grids to dry in a grid box.

iv.ix. Image in a TEM at low accelerating voltage.

7.3. Representative results

The methods described here enable detailed study of the simple and compound eyes of ants. Imaging the dorsal view of the head using Z-stack photomicrography techniques allows one to obtain an overview of the layout of the visual system (**Figure 7.1**). This is good preparation for dissections and to determine the required sectioning angle. This technique is also useful for taking measurements such as head width, eye length, and ocellar lens diameters. SEM imaging also gives detailed overview images but additionally allows acquisition of high magnification and high resolution images. Particular regions of interest in the eye can be examined in detail and variations in lens shape can be identified (**Figure 7.2**). SEM images are especially useful for resolving ants with small eyes and ocelli. The cornea replicas provide information on the shape, size, and number of lenses in each eye (**Figure 7.3**). Semi-thin sections imaged using LM techniques allow investigation of the gross internal anatomy of the eye (**Figure 7.4** and **Figure 7.5**); this includes the thickness of the lens, diameter of the crystalline cone, presence of a crystalline cone tract, shape, width, and length of the rhabdom, mapping the dorsal rim area, and location of the primary and secondary pigment cells. This technique can be nicely complemented by ultra-thin sections imaged using TEM. This latter technique permits the study of ultrastructure especially, the microvillar orientation (**Figure 7.4**) and other smaller structures (e.g. width of the constricted crystalline cone tract, **Figure 7.5**).

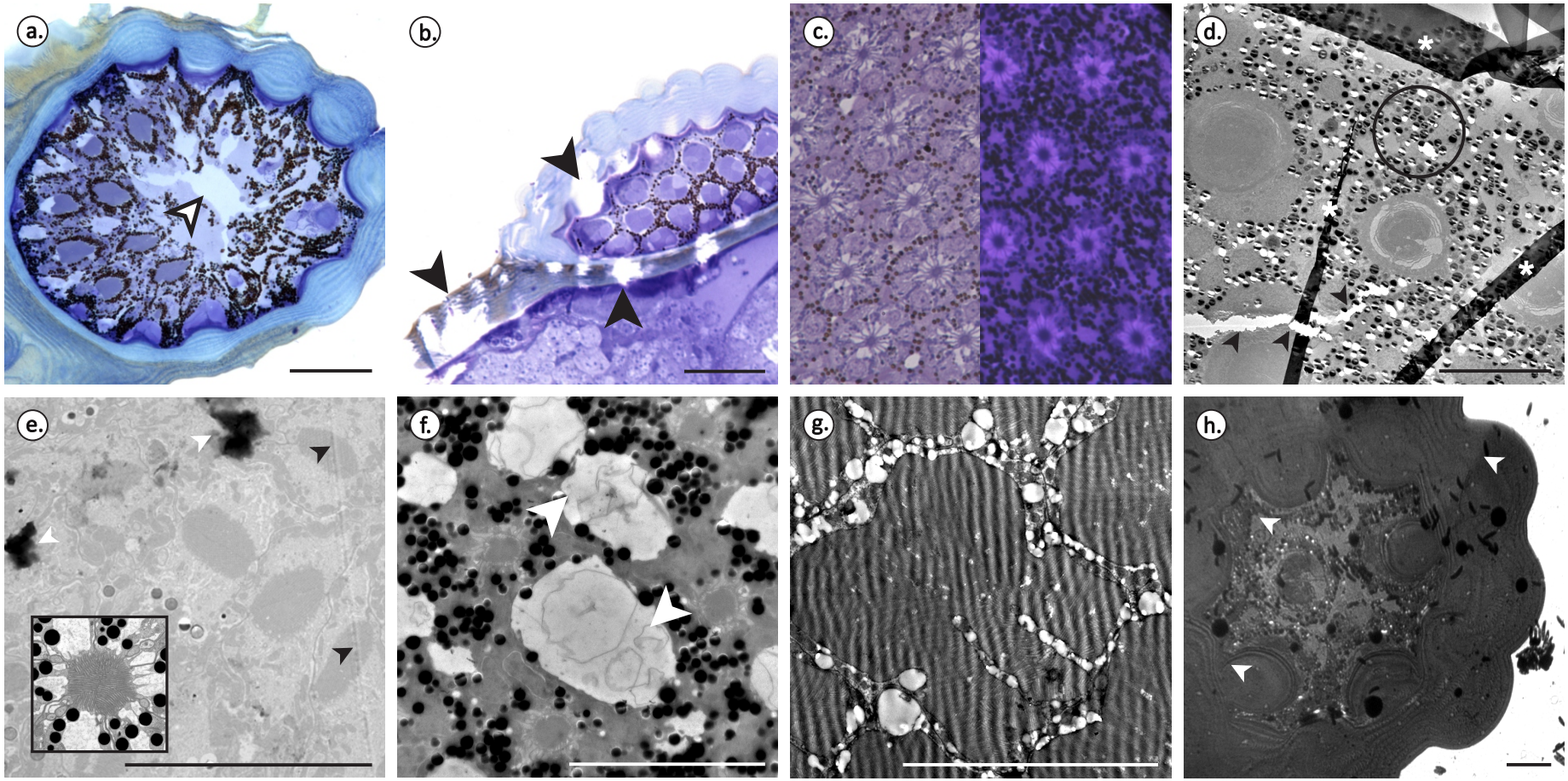

Figure 7.6. Common problems with semi-thin and ultra-thin sections (fixation and infiltration, cutting and staining). (a) Poor fixation of tissue due to inadequate penetration (arrow) in a semi-thin section of *Pheidole* species; (b) ripping during sectioning in *Iridomyrmex calvus* (semi-thin); (c) perfect staining (left) and over staining (right) with toluidine blue in *Myrmecia croslandi*; (d) pigment (circle) and tissue ripping during sectioning (arrows) due to poor matching of the resin and tissue density (resin too soft). Folding of the section (asterisks), can happen when collecting sections from the knife boat; (e) poor contrast due to insufficient staining (compare to inset), lead citrate crystals (white arrows) from exposure to CO_2, and vertical knife mark (black arrows); (f) holes in the tissue (white arrows) caused by poor fixation in a *Melophorus hirsutus* compound eye; (g) resin too soft, leads to chitter when sectioning seen as vertical ripples in the section; (h) section too thick (~ 100 nm) resulted in dark image with poor contrast, contaminated distilled water lead to bacteria and particulate matter scattered throughout the section (white arrows) in *Pheidole* species. Scale bar = 25 µm (a–b), 10 µm (c–h).

7.4. Discussion

The suite of methods outlined above allow for an effective investigation into the optical system of ants and other insects. These techniques inform our understanding of sampling resolution, optical sensitivity, and potential polarization sensitivity of the eye under study. This knowledge provides an important foundation for physiological and behavioural investigation into their visual capabilities. Furthermore, while the methods detailed here have focused on ant visual systems, these techniques can be used on other insects, albeit with slight modifications in the protocol (e.g. increasing duration of fixation and infiltration in thicker tissues). Slightly modified protocols have been used to characterize the visual systems of a variety of insects including cicadas (Ribi and Zeil, 2015), flies (Zeil, 1983), bees (Ribi et al., 2011), wasps (Ribi, 1978a), butterflies (Ribi, 1978b), and moths (Lau et al., 2007). These methods are extremely useful and can be modified to apply to a variety of study systems. Although most of the techniques outlined here have been in use for some time, this article takes the opportunity to bring them together in the context of studying the ant's optical system to compare alternative techniques and to identify common pitfalls.

There are many imaging techniques currently available that have overlapping applications and it can be difficult to assess which technique is appropriate for the task at hand. A relevant example here is choosing a technique for overview imaging. The external morphology of the head and eye and relative positioning of the optical system on the head can be done using SEM or photomicrography. The strengths and weaknesses of these techniques have been reviewed (Wipfler et al., 2016), however, there are some special considerations when imaging eyes. When imaging the relative positioning and size of the eyes, both techniques have their advantages and disadvantages. SEM images lack colour information, so where pigmentation is relevant, photomicrography is better. However, SEM images can illustrate fine structures such as inter-ommatidial hairs and facet boundaries in greater detail and even reveal surface features not visible under photomicrography techniques (e.g. ocellar lenses and surface sculpturing of compound eye lenses). SEM is a versatile technique when it comes to exploratory imaging and identifying features of interest because it can operate on a large range of specimen sizes while still retaining very high resolution throughout this range. However, it is not as widely accessible as a dissection microscope and requires a higher level of expertise. There is often no single way of obtaining the information one

requires. In such a scenario, it is useful to consider what is available and where it is most important to invest resources.

Nail-polish replicas of the cornea have proven to be most useful in obtaining the most accurate measure of facet numbers and facet diameters. This has now been used in a variety of insects (Narendra et al., 2011; Ribi and Zeil, 2015; Somanathan et al., 2009; Streinzer et al., 2013). While the quality of the images acquired from an SEM is far superior, the curvature of the eye prevents accurate measurements of the whole facet array. Mapping the facet size and facet distribution should also be feasible from scans acquired from micro-computed tomography (Taylor et al., 2016).

In both the LM and TEM techniques, it often is difficult to know whether the sample has been prepared and processed well until the final stage of imaging. To avoid complications, it is important to establish good practices such as maintaining clean working spaces and tools, preparing fresh solutions regularly, and thoroughly filtering water. Contaminants that are invisible to the naked eye can ruin EM samples. For this reason, it can be useful to wipe down surfaces and instruments using a solvent, such as ethanol or acetone, and a non-lint producing wipe. This is most relevant when sectioning, staining EM sections, and when preparing SEM samples. Similarly, distilled water sources can present problems and introduce contaminants so it is always best to check filters, change them regularly, and always use freshly filtered water (do not store). Most fixatives, stains, and embedding materials cannot be stored indefinitely and it is important to label all solutions with the date of preparation. It is important to take a systematic approach and set aside enough time to carry out protocols without interruptions.

Adapting techniques to different species is always a matter of trial and error. When working within Formicidae, the main differences lie in the size of the animal and the muscle mass within the head. Ants with more musculature in their head will typically take longer to fix. With very large ants, it is best to remove the mandibular muscles, trachea, and mandibular glands, while ensuring minimum interference with the neural tissue. In small ants and those with few mandibular muscles, it is possible to achieve adequate fixation by just removing the mandibles and exposing the clypeal region. In these cases, small holes using minutiae pins can be made on the head to improve fixation.

It is important to note that environmental conditions can also affect preparations. Hot and humid environments (especially field stations in the

tropics) can prove to be a challenge during the infiltration stage. Warm conditions can lead resins to partially polymerize prematurely, resulting in the unused resin becoming increasingly more viscous. In this case, the best option is to store the resin in small, single use, containers in the fridge or freezer. Cooling fixatives can be helpful to counter faster tissue decay in warm conditions. However, cooled solutions will disperse more slowly which means that treatment times should be extended to ensure proper penetration.

With these cautions in mind, investigation into the optical system of ants and other insects can prove very rewarding. Studying the visual system allows us to estimate the size of visual fields, interommatidial angles, optical sensitivity and sampling resolutions. Understanding the anatomy of the eye informs our understanding and interpretation of animal behaviour. For example, anatomy sometimes allows us to make predictions on the visual capabilities of animals such as whether they are diurnal or nocturnal, which may not have been previously documented. Given the current knowledge about the visual system of handful of ants, we hope our methods will inspire biologists and myrmecologists to investigate the compound eye and ocelli in ants to further our understanding.

7.5. References

Ali, M.T., Urbani, B.C., Billen, J., 1992. Multiple jumping behaviors in the ant *Harpegnathos saltator*. Naturwissenschaften 79, 374-376.

Bulova, S., Purce, K., Khodak, P., Sulger, E., O'Donnell, S., 2016. Into the black and back: the ecology of brain investment in Neotropical army ants (Formicidae: Dorylinae). The Science of Nature 103, 1-11.

Dacke, M., Nordström, P., Scholtz, C.H., 2003. Twilight orientation to polarised light in the crepuscular dung beetle *Scarabaeus zambesianus*. Journal of Experimental Biology 206, 1535-1543.

Fent, K., Wehner, R., 1985. Ocelli: a celestial compass in the desert ant *Cataglyphis*. Science (New York, N.Y.) 228, 192-194.

Greiner, B., Ribi, W.A., Warrant, E.J., 2004. Retinal and optical adaptations for nocturnal vision in the halictid bee *Megalopta genalis*. Cell and Tissue Research 316, 377-390.

Hölldobler, B., Wilson, E.O., 1990. The Ants. The Belknap Press of Harvard University Press, Cambridge, Massachusetts.

Lattke, J.E., 2000. Specimen Processing: Building and Curating an Ant Collection, In: Alonso, L.E., Agosti, D., Majer, J.D. (Eds.), Ants: Standard Methods for Measuring and Monitoring Biodiversity. Smithsonian Institution Press.

Lau, T.F.S., Gross, E.M., Meyer-Rochow, V.B., 2007. Sexual dimorphism and light/dark adaptation in the compound eyes of male and female *Acentria ephemerella* (Lepidoptera: Pyraloidea: Crambidae). European Journal of Entomology 104, 459.

Moser, J.C., Reeve, J.D., Bento, J., eacute, Maur, iacute, S., c., Della Lucia, T., C., n.M., Cameron, R.S., Heck, N.M., 2004. Eye size and behaviour of day- and night-flying leafcutting ant alates. Journal of Zoology 264, 69-75.

Narendra, A., Greiner, B., Ribi, W.A., Zeil, J., 2016a. Light and dark adaptation mechanisms in the compound eyes of *Myrmecia* ants that occupy discrete temporal niches. Journal of Experimental Biology 219, 2435-2442.

Narendra, A., Ramirez-Esquivel, F., Ribi, W.A., 2016b. Compound eye and ocellar structure for walking and flying modes of locomotion in the Australian ant, *Camponotus consobrinus*. Scientific Reports 6, 22331.

Narendra, A., Reid, S.F., Greiner, B., Peters, R.A., Hemmi, J.M., Ribi, W.A., Zeil, J., 2011. Caste-specific visual adaptations to distinct daily activity schedules in Australian *Myrmecia* ants. Proceedings of the Royal Society B: Biological Sciences 278, 1141-1149.

Narendra, A., Reid, S.F., Hemmi, J.M., 2010. The twilight zone: ambient light levels trigger activity in primitive ants. Proceedings of the Royal Society B: Biological Sciences 277, 1531-1538.

Ribi, W.A., 1978a. Colour receptors in the eye of the digger wasp, *Sphex cognatus* Smith: evaluation by selective adaptation. Cell and Tissue Research 195, 471-483.

Ribi, W.A., 1978b. Ultrastructure and migration of screening pigments in the retina of *Pieris rapae* L.(Lepidoptera, Pieridae). Cell and Tissue Research 191, 57-73.

Ribi, W.A., 1987. A Handbook in Biological Electron Microscopy. Switzerland, 106.

Ribi, W.A., Warrant, E., Zeil, J., 2011. The organization of honeybee ocelli: regional specializations and rhabdom arrangements. Arthropod Structure & Development 40, 509-520.

Ribi, W.A., Zeil, J., 2015. The visual system of the Australian 'Redeye' cicada (*Psaltoda moerens*). Arthropod Structure & Development 44, 574-586.

Schafer, R., Sanchez, T.V., 1976. The nature and development of sex attractant specificity in cockroaches of the genus *Periplaneta*. I. Sexual dimorphism in the distribution of antennal sense organs in five species. Journal of Morphology 149, 139-157.

Somanathan, H., Warrant, E.J., Borges, R.M., Wallén, R., Kelber, A., 2009. Resolution and sensitivity of the eyes of the Asian honeybees *Apis florea*, *Apis cerana* and *Apis dorsata*. Journal of Experimental Biology 212, 2448-2453.

Stöckl, A.L., Ribi, W.A., Warrant, E.J., 2016. Adaptations for nocturnal and diurnal vision in the hawkmoth lamina. Journal of Comparative Neurology 524, 160-175.

Streinzer, M., Brockmann, A., Nagaraja, N., Spaethe, J., 2013. Sex and caste-specific variation in compound eye morphology of five honeybee species. PloS one 8, e57702.

Taylor, G.J., Ribi, W., Bech, M., Bodey, A.J., Rau, C., Steuwer, A., Warrant, E.J., Baird, E., 2016. The dual function of orchid bee ocelli as revealed by X-ray microtomography. Current Biology 26, 1319-1324.

Warrant, E., Dacke, M., 2016. Visual navigation in nocturnal insects. Physiology 31, 182-192.

Warrant, E.J., Kelber, A., Gislén, A., Greiner, B., Ribi, W., Wcislo, W.T., 2004. Nocturnal vision and landmark orientation in a tropical halictid bee. Current Biology 14, 1309-1318.

Wehner, R., 2003. Desert ant navigation: how miniature brains solve complex tasks. Journal of Comparative Physiology A 189, 579-588.

Weiser, M.D., Kaspari, M., 2006. Ecological morphospace of New World ants. Ecological Entomology 31, 131-142.

Wipfler, B., Pohl, H., Yavorskaya, M.I., Beutel, R.G., 2016. A review of methods for analysing insect structures - the role of morphology in

the age of phylogenomics. Current Opinion in Insect Science 18, 60-68.

Zeil, J., 1983. Sexual dimorphism in the visual system of flies: the compound eyes and neural superposition in Bibionidae (Diptera). Journal of Comparative Physiology A 150, 379-393.

Zeil, J., 2012. Visual homing: an insect perspective. Current Opinion in Neurobiology 22, 285-293.

7.6. Appendices

In this chapter a number of techniques for the study of ant eye anatomy were described. Some of these can be adapted for the study of antennae. Here are some examples of techniques using light microscopy (for details on using SEM techniques see **Chapter 2**).

Light microscopy and Z-stacking

In this chapter techniques for imaging eyes and whole ant heads with full depth of field are described in section 1.2. Z-stacking can be used to study antenna whole-mounts as shown in Sf 1. Here antennae of *Iridomyrmex calvus* have been treated with 10% KOH overnight to clear the cuticle, after rinsing in distilled water the whole antenna is immersed in 0.1M $AgNO_3$ solution for 10 minutes followed by another rinse and then 10 minutes in photographic developer (Ilford ID-11, for black and white film), this method was modified from Schafer and Sanchez (1976). The whole antenna can then be mounted on a glass slide, coverslips can be affixed using Cytoseal (Electron Microscopy Sciences) or an appropriate embedding medium or a temporary mount can be prepared using distilled water. Imaging in this case was done using a Leica DM5500B compound microscope equipped with a DFC365FX monochrome camera. Multiple images at different focal depths (approx. 10-60 images) are captured and then stacked into a single image using the ZereneStacker v1.04 (Zerene Systems, LLC) "PMax" function.

This kind of preparation can be adapted to image different aspects of antennal anatomy. Generally, using some kind of bleaching agent will be more important for larger specimens with thicker, more sclerotised cuticle; small specimens may be translucent enough to not require this step. The use of stains that highlight areas of interest, such as silver nitrate which stains porous areas (see Sf 1. a and b), can be important as the complex structure of the antenna can be difficult for Z-stacking software to interpret (e.g. note the hazy aura around the antenna in Sf 1. c).

Nail polish replicas

Although this technique was not thoroughly trialled, it is possible to create fine enough nail polish replicas of the antenna to study sensilla. Some types of sensilla, such as sensilla basiconica, are distinctive enough to be

easily identified in this manner while others are more difficult to differentiate (e.g. sensilla chaetica and TII). This technique may be useful for studying the whole antennal surface (dorsal and ventral) in a cheaper but lower resolution manner than SEM.

Semi- and ultra-thin sectioning

These techniques can be used to study the internal ultrastucture of sensilla with little modification to the protocols outlined in this chapter. The main hurdles to overcome are ensuring adequate access for fixation and infiltration and matching of the resin hardness to the hardness of the cuticle. The protocol may need to be tweaked from species to species depending on the size of the antenna, cuticle thickness and hardness.

Some notes and recommendations for SEM

Handling and mounting antennae differs from mounting whole heads for eye imaging in a few ways. Antennae are thin and covered in hairs so they are prone to building up static and attracting microfibers, for this reason it is particularly important to clean all surfaces with ethanol before mounting specimens. It is best to keep specimens in ethanol (Sf 3. a) until right before mounting on aluminium stubs. Specimens should then be taken out and placed on a clean petri dish and left for the ethanol to evaporate before placing on adhesive carbon tape or tabs. If the ethanol is not allowed to evaporate first it will partially dissolve the adhesive on the carbon tape/tab. After coating specimens antennae in particular have to be checked again as the vacuum of the coater can make the antennomeres shift (Sf 3. b, c, d). If antennae have shifted it is best to use the finest possible tool either fine forceps, entomological or minutiae pins. If possible adjust positioning without directly touching the antennomere or area that is to be imaged as the gold coating is very likely to be scraped off (see Sf 3. e). Labelling on the stubs themselves is difficult because they are very small. If there is space to write on the stub permanent ink can be used to label the stubs, if done after coating the label will be legible under the SEM illumination. If specimens are to be stored, it is best to number the stub underside and store with a paper card where details can be written out in detail in archival ink.

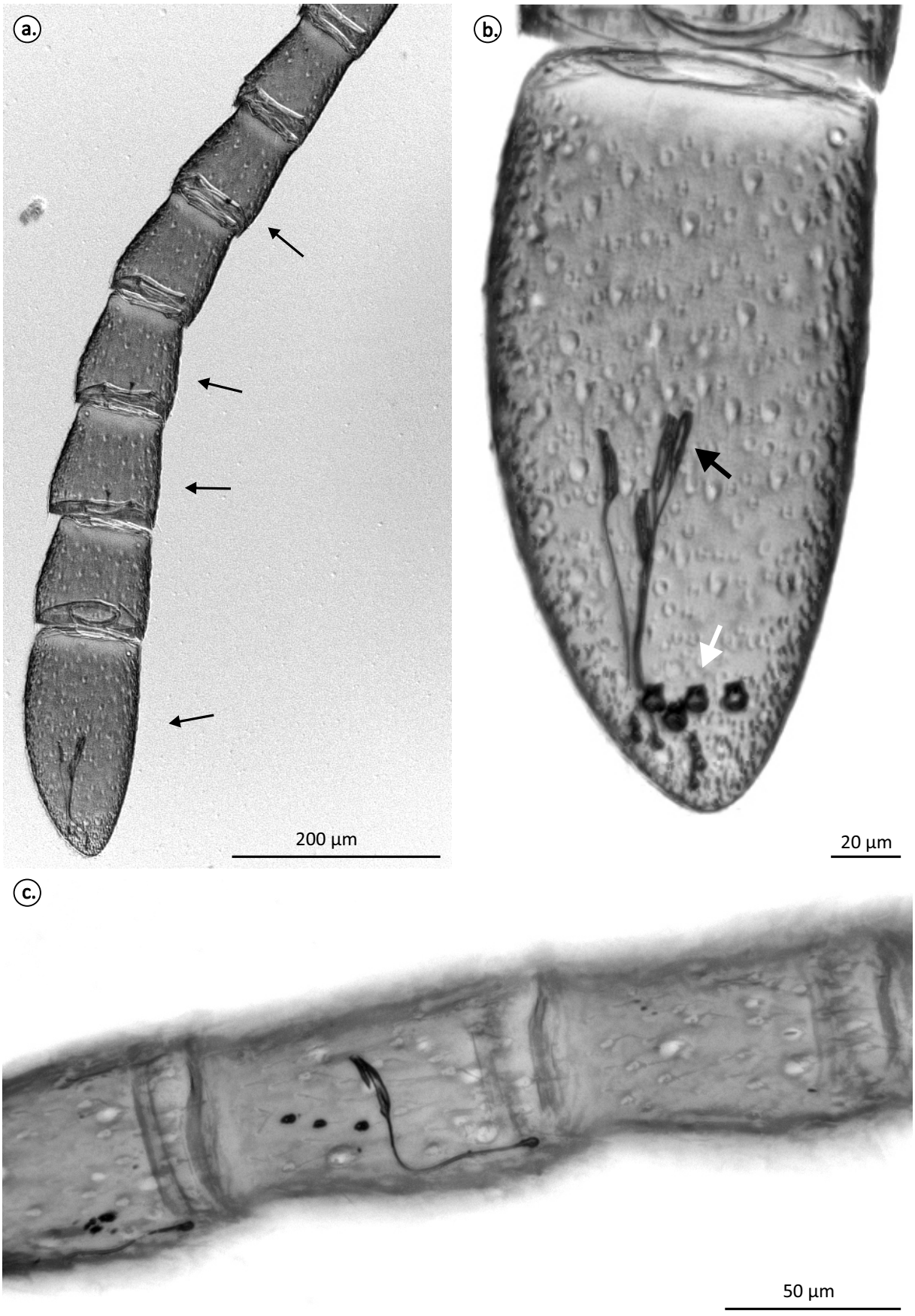

Supplementary Figure 7.1. Silver nitrate stained, whole-mounted, *Iridomyrmex calvus* antennae highlighting internal sensilla (sensilla coeloconica and ampullacea). (a) Low magnification image showing the 8 distal antennomeres of the flagellum, black arrows indicate antennomeres bearing internal sensilla; (b) high magnification image of the apical segment showing sensilla ampullacea (black arrow) and sensilla coeloconica (white arrow); (c) Z-stacking can lead to some artefacts such as the hazy aura around this segment of antenna.

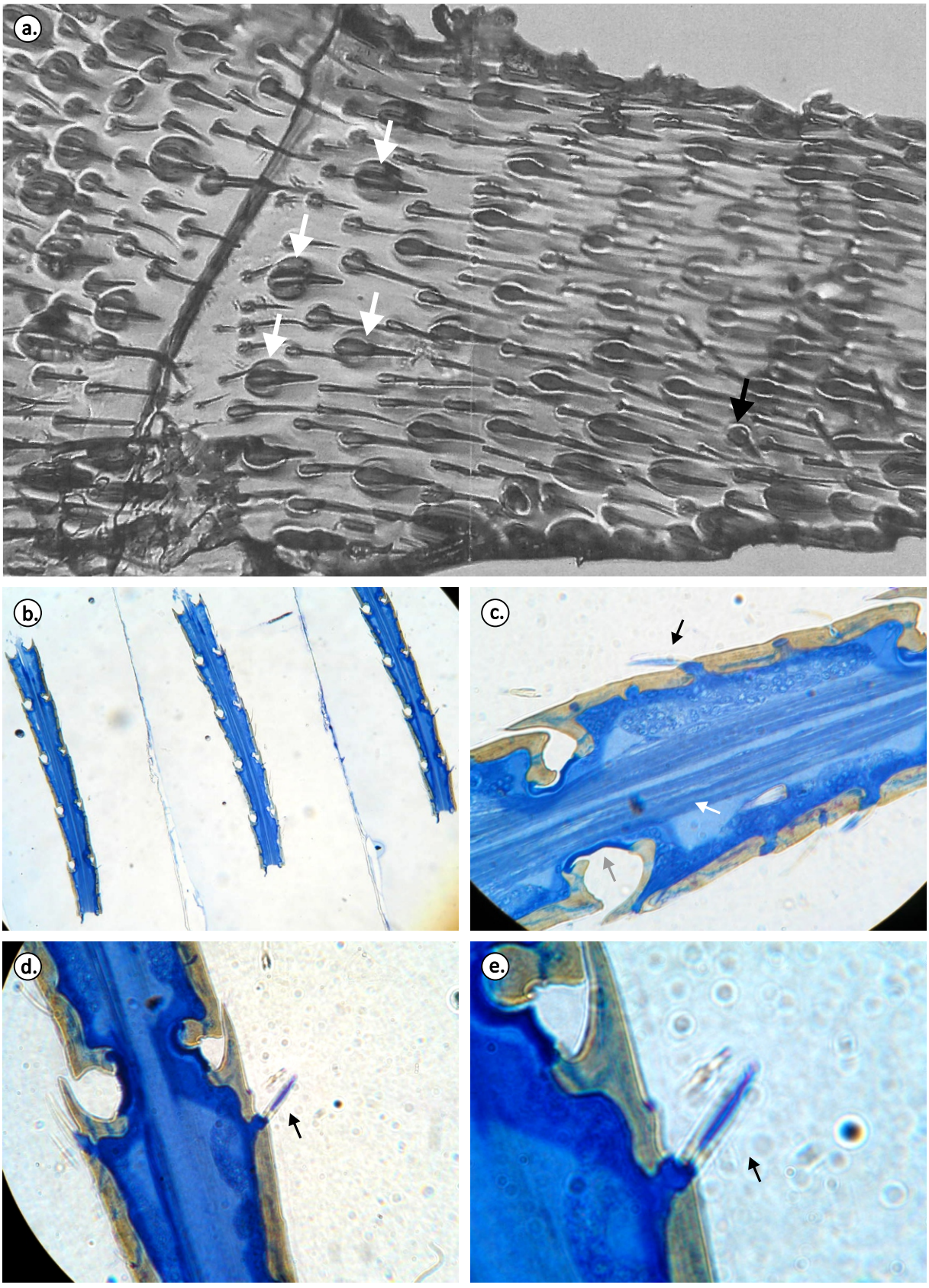

Supplementary Figure 7.2. Nail polish replica of an ant antenna and examples of semi-thin sections of antennae of *Notoncus ectatommoides*. (a) Nail polish replica of an ant antenna showing some identifiable sensilla, sensillum basiconicum (black arrow) and some sensilla trichodea curvata (white arrows), image courtesy of Willi Ribi; (b) ribbon of semi-thin serial sections; (c) semi-thin section showing some features of interest: sensillum tirchodeum curvatum (black arrow) with underlying neuron cell bodies (blue granular material), antennal nerve (white arrow), inter-antennomere joint made up of soft unsclerotised cuticle (grey arrow); (d) section showing a sensillum basiconicum section (black arrow); (e) same as (d) in higher magnification.

Supplementary Figure 7.3. Some of the equipment used for SEM specimen preparation. (a) Specimens stored in 70% ethanol; (b) sputter coater being used to coat specimens in gold (c); (d) dissecting microscopes are useful to check specimens after coating; (e) tools and equipment used for mounting specimens: 1. carbon tabs (smooth grain), 2. double-sided carbon tape (rough grain), 3. aluminum stubs, 4. razor blade (for cutting carbon tabs and tape as well as amputating antennae), 5. stub grasping forceps, 6. minutia pin mounted on a bamboo stick (used to manipulate small specimens), 7. entomological pin (used to manipulate specimens), 8. fine forceps, 9. archival ink pen for labelling specimens, 10. thicker permanent marker can be used to label stubs after coating.